MUTATIONS OF THE TRYPSINOGEN ACTIVATION PEPTIDE IN HEREDITARY PANCREATITIS

Andrea Geisz

Ph.D. Thesis

Supervisor at Boston University:	Miklós Sahin-Tóth, M.D., Ph.D.
Supervisors at University of Szeged:	Péter Hegyi, M.D., Ph.D., D.Sc
	Zoltán Rakonczay Jr., M.D., Ph.D., D.Sc.

First Department of Medicine

University of Szeged

Szeged, Hungary

2013

Articles closely related to the subject of the thesis and cited in the thesis

I. **Geisz A**, Hegyi P, Sahin-Tóth M. Robust autoactivation, chymotrypsin C independence and diminished secretion define a subset of hereditary pancreatitis associated cationic trypsinogen mutants. *FEBS J* (2013 Apr 18, Epub ahead of print), doi:10.1111/febs.12292 **[IF: 3.79]**

II. Joergensen MT*, **Geisz A***, Brusgaard K, Schaffalitzky de Muckadell OB, Hegyi P, Gerdes A, Sahin-Tóth M. Intragenic duplication: a novel mutational mechanism in hereditary pancreatitis. *Pancreas* 40, 540–546 (2011). *Equal contributors with shared first authorship. **[IF: 2.386]**

Articles related to the subject of the thesis and cited in the thesis

III. Pallagi P, Venglovecz V, Rakonczay Z Jr, Borka K, Korompay A, Ózsvári B, Judák L, Sahin-Tóth M, **Geisz A**, Schnúr A, Maléth J, Takács T, Gray MA, Argent BE, Mayerle J, Lerch MM, Wittman T, Hegyi P. Trypsin reduces pancreatic ductal bicarbonate secretion by inhibiting CFTR Cl^- channels and luminal anion exchangers. *Gastroenterology* 141, 2228–2239.e6 (2011). **[IF: 11.675]**

IV. Czepán M, Rakonczay Z Jr, Varró A, Steele I, Dimaline R, Lertkowit N, Lonovics J, Schnúr A, Biczó G, **Geisz A**, Lázár G, Simonka Z, Venglovecz V, Wittmann T, Hegyi P. NHE1 activity contributes to migration and is necessary for proliferation of human gastric myofibroblasts. *Pflugers Arch* 463**,** 459–475 (2012). **[IF: 4.463]**

Article not related to the subject of the thesis

V. Zádori D*, **Geisz A***, Vámos E, Vécsei L, Klivényi P. Valproate ameliorates the survival and the motor performance in a transgenic mouse model of Huntington's disease. *Pharmacol Biochem Behav* 94, 148–153 (2009). *Equal contributors with shared first authorship. **[IF: 2.967]**

Number of full publications:	5 (3 first author)
Cumulative impact factor:	25.281

TABLE OF CONTENTS

ABBREVIATIONS

BSA	bovine serum albumin
CASR	calcium sensing receptor
CFTR	cystic fibrosis transmembrane conductance regulator
CP	chronic pancreatitis
CTRC	human chymotrypsinogen C
CTRB1	human chymotrypsinogen B1
CTRB2	human chymotrypsinogen B2
CTRL1	human chymotrypsinogen like enzyme 1
DMEM	Dulbecco's modified Eagle's medium
EDTA	ethylene diamine tetraacetic acid
ELA2A	human proelastase 2A
ELA3A	human proelastase 3A
ELA3B	human proelastase 3B
FBS	fetal bovine serum
HCP	hereditary chronic pancreatitis
HEK	human embryonic kidney
HP	hereditary pancreatitis
HPLC	high-performance liquid chromatography
HRP	horseradish peroxidase
ICP	idiopathic chronic pancreatitis
IPTG	Isopropyl β-D-1-thiogalactopyranoside
MRCP	Magnetic resonance cholangiopancreatography
MWCO	molecular weight cut off
PCR	polymerase chain reaction
PRSS1	human cationic trypsinogen
PRSS2	human anionic trypsinogen
PRSS3	human mesotrypsinogen
PVDF	polyvinylidene difluoride
SBTI	soybean trypsin inhibitor
SDS	sodium dodecyl sulfate

SDS-PAGE	sodium dodecyl sulfate polyacrylamide gel electrophoresis
SPINK1	serine protease inhibitor, Kazal type 1
TAP	trypsinogen activation peptide
TCA	trichloroacetic acid
TCP	tropical chronic pancreatitis

1 INTRODUCTION

1.1 Chronic pancreatitis

Chronic pancreatitis (CP) is a disease of the pancreas characterized by chronic inflammation, progressive fibrosis, variable pain and loss of exocrine and endocrine function. CP can be classified into several subtypes which include alcoholic chronic pancreatitis (ACP), idiopathic chronic pancreatitis (ICP), tropical chronic pancreatitis (TCP) and hereditary chronic pancreatitis (HCP). Heavy alcohol consumption is a prominent risk factor of the disease but the mechanism by which alcohol induces pancreatic inflammation is poorly understood [[1]]. In about 10-30% of the cases, no causal agent can be identified and these patients are labeled as having ICP. TCP is a juvenile form of chronic calcific non-alcoholic pancreatitis, prevalent in tropical developing countries. HCP is an autosomal dominant genetic disorder that accounts for approximately 1-2 % of pancreatitis patients. Clarifying the pathomechanism of genetically determined CP helps to understand the pathophysiology of all other forms of the disorder and may result in more effective therapy and prevention.

1.2 Genetic factors in chronic pancreatitis

In recent years, several genetic risk factors for CP have been identified. Rare mutations affecting the human cationic trypsinogen (*PRSS1*) gene directly cause the disease [[2,3]]. Mutations in the *PRSS1* gene increase activation of trypsinogen and cause an autosomal dominant hereditary pancreatitis or act as a risk factor for sporadic cases [[4]]. Surprisingly, the G191R variant in the human anionic trypsinogen gene (*PRSS2*) protects against pancreatitis by stimulating trypsinogen autodegradation [[5]]. Genetic alterations in the serine protease inhibitor Kazal type 1 (*SPINK1*), an important pancreatic trypsin inhibitor have been found in association with ICP, ACP, and TCP [[6,7]]. Mutations in the *SPINK1* gene decrease the expression of the inhibitory protein, and thereby increase trypsinogen activation. Another risk factor for CP are mutations in the cystic fibrosis transmembrane conductance regulator gene (*CFTR*) [[8,9,10,11]]. *CFTR* mutations might impair bicarbonate secretion and facilitate trypsinogen activation through altered intraductal pH and/or decreased ductal washout. Furthermore, recent investigations confirmed chymotrypsin C (*CTRC*), a significant component of the trypsin activation

cascade, as a new susceptibility gene for CP [12]. CTRC variants can cause loss of CTRC function by different mechanisms: reduced secretion, catalytic defect or increased degradation by trypsin. Finally, mutations in the calcium sensing receptor gene (CASR) have been reported in CP. CASR might be a regulator of pancreatic juice calcium concentration by stimulating ductal electrolyte and fluid secretion [13,14].

1.3 Hereditary chronic pancreatitis

HCP is a very rare type of early onset chronic pancreatitis. It is defined as an autosomal dominant genetic disorder characterized by incomplete penetrance and variable expressivity [15]. HCP is diagnosed when there are recurrent episodes of pancreatitis from childhood, a positive family history and other causes of pancreatitis such as alcohol abuse, trauma, infection, medication, gallstones and metabolic disorders have been excluded. The disease was first described by Comfort and Steinberg in the early 1950's when they recognized that CP may accumulate in selected families suggesting a genetic background [16]. In 1996, an association between HCP and the long arm of chromosome 7 (7q35) was found by genetic linkage analysis with microsatellite markers by three independent teams [17,18,19]. In the same year, Whitcomb *et al.* identified the first genetic defect of the *PRSS1* gene when they sequenced two of the functional trypsinogen genes and discovered a disease causing mutation, which was the R122H variant [2]. Subsequently, this was independently confirmed by other studies [20,21,22].

Heterozygous mutations in the serine protease 1 (*PRSS1*) gene have been identified as causative genetic changes in 25-80% of cases in different studies. The *PRSS1* gene encodes human cationic trypsinogen, the dominant digestive proenzyme in human pancreatic secretions. Up to now, approximately 70% of the identified HCP cases carry the R122H mutation and about 20 % the N29I mutation. In the remaining 10% of the documented variants, there is an interesting subgroup composed by mutations affecting the activation peptide of human cationic trypsinogen [3]. The discovery that the disease is associated with *PRSS1* mutations demonstrates that trypsinogen plays a central role in the pathogenesis of human pancreatitis. The biochemical mechanism behind the genetic factors involves increased ectopic activation of trypsin in the pancreas and failure of protective mechanisms responsible for trypsin inactivation.

1.4 Human trypsinogens

Among the pancreatic enzymes trypsinogen is the most abundant digestive proteolytic proenzyme in the pancreatic juice. The human pancreas secretes three trypsinogen isoforms encoded by the *PRSS* genes 1, 2 and 3. On the basis of their isoelectric point and relative electrophoretic mobility, the three trypsinogen species are commonly referred to as cationic trypsinogen (*PRSS1*), anionic trypsinogen (*PRSS2*) and mesotrypsinogen (*PRSS3*). Cationic trypsinogen and anionic trypsinogen make up the bulk of secreted trypsinogen, whereas mesotrypsinogen accounts for 2% to 10% [[23,24]]. Human trypsinogens are synthesized as pre-pro-enzymes with a signal peptide of 15 amino acids which is removed on entry into the endoplasmic reticulum lumen. The proenzymes are packaged into zymogen granules and eventually secreted into the pancreatic juice. Physiological activation of trypsinogen takes place in the duodenum, where enteropeptidase specifically cleaves the Lys23-Ile24 peptide bond and this activating cleavage removes a typically 8 amino-acid long activation peptide [[25]]. Trypsin can also activate trypsinogen, in a process termed autoactivation which facilitates digestive zymogen activation in the duodenum, but may induce pancreatitis if occurs prematurely in the pancreas. Compared with trypsinogens from other species, human cationic trypsinogen exhibits an usually high propensity for autoactivation, and this stimulatory effect is especially strong in the case of activation peptide mutations [[26,25,27]].

1.5 Mutations in the trypsinogen activation peptide

The trypsinogen activation peptide (TAP) is an eight amino acid long N-terminal sequence containing a strongly conserved tetra-Asp motif preceding the Lys23-Ile24 scissile peptide bond. The characteristic tetra-Asp sequence is presumed to serve as an enteropeptidase recognition motif [[28]]. Previous data from our laboratory showed that in human cationic trypsinogen the negatively charged tetra-Asp sequence plays only a limited role in enteropeptidase recognition, but it is essential for suppression of autoactivation [[26]]. It has also been demonstrated that millimolar concentrations of Ca^{2+}, which binds to the above mentioned tetra-Asp motif in the activation peptide and shields the negative charges, can increase trypsinogen activation [[29]]. Thus, mutations that neutralize any of the Asp residues in the activation peptide, are expected to cause increased autoactivation of trypsinogen. In addition to the relatively common A16V mutation, there were three other mutations in the activation peptide of human cationic

trypsinogen found in association with hereditary pancreatitis namely D19A, D22G and K23R variants (Table 1) [22,25,30,31].

Region	Nucleotide change	Amino acid change	Number of CP carriers reported	Number of non-CP carriers reported
exon-2	c.47C>T	p.A16V	~38	23
	c.56A>C	p.D19A	1	
	c.65A>G	p.D22G	2	1
	c.68A>G	p.K23R	2	

Table 1. Hereditary pancreatitis-associated mutations in the activation peptide of human cationic trypsinogen. Note that only changes in exon-2 affect the mature trypsinogen protein.

All four TAP mutations were identified in the heterozygous state, and mutations D22G and K23R were found only in a single family each (see details at www.pancreasgenetics.org). Mutation A16V exhibited variable penetrance and was also found in sporadic cases with no family history [32].

Although these activation peptide mutations are fairly rare, their functional characterization strongly contributed to the elucidation of the pathomechanism of genetically determined pancreatitis. Biochemical analyses of TAP mutants D19A, D22G and K23R revealed that the common phenotypic change is a markedly increased propensity for autoactivation [25,26, 27]. In fact, these mutations offered the first convincing evidence that increased autoactivation was a pathologically relevant mechanism in hereditary pancreatitis. However, even though TAP mutations stimulate autoactivation in a dramatic manner, these variants cause the same clinical phenotype as the most frequent R122H and N29I mutations. Mutations D19A and D22G eliminate Asp residues from the characteristic tetra-Asp motif and thereby mitigate its inhibitory effect. Mutation K23R changes the P1 Lys residue to Arg, which is preferred by trypsin owing to a favorable electrostatic interaction in the specificity pocket of the protease [25]. Mutation A16V has no direct effect on autoactivation; however, it increases N-terminal processing of the activation peptide by chymotrypsin C, which, in turn, leads to increased autoactivation of cationic trypsinogen [33,34]. Recent studies demonstrated that increased autoactivation of activation peptide mutants can occur intracellularly and result in decreased trypsinogen secretion and apoptotic acinar cell death [27].

1.6 The regulatory effect of chymotrypsin C

Functional characterization of HCP-associated *PRSS1* mutations revealed that there are at least two pathological pathways mediating increased pancreatitis risk. Mutations exert their effect via a so-called trypsin-dependent pathological pathway by

directly increasing trypsinogen autoactivation or by altering the chymotrypsin-C (CTRC)-dependent activation and/or degradation of cationic trypsinogen [34]. Alternatively, *PRSS1* mutations can cause misfolding, intracellular retention and degradation with consequent endoplasmatic reticulum stress [35].

The mechanism of action for the most frequently found mutations have been recently elucidated and involves increased resistance against CTRC-mediated degradation and/or increased sensitivity to CTRC-dependent stimulation of autoactivation [34]. CTRC is a pancreatic serine protease which controls autoactivation of human cationic trypsinogen by selectively cleaving regulatory sites within the TAP and the calcium binding loop. The dominant effect of CTRC is trypsinogen degradation, which is triggered by cleavage of the Leu81-Glu82 peptide bond in the calcium binding loop and is facilitated by a trypsin-mediated autolytic cleavage of the Arg122-Val123 peptide bond [12,34]. CTRC also degrades active trypsin by the same mechanism but at a slower rate. It has been shown that HCP-associated mutations N29I, N29T, V39A, R122C and R122H decrease or block cleavages at these sites and thereby increase trypsin levels generated during autoactivation [34].

A secondary, less prominent effect of CTRC on autoactivation is mediated by cleavage of the activation peptide of cationic trypsinogen at the Phe18-Asp19 peptide bond (Figure 1) [33]. In human cationic trypsinogen, inhibition of autoactivation is dependent on Asp218, which participates in a repulsive electrostatic interaction with the tetra-Asp motif. CTRC cleavage at the Phe18-Asp19 peptide bond results in a shortened activation peptide, causing partial liberation of the inhibitory interaction with Asp218 and increased autoactivation. Earlier studies proved that pancreatitis-associated mutations A16V and, to a lesser extent, N29I increase N-terminal processing of the activation peptide by CTRC and thereby stimulate trypsinogen autoactivation [33,34].

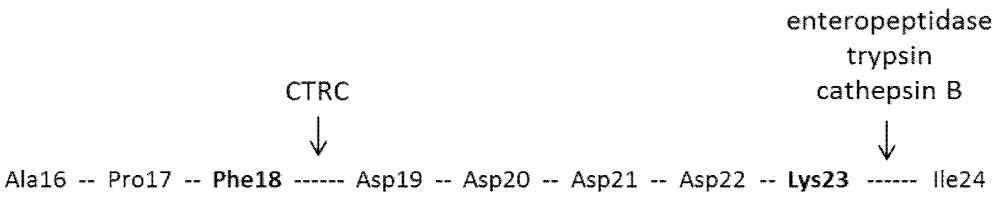

Figure 1. Amino-acid sequence and the cleavage sites of human cationic trypsinogen activation peptide

2 AIMS OF THE STUDY

Mutations in the *PRSS1* gene increase autoactivation of human cationic trypsinogen which explains the higher risk for pancreatitis in carriers. Based on the hypothesis that HCP-associated mutations may exert their effect in a chymotrypsin C (CTRC)-dependent manner, autoactivation of trypsinogen mutants has recently been studied in the presence of CTRC. The mechanism of action for the most frequently found variants involves increased resistance against CTRC-mediated degradation and/or increased sensitivity to CTRC-dependent stimulation of autoactivation.

2.1 Characterization of the K23_I24insIDK *PRSS1* mutation

In a hereditary pancreatitis family from Denmark, we identified a novel intragenic duplication of 9 nucleotides in exon 2 of the *PRSS1* gene (c.63_71dup) which at the amino-acid level resulted in the insertion of three amino acids within the activation peptide of cationic trypsinogen (K23_I24insIDK). Our aim was to **characterize the effect of the novel K23_I24insIDK *PRSS1* alteration on the function of human cationic trypsinogen**. Our specific aims were:

1. To investigate the effect of the K23_I24insIDK mutation on autoactivation
2. To investigate the effect of the K23_I24insIDK mutation on enteropeptidase and cathepsin B-mediated trypsinogen activation
3. To investigate the effect of the K23_I24insIDK mutation on trypsinogen secretion

2.2 Investigation of trypsinogen activation in the presence of chymotrypsin C

In light of the recently discovered CTRC-dependent unifying pathomechanism for HCP, **this study was further aimed at clarifying the role of CTRC in the mechanism of action of the activation peptide mutations.** Our specific aims were:

1. To investigate the effect of TAP mutations on autoactivation
2. To investigate the effect of CTRC on the autoactivation of trypsinogen activation peptide mutations
3. To elucidate the effect of mutations on CTRC specificity in activation peptide cleavage
4. To determine the effect of mutations on the Ca^{2+} binding affinity of the activation peptide
5. To investigate the effect of mutations on trypsinogen secretion

3 EXPERIMENTAL PROCEDURES

3.1 Nomenclature

Nucleotide numbering in genes encoding human pancreatic proteases reflects coding DNA numbering with +1 corresponding to the A of the ATG translation initiation codon in the reference sequence. Amino acid residues were numbered starting with the initiator methionine of the primary translation product, in accordance with the recommendations of the Human Genome Variation Society. Note that the ELA (elastase) gene nomenclature for the five human pancreatic elastase genes have recently been changed to CELA (chymotrypsin-like elastase). In this thesis, I use the old ELA nomenclature.

3.2 Patients

Our study was approved by the Scientific Ethics Committee of the Odense University Hospital and the Danish Data Protection Agency. The diagnosis of CP was based on the criteria used by The European Registry of Hereditary Pancreatitis and Familial Pancreatic Cancer (EUROPAC) which require two first degree relatives or three or more second degree relatives in two or more generations with recurrent acute pancreatitis, and/or CP for which there are no known precipitating factors. The family received genetic counseling before they gave their informed consent to participate in the study. A questionnaire recording symptoms, clinical tests and medical history was completed. After discovery of the mutation, the grandparents and the siblings of the father were also tested.

3.3 Genetic analyses

Blood samples were drawn from the index patient, his brother and his father into tubes with ethylene diamine tetraacetic acid (EDTA) and stored at –20 ^{o}C. Genomic DNA was extracted from full blood using the Maxwell® (Promega, Ramcon Denmark) DNA purification robot. The samples were tested for small deletions, insertions and point mutations in all exons and the exon-intron boundaries of the *PRSS1* (GenBank NM_002769.3) and *SPINK1* (GenBank NM_003122.3) genes using DHPLC (WAVE 3500HT High Sensitivity System; Transgenomic Inc, Elancourt, France). Variants in the *PRSS1* gene were categorized as polymorphisms if they were identified in control

samples with a comparable frequency. Samples with deviating chromatographic profiles were sequenced in both directions using the BigDye® Terminator v3.1 Cycle Sequencing Kit (Applied Biosystems) and analyzed on an automated ABI PRISM® 3100 (Applied Biosystems). The presence of *PRSS1* gene duplication or triplication was excluded using the rapid polymerase chain reaction (PCR)-based method described by Chauvin et al., 2009 [36]. Genomic DNA was also tested for 33 *CFTR* (GenBank NM_000492.3) mutations: 394delTT, p.R553X, 621+1G>T, p.R1162X, 1717-1G>A, 3659delC, p.G542X, 2183A>G, p.W1282X, 1078delT, 711+1G>T, p.F508del, p.S549N, I507del, p.S549R, 2184delA, p.G551D, p.G85E, p.N1303K, p.R560T, p.R117H, p.R347H, p.R347P, p.R334W, 2789+5G>A, 3849+10kbC>T, p.A445E, 3120+1G>A, p.V520F, 1898+1G>A, 3876delA, 3905insT and IVS8-5T.

3.4 Plasmid construction and mutagenesis

The pTrapT7 intein and pcDNA3.1(-) expression plasmids harboring the coding DNA for human pancreatic digestive proteases were constructed previously in our laboratory. [12,33,37,38]. To increase expression levels in cell transfection experiments, the TAP mutations were transferred into the pcDNA3.1(-) p.K237D/p.N241D mutant *PRSS1* background [39]. Mutations in *PRSS1* were generated by overlap extension PCR mutagenesis with the mutagenic primers listed in Table 2. A typical PCR mixture contained 200 µM dNTP, 2 µM of each primer, DNA template, 0.05 U/µl HotStarTaq DNA Polymerase (Qiagen) in a total volume of 50 µL. 35 cycles of 30 sec denaturation at 94 ºC, 30 sec annealing at 55-65 ºC and 1 min extension at 72 ºC were performed. PCR products were analyzed by conventional submarine horizontal agarose gel electrophoresis.

PRIMER NAME	PRIMER SEQUENCE
intein constructs	
D19A sense	5'- GCT CCT TTC GCT GAT GAT GAC -3'
D19A antisense	5'- GTC ATC ATC AGC GAA AGG AGC -3'
D22G sense	5'– GAT GAT GAT GGC AAG ATC GTT -3
D22G antisense	5'– AAC GAT CTT GCC ATC ATC ATC -3'
IDK sense	5' – CAA GAT TGA CAA GAT CGT TGG AGG ATA CAA CTG CGA AGA - 3'
IDK antisense	5' – CCA ACG ATC TTG TCA ATC TTG TCA TCA TCA TCG AAA GGA - 3'
K23R sense	5'- GAT GAT GAT GAC AGG ATC GTT GGA -3
K23R antisense	5'- TCC AAC GAT CCT GTC ATC ATC ATC -3'
pcDNA3.1(-) constructs	
D19A sense	5'- GCT GCC CCC TTT GCT GAT GAT GAC -3'
D19A antisense	5'- GTC ATC ATC AGC AAA GGG GGC AGC -3'
D22G sense	5'- GAT GAT GAT GGC AAG ATC GTT -3'
D22G antisense	5'- AAC GAT CTT GCC ATC ATC ATC -3'
IDK sense	5' – CAA GAT TGA CAA GAT CGT TGG GGG CTA CAA CTG TGA GGA - 3'
IDK antisense	5' – CCA ACG ATC TTG TCA ATC TTG TCA TCA TCA TCA AAG GGG - 3'
K23R sense	5'- GAT GAT GAT GAC AGG ATC GTT GGG GGC -3'
K23R antisense	5'- GCC CCC AAC GAT CCT GTC ATC ATC ATC -3'

Table 2. Oligonucleotides used for PCR mutagenesis.

3.5 Expression of cationic trypsinogen

Wild-type and mutant trypsinogens were expressed in the aminopeptidase P deficient LG-3 *E. coli* strain as fusions with a self-splicing mini-intein. This expression system produces recombinant trypsinogen with uniform, authentic N termini [[37,40]]. Transformants were grown in 200 mL Luria-Bertani medium (LB) at 30 ºC. When culture density reached OD 0.5 at 600 nm (OD_{600}), expression of trypsinogen was induced by shifting the incubation temperature to 42 ºC for 30 min which induces the expression of T7 RNA polymerase encoded on plasmid pGPI-2 under the control of temperature-sensitive λ repressor. Adding isopropyl-1-thio-β,D-galactopyranoside (IPTG) to a final concentration of 1 mM derepressed the lac operator which is positioned between the T7 promoter and the intein-trypsinogen fusion gene in the pTrapT7 plasmid. After induction, cells were grown for an additional 5 h at 30 ºC. Expression was verified by analyzing the inclusion body fraction by 15% SDS-PAGE and Coomassie Blue staining (Figure 2.).

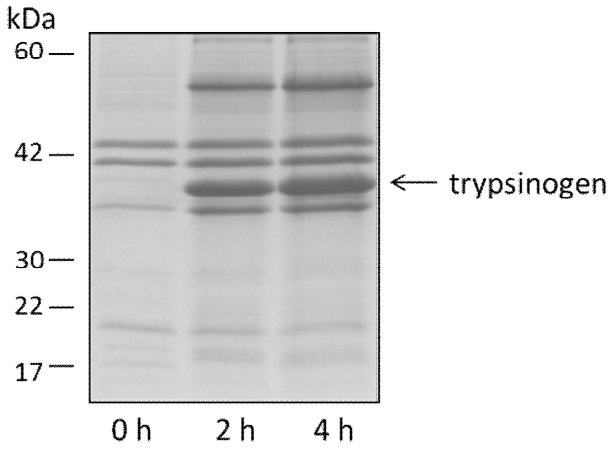

Figure 2. Human cationic trypsinogen (PRSS1) expressed in aminopeptidase P deficient LG-3 *E. coli* cells. Inclusion bodies prepared from 1 mL cell culture were analyzed by 15% reducing SDS-PAGE followed by Coomassie Blue staining.

3.6 Refolding and purification of cationic trypsinogen

Harvested LG-3 *E. coli* cells were resuspended in 0.1 M Tris-HCl pH 8.0, 5 mM K-EDTA at 0.8 mL per 10 mL original culture volume, and inclusion bodies were isolated by sonication (3 x 20 s, Heat Systems Ultrasonic cell disruptor, Model W-200R with a microtip probe, continuous mode, power setting 4) and centrifugation (13,200 rpm, 5 min, Eppendorf microcentrifuge, 4 ºC). The pellet was washed twice with 1 mL of 0.1 M Tris-HCl (pH 8.0), 5 mM K-EDTA, dissolved in 500 µL of 4M guanidine-HCl, 0.1 M Tris-HCl (pH 8.0), 2 mM K-EDTA, 30 mM dithiothreitol (final concentrations), and incubated at 37 ºC for 30 min to reduce trypsinogens. Denaturated trypsinogens were rapidly diluted in 50 mL refolding buffer (0.9 M guanidine-HCl, 0.1 M Tris-HCl (pH 8.0), 2 mM K-EDTA, 1 mM L-cysteine, and 1 mM L-cystine), stirred under argon for 5 min, and incubated overnight at 4 ºC. The solution was diluted with 50 mL of 0.4 M NaCl, centrifuged for 15 min at 15,000 rpm and loaded onto 2 mL ecotin-affinity column. The column was washed with 20 mM Tris-HCl (pH 8.0) 0.2 M NaCl and trypsinogens were eluted with 50 mM HCl. To stabilize trypsinogens against autoactivation the elution solution also contained 100 mM NaCl.

3.7 Expression of proelastase 2A

The pTrap-T7 constructs encoding proelastase 2A (*ELA2A*) were transformed into *E. coli* BL21(DE3) carrying a chromosomal copy of T7 RNA polymerase under the control of the *lacZ* promoter. The transformants were grown in 200 mL of LB medium containing 100 µg/mL ampicillin at 37 ºC. When culture density reached OD 0.5 at 600

nm (OD_{600}), expression of proelastase was induced by adding IPTG to a final concentration of 1 mM. After induction, cells were grown for an additional 4 h at 37 ºC. Cells were harvested and inclusion bodies were isolated by sonication and centrifugation, as described above.

3.8 Refolding and purification of proelastase 2A

The inclusion body pellet was washed twice with 1.5 mL of 0.1 M Tris-HCl (pH 8.0) and dissolved in 1 mL of unfolding solution [6 M guanidine-HCl, 50 mM Tris-HCl (pH 8.0) and 5 mM DTT] to ~20 mg of inclusion bodies. Dithiothreitol was added to a final concentration of 30 mM, and ELA2A protein was completely reduced at room temperature for 2 h. Denatured ELA2A protein was then rapidly diluted into 50 mL of refolding buffer (0.9 M guanidine-HCl, 0.1 M Tris-HCl (pH 8.0), 30 mM L-cysteine, 30 mM L-cystine), slowly stirred under argon for 5 min at room temperature, and kept at 4 °C overnight. To remove any leftover contaminants and misfolded protein, the renatured ELA2A protein solution was diluted 2-fold with 50 ml of 0.1 M Tris-HCl (pH 8.0) and applied directly to a 2 mL ecotin affinity column [[38]]. The column was washed with 20 mM Tris-HCl (pH 8.0)/0.2 M NaCl, and ELA2A was eluted with 50 mM HCl. ELA2A was then activated using 10 nM human anionic trypsin in 0.1 M Tris (pH 8.0), 0.05% Tween-20 (final concentrations) and enzyme concentrations were determined by active site titration with ecotin [[41]].

3.9 Expression and purification of human chymotrypsinogens and proelastase ELA3A and ELA3B

Deca-histidine (10 His)-tagged forms of human chymotrypsinogens CTRB1, CTRB2, CTRC and CTRL1 and proelastases ELA3A and ELA3B proteins were expressed in human embryonic kidney (HEK 293T) cells with transient transfection using 30 µg of the pcDNA expression plasmid and then purified from the conditioned medium with nickel-affinity chromatography. Approximately 150-200 mL of conditioned medium was used for purification on a nickel-nitrilotriacetic acid Superflow cartridge (Qiagen) equilibrated with Buffer NPI-20 [50mM NaH_2PO_4, 300 mM NaCl, and 20 mM imidazole (pH 8.0)]. The medium was loaded onto the column at a flow rate of 4 mL/min using a loading pump, and the column was washed with Buffer NPI-20 until the absorbance at 280 nm returned to the base line. The purified protein was then eluted with Buffer NPI-250 [50 mM NaH_2PO_4, 300 mM NaCl, and 250 mM imidazole (pH 8.0)] at a flow rate of 2 mL/min, and 5 mL fractions were collected. Aliquots (100 µL) of the fractions were

analyzed by 15% SDS-PAGE and Coomassie Blue staining, and peak fractions were pooled and dialyzed for 24 h against two changes of 3.5 liters of 50 mM NaH_2PO_4 buffer (pH 8.0) containing 300 mM NaCl. The dialyzed proenzyme solution was concentrated using a Vivaspin concentrator (10-kDa molecular mass cutoff). Pancreatic zymogens were then activated using 10 nM human cationic trypsin, and enzyme concentrations were determined by active site titration with ecotin [41]. The final working CTRC stock solution was diluted to 500 nM in 0.1 M Tris-HCl (pH 8.0) and 0.05% Tween 20.

3.10 Concentration determination of pancreatic enzymes

The concentration of proteases were determined by active-site titration against the pan-protease inhibitor ecotin Ecotin was overexpressed previously in *E. coli* BL21(DE3) and purified from the periplasm as described in [42]. The concentration of ecotin was then determined by titration against active site-titrated bovine trypsin. This ecotin batch served then as a universal titrant for all studies. Enzymes at 25-100 nM estimated concentration (calculated from their ultraviolet absorbance at 280 nm, using the theoretical extinction coefficients) was added to 0-100 nM ecotin (two-fold serial dilution in 0.1 M Tris-HCl (pH 8.0) with 1 mM $CaCl_2$) in a total volume of 100 µL. After 1 hour incubation at room temperature, free enzyme activity was measured as described below. Titrations were performed using protease concentrations at least 2 orders of magnitude above the K_D values. Substrate was given in a 5 µL volume so as not to perturb the equilibrium. The measured enzyme activity values were plotted as a function of the total inhibitor concentration. The equivalence point was determined by extrapolation of the linear portion of the curve to the x axis. This represents the inhibitor concentration equal to the enzyme concentration.

3.11 Trypsin activity assay

Trypsin activity was measured with the synthetic chromogenic substrate, *N*-benzyloxycarbonyl-Gly-Pro-Arg-*p*-nitroanilide at 0.14 mM final concentration. One-minute time courses of *p*-nitroaniline release were followed at 405 nm in 0.1 M Tris-HCl (pH 8.0) and 1 mM $CaCl_2$ at room temperature using a SpectramaxPlus 384 microplate reader. Rates of substrate hydrolysis were determined from fits to the initial linear portion of the curves.

3.12 Trypsinogen autoactivation in the presence of chymotrypsin C

Trypsinogen at 1 μM concentration was incubated in the absence or presence of 25 nM human CTRC, as indicated, and 10 nM cationic trypsin in 0.1 M Tris-HCl (pH 8.0), 100 mM NaCl, 1 mM $CaCl_2$ and 0.05% Tween-20 (final concentrations) at 37 ºC. At given times, 2 μL aliquots were withdrawn and mixed with 48 μL assay buffer containing 0.1 M Tris-HCl (pH 8.0), 1mM $CaCl_2$, and 0.05% Tween-20. Trypsin activity was measured by adding 150 μL 200 μM N-CBZ-Gly-Pro-Arg-p-nitroanilide substrate (dissolved in 0.1 M Tris-HCl (pH 8.0), 1 mM $CaCl_2$ and 0.05% Tween-20) and following the release of the yellow p-nitroanilin at 405 nm in a SpectraMax plus384 microplate reader for 1 min. Reaction rates were calculated from fits to the initial linear portions of the curves.

3.13 Gel electrophoresis and densitometry

Trypsinogen samples were precipitated with trichloroacetic acid (10% final concentration), and the precipitate was recovered by centrifugation, dissolved in 20 mL of Laemmli sample buffer containing 100 mM DTT (final concentration), and heat-denatured at 95 °C for 5 min. Electrophoretic separation was performed on 15% SDS-polyacrylamide mini gels in standard Tris-glycine buffer. The samples of trypsinogen N-terminal processing experiments were analyzed by 15% non-reducing SDS-PAGE. Gels were stained for 30 min with 0.5% Brilliant Blue R-250 dissolved in 40% methanol and 10% acetic acid and destained overnight with 30% methanol and 10% acetic acid. Quantitation of bands was carried out with the Quantity One 4.6.9 software (Bio-Rad). Rectangles were drawn around each band of interest, and an identical rectangle was used in each lane for background subtraction.

3.14 Cell culture and transfection

HEK 293T cells were cultured in six-well tissue culture plates (10^6 cells per well) in Dulbecco's modified Eagle medium (DMEM) supplemented with 10% fetal bovine serum (FBS), 4 mM glutamine, and 1% penicillin/streptomycin at 37 °C in 5% CO_2. Transfections were performed using 2 μg expression plasmid and 5μL Lipofectamine 2000 (Invitrogen, Carlsbad, CA) in 2 mL DMEM medium. After overnight incubation, cells were washed and the transfection medium was replaced with 1 mL OptiMEM reduced serum medium. Time courses of expression were measured starting from this medium change and were followed for 12 h.

3.15 Measurement of trypsin activity in conditioned media

Aliquots (50 µL) of conditioned media were supplemented with 5 µL 1 M Tris-HCl (pH:8.0) and 1 µL 0.5 M $CaCl_2$ and trypsinogens were activated by adding 1 µL 1.4 µg/mL human enteropeptidase (R&D Systems, Minneapolis, MN). After incubation for 1 h at 37 °C, a 50 µL aliquot was removed and mixed with 150 µL 200 µM N-CBZ-Gly-Pro-Arg-p-nitroanilide substrate. Activity was determined as described above.

3.16 Western blot analysis

Aliquots of conditioned media (20 µL per lane) were directly mixed with sample buffer, electrophoresed on Tris-glycine minigels and transferred onto an Immobilon-P polyvinylidene difluoride (PVDF) (Millipore Corporation, Bedford, MA) membrane at 300 mA for 1.5 h. The membrane was blocked with 5% milk powder dissolved in phosphate-buffered saline supplemented with 0.1% Tween-20 (final concentration), at 4 °C overnight. Trypsinogen was detected with a sheep polyclonal antibody (R&D Systems, #AF3848) used at a dilution of 1:2000 followed by horse-radish peroxidase (HRP)-conjugated donkey polyclonal anti-sheep IgG (R&D Systems, #HAF016) used at 1:2000 dilution. Incubations with primary and secondary antibodies were performed at room temperature for 1 h each. HRP was detected using the SuperSignal West Pico Chemiluminescent Substrate (Thermo Scientific).

3.17 N-terminal sequencing

N-terminal sequencing uses a chemical process based on the technique developed by Pehr Edman in the 1950's [43]. This method excises amino acids sequentially from the N terminus of proteins, which are then identified by high-performance liquid chromatography (HPLC). Protein samples were run on 15% Tris-glycine gels under reducing conditions and were transferred to Immobilon-P membrane at 300 mA for 1.5h. The membrane was stained with Coomassie Blue for 5 min followed by destaining with 50% methanol and dried at room temperature. Protein sequencing was performed by David McCourt (Midwest Analytical Inc., St. Louis, Missouri, USA).

4 RESULTS

4.1 A novel mutation in the PRSS1 gene is associated with hereditary pancreatitis

The criteria of the diagnosis of HCP have been changing over the years and may vary from centre to centre. We use the criteria also used by EUROPAC (The European Registry of Hereditary Pancreatitis and Familial Pancreatic Cancer) based on two first-degree relatives or three or more second-degree relatives, in two or more generations with recurrent acute pancreatitis, and/or CP for which there are no known precipitating factors [44].

There are three affected members within the study family which satisfy the formal criteria mentioned above (Figure 3). The index patient is a 2-year-old boy from Denmark who presented with ascites and a history of recurrent attacks of abdominal pain, diarrhea and vomiting for 4 months. A preoperative magnetic resonance cholangiopancreatography revealed a pancreatic fistula as the cause for the ascites, and also disclosed pancreas divisum, duct irregularities and multiple cysts in the pancreatic head and tail. The tail of the pancreas was resected and pancreatico-jejunostomy was performed. After resection, the ascites production ceased and the patient recovered. The father of the index patient was diagnosed with CP at the age of 21, which was initially attributed to a bicycle accident, which had happened at age 13. The father underwent resection of the tail of the pancreas at the age of 27 because of repeated attacks of upper abdominal pain. The index patient's younger brother also developed abdominal pain, diarrhea and elevated blood amylase at the age of 2, but pancreatic edema was not detected by ultrasonography. Interestingly, no other case of pancreatitis could be confirmed in the rest of the extended family, suggesting that the causative mutation may have occurred *de novo* in the father. Non-paternity was excluded by DNA microsatellite analysis (Identifiler kit, Applied Biosystems).

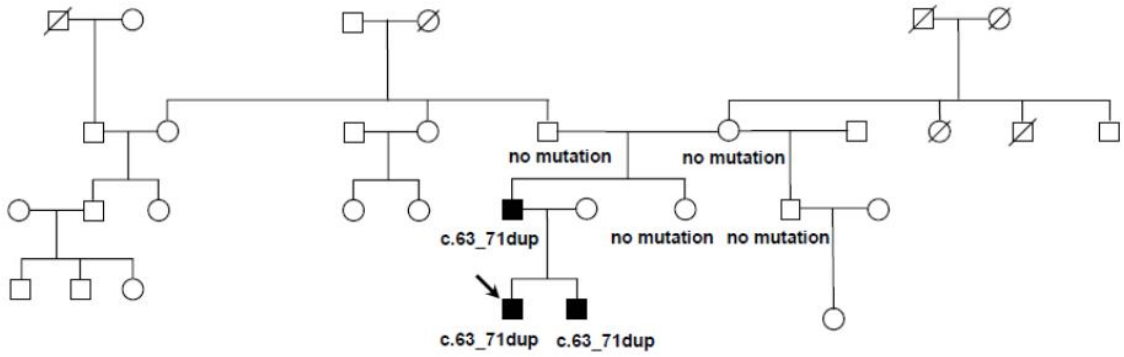

Figure 3. Pedigree of the studied family with hereditary pancreatitis from Denmark. Heterozygous carriers of the c.63_71dup (K23_I24insIDK) mutation are indicated. Subjects affected with idiopathic chronic pancreatitis are shown by solid black symbols. Crossed symbols designate deceased subjects. The arrow points to the index patient.

4.2 The identified intragenic duplication

DNA sequence analysis of the *PRSS1* gene in the index patient showed a so far unreported duplication in exon 2. As demonstrated by the electropherogram (Figure 4), the forward sequencing of exon 2 showed mixed signals starting at nucleotide position c.72 due to a heterozygous nine-nucleotide insertion. The inserted sequence is TGACAAGAT, which corresponds to *PRSS1* sequence between c.63 and c.71. Thus, the insertion represents a short intragenic duplication (c.63_71dup), which has never been described in trypsinogen genes so far. Sequencing of exon 2 with a reverse primer confirmed the duplication. No other mutations were identified in the *PRSS1* gene. The previously reported large-scale trypsinogen duplication and triplication was excluded [36,45,46,47]. The c.63_71dup mutation was also present in the father and the brother but not in the grandparents or in the father's sister and half-brother, indicating that the mutation was *de novo* created in the father. All affected family members were negative for *SPINK1* mutations and a select panel of *CFTR* mutations. From the same geographical region 200 healthy controls (400 chromosomes) were included in the mutational screening, but we did not find the c.63_71dup mutation among them.

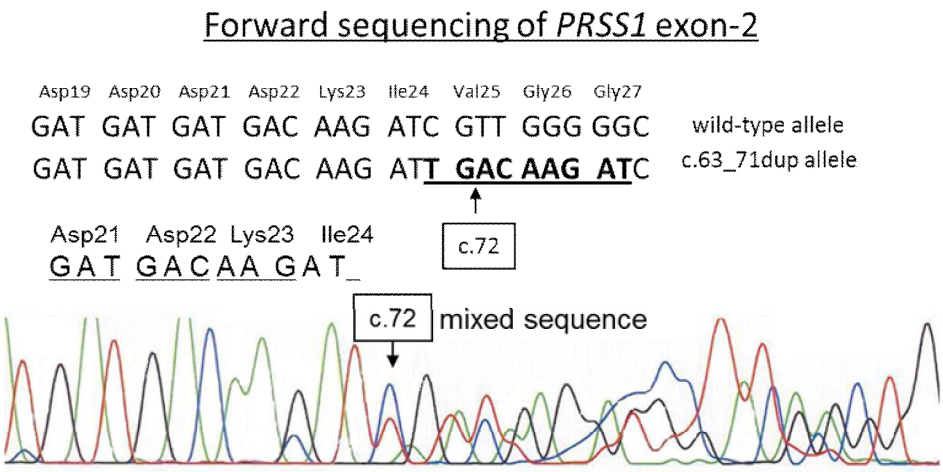

Figure 4. Sequence analysis of exon-2 of the *PRSS1* gene from genomic DNA of the index patient carrying a heterozygous c.63_71dup (K23_I24insIDK) mutation.

4.3 Changes in the trypsinogen activation peptide

The activation peptide of human cationic trypsinogen is an 8 amino-acid long N-terminal extension which is cleaved off during activation at the Lys23-Ile24 peptide bond by the physiological activator enteropeptidase or by the pathological activators trypsin and cathepsin B. The identified c.63_71dup mutation creates an insertion of the Ile-Asp-Lys (IDK) sequence within the activation peptide between amino acids Lys23 and Ile24 (K23_I24insIDK) (Figure 5). This insertion changes the P1-P5 (Schechter-Berger numbering where P1 is Lys23) positions of the activation peptide to Asp-Lys-Ile-Asp-Lys, effectively eliminating two of the tetra-Asp residues which has been shown to be an important suppressor of trypsin-mediated activation (autoactivation) [[26]]. It has been previously described that mutations which alter the tetra-Asp motif (D19A, D22G) were shown to increase autoactivation of cationic trypsinogen, suggesting a similar phenotype for the K23_I24insIDK mutant as well [[25,26,27,31]]. With this insertion the mutation creates an extra Lys-Ile peptide bond; which provides an additional target for hydrolysis by trypsin and enteropeptidase.

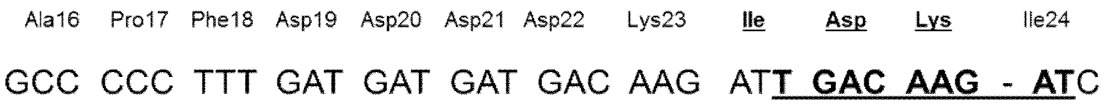

Figure 5. Nucleotide and amino-acid sequence of the wild-type and c.63_71dup (K23_I24insIDK) mutant cationic trypsinogen activation peptides.

4.4 Activation characteristics of K23_I24insIDK mutant cationic trypsinogen

4.4.1 Trypsin mediated trypsinogen activation: Autoactivation

When we studied the effect of the K23_I24insIDK mutation on the activation of cationic trypsinogen, we observed that the mutant trypsinogen preparations were highly unstable and spontaneous conversion to trypsin occurred rapidly, suggesting that the K23_I24insIDK mutant exhibits markedly increased autoactivation. Indeed, when autoactivation of wild-type and mutant trypsinogens were compared in a quantitative manner (pH 8.0, 37 ^{o}C), the mutant autoactivated at rates that were >10-fold higher relative to wild-type trypsinogen (Figure 6).

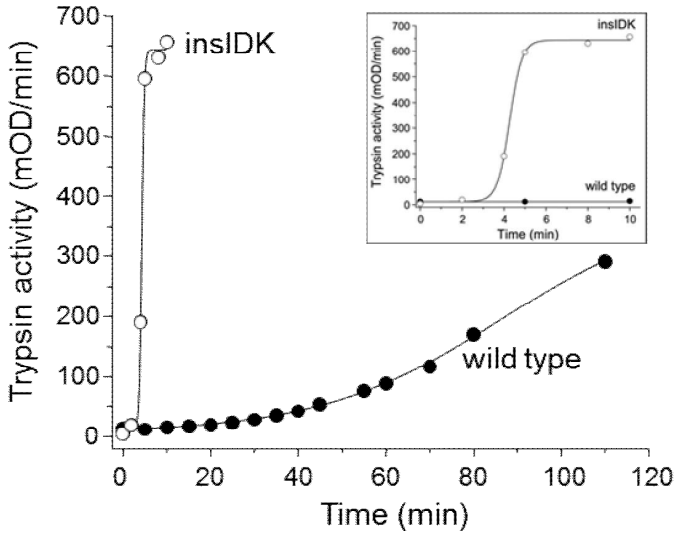

Figure 6. Effect of the K23_I24insIDK mutation on the activation of human cationic trypsinogen by trypsin (autoactivation). Trypsinogens at 2 µM concentration were incubated with 40 nM human cationic trypsin (initial concentration) at 37 ^{o}C in 0.1 M Tris-HCl (pH 8.0), 1 mM $CaCl_2$, and 40 mM NaCl (final concentrations) in 100 µL final volume. Aliquots (2 µL) were withdrawn at indicated times and trypsin activity was determined. Trypsin activity was expressed as percentage of the maximal activity.

The catalytic mechanism of trypsin requires an intact catalytic triad which is composed of a serine, histidine and aspartic acid residues [48]. Elimination of these amino acids would result in a protein which does not have enzymatic activity. Therefore, to characterize the autoactivation kinetics in a more precise manner, we generated catalytically inactive versions of wild-type and mutant trypsinogens by mutation of Ser200 to Ala (S200A). The use of the S200A-trypsinogens allowed us to measure exact rates of trypsin-mediated trypsinogen activation by controlling the trypsin concentration in the reactions. Because activation of S200A-trypsinogen does not result in enzymatic activity, the activation reactions were followed by the mobility shift on SDS-PAGE. For comparison, in these experiments we included the D22G mutant as a previously well-characterized example of the activation peptide mutants [25,27,31]. As shown in Figure 7, 100 nM human cationic trypsin converted the 2 µM S200A (wild-type) trypsinogen to

trypsin at a very low rate and appreciable trypsin levels were seen only after 60 min incubation (pH 8.0, 37 °C). In contrast, K23_I24insIDK/S200A trypsinogen was completely activated to trypsin within 30 min, whereas complete conversion of the D22G/S200A mutant took about 60 min. Thus, as judged from the half-lives of S200A trypsinogens, the rate of trypsin-mediated trypsinogen activation is>10-fold higher for both the K23_I24insIDK and D22G mutants, relative to wild-type trypsinogen. These data are in agreement with the activity based assay using catalytically competent trypsinogens, as shown in (Figure 6).

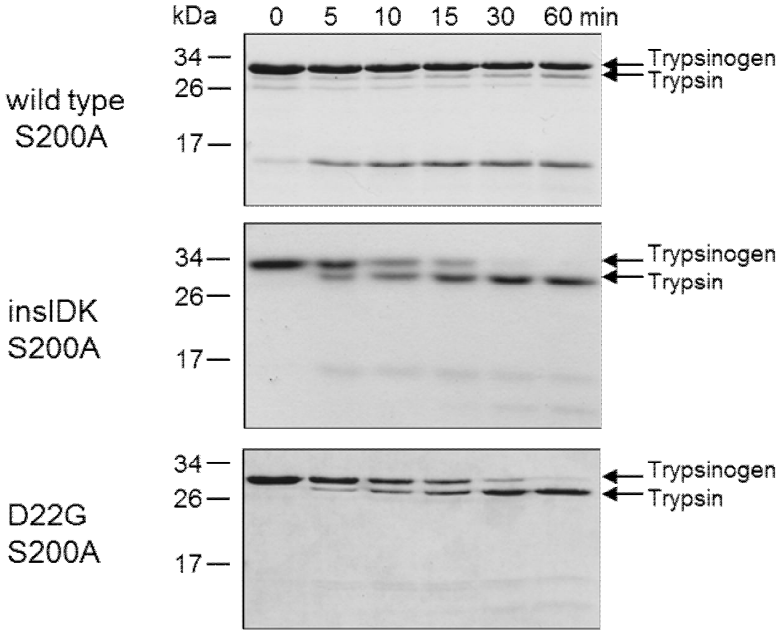

Figure 7. Effect of the K23_I24insIDK mutation on the activation of human cationic trypsinogen by trypsin (autoactivation). Trypsinogens carrying the S200A mutation were incubated with 100 nM human cationic trypsin at 37 °C in 0.1 M Tris-HCl (pH 8.0) and 1 mM $CaCl_2$ in 100 µL final volume. At the indicated times, reactions were precipitated with 10% trichloroacetic acid (final concentration) and analyzed by 15% SDS-PAGE and Coomassie Blue staining. The lower molecular weight bands represent double-chain forms of trypsinogen and trypsin cleaved at the Arg122-Val123 peptide bond. insIDK = K23_I24insIDK.

4.4.2 Enteropeptidase mediated activation

Owing to the robust autoactivation of the K23_I24insIDK mutant, we were unable to measure enteropeptidase-mediated trypsinogen activation using the catalytically active proteins. Therefore, we monitored enteropeptidase-mediated activation of the S200A-trypsinogens on SDS-PAGE. Figure 8 demonstrates that activation of the K23_I24insIDK and D22G mutants were comparable to that of wild-type (pH 8.0, 37 °C). The results are in accord with our previous studies showing that the TAP plays no significant role in the recognition of human cationic trypsinogen by human enteropeptidase.

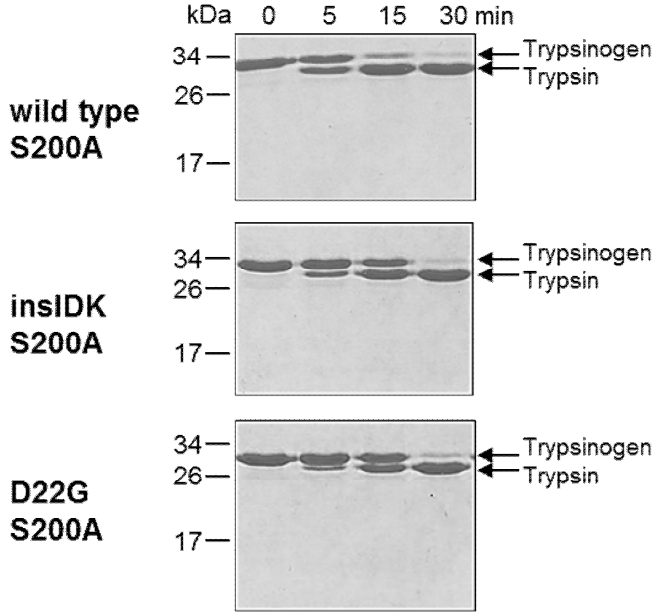

Figure 8. Effect of the K23_I24insIDK mutation on the activation of human cationic trypsinogen with enteropeptidase. Trypsinogens carrying the S200A mutation were activated with human enteropeptidase (28 ng/mL final concentration) at 37 °C in 0.1 M Tris-HCl (pH 8.0) and 1 mM $CaCl_2$ in 100 µL final volume. At the indicated times, reactions were precipitated with 10% trichloroacetic acid (final concentration) and analyzed by 15% SDS-PAGE and Coomassie Blue staining. insIDK = K23_I24insIDK.

This finding is somewhat surprising, as the tetra-Asp motif in the TAP has been known as a specific recognition motif for enteropeptidase, at least in the context of the bovine enzymes [28].

4.4.3 Cathepsin B mediated activation

The lysosomal cysteine protease cathepsin B has been recognized as a pathological activator of trypsinogen in models of experimental acute pancreatitis [49,50,51,52]. We tested the effect of the K23_I24insIDK mutation on cathepsin B-mediated trypsinogen activation at pH 4.0, where autoactivation is minimal. Remarkably, the mutant was activated by cathepsin B at a markedly elevated rate, which seemed approximately 5-10-fold higher than that of wild-type (Figure 9).

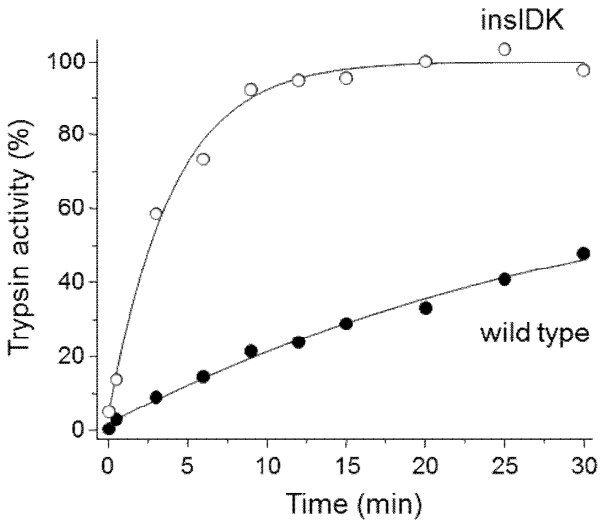

Figure 9. Effect of the p.K23_I24insIDK mutation on the activation of human cationic trypsinogen with cathepsin B. Trypsinogens at 2 µM concentration were activated with human cathepsin B (37 µg/mL, ~1.3 µM) at 37 °C in 0.1 M Na-acetate buffer (pH 4.0), 1 mM K-EDTA and 1 mM dithiothreitol (final concentrations) in 50 µL final volume. Aliquots (2 µL) were withdrawn at indicated times and trypsin activity was determined. Trypsin activity was expressed as percentage of the maximal activity.

Using S200A-trypsinogens, we measured the rates of conversion in a more precise manner and found that the K23_I24insIDK mutant was activated by cathepsin B 10-fold faster than wild-type cationic trypsinogen (Figure 10). As described previously, mutant D22G was resistant to cathepsin B mediated activation [27,53]. More recently, cathepsin L was shown to degrade trypsinogen and active trypsin accumulation during pancreatitis was attributed not only to cathepsin B-mediated activation but also to a defect in cathepsin L-mediated degradation [54,55]. We found no change in the degradation of the K23_I24insIDK mutant by cathepsin L (pH 4.0, 37 °C) as compared to wild-type cationic trypsinogen (data not shown).

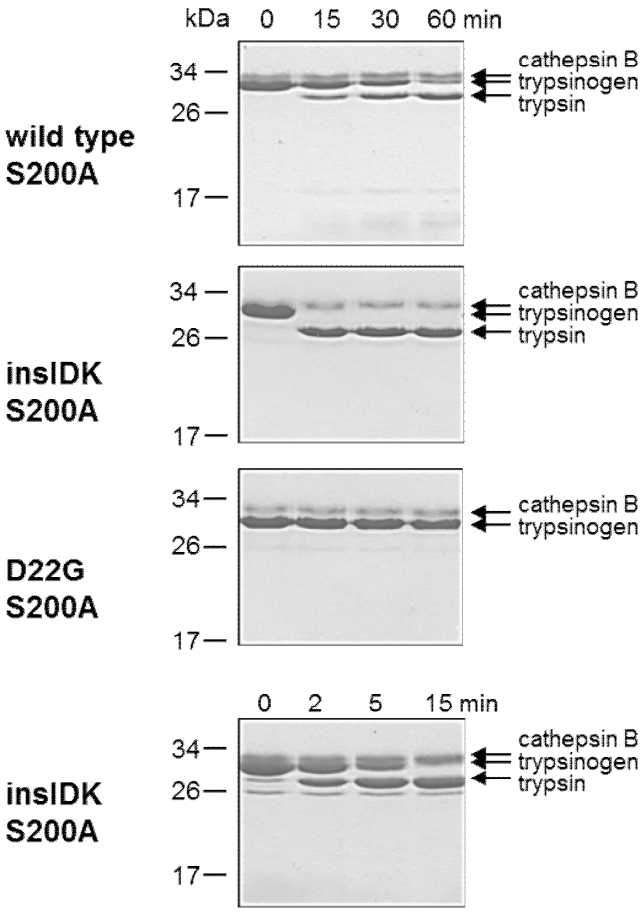

Figure 10. Effect of the K23_I24insIDK mutation on the activation of human cationic trypsinogen with cathepsin B. Trypsinogens carrying the p.S200A mutation were activated with human cathepsin B (37 µg/mL, ~1.3 µM; 74 µg/mL, ~2.6 µM for p.D22G) at 37 °C in 0.1 M Na-acetate buffer (pH 4.0) 1 mM K-EDTA and 1 mM dithiothreitol in 100 µL final volume. At the indicated times, reactions were precipitated with 10% trichloroacetic acid (final concentration) and analyzed by 15% SDS-PAGE and Coomassie Blue staining. p.insIDK = K23_I24insIDK.

4.5 Cleavage of the activation peptide in the K23_I24insIDK mutant cationic trypsinogen

The mutant activation peptide sequence contains two Lys-Ile peptides bonds (Figure 5). Although activation of trypsinogen to trypsin requires proteolysis of the second site, cleavage after the first Lys may modify the efficiency of the second cleavage. Therefore, we sought to clarify whether both sites were cleaved. For these experiments we used the S200A-trypsinogens which we activated with trypsin (pH 8.0), enteropeptidase (pH 8.0) and cathepsin B (pH 4.0). The activation reactions were separated on SDS-PAGE, transferred to PVDF membranes and trypsin bands were subjected to N-terminal sequence analysis by Edman-degradation. To capture cleavage intermediates, we sequenced trypsin bands early in the reaction when less than half of the trypsinogen was converted to a trypsin band. We found that trypsin and cathepsin B cleaved the second (activating) Lys-Ile peptide bond only, whereas enteropeptidase cleaved both Lys-Ile peptide bonds with equal efficacy. Cleavage after the first Lys-Ile peptide bond resulted in an N-terminally truncated trypsinogen, which was eventually completely cleaved at the second Lys-Ile peptide bond by enteropeptidase (Figure 11).

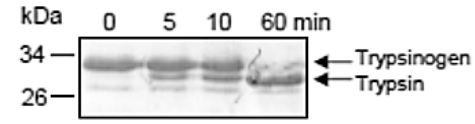

APFDDDDK**IDK**IVGGY

10 min	IDKIV	~60%
	IVGGY	~40%
60 min	IVGGY	100%

Figure 11. N-terminal sequencing of the K23_I24insIDK, S200A mutant activated with enteropeptidase. Activation was performed with human enteropeptidase (28 ng/mL final concentration) at 37 °C in 0.1 M Tris-HCl (pH 8.0) and 1mM $CaCl_2$ in 100 µL final volume. At the indicated times reactions were precipitated with 10% trichloroacetic acid (final concentration) and samples were electrophoresed on 15% SDS-PAGE. Proteins were transferred to Immobilon-P PVDF membrane and stained with Coomassie Blue for 5 min followed by destaining with 50% methanol. The trypsin bands at 10 min and 60 min were sequenced by Edman degradation chemistry and the determined N-terminal 5 amino-acids are indicated. The N-terminal sequence of K23_I24insIDK trypsinogen including the first 5 residues of trypsin is indicated as reference.

4.6 Autoactivation of hereditary pancreatitis associated activation peptide mutants in the absence and presence of chymotrypsin C

In addition to the newly identified K23_I24insIDK *PRSS1* mutation, we aimed to analyze the autoactivation of previously characterized variants affecting the TAP (Table 1). While mutations D19A, D22G and K23R were caused by missense point mutations, the K23_I24insIDK variant was induced by an intragenic duplication in the exon2 of the *PRSS1* gene.

Studies focusing on mutations in human cationic trypsinogen have demonstrated that changes in the autoactivation may result in an increased risk for CP. A number of recent investigations revealed that cationic trypsinogen and trypsin are under the regulation of CTRC which draws the conclusion that pancreatitis associated mutants may exert their effect in a CTRC dependent manner [34,56]. To find out whether increased autoactivation is caused directly by mutational impact or influenced by the regulatory effect of CTRC we investigated the autoactivation properties of TAP mutations. Autoactivation of human cationic trypsinogen in the presence of 25 nM CTRC results in a slight increase in the rate accompanied by a marked reduction in final trypsin levels attained (Figure 12). The increased rate is due to N-terminal processing of the activation peptide by CTRC, whereas the reduced trypsin levels are a consequence of CTRC-dependent trypsinogen degradation. Recently, we demonstrated that mutations commonly associated with hereditary pancreatitis exert their effect primarily in the presence of CTRC. A typical case is shown for the most frequent R122H mutation in Figure 12, which in the absence of CTRC increases autoactivation only slightly (1.2-fold). In the presence of CTRC, however, autoactivation of wild-type trypsinogen is drastically suppressed, while mutant R122H autoactivates at an increased rate and reaches high trypsin levels.

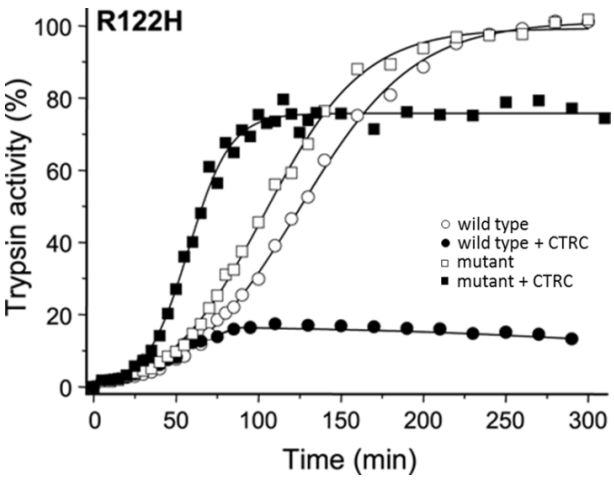

Figure 12. Autoactivation of wild type and R122H mutant human cationic trypsinogen in the absence and presence of chymotrypsin C (CTRC). Wild-type (circles) and mutant (squares) trypsinogen were incubated at 1 µM with 10 nM initial trypsin in 0.1 M Tris-HCl (pH 8.0), 1 mM $CaCl_2$, 100 mM NaCl and 0.05% Tween 20, at 37 °C, in the absence (empty symbols) or presence (solid symbols) of 25 nM CTRC (final concentrations). Aliquots (2 µL) were withdrawn at the indicated times and trypsin activity was determined as described in *Experimental Procedures*. Trypsin activity was expressed as percentage of the maximal activity in the absence of CTRC. Representative experiments from two replicates are shown.

When mutants D19A, D22G, K23R and K23_I24insIDK were tested under similar conditions, a markedly different phenotype became apparent (Figure 13). All four mutations increased the rate of trypsinogen autoactivation robustly (3.9-fold, 9.2-fold, 5.7-fold and 17.5-fold, respectively) even in the absence of CTRC, in agreement with previous observations [25]. Similarly, in the presence of CTRC, all four mutants autoactivated markedly faster than wild-type trypsinogen and reached much higher trypsin levels, which then slowly decreased due to CTRC-mediated trypsin degradation. Peak trypsin levels correlated with the rate of autoactivation and were higher in mutants D22G and K23_I24insIDK versus D19A and K23R. Surprisingly, even in the presence of CTRC, TAP mutants autoactivated much faster than the reference mutant R122H. Thus, the estimated rates of autoactivation for mutants D19A, D22G, K23R and K23_I24insIDK were approximately 3-fold, 10-fold, 3-fold and 10-fold higher than that of mutant R122H, in the presence of CTRC.

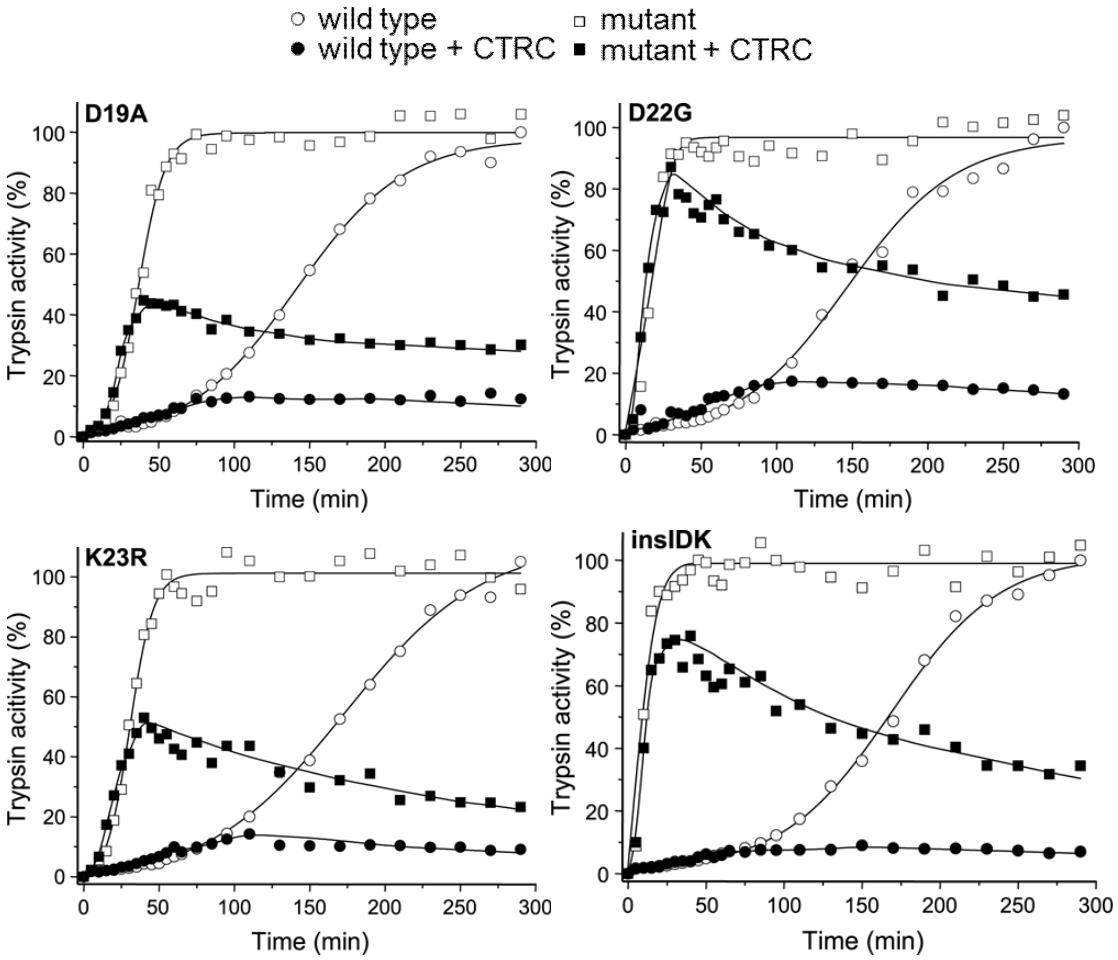

Figure 13. Autoactivation of human cationic trypsinogen and activation peptide mutants in the absence and presence of chymotrypsin C (CTRC). Wild-type (circles) and mutant (squares)

trypsinogens were incubated at 1 µM with 10 nM initial trypsin in 0.1 M Tris-HCl (pH 8.0), 1 mM $CaCl_2$, 100 mM NaCl and 0.05% Tween 20, at 37 °C, in the absence (empty symbols) or presence (solid symbols) of 25 nM CTRC (final concentrations). Aliquots (2 µL) were withdrawn at the indicated times and trypsin activity was determined as described in *Experimental Procedures*. Trypsin activity was expressed as percentage of the maximal activity in the absence of CTRC. Representative experiments from two replicates are shown. Mutant K23R_I24insIDK is denoted as insIDK.

4.7 Chymotrypsin C mediated degradation: Cleavage of the Leu81-Glu82 peptide bond in the activation peptide mutants

Mutation caused defect in the CTRC-dependent degradation during autoactivation can be crucial in the trypsin activity regulation. Because the activation peptide is not in the proximity of the calcium binding loop, mutations D19A, D22G, K23R and K23_I24insIDK are unlikely to affect CTRC-mediated trypsinogen degradation. We tested this assumption experimentally and found that cleavage of the Leu81-Glu82 peptide bond by CTRC was unchanged in the activation peptide mutants compared to wild-type cationic trypsinogen (Figure 14).

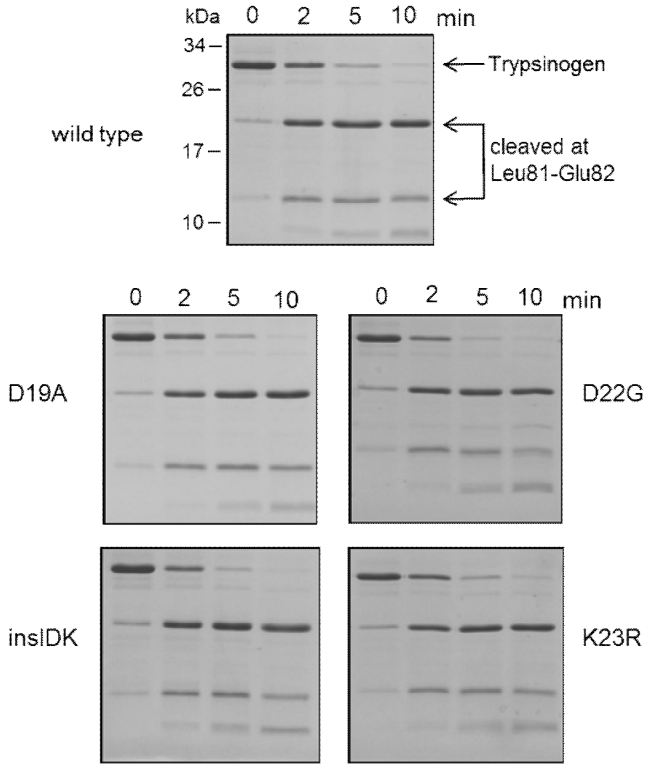

Figure 14. Cleavage of Leu81-Glu82 peptide bond in human cationic trypsinogen and activation peptide mutants by chymotrypsin C (CTRC). Wild-type and mutant trypsinogen were incubated at 2 µM with 20 nM CTRC in 0.1M Tris-HCl (pH 8.0) (final concentrations), at 37 °C. Trypsinogens also contained the S200A mutation to prevent autoactivation. At the indicated times reactions were terminated by precipitation with 10% trichloroacetic acid (final concentration) and analyzed by 15% reducing SDS-PAGE and Coomassie Blue staining. Representative gels of two or three experiments are shown.

The densitometric evaluation of SDS-PAGE analysis confirmed that the CTRC-mediated degradation of wild-type and acivation peptide mutant trypsinogens were comparable (Figure 15).

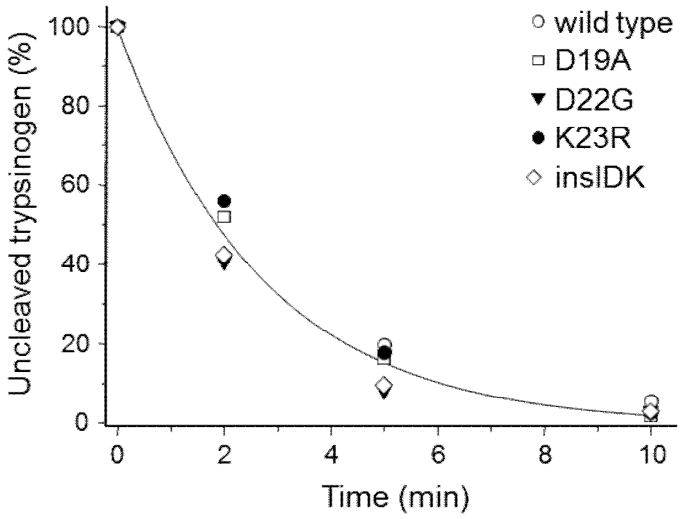

Figure 15. Cleavage of Leu81-Glu82 peptide bond in human cationic trypsinogen and activation peptide mutants by chymotrypsin C (CTRC). Densitometric analysis of stained gels showing the changes in the intensity of the unprocessed, intact trypsinogen band. Error bars were omitted for clarity, the error was within 10% of the mean. Mutant K23_I24insIDK is denoted as insIDK.

4.8 Elevated autoactivation by chymotrypsin C: N-terminal processing of activation peptide mutants

CTRC cleaves the Phe18-Asp19 peptide bond in the TAP and removes three amino acids from the N terminus (Figure 1). This, in turn, results in increased autoactivation of cationic trypsinogen. The N-terminal truncation of the activation peptide is readily detectable by non-reducing SDS-PAGE as a small mobility shift. To assess whether the activation peptide mutations altered CTRC-mediated N-terminal processing, we incubated wild-type and mutant trypsinogens with 50 nM CTRC at pH 8.0, in 1 mM $CaCl_2$, to minimize cleavage after Leu81. To prevent autoactivation during the incubation, we used an inactive trypsinogen background in which the catalytic Ser200 was changed to Ala (S200A). Figures 16 A and B demonstrate that mutant D19A exhibited 4-fold increased N-terminal processing, whereas mutants D22G, K23R and K23_I24insIDK were processed at rates comparable with wild type. Inspection of the early time points of the autoactivation curves in the presence of CTRC (see Figure 13, compare black with white symbols) reveals that N-terminal processing by CTRC increases the rate of autoactivation for mutants D19A, D22G and K23R. Surprisingly, the enhanced processing of mutant D19A did not translate to a more robust autoactivation increase than seen in mutants D22G or K23R (Figure 13). Similarly, even though mutant

K23_I24insIDK was processed normally, this modification had no impact on autoactivation.

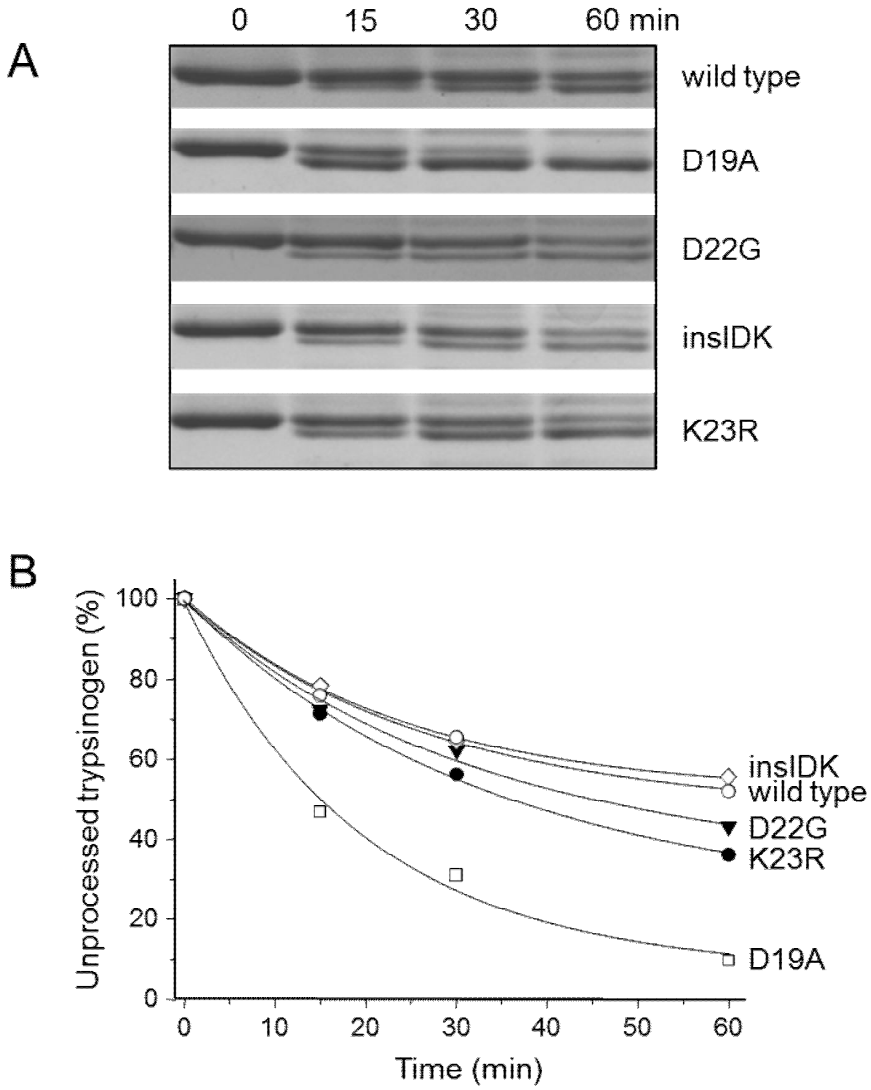

Figure 16. N-terminal processing of human cationic trypsinogen and activation peptide mutants by chymotrypsin C (CTRC).***A***, Wild-type and mutant trypsinogen were incubated at 2 µM with 50 nM CTRC in 0.1 M Tris-HCl (pH 8.0), 1 mM $CaCl_2$ and 100 mM NaCl (final concentrations), at 37 °C. Trypsinogens also contained the S200A mutation to prevent autoactivation. At the indicated times reactions were terminated by precipitation with 10% trichloroacetic acid (final concentration) and samples were analyzed by 15% non-reducing SDS-PAGE and Coomassie Blue staining. Relevant segments of representative gels demonstrate the small mobility shift of the trypsinogen band caused by CTRC-mediated cleavage of the activation peptide. ***B***, Densitometric analysis of stained gels showing the changes in the intensity of the unprocessed, intact trypsinogen band as a percentage of the total intensity of the processed and unprocessed bands.

CTRC-mediated cleavage of the Phe18-Asp19 peptide bond in the TAP is highly specific and other human chymotrypsins (CTRB1, CTRB2, CTRL1) and elastases (ELA2A, ELA3A, ELA3B) do not catalyze this reaction (Figure 17). We considered the

possibility that activation peptide mutations might allow for cleavages by proteases other than CTRC, however, this was not the case. None of the mutant activation peptides was cleaved by any of the chymotrypsins or elastases tested in Figure 17 (data not shown).

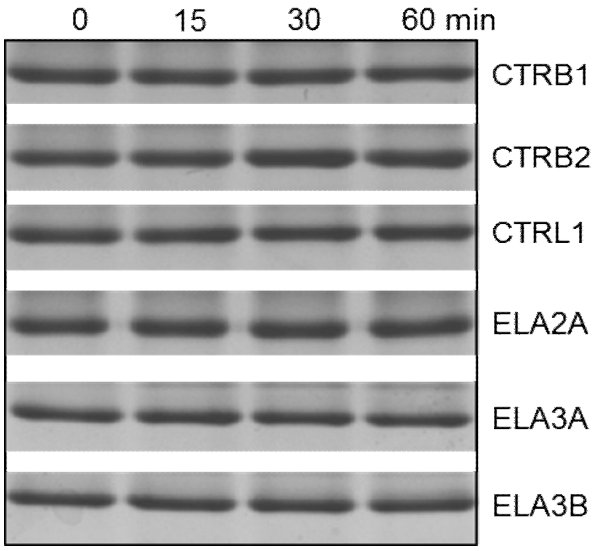

Figure 17. N-terminal processing of the activation peptide is specific for CTRC. Wild-type and mutant trypsinogens were incubated with 50 nM of the indicated human pancreatic chymotrypsins and elastases and reactions were analyzed as described above. For clarity, only the wild-type dataset is shown; none of the mutants was cleaved by any of the proteases tested. Mutant K23R_I24insIDK is denoted as insIDK.

4.9 Effect of the activation peptide mutations on calcium binding

The tetra-Asp motif in the TAP binds Ca^{2+}, which stimulates autoactivation in a concentration-dependent manner. To determine the effect of the activation peptide mutations on the calcium binding affinity of the activation peptide, we measured the rate of N-terminal processing by CTRC as a function of increasing calcium concentrations. For these experiments we used trypsinogen constructs carrying the L81A and S200A mutations to prevent unwanted cleavage at Leu81 by CTRC and to avoid trypsinogen autoactivation during incubations. As shown in Figure 18, calcium inhibited cleavage of the Phe18-Asp19 peptide bond by CTRC in wild-type cationic trypsinogen with a K_D value around 1.9 mM. Calcium dependence of N-terminal processing by CTRC was comparable for the activation peptide mutants. The calculated K_D values for mutants D19A, D22G, K23R and K23_I24insIDK were 1.1 mM, 1.3 mM, 2.6 mM and 1.3 mM, respectively. Inspection of Figure 18B suggests that these values fall within the experimental error of the method. When the entire dataset including wild-type and mutants was fit with a single curve a K_D of 1.6±0.2 mM was obtained. We conclude that calcium binding to the activation peptide is not affected by the activation peptide mutations.

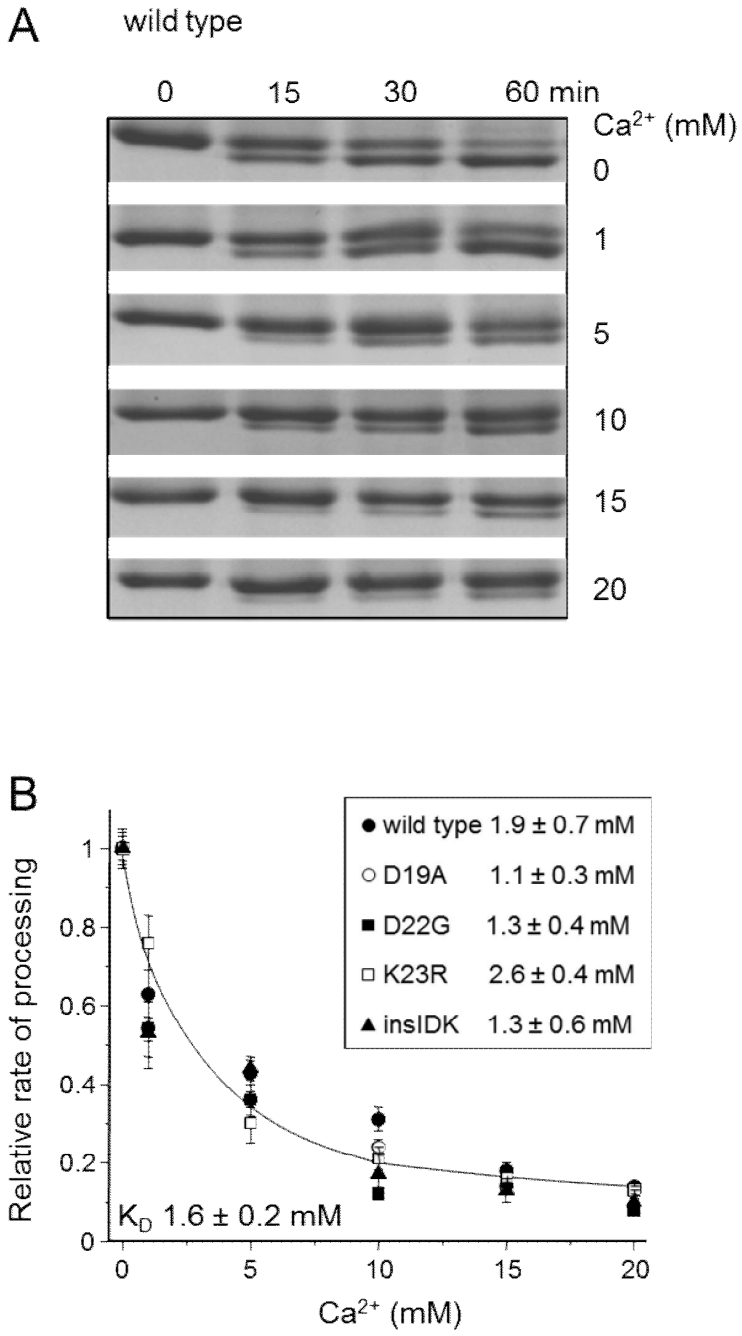

Figure 18. Effect of calcium on the N-terminal processing of the trypsinogen activation peptide by chymotrypsin C (CTRC). ***A,*** Wild-type and mutant trypsinogen were incubated at 2 µM with 50 nM CTRC in 0.1 M Tris-HCl (pH 8.0) and 100 mM NaCl in the absence or presence of $CaCl_2$ (Ca^{2+}) at the indicated concentrations, at 37 °C. Trypsinogens also contained the S200A mutation to prevent autoactivation and the L81A mutation to prevent CTRC cleavage after Leu81 in the absence of calcium. At the indicated times reactions were terminated and analyzed as described in Figure 19A. As an example, the relevant gel segments for wild-type are shown. Similar gel sets were generated for all mutants and used to determine reaction rates, as described below. ***B,*** Densitometric analysis was performed as given in Figure 18B. Rates of processing were calculated from linear fits to semilogarithmic graphs and plotted as a function of the calcium concentration with errors of the fits also shown. The equilibrium binding constants (KD) for calcium were calculated from fits to the $y = y(min)+[y(max)-y(min)] / 1+[Ca^{2+}]/KD$ equation where y is the measured reaction rate, y(max) is the maximal reaction rate in the absence of calcium and y(min) is the residual reaction rate under fully saturating calcium concentrations. The error of the fits is also indicated. Mutant K23R_I24insIDK is denoted as insIDK.

4.10 Effect of calcium on autoactivation of the activation peptide mutants

Calcium binding to the tetra-Asp motif in the TAP stimulates autoactivation. Even though the activation peptide mutations appear to bind calcium normally, the effect of calcium on autoactivation may be altered.

When autoactivation of wild-type and mutant trypsinogens were measured in the presence of 0, 1, 5 and 10 mM calcium, wild-type trypsinogen and mutants D19A and K23R were stimulated in a concentration dependent manner, whereas autoactivation of

mutants D22G and K23R_I24insIDK was insensitive to calcium (Figure 19). Although the half-maximal stimulatory calcium concentration was difficult to determine due to the confounding effect of degradation in the absence of calcium, it appeared that calcium dependence of autoactivation of wild-type, D19A and K23R trypsinogens was consistent with the K_D values obtained for binding of calcium to the activation peptide. The effect of calcium on the autoactivation of mutant D19A seemed to saturate at a lower concentration when compared to mutant K23R, which might reflect a true but small difference in binding affinity (see K_D values above). The observations indicate that activation peptide mutations do not affect binding of calcium to the activation peptide but may diminish the functional effect of calcium binding.

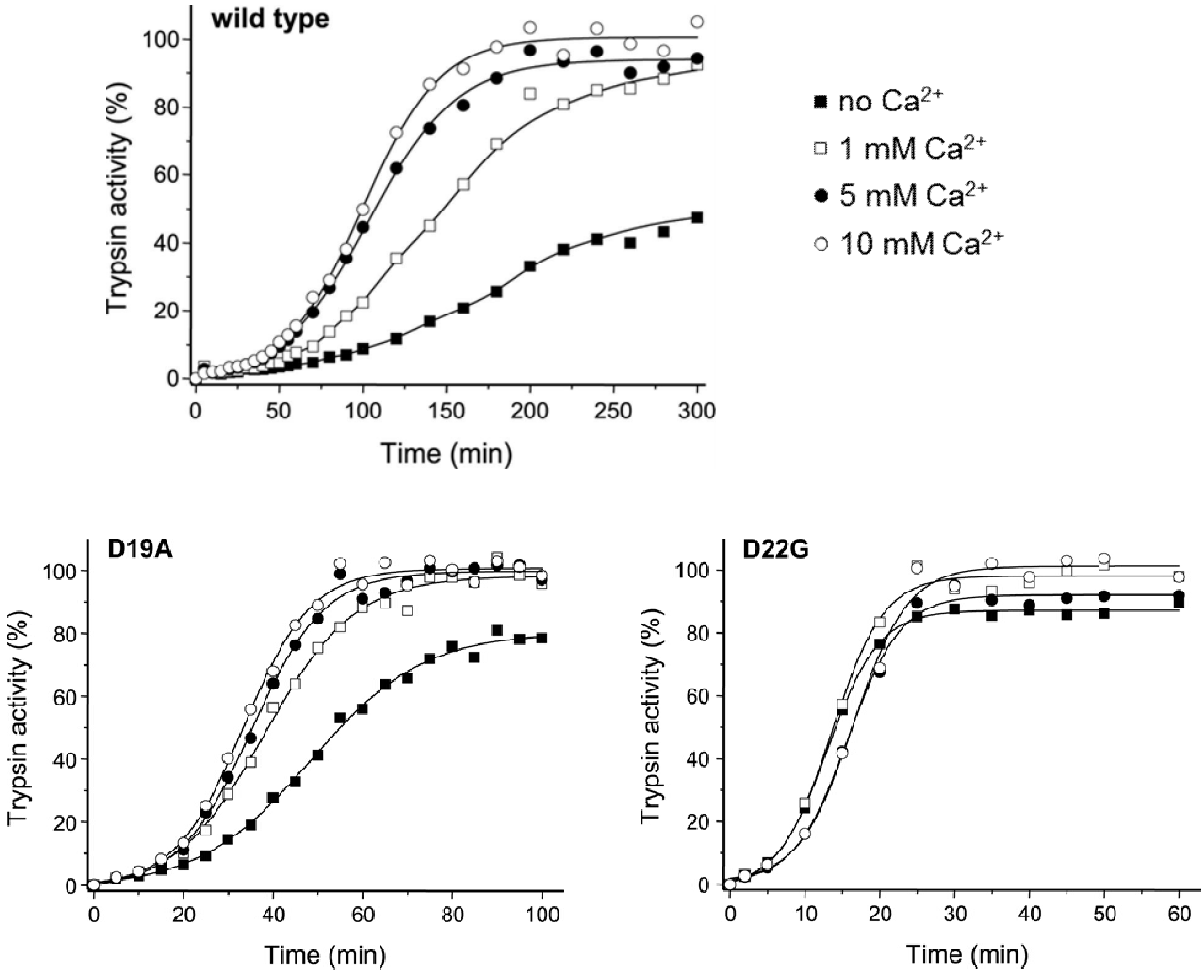

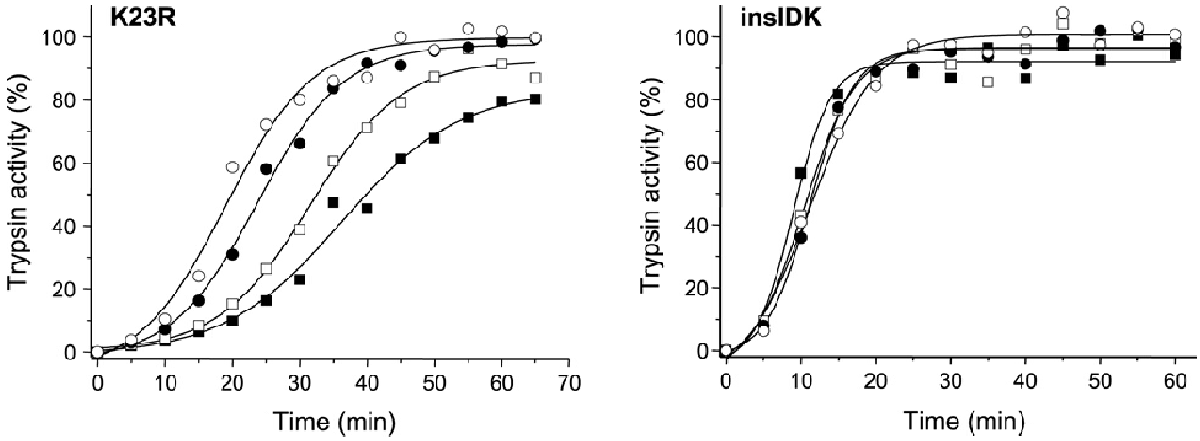

Figure 19. Effect of calcium on the autoactivation of human cationic trypsinogen and activation peptide mutants. Wild-type and mutant trypsinogen were incubated at 1 µM with 10 nM initial trypsin in 0.1 M Tris-HCl (pH 8.0), 100 mM NaCl, and 0.05% Tween 20, at 37 °C, in the absence or presence of $CaCl_2$ (Ca^{2+}) at the indicated concentrations. At given times 2 µL aliquots were removed and trypsin activity was determined as described in *Experimental Procedures*. Trypsin activity was expressed as percentage of the maximal activity in the presence of 10 mM $CaCl_2$. Mutant K23_I24insIDK is denoted as insIDK.

4.11 Secretion of trypsinogen activation peptide mutants from transiently transfected HEK 293T cells

4.11.1 Secretion of the K23_I24insIDK mutant

The biochemical properties of the activation peptide mutants described so far suggest that these mutations should be associated with a more severe clinical phenotype than mutation R122H. However, this is not the case. Recently, we demonstrated that activation peptide mutants that undergo robust autoactivation in the test tube were also autoactivating inside living cells [27]. Intracellular autoactivation resulted in diminished trypsinogen secretion and eventual cell death of acinar cells. To test whether or not secretion of the strongly autoactivating K23_I24insIDK mutant would be reduced, we transfected HEK 293T cells with wild-type and K23_I24insIDK mutant cationic trypsinogen and measured secretion of trypsinogens from the conditioned medium by activity assays and immunoblot. As shown in Figure 20, mutantK23_I24insIDK was secreted to significantly lower levels than wild-type cationic trypsinogen, indicating that the K23_I24insIDK mutant suffered intracellular autoactivation.

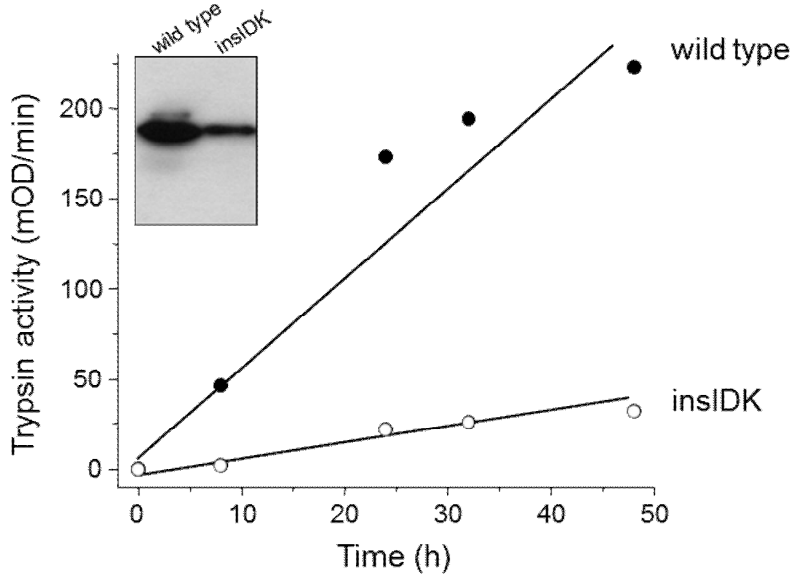

Figure 20. Secretion of the p.K23_I24insIDK cationic trypsinogen mutant from transiently transfected HEK 293T cells. At 8, 24, 32 and 48 hours after transfection conditioned media were collected and 20 µL medium was supplemented with 0.1 M Tris-HCl (pH 8.0) and 1 mM $CaCl_2$ to 50 µL volume and trypsinogen was activated with 28 ng/mL human enteropeptidase for 1 h at 37 ^{o}C. Trypsin activity was then measured by adding 150 µL of the chromogenic substrate, *N*-benzyloxycarbonyl-Gly-Pro-Arg-*p*-nitroanilide to 0.14 mM final concentration. Trypsin activities were expressed as percent of the 48 h wild-type activity. The average of 2 independent transfection experiments is shown. For clarity, the error bars have been omitted; the standard error of the mean was within 15%. Inset: Eight hours after transfection 20 µL aliquots of conditioned media were electrophoresed on 15% SDS-polyacrylamide gels and analyzed by western blotting as described in *Experimental Procedures*.

4.11.2 Secretion of all four activation peptide mutants

We previously found that secretion of activation peptide mutants from transfected cells was reduced, although the four mutants have never been studied in a comparative manner within the same experiment. To establish whether this secretion defect might be a mechanism that partly offsets the drastically increased autoactivation, we quantified secretion of wild-type and mutant trypsinogens from transiently transfected HEK 293T cells. For these experiments we used a short time course (12 h) to prevent autoactivation in the medium and consequent trypsinization of the cells. We measured trypsin activity in the conditioned media after enteropeptidase-mediated activation (Figure 21A) and trypsinogen levels by western blotting (Figure 21B). We found that the activation peptide mutants were secreted at significantly lower levels than wild-type trypsinogen, in agreement with previous observations. Importantly, secretion rates for the mutants were inversely proportional with their ability to autoactivate (D19A>K23R>D22G ≈K23_I24insIDK).

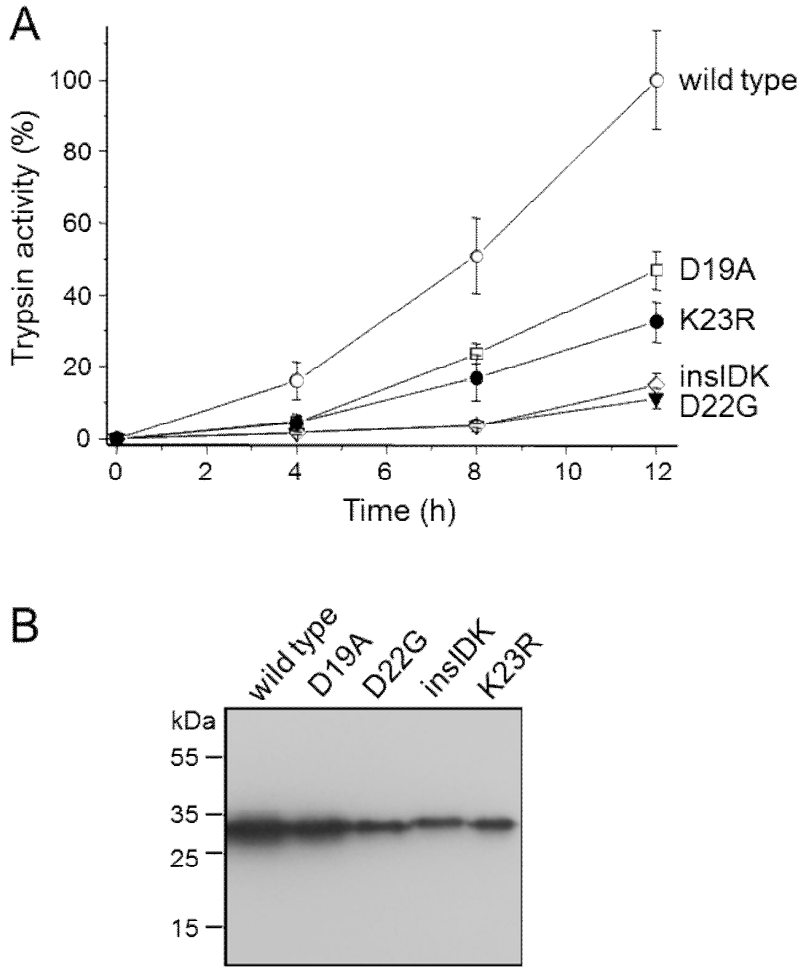

Figure 21. Secretion of human cationic trypsinogen and activation peptide mutants from transiently transfected HEK 293T cells. Trypsinogen expression constructs also contained the K237D and N241D mutations which improve secretion from transfected cells. ***A***, At 4, 8 and 12 hours after transfection conditioned media were collected and trypsin activity was measured as described under *Experimental Procedures*. Trypsin activity was expressed as percentage of the 12 h wild-type activity. The average of three independent transfection experiments with standard deviation is shown. ***B***, Aliquots (20 µL) of conditioned media collected at 12 h were electrophoresed on 15% SDS-polyacrylamide gels and analyzed by western blotting, as described in *Experimental Procedures*. A representative blot of three is shown. Mutant K23R_I24insIDK is denoted as insIDK.

5 DISCUSSION

There are a number of important observations in this study which set it apart from a typical mutation account.

We reported first an intragenic duplication within the *PRSS1* gene in association with HCP. The human trypsinogen genes are located on chromosome 7q35, intercalated between the beta T-cell receptor genes; at a locus highly active in recombination. This organization seems beneficial for the evolution of trypsinogens which tend to undergo extensive gene-duplication and gene-loss events during speciation resulting in distinctive trypsinogen gene families [25,57]. On the other hand, unwanted genetic rearrangements -- such as gene-conversions, duplications or triplications -- can result in novel pathogenic alleles in hereditary pancreatitis [36,45,46,47,57,58]. In contrast to the previously reported large-scale gene duplications, in our family the duplication was confined only to a nine-nucleotide segment within exon 2 without any evidence of more extensive genetic changes. Interestingly, the duplication was identified only in the father and his two sons (Figure 3), while it was absent in the grandparents or in the father's siblings, indicating that it was *de novo* generated in the father. Ours is the second report on capturing a mutational event leading to hereditary pancreatitis. Simon *et al.* (2002) found a *de novo* R122H mutation in their cohort and their subsequent studies indicated that *PRSS1* mutations are characteristically not inherited from a common founder, even when local clustering of families is observed [59,60].

Intragenic duplications are likely to result in a frame shift and truncated, non-functional protein. In this case, however, the reading frame was kept and at the amino-acid level the duplication generated an insertion within the TAP (Figure 5). As expected from this alteration, the activation properties of cationic trypsinogen have been affected in profound ways. Trypsin-mediated trypsinogen activation (autoactivation) and cathepsin B-mediated trypsinogen activation were both increased by an order-of-magnitude; an effect size never before seen with the known *PRSS1* mutants. With respect to autoactivation, the K23_I24insIDK mutant's phenotype is consistent with the reported properties of other *PRSS1* mutations affecting the activation peptide (D19A, D22G, and K23R), which all result in markedly increased autoactivation [25,26,27,31]. Mechanistically, the increased autoactivation of K23_I24insIDK is explained by the disruption of inhibitory interactions between the negatively charged tetra-Asp motif in the activation

peptide and trypsin [26]. In the K23_I24insIDK mutant Asp21 is replaced with a hydrophobic Ile residue and Asp20 by a positively charged Lys (Figure 5).

Cathepsin B has long been known as a pathological activator of trypsinogen in experimental models of acute pancreatitis, cerulein-induced pancreatitis in particular [49,50,51,52]. The effect of hereditary pancreatitis-associated mutations on cathepsin B-mediated trypsinogen activation has been studied in detail previously. Mutants D19A, N29I, N29T, E79K and R122H exhibited unchanged activation characteristics; whereas mutant K23R was activated slowly, and mutant D22G was resistant to activation by cathepsin B [27,51,52,61]. MutantK23_I24insIDK is the first cationic trypsinogen variant that exhibits increased sensitivity to cathepsin B-mediated activation and thus stands in contrast with all other PRSS1 mutants studied to date. We believe this property is related to the longer activation peptide which allows extended contacts with the activating enzyme.

Another important objective of the present study was to investigate the effect of CTRC on the autoactivation of trypsinogen activation peptide mutants D19A, D22G, K23R and K23_I24insIDK found in hereditary pancreatitis. Previously, we demonstrated that wild-type cationic trypsinogen is largely degraded by CTRC during autoactivation, whereas hereditary pancreatitis associated mutants N29I, N29T, V39A, R122C and R122H exhibited resistance to CTRC-mediated degradation and autoactivated to higher trypsin levels. In addition, we found that mutations A16V and N29I increased CTRC-mediated cleavage of the activation peptide, and thereby accelerated autoactivation [34]. We speculated that activation peptide mutants might also affect processing of the activation peptide by CTRC and/or alter the effect of this cleavage, perhaps even resulting in decreased autoactivation. This would then offer an explanation for the puzzling observation that the robust autoactivation of activation peptide mutants is not accompanied by a more severe clinical picture.

Our results confirmed that even in the absence of CTRC activation peptide mutants autoactivated at markedly increased rates (~4-18-fold). In the presence of CTRC, activation rates were further increased slightly (D19A, D22G, K23R) or remained unchanged (K23_I24insIDK), indicating that the robust autoactivation of the activation peptide mutants is mostly independent of CTRC. Peak trypsin levels attained during autoactivation positively correlated with the rate of autoactivation, indicating that faster conversion of trypsinogen to trypsin results in higher trypsin levels, as trypsin is less sensitive to CTRC-mediated degradation than trypsinogen. As expected, the mutations

had no effect on CTRC cleavage of the Leu81-Glu82 peptide bond in the calcium binding loop and consequent trypsinogen degradation. Importantly, when compared to the most common pancreatitis-associated mutant R122H, in the presence of CTRC the activation peptide mutants still exhibited much higher rates of autoactivation (~3-10-fold).

N-terminal processing of the activation peptide at Phe18 by CTRC was unchanged in mutants D22G, K23R and K23_I24insIDK, whereas mutant D19A was processed at 4-fold increased rate. This finding is consistent with recent mutagenesis studies in the calcium binding loop of cationic trypsinogen, which demonstrated that mutation of Glu82 to Ala increased cleavage after Leu81 about 3-fold, indicating that acidic residues at the P1' position hinder cleavage by CTRC. Surprisingly, however, the increased processing of mutant D19A was paralleled only with a slight increase in the rate of autoactivation, suggesting that Asp19 is important for mediating the functional effect of N-terminal processing. Thus, shortening the activation peptide by CTRC may increase autoactivation by partly relieving the inhibitory interaction between Asp218 and Asp19. This effect is probably due to neutralization of the negative charge on Asp19 by the newly created proximity of the positively charged amino terminus. Similarly, mutation D19A would increase autoactivation by neutralizing Asp19 but at the same time it would diminish the effect of N-terminal processing by CTRC. This notion is supported by the observations that the extent of the autoactivation increase either by CTRC processing or by mutation D19A is comparable, approximately 3-4-fold. The stimulatory effect of CTRC cleavage on autoactivation was also abolished in mutant K23_I24insIDK, which may be readily explained by sterical uncoupling of the original tetra-Asp motif from the activation site by the three-amino-acid insertion (Figure 5). Furthermore, previous experiments indicated that trypsin-mediated activation (i.e. autoactivation) of the K23_I24insIDK mutant most likely proceeds by sequential cleavage of the two lysyl peptide bonds found in the mutated activation peptide. In this case, cleavage of the N-terminal Lys-Ile peptide bond would eliminate the N-terminal eight amino acids together with any effect of CTRC-dependent processing.

Calcium in millimolar concentrations stimulates autoactivation presumably by binding to the activation peptide and shielding the inhibitory negative charges of the tetra-Asp motif. Using the CTRC-dependent processing of the activation peptide as readout, we determined the calcium binding affinity of wild-type and mutant activation peptides (Figure 19). Unexpectedly, mutant and wild-type trypsinogens bound calcium at the activation peptide with comparable affinities, 1.6 mM on average. This observation

suggests that calcium probably engages only two or three Asp side chains and elimination of one of the four Asp residues either by mutation D19A or D22G is tolerated. When the functional effect of calcium binding was investigated, however, we found that autoactivation of mutants D22G and K23_I24insIDK were insensitive to calcium. The results suggest that the stimulatory effect calcium on autoactivation is mediated through binding to Asp22 and neutralizing its negative charge. During autoactivation, Asp22 in the activation peptide binds to the S2 subsite on trypsin, a conserved hydrophobic pocket formed by His63, Leu104 and Trp216, and this unfavorable interaction may be alleviated by calcium. In the K23_I24insIDK mutant, calcium likely binds only to the original tetra-Asp motif, which is now further removed from the activation peptide bond. The Asp-Ile-Lys-Asp sequence preceding the activation site does not seem competent to bind calcium. Furthermore, as pointed out above, during autoactivation the N-terminal eight amino acids are removed before cleavage at the activation peptide takes place.

The biochemical properties of the TAP mutants do not explain why the markedly increased autoactivation is not associated with a more severe clinical presentation of hereditary pancreatitis with complete penetrance and early onset. Typical penetrance of hereditary pancreatitis in families with the R122H mutation is 70-90% and the average age of onset is 14 years with a range of 2-20 years. Although clinical data for the rare activation peptide mutations is relatively scant, mutation D22G was also identified in the unaffected 20 year old sister of the index patient, indicating incomplete penetrance. Published ages of diagnosis indicated some early onset (K23_I24insIDK 2 y, D22G 8 y) and some late onset cases (D19A 17 y, K23_I24insIDK 21 y), consistent with typical HCP. Previously, we observed that secretion of activation peptide mutants was compromised from transfected cells due to intracellular autoactivation and ensuing degradation. We extended these studies here and quantitatively compared, for the first time, cellular secretion of all four activation peptide mutants to determine whether reduced secretion could offset the effect of increased autoactivation. Indeed, we confirmed not only that all four activation peptide mutants were secreted at lower levels than wild-type trypsinogen, but also that the secretion defect inversely correlated with the rates of autoactivation. Our observations indicate that nature carefully titrated trypsinogen secretion against autoactivation propensity, to curb the risk for excessive pathological intra-pancreatic trypsinogen activation in carriers of the activation peptide mutations.

Our results define the TAP mutations D19A, D22G, K23R and K23_I24insIDK as a special subset of hereditary-pancreatitis associated mutations which stimulate

autoactivation largely independently of CTRC and this robust effect is compensated by their reduced secretion. Taken together with previous studies, the observations indicate that human cationic trypsinogen mutations may increase autoactivation by several independent but not mutually exclusive mechanisms in HCP (Figure 22): (i) increased secretion, as seen with copy number mutations; (ii) resistance to CTRC-mediated degradation; (iii) increased processing of the activation peptide by CTRC and (iv) direct stimulation of autoactivation, as demonstrated here for the activation peptide mutations.

Despite considerable progress in the field, greater understanding into the underlying mechanisms of disease is much needed. The central role of trypsin is also supported by observations based on protective mechanisms evolved to curtail premature activation of the zymogen. It has been shown that under physiological conditions bicarbonate secretion by pancreatic ductal epithelial cells is not only important for elevating the pH in the duodenum, but also for keeping digestive enzymes in an inactive state. This raises the question whether the decreased pH would contribute in the early trypsin activation. Our research group found that prematurely activated trypsin in the ductal tree inhibits bicarbonate transport leading to a vicious cycle generating a further decrease in pH and enhanced trypsinogen activation, which will favour development of pancreatitis [62].

The complex understanding of inflammatory disorders invokes further insight of other pathomechanistic processes involving the role of ion transporters in the disease development. It has been reported that acid/base transporters have a great impact on cell function and they also may have specific contributions to cancer development [63]. Since individuals with CP have an increased risk for pancreatic cancer -which is still one of the deadliest of human tumors- extending the research towards ion exchangers should be considered.

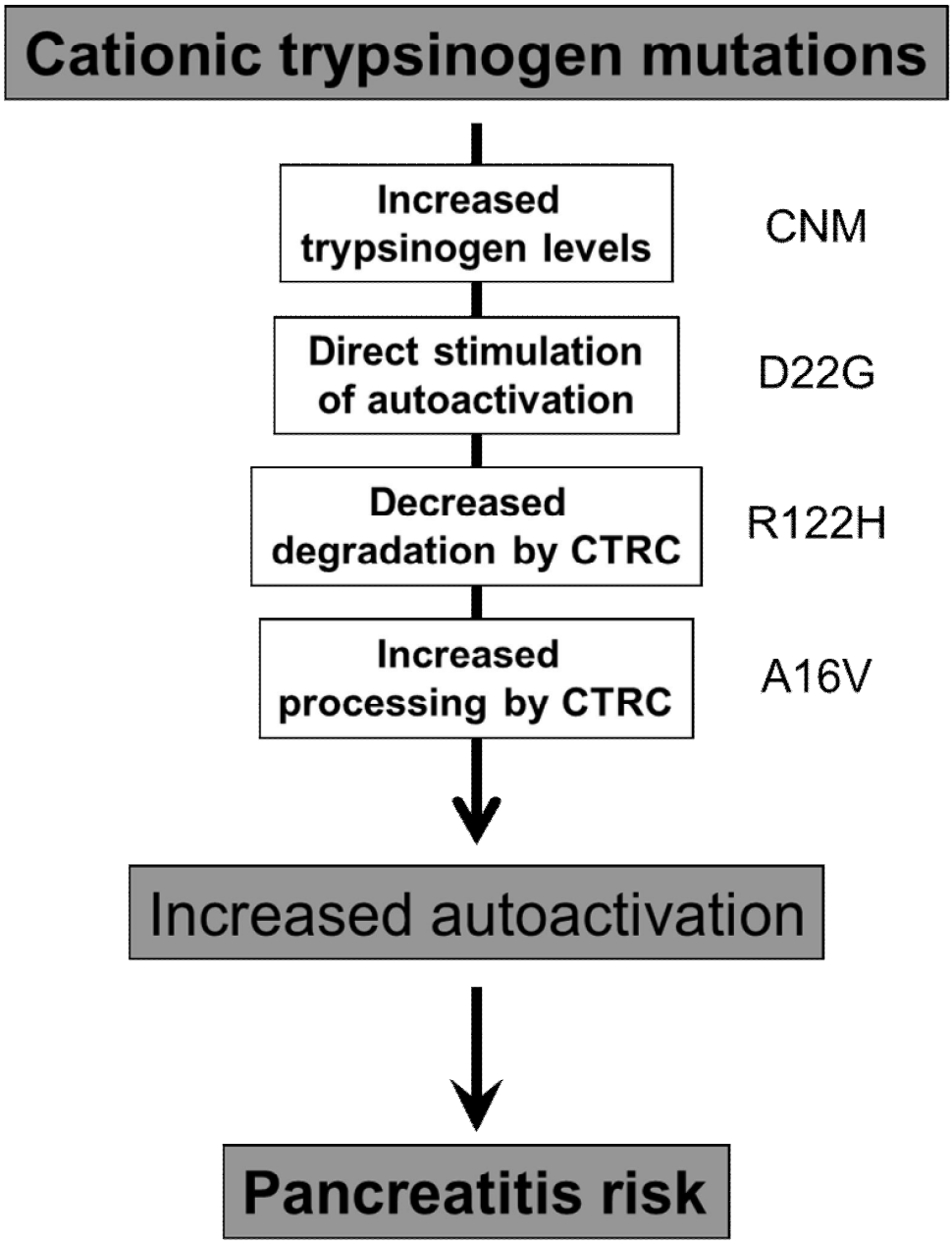

Figure 23. Mechanisms of increased autoactivation in hereditary pancreatitis associated with human cationic trypsinogen mutations. Copy number mutations (CNM) increase trypsinogen expression. Activation peptide mutations D19A, D22G, K23R, and K23_I24insIDK directly stimulate autoactivation. Mutations N29I, N29T, V39A, R122C, and R122H inhibit CTRC-dependent trypsinogen degradation. Mutations A16V and N29I stimulate N-terminal processing of the trypsinogen activation peptide by CTRC. A prominent example for each mechanism is indicated.

6 SUMMARY

Hereditary chronic pancreatitis is caused by missense mutations in human cationic trypsinogen. A subset of mutations alters the activation peptide and increases autoactivation of trypsinogen to trypsin. It has recently been demonstrated that trypsinogen mutations cause hereditary pancreatitis by altering its proteolytic regulation by chymotrypsin C (CTRC). CTRC stimulates trypsinogen autoactivation by processing the activation peptide to a shorter form and also promotes degradation by cleaving the calcium binding loop in trypsinogen. Mutations render trypsinogen resistant to CTRC-mediated degradation and/or increase processing of the activation peptide by CTRC.

In a hereditary pancreatitis family from Denmark we identified an intragenic duplication of 9 nucleotides in exon-2 of the *PRSS1* gene which at the protein level results in a 3 amino-acid insertion within the activation peptide (K23_I24insIDK). The aim of this work was to study and characterize the novel K23_I24insIDK *PRSS1* mutation on the function of human cationic trypsinogen. In light of the recently discovered CTRC-dependent unifying pathomechanism for hereditary-pancreatitis, this study was further aimed at clarifying the role of CTRC in the mechanism of action of the activation peptide mutations.

Human pancreatic enzymes were produced recombinantly and purified to homogeneity. Trypsinogen activation was followed by enzymatic assays and SDS-PAGE. Trypsinogen secretion was measured from transfected HEK 293T cells.

Our results demonstrate that activation of the K23_I24insIDK mutant by trypsin or by cathepsin B is markedly increased confirming the significance of the trypsin-dependent pathological pathway in hereditary pancreatitis. When we investigated the autoactivation properties of all four trypsinogen activation peptide mutations (D19A, D22G, K23R, and K23_I24insIDK) and their possible interaction with CTRC, we found that all four activation peptide mutations robustly increased trypsinogen autoactivation, both in the presence and absence of CTRC. Degradation of activation peptide mutants by CTRC was unchanged and processing of the activation peptide was increased only in the D19A mutant by 4-fold. Surprisingly, however, increased processing had essentially no effect on autoactivation. Finally, the activation peptide mutants exhibited reduced secretion from transfected cells, and secreted trypsinogen levels were inversely proportional with autoactivation rates.

We conclude that D19A, D22G, K23R and K23_I24insIDK form a special subset of hereditary pancreatitis-associated mutations characterized by robust autoactivation that is largely independent of CTRC and decreased cellular secretion, which is inversely proportional to their ability to autoactivate. The combination of these unique properties adequately explains the observed clinical effects of these mutations.

7 ACKNOWLEDGEMENTS

I am grateful to **professors János Lonovics** and **Tibor Wittmann,** past and present chairs of the First Department of Medicine, University of Szeged, for affording me the opportunity to participate in their Ph.D. program.

I would like to express my deepest and sincere gratitude to my mentors and advisors **professor Miklós Sahin-Tóth** at the Department of Molecular and Cell Biology in the Boston University Medical Center and **professor Péter Hegyi** at the First Department of Medicine, University of Szeged. I admire their broad knowledge of science, their way of analyzing scientific problems, and their ability to come up with exciting new ideas. I am most grateful for their patient guidance and inspiration during my Ph.D. studies.

It also gives me great pleasure to acknowledge the support and help of **associate professor Zoltán Rakonczay Jr.** and thank him for constructive discussions of my work and for his valuable suggestions.

I would also like to thank **my colleagues** at Boston University, **Zsolt Rónai**, **Éva Keresztúri**, **András Szabó**, **Melinda Bence** and **Vera Sahin-Tóth** for introducing me to all the research techniques and for their caring support during my first steps in the Sahin-Tóth laboratory. I owe warm thanks to all of my **colleagues** at the University of Szeged for all the emotional support, their weekly dose of humor, their kindness and for having had the opportunity to work with them.

This work was supported by National Development Agency grants in Szeged (TÁMOP-4.2.2.A-11/1/KONV-2012-0035, TÁMOP-4.2.2.A-11/1/KONV-2012-0073, TÁMOP-4.2.2-11/1/KONV-2012-0052), NIH grants R01DK058088, R01DK082412, R01DK082412-S2 and R01DK095753 in Boston, a scholarship from the Rosztoczy Foundation, and a mini-sabbatical grant from the American Pancreatic Association.

I dedicate this thesis to **my parents** who always valued education and taught me hard work, perseverance, humility, honesty and integrity. I thank you for your endless love, support and encouragement.

8 REFERENCES

1. Ammann, R. W. The natural history of alcoholic chronic pancreatitis. *Intern. Med.* **40,** 368–375 (2001).
2. Whitcomb, D. C. *et al.* Hereditary pancreatitis is caused by a mutation in the cationic trypsinogen gene. *Nat. Genet.* **14,** 141–145 (1996).
3. Szmola, R. & Sahin-Tóth, M. Uncertainties in the classification of human cationic trypsinogen (PRSS1) variants as hereditary pancreatitis-associated mutations. *J. Med. Genet.* **47,** 348–350 (2010).
4. Whitcomb, D. C. *et al.* Common genetic variants in the CLDN2 and PRSS1-PRSS2 loci alter risk for alcohol-related and sporadic pancreatitis. *Nat. Genet.* **44,** 1349–1354 (2012).
5. Witt, H. *et al.* A degradation-sensitive anionic trypsinogen (PRSS2) variant protects against chronic pancreatitis. *Nat. Genet.* **38,** 668–673 (2006).
6. Witt, H. *et al.* Mutations in the gene encoding the serine protease inhibitor, Kazal type 1 are associated with chronic pancreatitis. *Nat. Genet.* **25,** 213–216 (2000).
7. Pfützer, R. H. *et al.* SPINK1/PSTI polymorphisms act as disease modifiers in familial and idiopathic chronic pancreatitis. *Gastroenterology* **119,** 615–623 (2000).
8. Sharer, N. *et al.* Mutations of the cystic fibrosis gene in patients with chronic pancreatitis. *N. Engl. J. Med.* **339,** 645–652 (1998).
9. Cohn, J. A. *et al.* Relation between mutations of the cystic fibrosis gene and idiopathic pancreatitis. *N. Engl. J. Med.* **339,** 653–658 (1998).
10. Noone, P. G. *et al.* Cystic fibrosis gene mutations and pancreatitis risk: relation to epithelial ion transport and trypsin inhibitor gene mutations. *Gastroenterology* **121,** 1310–1319 (2001).
11. Truninger, K. *et al.* Mutations of the cystic fibrosis gene in patients with chronic pancreatitis. *Am. J. Gastroenterol.* **96,** 2657–2661 (2001).
12. Szmola, R. & Sahin-Tóth, M. Chymotrypsin C (caldecrin) promotes degradation of human cationic trypsin: identity with Rinderknecht's enzyme Y. *Proc. Natl. Acad. Sci. U.S.A.* **104,** 11227–11232 (2007).

13. Baudry, C. *et al.* Recurrent acute pancreatitis caused by association of a novel mutation of the calcium-sensing receptor gene and a heterozygous mutation of the SPINK1 gene. *Pancreas* **39,** 420–421 (2010).

14. Felderbauer, P. *et al.* Mutations in the calcium-sensing receptor: a new genetic risk factor for chronic pancreatitis? *Scand. J. Gastroenterol.* **41,** 343–348 (2006).

15. Rebours, V. *et al.* The natural history of hereditary pancreatitis: a national series. *Gut* **58,** 97–103 (2009).

16. COMFORT, M. W. & STEINBERG, A. G. Pedigree of a family with hereditary chronic relapsing pancreatitis. *Gastroenterology* **21,** 54–63 (1952).

17. Whitcomb, D. C. *et al.* A gene for hereditary pancreatitis maps to chromosome 7q35. *Gastroenterology* **110,** 1975–1980 (1996).

18. Le Bodic, L. *et al.* The hereditary pancreatitis gene maps to long arm of chromosome 7. *Hum. Mol. Genet.* **5,** 549–554 (1996).

19. Pandya, A. *et al.* Linkage studies in a large kindred with hereditary pancreatitis confirms mapping of the gene to a 16-cM region on 7q. *Genomics* **38,** 227–230 (1996).

20. Gorry, M. C. *et al.* Mutations in the cationic trypsinogen gene are associated with recurrent acute and chronic pancreatitis. *Gastroenterology* **113,** 1063–1068 (1997).

21. Teich, N., Mössner, J. & Keim, V. Mutations of the cationic trypsinogen in hereditary pancreatitis. *Hum. Mutat.* **12,** 39–43 (1998).

22. Férec, C. *et al.* Mutations in the cationic trypsinogen gene and evidence for genetic heterogeneity in hereditary pancreatitis. *J. Med. Genet.* **36,** 228–232 (1999).

23. Guy, O., Lombardo, D., Bartelt, D. C., Amic, J. & Figarella, C. Two human trypsinogens. Purification, molecular properties, and N-terminal sequences. *Biochemistry* **17,** 1669–1675 (1978).

24. Rinderknecht, H., Renner, I. G., Abramson, S. B. & Carmack, C. Mesotrypsin: a new inhibitor-resistant protease from a zymogen in human pancreatic tissue and fluid. *Gastroenterology* **86,** 681–692 (1984).

25. Chen, J.-M. *et al.* Evolution of trypsinogen activation peptides. *Mol. Biol. Evol.* **20,** 1767–1777 (2003).

26. Nemoda, Z. & Sahin-Tóth, M. The tetra-aspartate motif in the activation peptide of human cationic trypsinogen is essential for autoactivation control but not for enteropeptidase recognition. *J. Biol. Chem.* **280,** 29645–29652 (2005).

27. Kereszturi, E. & Sahin-Tóth, M. Intracellular autoactivation of human cationic trypsinogen mutants causes reduced trypsinogen secretion and acinar cell death. *J. Biol. Chem.* **284,** 33392–33399 (2009).

28. Lu, D. *et al.* Crystal structure of enteropeptidase light chain complexed with an analog of the trypsinogen activation peptide. *J. Mol. Biol.* **292,** 361–373 (1999).

29. Kukor, Z., Tóth, M. & Sahin-Tóth, M. Human anionic trypsinogen: properties of autocatalytic activation and degradation and implications in pancreatic diseases. *Eur. J. Biochem.* **270,** 2047–2058 (2003).

30. Witt, H., Luck, W. & Becker, M. A signal peptide cleavage site mutation in the cationic trypsinogen gene is strongly associated with chronic pancreatitis. *Gastroenterology* **117,** 7–10 (1999).

31. Teich, N. *et al.* Chronic pancreatitis associated with an activation peptide mutation that facilitates trypsin activation. *Gastroenterology* **119,** 461–465 (2000).

32. Grocock, C. J. *et al.* The variable phenotype of the p.A16V mutation of cationic trypsinogen (PRSS1) in pancreatitis families. *Gut* **59,** 357–363 (2010).

33. Nemoda, Z. & Sahin-Tóth, M. Chymotrypsin C (caldecrin) stimulates autoactivation of human cationic trypsinogen. *J. Biol. Chem.* **281,** 11879–11886 (2006).

34. Szabó, A. & Sahin-Tóth, M. Increased activation of hereditary pancreatitis-associated human cationic trypsinogen mutants in presence of chymotrypsin C. *J. Biol. Chem.* **287,** 20701–20710 (2012).

35. Kereszturi, É. *et al.* Hereditary pancreatitis caused by mutation-induced misfolding of human cationic trypsinogen: A novel disease mechanism. *Human Mutation* **30,** 575–582 (2009).

36. Chauvin, A. *et al.* Elucidation of the complex structure and origin of the human trypsinogen locus triplication. *Hum. Mol. Genet.* **18,** 3605–3614 (2009).

37. Király, O. *et al.* Expression of human cationic trypsinogen with an authentic N terminus using intein-mediated splicing in aminopeptidase P deficient Escherichia coli. *Protein Expr. Purif.* **48,** 104–111 (2006).

38. Szepessy, E. & Sahin-Tóth, M. Inactivity of recombinant ELA2B provides a new example of evolutionary elastase silencing in humans. *Pancreatology* **6,** 117–122 (2006).

39. Rónai, Z. *et al.* A common African polymorphism abolishes tyrosine sulfation of human anionic trypsinogen (PRSS2). *Biochem. J.* **418,** 155–161 (2009).

40. Király, O., Guan, L. & Sahin-Tóth, M. Expression of recombinant proteins with uniform N-termini. *Methods Mol. Biol.* **705,** 175–194 (2011).

41. Szabó, A. *et al.* High affinity small protein inhibitors of human chymotrypsin C (CTRC) selected by phage display reveal unusual preference for P4' acidic residues. *J. Biol. Chem.* **286,** 22535–22545 (2011).

42. Lengyel, Z., Pál, G. & Sahin-Tóth, M. Affinity purification of recombinant trypsinogen using immobilized ecotin. *Protein Expr. Purif.* **12,** 291–294 (1998).

43. Edman *et al.*. Method for Determination of the Amino Acid Sequence in Peptides. *ACTA CHEM SCAND* **vol. 4,** 283–293

44. Howes, N. *et al.* Clinical and genetic characteristics of hereditary pancreatitis in Europe. *Clin. Gastroenterol. Hepatol.* **2,** 252–261 (2004).

45. Masson, E., Le Maréchal, C., Delcenserie, R., Chen, J.-M. & Férec, C. Hereditary pancreatitis caused by a double gain-of-function trypsinogen mutation. *Hum. Genet.* **123,** 521–529 (2008).

46. Le Maréchal, C. *et al.* Hereditary pancreatitis caused by triplication of the trypsinogen locus. *Nat. Genet.* **38,** 1372–1374 (2006).

47. Masson, E. *et al.* Trypsinogen copy number mutations in patients with idiopathic chronic pancreatitis. *Clin. Gastroenterol. Hepatol.* **6,** 82–88 (2008).

48. Polgár, L. The catalytic triad of serine peptidases. *Cell. Mol. Life Sci.* **62,** 2161–2172 (2005).

49. Figarella, C., Miszczuk-Jamska, B. & Barrett, A. J. Possible lysosomal activation of pancreatic zymogens. Activation of both human trypsinogens by cathepsin B and spontaneous acid. Activation of human trypsinogen 1. *Biol. Chem. Hoppe-Seyler* **369** Suppl, 293–298 (1988).

50. Halangk, W. *et al.* Role of cathepsin B in intracellular trypsinogen activation and the onset of acute pancreatitis. *J. Clin. Invest.* **106,** 773–781 (2000).

51. Kukor, Z. *et al.* Presence of cathepsin B in the human pancreatic secretory pathway and its role in trypsinogen activation during hereditary pancreatitis. *J. Biol. Chem.* **277,** 21389–21396 (2002).

52. Saluja, A. K., Lerch, M. M., Phillips, P. A. & Dudeja, V. Why does pancreatic overstimulation cause pancreatitis? *Annu. Rev. Physiol.* **69,** 249–269 (2007).

53. Teich, N., Bödeker, H. & Keim, V. Cathepsin B cleavage of the trypsinogen activation peptide. *BMC Gastroenterol* **2,** 16 (2002).

54. Mareninova, O. A. *et al.* Impaired autophagic flux mediates acinar cell vacuole formation and trypsinogen activation in rodent models of acute pancreatitis. *J. Clin. Invest.* **119,** 3340–3355 (2009).

55. Wartmann, T. *et al.* Cathepsin L inactivates human trypsinogen, whereas cathepsin L-deletion reduces the severity of pancreatitis in mice. *Gastroenterology* **138,** 726–737 (2010).

56. Schnúr, A., *et al.*. Functional effects of 13 rare PRSS1 variants presumed to cause chronic pancreatitis. *Gut* (2013). doi:10.1136/gutjnl-2012-304331

57. Chen, J. M. & Ferec, C. Gene conversion-like missense mutations in the human cationic trypsinogen gene and insights into the molecular evolution of the human trypsinogen family. *Mol. Genet. Metab.* **71,** 463–469 (2000).

58. Teich, N. *et al.* Gene conversion between functional trypsinogen genes PRSS1 and PRSS2 associated with chronic pancreatitis in a six-year-old girl. *Hum. Mutat.* **25,** 343–347 (2005).

59. Simon, P. *et al.* Spontaneous and sporadic trypsinogen mutations in idiopathic pancreatitis. *JAMA* **288,** 2122 (2002).

60. Weiss, F. U. *et al.* Local clustering of PRSS1 R122H mutations in hereditary pancreatitis patients from Northern Germany. *Am. J. Gastroenterol.* **103,** 2585–2588 (2008).

61. Teich, N. *et al.* Interaction between trypsinogen isoforms in genetically determined pancreatitis: mutation E79K in cationic trypsin (PRSS1) causes increased transactivation of anionic trypsinogen (PRSS2). *Hum. Mutat.* **23,** 22–31 (2004).

62. Pallagi, P. *et al.* Trypsin reduces pancreatic ductal bicarbonate secretion by inhibiting CFTR Cl^- channels and luminal anion exchangers. *Gastroenterology* **141,** 2228–2239.e6 (2011).

63. Czepán, M. *et al.* NHE1 activity contributes to migration and is necessary for proliferation of human gastric myofibroblasts. *Pflugers Arch.* **463,** 459–475 (2012).

Articles closely related to the subject of the thesis and cited in the thesis

I.

Received Date : 05-Feb-2013

Revised Date : 30-Mar-2013

Accepted Date : 14-Apr-2013

Robust autoactivation, chymotrypsin C independence and diminished secretion define a subset of hereditary pancreatitis associated cationic trypsinogen mutants

Andrea Geisz[1,2], Péter Hegyi[2] and Miklós Sahin-Tóth[1]*

[1]Department of Molecular and Cell Biology, Henry M. Goldman School of Dental Medicine, Boston University, Boston, MA 02118; [2]First Department of Medicine, University of Szeged, Szeged, Hungary

Running title: Trypsinogen activation peptide mutants

Article type: Original Article

*Correspondence to Miklós Sahin-Tóth, 72 East Concord Street, Evans-433; Boston, MA 02118; Tel: (617) 414-1070; Fax: (617) 414-1041; E-mail: miklos@bu.edu

Keywords: trypsinogen, trypsin, chymotrypsin C, autoactivation, calcium binding, hereditary pancreatitis

SUMMARY

Mutations in human cationic trypsinogen cause hereditary pancreatitis by altering its proteolytic regulation of activation and degradation by chymotrypsin C (CTRC). CTRC stimulates trypsinogen autoactivation by processing the activation peptide to a shorter form but also

promotes degradation by cleaving the calcium binding loop in trypsinogen. Mutations render trypsinogen resistant to CTRC-mediated degradation and/or increase processing of the activation peptide by CTRC. Here we demonstrate that activation peptide mutations D19A, D22G, K23R and K23_I24insIDK robustly increased the rate of trypsinogen autoactivation, both in the presence and absence of CTRC. Degradation of the mutants by CTRC was unchanged and processing of the activation peptide was increased only in the D19A mutant by 4-fold. Surprisingly, however, this increased processing had only a minimal effect on autoactivation. The tetra-aspartate motif in the trypsinogen activation peptide binds calcium (K_D ~1.6 mM), which stimulates autoactivation. Unexpectedly, calcium binding was not compromised by any of the activation peptide mutations. Despite normal binding, autoactivation of mutants D22G and K23_I24insIDK was not stimulated by calcium. Finally, the activation peptide mutants exhibited reduced secretion from transfected cells, and secreted trypsinogen levels were inversely proportional with autoactivation rates. We conclude that D19A, D22G, K23R and K23_I24insIDK form a mechanistically distinct subset of hereditary pancreatitis associated mutations, which exert their effect primarily through direct stimulation of autoactivation, independently of CTRC. The potentially severe clinical impact of the markedly increased autoactivation is offset by diminished secretion, resulting in a clinical phenotype indistinguishable from typical hereditary pancreatitis.

Mutations in the serine protease 1 (*PRSS1*) gene that encodes human cationic trypsinogen cause hereditary pancreatitis [1, 2]. The mechanism of action for the most frequently found mutations have been recently elucidated and involves increased resistance against chymotrypsin C (CTRC)-mediated degradation and/or increased sensitivity to CTRC-dependent stimulation of autoactivation [3]. CTRC is a pancreatic serine protease which controls autoactivation of human cationic trypsinogen by selectively cleaving regulatory sites within the trypsinogen activation peptide and the calcium binding loop. The dominant effect of CTRC is trypsinogen degradation, which is triggered by cleavage of the Leu81-Glu82 peptide bond in the calcium binding loop and is facilitated by a trypsin-mediated autolytic cleavage of the Arg122-Val123 peptide bond [3, 4]. CTRC also degrades active trypsin by the same mechanism but at a slower rate. Hereditary pancreatitis-associated mutations N29I, N29T, V39A, R122C and R122H decrease or block cleavages at these sites and thereby increase trypsin levels generated during autoactivation [3].

A secondary, less prominent effect of CTRC on autoactivation is mediated by cleavage of the activation peptide of cationic trypsinogen at the Phe18-Asp19 peptide bond (Figure 1) [5]. The activation peptide is an 8 amino-acid N-terminal extension on trypsinogen, which becomes cleaved at the Lys23-Ile24 peptide bond during activation to trypsin (Figure 1). The activating cleavage may be catalyzed by the brush-border serine protease enteropeptidase (enterokinase) in the duodenum or by trypsin (i.e. autoactivation) in the pancreas. A characteristic feature of the activation peptide is the conserved tetra-Asp sequence, which is presumed to serve as an enteropeptidase recognition motif [6]. We found, however, that individual or combined mutations of these Asp residues had minimal effect on activation of human cationic trypsinogen by human enteropeptidase [7]. On the other hand, the tetra-Asp sequence was shown to inhibit autoactivation of trypsinogen, which is partly relieved by millimolar concentrations of calcium [7]. In human cationic trypsinogen, inhibition of autoactivation is also dependent on Asp218, which participates in a repulsive electrostatic interaction with the tetra-Asp motif [7]. CTRC cleavage at the Phe18-Asp19 peptide bond results in a shortened activation peptide, causing partial liberation of the inhibitory interaction with Asp218 and increased autoactivation [5] (Figure 1). Pancreatitis-associated mutations A16V and, to a lesser extent, N29I increase N-terminal processing of the activation peptide by CTRC and thereby stimulate trypsinogen autoactivation [3, 5].

In addition to the relatively common A16V mutation [8], there were four other mutations, D19A, D22G, K23R and K23_I24insIDK, in the activation peptide of human cationic trypsinogen found in association with hereditary pancreatitis (Figure 1) [9-12]. The K23_I24insIDK mutation results in the insertion of the Ile-Asp-Lys sequence between Lys23 and Ile24, which normally form the activating peptide bond (Figure 1). This insertion changes the tetra-Asp motif preceding Lys23 to Asp-Lys-Ile-Asp; effectively eliminating two of the inhibitory Asp residues. A number of previous studies demonstrated that mutations D19A, D22G, K23R and K23_I24insIDK markedly increased autoactivation of cationic trypsinogen [7, 9, 12, 13]. In fact, these mutations offered the first convincing evidence that increased autoactivation was a pathologically relevant mechanism in hereditary pancreatitis.

In light of the recently discovered CTRC-dependent unifying pathomechanism for hereditary-pancreatitis, the present study was aimed at clarifying the role of CTRC in the

mechanism of action of the activation peptide mutations. Because of their location, the mutations are unlikely to affect trypsinogen degradation but may have profound effects on CTRC-mediated processing of the activation peptide. Furthermore, we sought to elucidate how the biochemical phenotype of strikingly increased autoactivation can be reconciled with the clinical phenotype of these mutations which is typical of hereditary pancreatitis and does not indicate increased severity or penetrance. Our results demonstrate that D19A, D22G, K23R and K23_I24insIDK form a special subset of hereditary pancreatitis-associated mutations characterized by robust autoactivation that is largely independent of CTRC and decreased cellular secretion, which is inversely proportional to their ability to autoactivate. The combination of these unique properties adequately explains the observed clinical effect of these mutations.

RESULTS

Autoactivation of activation peptide mutants in absence and presence of CTRC. We studied four mutations which cause alterations in the conserved region of the activation peptide of human cationic trypsinogen, D19A, D22G, K23R and K23_I24insIDK (Figure 1). The A16V mutation which affects the N-terminal residue of the activation peptide was characterized in a recent study [3].

Autoactivation of human cationic trypsinogen in the presence of 25 nM CTRC resulted in a slight increase in the rate accompanied by a marked reduction in final trypsin levels attained (Figure 2). The increased rate is due to N-terminal processing of the activation peptide by CTRC, whereas the reduced trypsin levels are a consequence of CTRC-dependent trypsinogen degradation [3]. Recently, we demonstrated that mutations commonly associated with hereditary pancreatitis exert their effect primarily in the presence of CTRC [3]. A typical case is shown for the archetypal R122H mutation in Figure 2, which in the absence of CTRC increased autoactivation only slightly (1.2-fold). In the presence of CTRC, however, autoactivation of wild-type trypsinogen was drastically suppressed, while mutant R122H autoactivated at an increased rate and reached high trypsin levels.

When mutants D19A, D22G, K23R and K23_I24insIDK were tested under similar conditions, a markedly different phenotype became apparent. All four mutations increased the rate of trypsinogen autoactivation robustly (3.9-fold, 9.2-fold, 5.7-fold and 17.5-fold, respectively) even in the absence of CTRC, in agreement with previous observations [9, 12].

Similarly, in the presence of CTRC, all four mutants autoactivated markedly faster than wild-type trypsinogen and reached much higher trypsin levels, which then slowly decreased due to CTRC-mediated trypsin degradation. Peak trypsin levels correlated with the rate of autoactivation and were higher in mutants D22G and K23_I24insIDK versus D19A and K23R. Surprisingly, even in the presence of CTRC, activation peptide mutants autoactivated much faster than the reference mutant R122H. Thus, the estimated rates of autoactivation were approximately 3-fold higher for mutants D19A and K23R and 10-fold higher for mutants D22G and K23_I24insIDK, relative to mutant R122H.

Cleavage of the Leu81-Glu82 peptide bond by CTRC in activation peptide mutants. Because the activation peptide is not in the proximity of the calcium binding loop, mutations D19A, D22G, K23R and K23_I24insIDK are unlikely to affect CTRC-mediated trypsinogen degradation. We tested this assumption experimentally and found that cleavage of the Leu81-Glu82 peptide bond by CTRC was unchanged in the activation peptide mutants compared to wild-type cationic trypsinogen (Figure 3).

N-terminal processing of activation peptide mutants by CTRC. CTRC cleaves the Phe18-Asp19 peptide bond in the trypsinogen activation peptide and removes three amino acids from the N terminus (Figure 1) [5]. This, in turn, results in increased autoactivation of cationic trypsinogen. The N-terminal truncation of the activation peptide is readily detectable by non-reducing SDS-PAGE as a small mobility shift. To assess whether the activation peptide mutations altered CTRC-mediated N-terminal processing, we incubated wild-type and mutant trypsinogens with 50 nM CTRC at pH 8.0, in 1 mM $CaCl_2$, to minimize cleavage after Leu81. To prevent autoactivation during the incubation, we used an inactive trypsinogen background in which the catalytic Ser200 was changed to Ala (S200A). Figure 4A and B demonstrate that mutant D19A exhibited 4-fold increased N-terminal processing, whereas mutants D22G, K23R and K23_I24insIDK were processed at rates comparable with wild type. Inspection of the early time points of the autoactivation curves in the presence of CTRC (see Figure 2, compare black with white symbols) reveals that N-terminal processing by CTRC increased the rate of autoactivation for mutants D19A, D22G and K23R. Surprisingly, the enhanced processing of mutant D19A did not translate to a more robust autoactivation increase than seen in mutants

D22G or K23R (see Figure 2). Similarly, even though mutant K23_I24insIDK was processed normally, this modification had no impact on autoactivation.

CTRC-mediated cleavage of the Phe18-Asp19 peptide bond in the trypsinogen activation peptide is highly specific and other human chymotrypsins (CTRB1, CTRB2, CTRL1) and elastases (ELA2A, ELA3A, ELA3B) do not catalyze this reaction (Figure 4C). We considered the possibility that activation peptide mutations might allow for cleavages by proteases other than CTRC, however, this was not the case. None of the mutant activation peptides was cleaved by any of the chymotrypsins or elastases tested in Figure 4C (data not shown).

Effect of activation peptide mutations on calcium binding. To determine the effect of the activation peptide mutations on the calcium binding affinity of the activation peptide, we measured the rate of N-terminal processing by CTRC as a function of increasing calcium concentrations. For these experiments we used trypsinogen constructs carrying the L81A and S200A mutations to prevent unwanted cleavage at Leu81 by CTRC and to avoid trypsinogen autoactivation during incubations. As shown in Figure 5, calcium inhibited cleavage of the Phe18-Asp19 peptide bond by CTRC in wild-type cationic trypsinogen with a K_D value around 1.9 mM. Calcium dependence of N-terminal processing by CTRC was comparable for the activation peptide mutants (Figure 5B). The calculated K_D values for mutants D19A, D22G, K23R and K23_I24insIDK were 1.1 mM, 1.3 mM, 2.6 mM and 1.3 mM, respectively. Inspection of Figure 5B suggests that these values fall within the experimental error of the method. When the entire dataset including wild-type and mutants was fitted with a single curve a K_D of 1.6±0.2 mM was obtained. We conclude that calcium binding to the activation peptide is not affected by the activation peptide mutations.

Effect of calcium on autoactivation of activation peptide mutants. Calcium binding to the tetra-aspartate motif in the trypsinogen activation peptide stimulates autoactivation [14, 15]. Even though the activation peptide mutants appear to bind calcium normally, the effect of calcium on autoactivation may be altered. When autoactivation of wild-type and mutant trypsinogens was measured in the presence of 0, 1, 5 and 10 mM calcium, wild-type trypsinogen and mutants D19A and K23R were stimulated in a concentration dependent manner, whereas autoactivation of mutants D22G and K23_I24insIDK was insensitive to calcium (Figure 6).

Although the half-maximal stimulatory calcium concentration was difficult to determine due to the confounding effect of degradation in the absence of calcium, it appeared that calcium dependence of autoactivation of wild-type, D19A and K23R trypsinogens was consistent with the K_D values obtained for binding of calcium to the activation peptide. The effect of calcium on the autoactivation of mutant D19A seemed to saturate at a lower concentration when compared to mutant K23R, which might reflect a true but small difference in binding affinity (see K_D values above). The observations indicate that activation peptide mutations do not affect binding of calcium to the activation peptide but may diminish the functional effect of calcium binding.

Secretion of activation peptide mutants from transfected 293T cells. The biochemical properties of the activation peptide mutants described so far suggest that these mutations should be associated with a more severe clinical phenotype than mutation R122H. However, this is not the case. Previously, we found that secretion of activation peptide mutants from transfected cells was reduced, although the four mutants have never been studied in a comparative manner within the same experiment [12, 13]. We also demonstrated that the secretion loss was related to intracellular autoactivation and degradation [13]. To establish whether this secretion defect might be a mechanism that partly offsets the drastically increased autoactivation, we quantified secretion of wild-type and mutant trypsinogens from transiently transfected human embryonic kidney (HEK) 293T cells. The use of HEK 293T cells for cellular secretion studies is a compromise, as efficient transfection of pancreatic acinar cells is not feasible. For these experiments we used a short time course (12 h) to prevent autoactivation in the medium and consequent trypsinization of the cells. We measured trypsin activity in the conditioned media after enteropeptidase-mediated activation (Figure 7A) and trypsinogen levels by western blotting (Figure 7B). We found that the activation peptide mutants were secreted at significantly lower levels than wild-type trypsinogen, in agreement with previous observations [12, 13]. Importantly, secretion rates for the mutants were inversely proportional with their ability to autoactivate (D19A > K23R > D22G ≈ K23_I24insIDK).

DISCUSSION

The primary objective of the present study was to investigate the effect of CTRC on the autoactivation of trypsinogen activation peptide mutants D19A, D22G, K23R and

K23_I24insIDK found in hereditary pancreatitis. Previously, we demonstrated that wild-type cationic trypsinogen is largely degraded by CTRC during autoactivation, whereas hereditary pancreatitis associated mutants N29I, N29T, V39A, R122C and R122H exhibited resistance to CTRC-mediated degradation and autoactivated to higher trypsin levels [3]. In addition, we found that mutations A16V and N29I increased CTRC-mediated cleavage of the activation peptide, and thereby accelerated autoactivation (see Figure 1) [3, 5]. We speculated that activation peptide mutants might also affect processing of the activation peptide by CTRC and/or alter the effect of this cleavage, perhaps even resulting in decreased autoactivation. This would then offer an explanation for the puzzling observation that the robust autoactivation of activation peptide mutants is not accompanied by a more severe clinical picture.

Our results confirmed that even in the absence of CTRC activation peptide mutants autoactivated at markedly increased rates (~4-18-fold) [9, 12]. In the presence of CTRC, activation rates were further increased slightly (D19A, D22G, K23R) or remained unchanged (K23_I24insIDK), indicating that the robust autoactivation of the activation peptide mutants is mostly independent of CTRC. Peak trypsin levels attained during autoactivation positively correlated with the rate of autoactivation, indicating that faster conversion of trypsinogen to trypsin results in higher trypsin levels, as trypsin is less sensitive to CTRC-mediated degradation than trypsinogen. As expected, the mutations had no effect on CTRC cleavage of the Leu81-Glu82 peptide bond in the calcium binding loop and consequent trypsinogen degradation. Importantly, when compared to the most common pancreatitis-associated mutant R122H, in the presence of CTRC the activation peptide mutants still exhibited much higher rates of autoactivation (~3-10-fold).

N-terminal processing of the activation peptide at Phe18 by CTRC was unchanged in mutants D22G, K23R and K23_I24insIDK, whereas mutant D19A was processed at 4-fold increased rate. This finding is consistent with recent mutagenesis studies in the calcium binding loop of cationic trypsinogen, which demonstrated that mutation of Glu82 to Ala increased cleavage after Leu81 about 3-fold, indicating that acidic residues at the P1' position hinder cleavage by CTRC [16]. Surprisingly, however, the increased processing of mutant D19A was paralleled only with a slight increase in the rate of autoactivation, suggesting that Asp19 is

important for mediating the functional effect of N-terminal processing. Thus, shortening the activation peptide by CTRC may increase autoactivation by partly relieving the inhibitory interaction between Asp218 and Asp19 [5, 7]. This effect is probably due to neutralization of the negative charge on Asp19 by the newly created proximity of the positively charged amino terminus. Similarly, mutation D19A would increase autoactivation by neutralizing Asp19 but at the same time it would diminish the effect of N-terminal processing by CTRC. This notion is supported by the observations that the extent of the autoactivation increase either by CTRC processing or by mutation D19A is comparable, approximately 3-4-fold [5, 9]. The stimulatory effect of CTRC cleavage on autoactivation was also abolished in mutant K23_I24insIDK, which may be readily explained by sterical uncoupling of the original tetra-Asp motif from the activation site by the three-amino-acid insertion (see Figure 1). Furthermore, previous experiments indicated that trypsin-mediated activation (i.e. autoactivation) of the K23_I24insIDK mutant most likely proceeds by sequential cleavage of the two lysyl peptide bonds found in the mutated activation peptide [12]. In this case, cleavage of the N-terminal Lys-Ile peptide bond would eliminate the N-terminal eight amino acids together with any effect of CTRC-dependent processing (see Figure 1).

Calcium in millimolar concentrations stimulates autoactivation presumably by binding to the activation peptide and shielding the inhibitory negative charges of the tetra-Asp motif [14, 15]. Using the CTRC-dependent processing of the activation peptide as readout, we determined the calcium binding affinity of wild-type and mutant activation peptides (see Figure 5). Unexpectedly, mutant and wild-type trypsinogens bound calcium at the activation peptide with comparable affinities, 1.6 mM on average. This observation suggests that calcium probably engages only two or three Asp side chains and elimination of one of the four Asp residues either by mutation D19A or D22G is tolerated. When the functional effect of calcium binding was investigated, however, we found that autoactivation of mutants D22G and K23_I24insIDK were insensitive to calcium. The results seem to lend some credence to the speculation that the stimulatory effect calcium on autoactivation is mediated through binding to Asp22 and neutralizing its negative charge. During autoactivation, Asp22 in the activation peptide binds to the S2 subsite on trypsin, a conserved hydrophobic pocket formed by His63, Leu104 and Trp216, and this unfavorable interaction may be alleviated by calcium. In the K23_I24insIDK

mutant, calcium likely binds only to the original tetra-Asp motif, which is now further removed from the activation peptide bond. The Asp-Lys-Ile-Asp sequence preceding the activation site does not seem competent to bind calcium. Furthermore, as pointed out above, during autoactivation the N-terminal eight amino acids are removed before cleavage at the activation peptide bond takes place (see Figure 1) [12]. Alternatively, another plausible interpretation for the data may be that for wild-type trypsinogen and mutants D19A and K23R the rate limiting step in the autoactivation reaction is calcium dependent, whereas for the rapidly autoactivating mutants D22G and K23_I24insIDK a calcium-insensitive step becomes rate determining.

The biochemical properties of the trypsinogen activation peptide mutants do not explain why the markedly increased autoactivation is not associated with a more severe clinical presentation of hereditary pancreatitis; i.e. with complete penetrance and earlier onset. Typical penetrance of hereditary pancreatitis in families with the R122H mutation is 70-90% and the median age of onset is 12 years with wide individual variability [1, 17]. Although clinical data for the rare activation peptide mutations is relatively scant, mutation D22G was also identified in the unaffected 20 year old sister of the index patient, indicating incomplete penetrance [10]. Published ages of diagnosis indicated both early onset (D22G 8 y, K23_I24insIDK 2 y) and late onset cases (D19A 17 y, K23_I24insIDK 21 y), consistent with typical hereditary pancreatitis [9, 10, 12]. Previously, we observed that secretion of activation peptide mutants was compromised from transfected cells due to intracellular autoactivation and ensuing degradation [12, 13]. We extended these studies here and quantitatively compared, for the first time, cellular secretion of all four activation peptide mutants to determine whether reduced secretion could offset the effect of increased autoactivation. Indeed, we confirmed not only that all four activation peptide mutants were secreted to lower levels than wild-type trypsinogen, but also that secretion rates inversely correlated with the rates of autoactivation. Our observations indicate that nature carefully titrated trypsinogen secretion against autoactivation propensity, to curb the risk for excessive pathological intra-pancreatic trypsinogen activation in carriers of the activation peptide mutations.

In summary, our results define the trypsinogen activation peptide mutations D19A, D22G, K23R and K23_I24insIDK as a special subset of hereditary-pancreatitis associated mutations which stimulate autoactivation largely independently of CTRC and this robust effect is

compensated by their reduced secretion. Taken together with previous studies, the observations indicate that human cationic trypsinogen mutations may increase autoactivation by several independent but not mutually exclusive mechanisms in hereditary pancreatitis (Figure 8): (i) increased secretion, as suggested for copy number mutations [18, 19]; (ii) resistance to CTRC-mediated degradation [3, 4]; (iii) increased processing of the activation peptide by CTRC [3, 5] and (iv) direct stimulation of autoactivation, as demonstrated here for the activation peptide mutations.

EXPERIMENTAL PROCEDURES

Nomenclature. Amino-acid residues in human cationic trypsinogen were numbered starting with the initiator methionine of the primary translation product, in accordance with the recommendations of the Human Genome Variation Society.

Plasmid construction and mutagenesis. The pTrapT7 intein-PRSS1, pcDNA3.1(-) PRSS1 and other expression plasmids harboring the coding DNA for human pancreatic digestive proteases have been described previously. [4, 5, 20, 21]. To increase expression levels in transfected HEK 293T cells, the trypsinogen activation peptide mutations were transferred to the pcDNA3.1(-) K237D/N241D background [22]. Mutations in human cationic trypsinogen were generated by PCR mutagenesis, cloned into the expression plasmids and verified by DNA sequencing.

Expression and purification of protease zymogens. Wild-type and mutant trypsinogens were expressed in the aminopeptidase P deficient LG-3 *E. coli* strain as fusions with a self-splicing mini-intein, as described in [20, 23]. This expression system produces recombinant trypsinogen with uniform, authentic N termini. Refolding and purification of trypsinogen by ecotin affinity chromatography was carried out as reported previously [23] with the following modification. To stabilize trypsinogens against autoactivation, the elution solution contained 50 mM HCl and 100 mM NaCl. Concentrations of trypsinogen preparations were determined from the UV absorbance at 280 nm using the extinction coefficient 37,525 M^{-1} cm^{-1}.

Expression in *E. coli*, in vitro refolding and purification of human proelastase ELA2A was performed as described previously [21]. Histidine-tagged forms of human chymotrypsinogens CTRB1, CTRB2, CTRC and CTRL1 and proelastases ELA3A and ELA3B were expressed in HEK 293T cells and purified from the conditioned medium using nickel-

affinity chromatography, as reported previously [3, 16]. ELA2A was activated using 10 nM human anionic trypsin [21] and other proteases were activated with immobilized bovine trypsin (Pierce/Thermo Fisher Scientific, Rockford, IL) in 0.1 M Tris-HCl (pH 8.0) and 0.05% Tween 20 (final concentrations) and the trypsin beads were removed by centrifugation. Active protease concentrations were determined by active site titration with ecotin, as described [24].

Trypsinogen autoactivation. Trypsinogen at 1 µM concentration was incubated in the absence or presence of 25 nM human CTRC, as indicated, and 10 nM cationic trypsin in 0.1 M Tris-HCl (pH 8.0), 100 mM NaCl, 1 mM $CaCl_2$ and 0.05% Tween 20 (final concentrations) at 37 ºC. At given times, 2 µL aliquots were withdrawn and mixed with 48 µL assay buffer containing 0.1 M Tris-HCl (pH 8.0), 1 mM $CaCl_2$, and 0.05% Tween 20. Trypsin activity was measured by adding 150 µL 200 µM N-CBZ-Gly-Pro-Arg-p-nitroanilide substrate (dissolved in 0.1 M Tris-HCl (pH 8.0), 1 mM $CaCl_2$ and 0.05% Tween 20) and following the release of the yellow p-nitroanilin at 405 nm in a SpectraMax plus 384 microplate reader (Molecular Devices, Sunnyvale, CA) for 1 min. Reaction rates were calculated from fits to the initial linear portions of the curves. Note that in the present study all experiments were performed in the presence of 100 mM NaCl, which resulted in slower autoactivation, compared to previous studies.

Cell culture and transfection. HEK 293T cells were cultured and transfected as described previously [25]. Transfections were performed using 2 µg expression plasmid and 5 µL Lipofectamine 2000 (Invitrogen, Carlsbad, CA) in 2 mL Dulbecco's Modified Eagle Medium (Invitrogen). After overnight incubation, cells were washed and the transfection medium was replaced with 1 mL OPTI-MEM I Reduced Serum Medium (Invitrogen). Time courses of expression were measured starting from this medium change and were followed for 12 hours. Trypsin activity in the conditioned media was measured after enteropeptidase activation, as described in [26]**.**

Gel electrophoresis and densitometry. Trypsinogen samples (75 µL of a 2 µM solution, corresponding to approximately 3.8 µg protein) were precipitated with trichloroacetic acid (10% final concentration), and the precipitate was recovered by centrifugation, dissolved in 20 µL Laemmli sample buffer with 100 mM dithiothreitol (final concentration), and heat-denatured at 95 °C for 5 min. Where non-reducing conditions are indicated, dithiothreitol was omitted from the sample buffer. Electrophoretic separation was performed on 15% SDS-polyacrylamide mini gels in standard Tris glycine buffer. Gels were stained with Brilliant Blue R-250 and destained as

described earlier [15]. Quantitation of bands was carried out with the Quantity One 4.6.9 software (Bio-Rad, Hercules, CA).

Western blot analysis. Aliquots (20 µL) of conditioned media were mixed with sample buffer, heat-denatured, electrophoresed on Tris-glycine minigels and transferred onto an Immobilon-P membrane (Millipore Corporation, Bedford, MA) at 300 mA for 1.5 h. The membrane was blocked with 5% milk powder dissolved in phosphate-buffered saline supplemented with 0.1% Tween 20 (final concentration), at 4 °C overnight. Trypsinogen was detected with a sheep polyclonal antibody (#AF3848, R&D Systems, Minneapolis, MN) used at a dilution of 1:2000 followed by horse-radish peroxidase (HRP)-conjugated donkey polyclonal anti-sheep IgG (#HAF016, R&D Systems) used at 1:2000 dilution, as described previously [26].

ACKNOWLEDGMENTS

This work was supported by NIH grants R01DK058088, R01DK082412, R01DK082412-S2 and R01DK095753 (to M.S-T). A.G. was also supported by a mini-sabbatical grant from the American Pancreatic Association. The authors thank András Szabó for help with plasmid construction and trypsinogen degradation assays; and Éva Kereszturi and Béla Ózsvári for performing preliminary experiments on calcium binding to the activation peptide.

REFERENCES

1. Whitcomb DC, Gorry MC, Preston RA, Furey W, Sossenheimer MJ, Ulrich CD, Martin SP, Gates LK Jr, Amann ST, Toskes PP, Liddle R, McGrath K, Uomo G, Post JC & Ehrlich GD (1996) Hereditary pancreatitis is caused by a mutation in the cationic trypsinogen gene. *Nat Genet* **14**, 141-145
2. Szmola R & Sahin-Tóth M (2010) Uncertainties in the classification of human cationic trypsinogen (*PRSS1*) variants as hereditary pancreatitis-associated mutations. *J Med Genet* **47**, 348-350
3. Szabó A & Sahin-Tóth M (2012) Increased activation of hereditary pancreatitis-associated human cationic trypsinogen mutants in presence of chymotrypsin C. *J Biol Chem* **287**, 20701-20710

4. Szmola R & Sahin-Tóth M (2007) Chymotrypsin C (caldecrin) promotes degradation of human cationic trypsin: identity with Rinderknecht's enzyme Y. *Proc Natl Acad Sci USA* **104**, 11227-11232

5. Nemoda Z & Sahin-Tóth M (2006) Chymotrypsin C (caldecrin) stimulates autoactivation of human cationic trypsinogen. *J Biol Chem* **281**, 11879–11886

6. Lu D, Fütterer K, Korolev S, Zheng X, Tan K, Waksman G & Sadler JE (1999) Crystal structure of enteropeptidase light chain complexed with an analog of the trypsinogen activation peptide. *J Mol Biol* **292**, 361-373

7. Nemoda Z & Sahin-Tóth M (2005) The tetra-aspartate motif in the activation peptide of human cationic trypsinogen is essential for autoactivation control but not for enteropeptidase recognition. *J Biol Chem* **280**, 29645-29652

8. Witt H, Luck W & Becker M (1999) A signal peptide cleavage site mutation in the cationic trypsinogen gene is strongly associated with chronic pancreatitis. *Gastroenterology* **117**, 7-10

9. Chen JM, Kukor Z, Le Maréchal C, Tóth M, Tsakiris L, Raguénès O, Férec C & Sahin-Tóth M (2003) Evolution of trypsinogen activation peptides. *Mol Biol Evol* **20**, 1767-1777

10. Teich N, Ockenga J, Hoffmeister A, Manns M, Mössner J & Keim V (2000) Chronic pancreatitis associated with an activation peptide mutation that facilitates trypsin activation. *Gastroenterology* **119**, 461-465

11. Férec C, Raguénès O, Salomon R, Roche C, Bernard JP, Guillot M, Quéré I, Faure C, Mercier B, Audrézet MP, Guillausseau PJ, Dupont C, Munnich A, Bignon JD & Le Bodic L (1999) Mutations in the cationic trypsinogen gene and evidence for genetic heterogeneity in hereditary pancreatitis. *J Med Genet* **36**, 228-232

12. Joergensen MT, Geisz A, Brusgaard K, Schaffalitzky de Muckadell OB, Hegyi P, Gerdes AM & Sahin-Tóth M (2011) Intragenic duplication: a novel mutational mechanism in hereditary pancreatitis. *Pancreas* **40**, 540-546

13. Kereszturi E & Sahin-Tóth M (2009) Intracellular autoactivation of human cationic trypsinogen mutants causes reduced trypsinogen secretion and acinar cell death. *J Biol Chem* **284**, 33392-33399

14. Abita JP, Delaage M & Lazdunski M (1969) The mechanism of activation of trypsinogen. The role of the four N-terminal aspartyl residues. *Eur J Biochem* **8**, 314-324

15. Kukor Z, Tóth M & Sahin-Tóth M (2003) Human anionic trypsinogen: properties of autocatalytic activation and degradation and implications in pancreatic diseases. *Eur J Biochem* **270**, 2047-2058
16. Szabó A & Sahin-Tóth M (2012) Determinants of chymotrypsin C cleavage specificity in the calcium-binding loop of human cationic trypsinogen. *FEBS J* **279**, 4283-4292
17. Howes N, Lerch MM, Greenhalf W, Stocken DD, Ellis I, Simon P, Truninger K, Ammann R, Cavallini G, Charnley RM, Uomo G, Delhaye M, Spicak J, Drumm B, Jansen J, Mountford R, Whitcomb DC, Neoptolemos JP & European Registry of Hereditary Pancreatitis and Pancreatic Cancer (EUROPAC) (2004) Clinical and genetic characteristics of hereditary pancreatitis in Europe. *Clin Gastroenterol Hepatol* **2**, 252-261
18. Le Maréchal C, Masson E, Chen JM, Morel F, Ruszniewski P, Levy P & Férec C (2006) Hereditary pancreatitis caused by triplication of the trypsinogen locus. *Nat Genet* **38**, 1372-1374
19. Masson E, Le Maréchal C, Chandak GR, Lamoril J, Bezieau S, Mahurkar S, Bhaskar S, Reddy DN, Chen JM & Férec C (2008) Trypsinogen copy number mutations in patients with idiopathic chronic pancreatitis. *Clin Gastroenterol Hepatol* **6**, 82-88
20. Király O, Guan L, Szepessy E, Tóth M, Kukor Z & Sahin-Tóth M (2006) Expression of human cationic trypsinogen with an authentic N terminus using intein-mediated splicing in aminopeptidase P deficient *Escherichia coli*. *Protein Expr Purif* **48**, 104-111
21. Szepessy E & Sahin-Tóth M (2006) Inactivity of recombinant ELA2B provides a new example of evolutionary elastase silencing in humans. *Pancreatology* 6, 117-122
22. Rónai Z, Witt H, Rickards O, Destro-Bisol G, Bradbury AR & Sahin-Tóth M (2009) A common African polymorphism abolishes tyrosine sulfation of human anionic trypsinogen (PRSS2). *Biochem J* **418**, 155-161
23. Király O, Guan L & Sahin-Tóth, M (2011) Expression of recombinant proteins with uniform N-termini. *Methods Mol Biol* **705**, 175–194
24. Szabó A, Héja D, Szakács D, Zboray K, Kékesi KA, Radisky ES, Sahin-Tóth M & Pál G. (2011) High affinity small protein inhibitors of human chymotrypsin C (CTRC) selected by phage display reveal unusual preference for P4' acidic residues. *J Biol Chem* **286**, 22535-22545

25. Beer S, Zhou J, Szabó A, Keiles S, Chandak GR, Witt H & Sahin-Tóth M (2012) Comprehensive functional analysis of chymotrypsin C (CTRC) variants reveals distinct loss-of-function mechanisms associated with pancreatitis risk. *Gut* Published Online First: 1 September 2012, doi:10.1136/gutjnl-2012-303090

26. Schnúr A, Beer S, Witt H, Hegyi P & Sahin-Tóth M (2013) Functional effects of 13 rare *PRSS1* variants presumed to cause chronic pancreatitis. *Gut* Published Online First: 1 March 2013, doi:10.1136/gutjnl-2012-304331

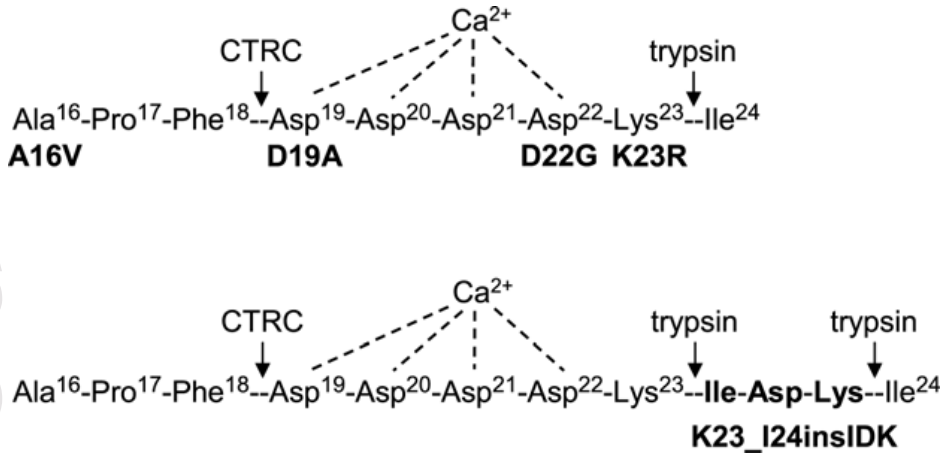

Figure 1. Pancreatitis-associated mutations in the activation peptide of human cationic trypsinogen. Proteolytic cleavage sites for trypsin and chymotrypsin C (CTRC) and the putative Ca^{2+} binding site are also indicated. See text for details. Note that the N-terminal amino-acid of mature trypsinogen is Ala16, as the 15 amino-acid long secretory signal peptide is removed in the endoplasmic reticulum. Properties of the A16V mutant were published recently and it was not included in the present study [3, 5].

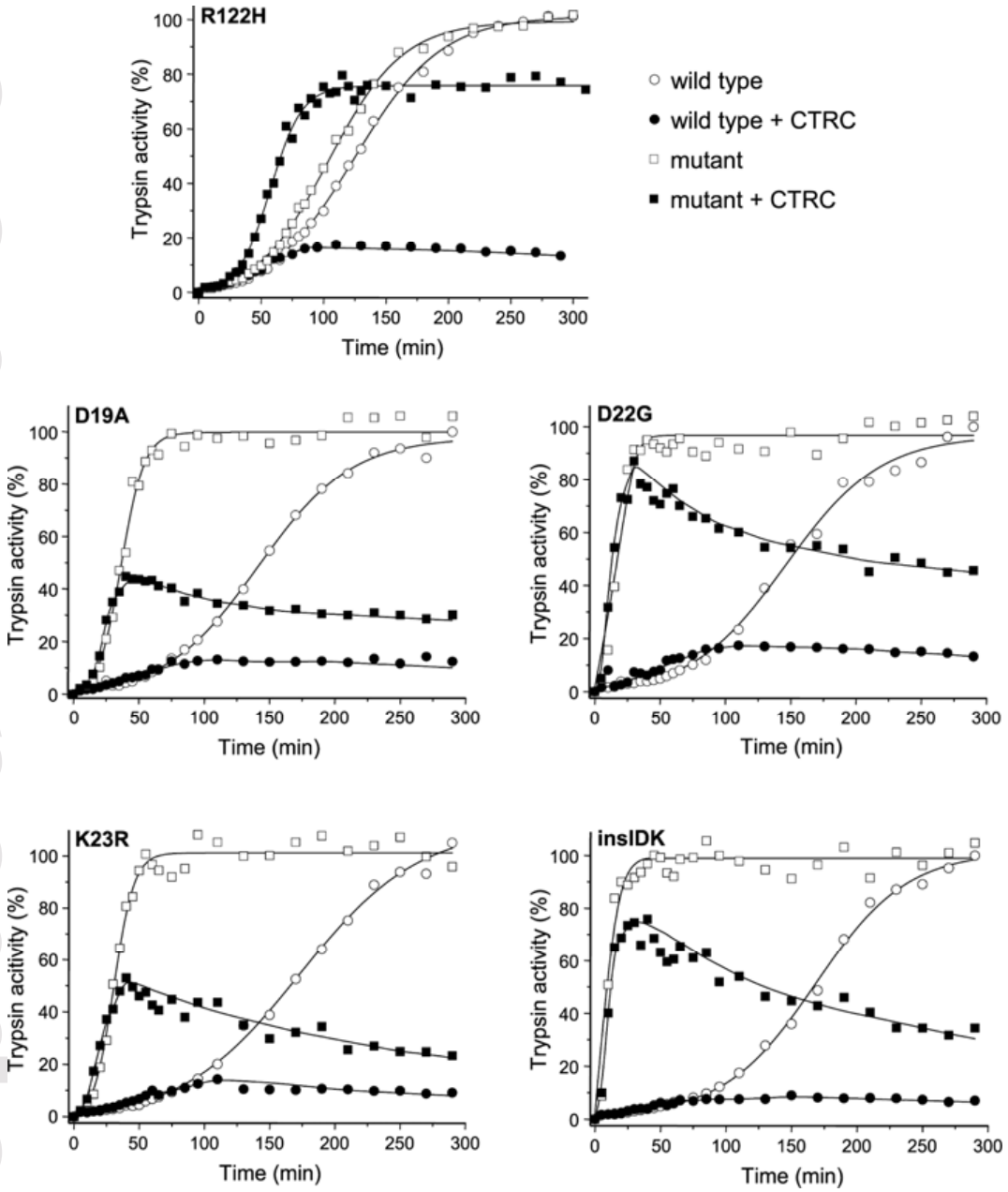

Figure 2. Autoactivation of human cationic trypsinogen and activation peptide mutants in the absence and presence of chymotrypsin C (CTRC). For comparison, mutant R122H was also included. Wild-type (circles) and mutant (squares) trypsinogen were incubated at 1 μM with 10 nM initial trypsin in 0.1 M Tris-HCl (pH 8.0), 1 mM $CaCl_2$, 100 mM NaCl and 0.05% Tween 20, at 37 °C, in the absence (empty symbols) or presence (solid symbols) of 25 nM CTRC (final concentrations). Aliquots (2 μL) were withdrawn at the indicated times and trypsin activity was

determined as described in *Experimental Procedures*. Trypsin activity was expressed as percentage of the maximal activity in the absence of CTRC. Representative experiments from two or three replicates are shown. Mutant K23_I24insIDK is denoted as insIDK.

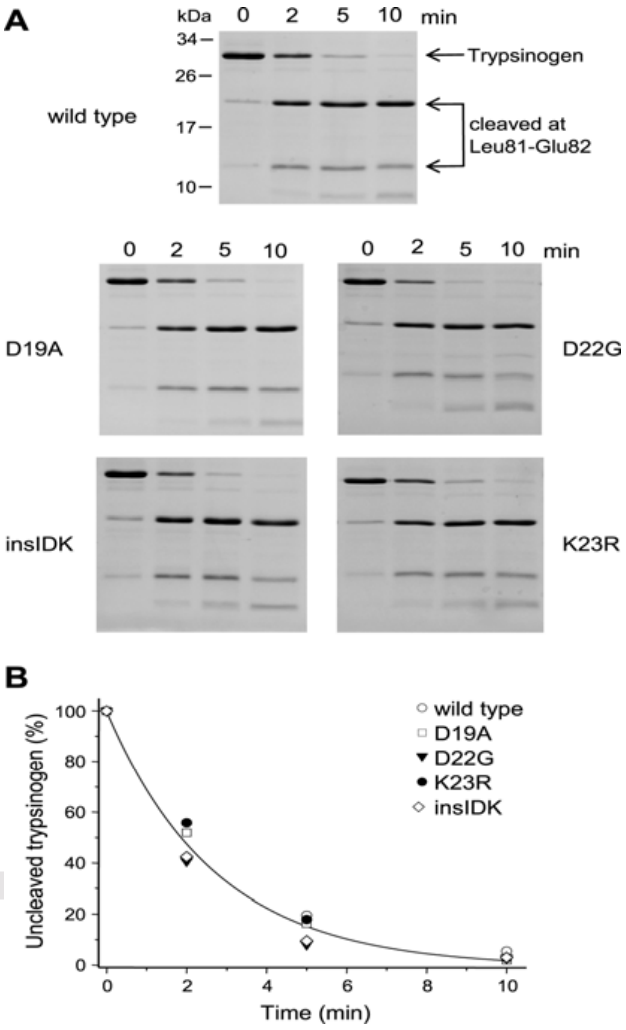

Figure 3. Cleavage of the Leu81-Glu82 peptide bond in human cationic trypsinogen and activation peptide mutants by chymotrypsin C (CTRC). Wild-type and mutant trypsinogen were incubated at 2 μM with 20 nM CTRC in 0.1 M Tris-HCl (pH 8.0) (final concentrations), at 37 °C. Trypsinogens contained the S200A mutation to prevent autoactivation. ***A***, At the indicated times reactions were terminated by precipitation of 75 μL aliquots (~3.8 μg protein) with 10% trichloroacetic acid (final concentration) and analyzed by 15% reducing SDS-PAGE and

Coomassie Blue staining. Representative gels of two or three experiments are shown. ***B***, Densitometric analysis of stained gels showing the changes in the intensity of the unprocessed, intact trypsinogen band. Error bars were omitted for clarity, the error was within 10% of the mean. Mutant K23_I24insIDK is denoted as insIDK.

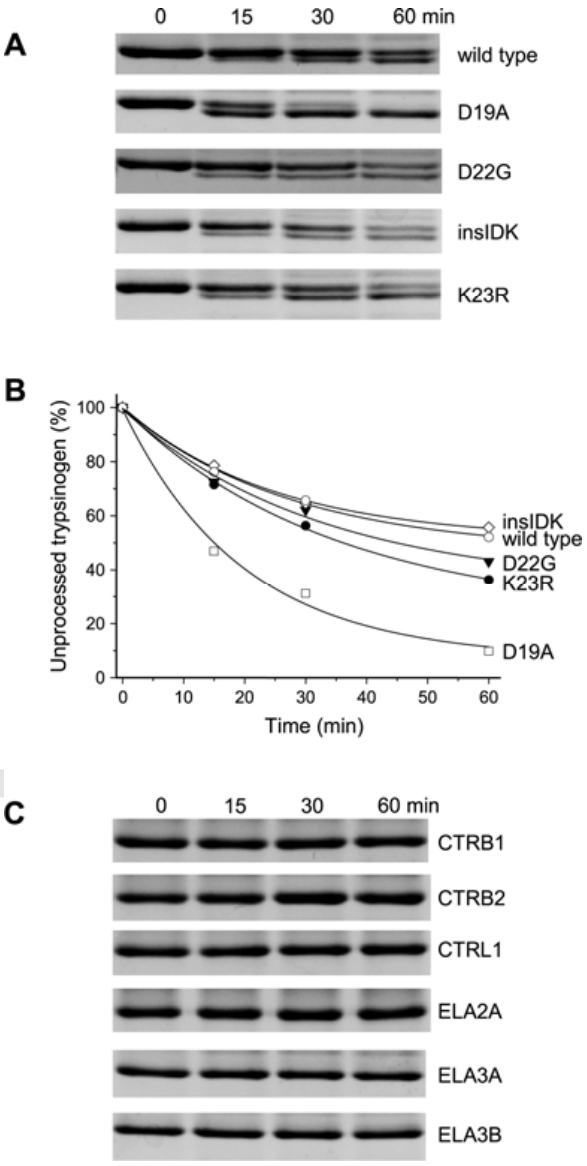

Figure 4. N-terminal processing of human cationic trypsinogen and activation peptide mutants by chymotrypsin C (CTRC). ***A***, Wild-type and mutant trypsinogen were incubated at 2 µM with 50 nM CTRC in 0.1 M Tris-HCl (pH 8.0), 1 mM $CaCl_2$ and 100 mM NaCl (final concentrations), at 37 °C. Trypsinogens contained the S200A mutation to prevent autoactivation. At the indicated times reactions were terminated by precipitation of 75 µL aliquots (~3.8 µg protein) with 10% trichloroacetic acid (final concentration) and samples were analyzed by 15% non-reducing SDS-PAGE and Coomassie Blue staining. Relevant segments of representative gels demonstrate the small mobility shift of the trypsinogen band caused by CTRC-mediated cleavage of the activation peptide (see Figure 1). ***B***, Densitometric analysis of stained gels showing the changes in the intensity of the unprocessed, intact trypsinogen band as percent of the total intensity of the processed and unprocessed bands. ***C***, N-terminal processing of the activation peptide is specific for CTRC. Wild-type and mutant trypsinogen were incubated with 50 nM of the indicated human pancreatic chymotrypsins and elastases and reactions were analyzed as described above. For clarity, only the wild-type dataset is shown; none of the mutants was cleaved by any of the proteases tested. Mutant K23_I24insIDK is denoted as insIDK.

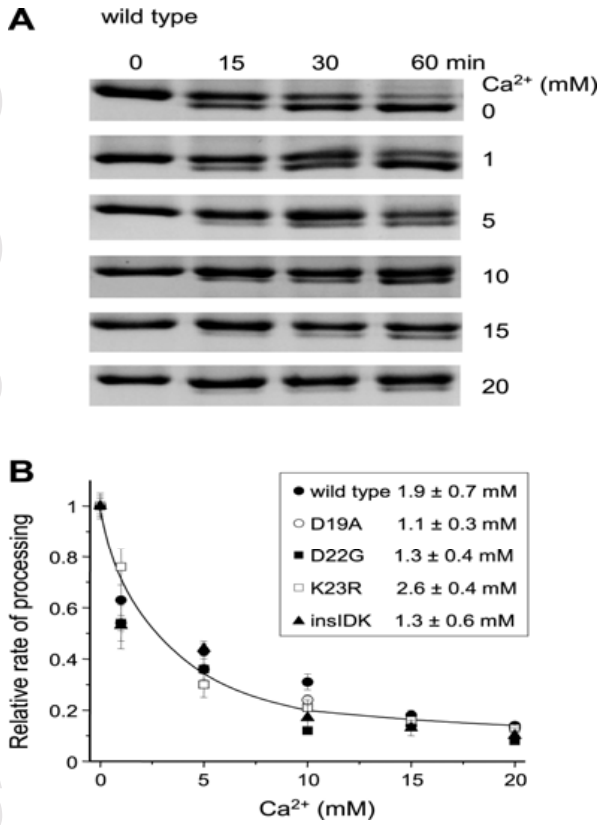

Figure 5. Effect of calcium on the N-terminal processing of the trypsinogen activation peptide by chymotrypsin C (CTRC). ***A***, Wild-type and mutant trypsinogen were incubated at 2 µM with 50 nM CTRC in 0.1 M Tris-HCl (pH 8.0) and 100 mM NaCl in the absence or presence of $CaCl_2$ (Ca^{2+}) at the indicated concentrations, at 37 °C. Trypsinogens contained the S200A mutation to prevent autoactivation and the L81A mutation to prevent CTRC cleavage after Leu81 in the absence of calcium. At the indicated times reactions were terminated and analyzed as described in Figure 4A. As an example, the relevant gel segments for wild type are shown. Similar gel sets were generated for all mutants and used to determine reaction rates, as described below. ***B***, Densitometric analysis was performed as given in Figure 4B. Rates of processing were calculated from linear fits to semilogarithmic graphs and plotted as a function of the calcium concentration with errors of the fits shown. The equilibrium binding constants (K_D) for calcium were calculated from fits to the $y = y(min)+[y(max)-y(min)] / 1+[Ca^{2+}]/K_D$ equation where y is the measured reaction rate, $y(max)$ is the maximal reaction rate in the absence of calcium and $y(min)$ is the residual reaction rate under fully saturating calcium concentrations. The error of the fits is also indicated. Mutant K23_I24insIDK is denoted as insIDK.

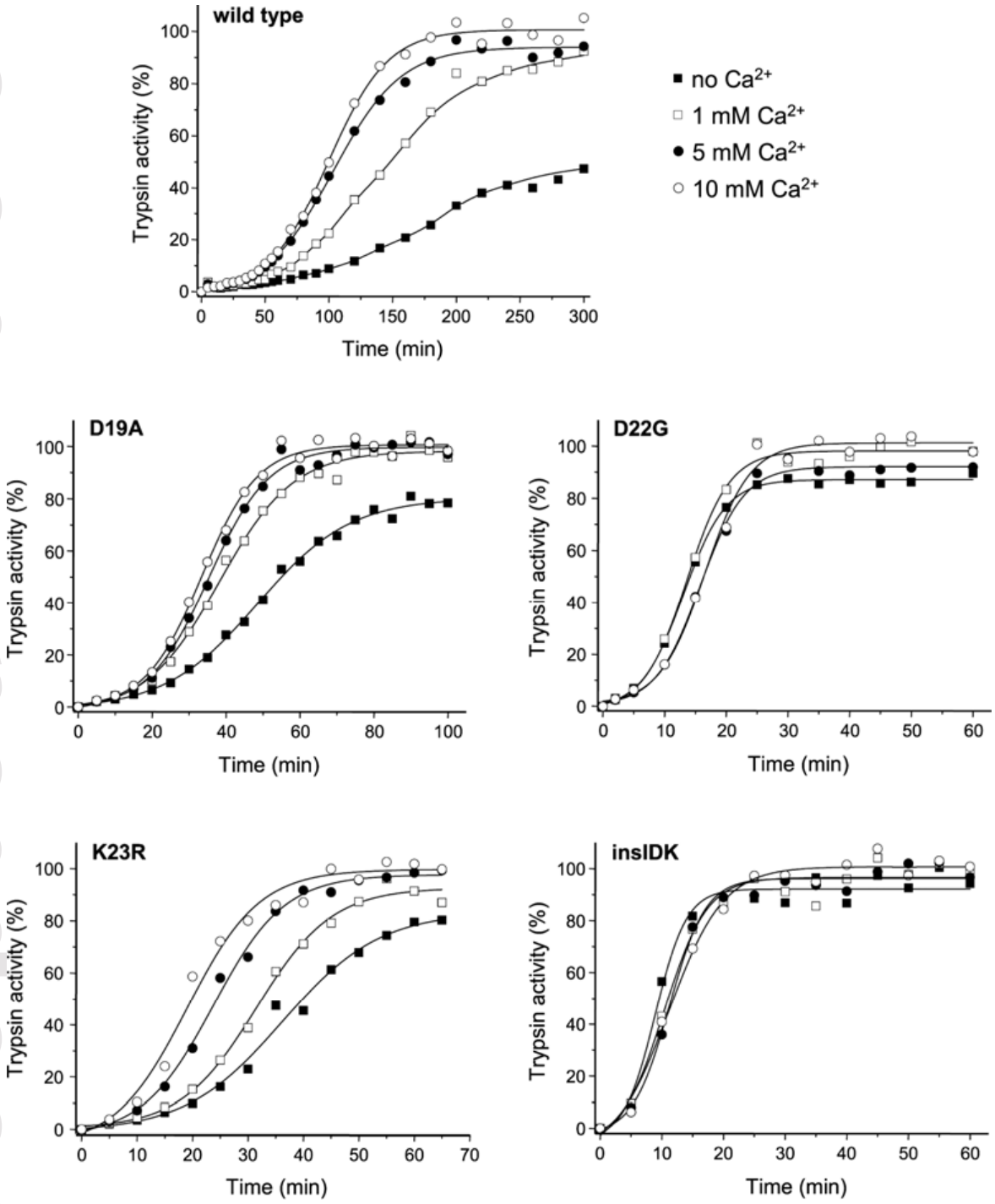

Figure 6. Effect of calcium on the autoactivation of human cationic trypsinogen and activation peptide mutants. Wild-type and mutant trypsinogen were incubated at 1 µM with 10 nM initial trypsin in 0.1 M Tris-HCl (pH 8.0), 100 mM NaCl, and 0.05% Tween 20, at 37 °C, in the

absence or presence of $CaCl_2$ (Ca^{2+}) at the indicated concentrations. At given times 2 µL aliquots were removed and trypsin activity was determined as described in *Experimental Procedures*. Trypsin activity was expressed as percentage of the maximal activity in the presence of 10 mM $CaCl_2$. Representative experiments from two or three replicates are shown. Mutant K23_I24insIDK is denoted as insIDK.

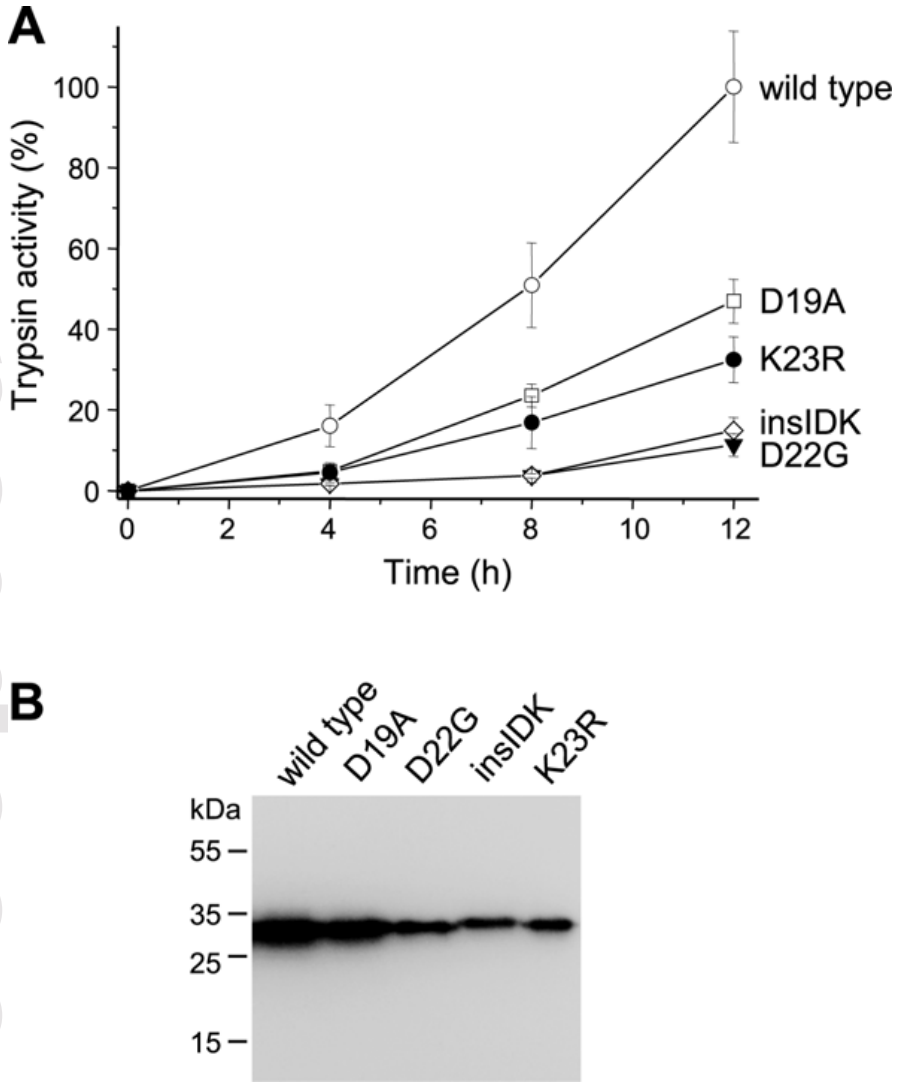

Figure 7. Secretion of human cationic trypsinogen and activation peptide mutants from transiently transfected HEK 293T cells. Trypsinogen expression constructs contained the K237D and N241D mutations which improve secretion from transfected cells [22]. ***A***, At 4, 8 and 12 hours after transfection conditioned media were collected and trypsin activity was measured as described under *Experimental Procedures*. Trypsin activity was expressed as percent of the 12 h wild-type activity. The average of three independent transfection experiments with standard deviation is shown. ***B***, Aliquots (20 μL) of conditioned media collected at 12 h were electrophoresed on 15% SDS-polyacrylamide gels and analyzed by western blotting, as described in *Experimental Procedures*. A representative blot of three is shown. Mutant K23_I24insIDK is denoted as insIDK.

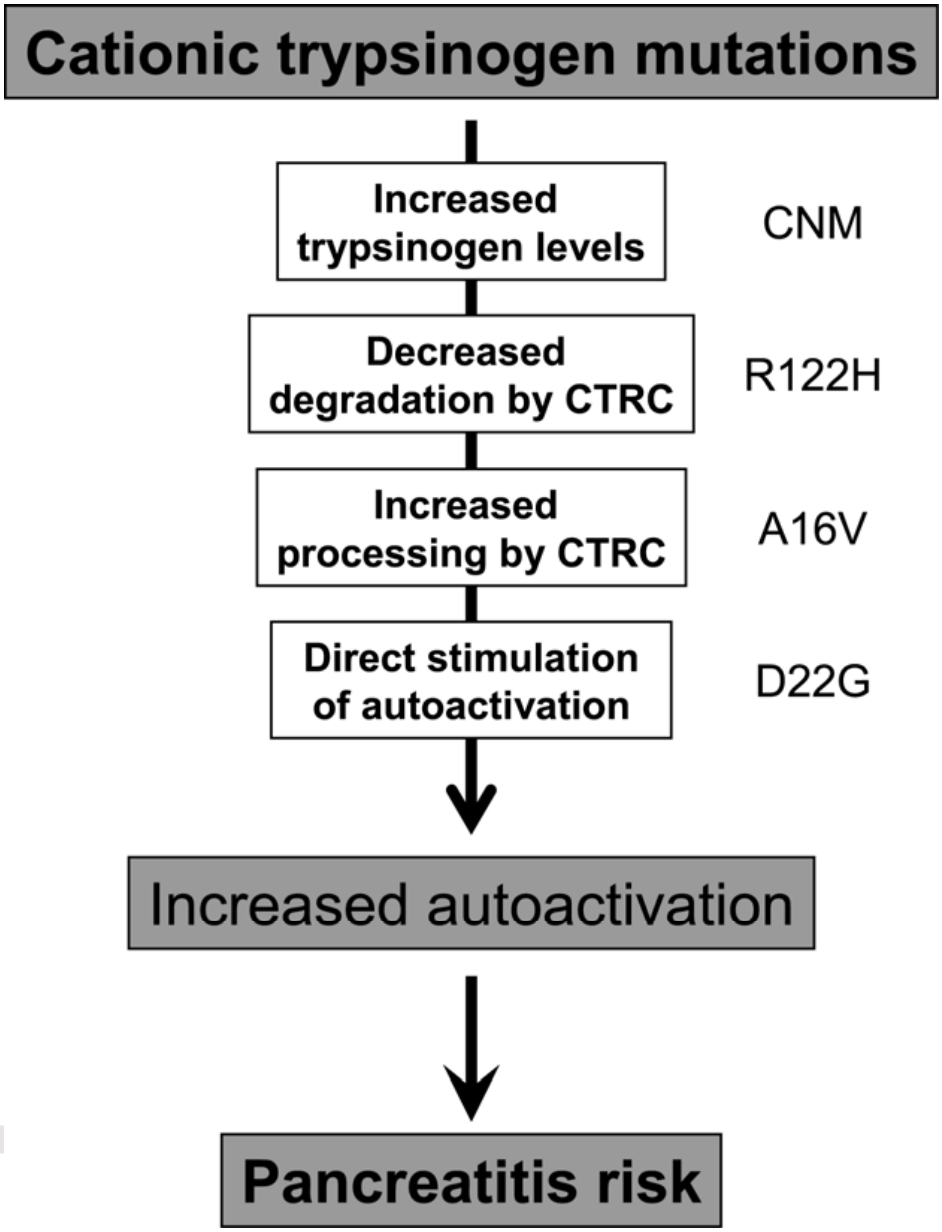

Figure 8. Mechanisms of increased autoactivation in hereditary pancreatitis associated with human cationic trypsinogen mutations. Copy number mutations (CNM) increase trypsinogen expression. Mutations N29I, N29T, V39A, R122C and R122H inhibit CTRC-dependent trypsinogen degradation. Mutations A16V and N29I stimulate N-terminal processing of the trypsinogen activation peptide by CTRC. Activation peptide mutations D19A, D22G, K23R and K23_I24insIDK directly stimulate autoactivation. A prominent example for each mechanism is indicated. See text for details.

II.

Intragenic Duplication

A Novel Mutational Mechanism in Hereditary Pancreatitis

Maiken T. Joergensen, MD, PhD, Andrea Geisz, MS,† Klaus Brusgaard, MS, PhD,‡*
Ove B. Schaffalitzky de Muckadell, MD, DMSci, Péter Hegyi, MD, PhD,§*
Anne-Marie Gerdes, MD, PhD,‡ and Miklós Sahin-Tóth, MD, PhD†

Objectives: In a hereditary pancreatitis family from Denmark, we identified a novel intragenic duplication of 9 nucleotides in exon-2 of the human cationic trypsinogen (*PRSS1*) gene (c.63_71dup) which at the amino-acid level resulted in the insertion of 3 amino acids within the activation peptide of cationic trypsinogen (p.K23_I24insIDK). The aim of the present study was to characterize the effect of this unique genetic alteration on the function of human cationic trypsinogen.

Methods: Wild-type and mutant cationic trypsinogens were produced recombinantly and purified to homogeneity. Trypsinogen activation was followed by enzymatic assays and sodium dodecyl sulfate–polyacrylamide gel electrophoresis. Trypsinogen secretion was measured from transfected HEK 293T cells.

Results: Recombinant cationic trypsinogen carrying the p.K23_I24insIDK mutation exhibited greater than 10-fold increased autoactivation. Activation by human cathepsin B also was accelerated by 10-fold. Secretion of the p.K23_I24insIDK mutant from transfected cells was diminished, consistent with intracellular autoactivation.

Conclusions: This is the first report of an intragenic duplication within the *PRSS1* gene causing hereditary pancreatitis. The accelerated activation of p.K23_I24insIDK by cathepsin B is a unique biochemical property not found in any other pancreatitis-associated trypsinogen mutant. In contrast, the robust autoactivation of the novel mutant confirms the notion that increased autoactivation is a disease-relevant mechanism in hereditary pancreatitis.

Key Words: hereditary pancreatitis, human cationic trypsinogen, PRSS1, intragenic duplication, autoactivation, cathepsin B, enteropeptidase

(*Pancreas* 2011;40: 540–546)

From the *Departments of Medical Gastroenterology, Odense University Hospital, University of Southern Denmark, Odense, Denmark; †Department of Molecular and Cell Biology, Boston University Henry M. Goldman School of Dental Medicine, Boston, MA; ‡Biochemistry, Pharmacology and Genetics, Odense University Hospital, University of Southern Denmark, Odense, Denmark; and §First Department of Internal Medicine, University of Szeged, Szeged, Hungary.

Received for publication May 27, 2010; accepted December 23, 2010.

Reprints: Maiken T. Joergensen, MD, PhD, Department of Medical Gastroenterology, Odense University Hospital, Sdr Boulevard 29, 5000 Odense C, Denmark (e-mail: maiken.t.joergensen@ouh.regionsyddanmark.dk).

This work was supported by grants from the Danish Cancer Society, the Dagmar Marshalls Foundation, the Fru Astrid Thaysens Legat, the Legat for Lægevidenskabelig grundforskning, the Ingemann O. Buch's Foundation 2004, the Lægernes Forsikringsforening af 1991 (to M.T.J), the National Institutes of Health (DK058088 to M.S.-T.), and a scholarship from the Rosztoczy Foundation (to A.G.).

These first (M.T.J.) and second authors (A.G.) contributed equally to this study.

Supplemental digital contents are available for this article. Direct URL citations appear in the printed text and are provided in the HTML and PDF versions of this article on the Journal's Web site (www.pancreasjournal.com).

Hereditary chronic pancreatitis is an autosomal dominant genetic disorder characterized by incomplete penetrance and variable expressivity.[1–6] Heterozygous mutations in the serine protease 1 (*PRSS1*) gene have been identified as causative genetic changes in 25% to 80% of cases in different studies. The *PRSS1* gene encodes human cationic trypsinogen, the most abundant digestive proenzyme in human pancreatic secretions. Approximately 70% of the mutation positive hereditary pancreatitis families carry the p.R122H mutation and approximately 20% the p.N29I mutation. In the remaining 10% of families, at least 10 different, relatively rare mutations have been identified, including a subset of mutations affecting the trypsinogen activation peptide (p.A16V, p.D19A, p.D22G, and p.K23R) (reviewed in [7]). The literature also reports 23 additional rare *PRSS1* variants, which have been found in patients with chronic pancreatitis; however, their pathogenic significance, if any, remains unknown (reviewed in [7]). Functional characterization of pancreatitis-associated *PRSS1* mutants revealed that increased trypsinogen autoactivation (trypsin-mediated trypsinogen activation) is a common phenotypic alteration at the protein level (see [1–8] and references therein). The increased propensity for autoactivation was especially notable in the activation peptide mutants.[9] More recent studies demonstrated that increased autoactivation of activation peptide mutants can occur intracellularly and result in decreased trypsinogen secretion and apoptotic acinar cell death.[10]

Although the vast majority of hereditary pancreatitis cases are caused by missense point mutations, other genetic mechanisms also have been recognized as potentially disease relevant. Mutation p.R122H is rarely caused by a dinucleotide change, possibly through a gene-conversion mechanism.[11,12] Gene conversion and duplication also can create functional hybrid trypsinogen genes carrying the p.N29I mutation.[13,14] Finally, duplication and triplication of the trypsinogen locus was described to result in hereditary pancreatitis in all likelihood because of a gene dosage effect.[14–17] In the present study, we report a novel mutational mechanism in a hereditary pancreatitis family from Denmark. We found that intragenic duplication of a 9 nucleotide sequence in exon-2 resulted in a 3–amino acid insertion in the trypsinogen activation peptide that dramatically altered the activation properties of human cationic trypsinogen.

MATERIALS AND METHODS

Materials

Human recombinant cathepsin B was a generous gift from Paul M. Steed (Research Department, Novartis Pharmaceuticals, Summit, NJ). Before use, cathepsin B was activated with 90 mM dithiothreitol (final concentration) for 30 minutes on ice. The *N*-benzyloxycarbonyl-Gly-Pro-Arg-*p*-nitroanilide trypsin substrate was from Sigma-Aldrich (St Louis, Mo). Recombinant human

pro-enteropeptidase (holoenzyme) was from R & D Systems (Minneapolis, Minn). Human pro-enteropeptidase (at 0.07 mg/mL, ~640 nM concentration) was activated with 50 nM human cationic trypsin in 0.1 M Tris-HCl (pH 8.0), 10 mM $CaCl_2$, and 2 mg/mL bovine serum albumin (final concentrations) for 30 minutes at room temperature. Ecotin was expressed and purified as reported previously.[18–20] Cell culture media and reagents were obtained from Invitrogen (Carlsbad, Calif).

Patients

This study was approved by the Scientific Ethics Committee and the Danish Data Protection Agency. The family received genetic counseling before they gave their informed consent to participate in the study. A questionnaire recording symptoms, clinical tests, and medical history was completed. A blood sample was drawn from the index patient, his brother, and his father into tubes with EDTA and stored at –20°C. After discovery of the mutation, the grandparents and the siblings of the father also were tested.

Nomenclature

Nucleotide numbering reflects coding DNA numbering with +1 corresponding to the A of the ATG translation initiation codon in the reference sequence. Amino acid residues are numbered starting with Met1 of human cationic pretrypsinogen. The first amino acid of cationic trypsinogen is Ala16.

Genetic Analyses

Genomic DNA was extracted from full blood using the Maxwell DNA purification robot (Promega, Ramcon, Denmark). The samples were tested for small deletions, insertions, and point mutations in all exons and the exon-intron boundaries of the *PRSS1* (GenBank NM_002769.3) and *SPINK1* (GenBank NM_003122.3) genes using DHPLC (WAVE 3500HT High Sensitivity System; Transgenomic Inc, Elancourt, France). Samples with deviating chromatographic profiles were sequenced in both directions using the BigDye Terminator v3.1 Cycle Sequencing Kit (Applied Biosystems, Carlsbad, Calif) and analyzed on an automated ABI PRISM 3100 (Applied Biosystems). The presence of *PRSS1* gene duplication or triplication was excluded using the rapid polymerase chain reaction–based method described by Chauvin et al.[17]

Genomic DNA also was tested for 33 *CFTR* (GenBank NM_000492.3) mutations: 394delTT, p.R553X, 621+1G>T, p.R1162X, 1717-1G>A, 3659delC, p.G542X, 2183A>G, p.W1282X, 1078delT, 711+1G>T, p.F508del, p.S549N, I507del, p.S549R, 2184delA, p.G551D, p.G85E, p.N1303K, p.R560T, p.R117H, p.R347H, p.R347P, p.R334W, 2789+5G>A, 3849+10kbC>T, p.A445E, 3120+1G>A, p.V520F, 1898+1G>A, 3876delA, 3905insT, and IVS8-5T.

Plasmid Construction and Mutagenesis

The pTrapT7 PRSS1, pTrapT7 PRSS1 p.S200A, and pcDNA3.1(−) PRSS1 expression plasmids were constructed previously.[21–24] The p.K23_I24insIDK mutation was generated by overlap extension polymerase chain reaction mutagenesis and cloned into the pTrapT7 and pcDNA3.1(−) expression plasmids. The p.K23_I24insIDK p.S200A and p.D22G p.S200A mutants were created in the pTrapT7 PRSS1 plasmid by cut and paste using the NcoI and XhoI restriction sites and the appropriate parent plasmids.

Expression and Purification of Cationic Trypsinogen

Wild-type, p.K23_I24insIDK, p.S200A, p.K23_I24insIDK/p.S200A, and p.D22G/p.S200A cationic trypsinogens were expressed in *Escherichia coli* BL21(DE3) as cytoplasmic inclusion bodies. Refolding and purification of trypsinogen on immobilized ecotin was carried out as reported previously[20–22] with the following modification. To stabilize the p.K23_I24insIDK mutant against autoactivation, 100 mM NaCl was included with the 50 mM HCl elution solution during ecotin affinity chromatography. Concentrations of trypsinogen solutions were determined from the UV absorbance at 280 nm using the extinction coefficient 36,160 M^{-1} cm^{-1} (http://ca.expasy.org/tools/protparam.html).

Trypsin Activity Assay

Trypsin activity was measured with the synthetic chromogenic substrate, *N*-benzyloxycarbonyl-Gly-Pro-Arg-*p*-nitroanilide at 0.14 mM final concentration. One-minute time courses of *p*-nitroaniline release were followed at 405 nm in 0.1 M Tris-HCl (pH 8.0) and 1 mM $CaCl_2$ at room temperature using a Spectramax Plus 384 microplate reader (Molecular Devices, Sunnyvale, Calif).

Cell Culture and Transfection

HEK 293T cells were cultured in 6-well tissue culture plates (10^6 cells per well) in Dulbecco modified Eagle medium supplemented with 10% fetal bovine serum, 4 mM glutamine, and 1% penicillin/streptomycin at 37°C in 5% CO_2. Transfections were performed using 2 μg expression plasmid and 10 μL Lipofectamine 2000 in 2 mL Dulbecco modified Eagle medium. After overnight incubation at 37°C, cells were washed, and the transfection medium was replaced with 2 mL OptiMEM reduced serum medium. Time courses of expression were measured starting from this medium change and were followed for 48 hours.

Western Blot Analysis

Aliquots of conditioned media (20 μL per lane) were electrophoresed on Tris-glycine minigels and transferred onto an Immobilon-P membrane (Millipore, Billerica, Mass). The membrane was blocked with 5% milk powder solution at 4°C overnight and incubated with sheep polyclonal antibody against human cationic trypsinogen (R&D Systems, AF3848) at a dilution of 1:2000 for 1 hour at room temperature, followed by incubation with horseradish peroxidase–conjugated donkey polyclonal antisheep immunoglobulin G (R&D Systems, HAF016), used at 1:2000 dilution, for 1 hour at room temperature. Horseradish peroxidase was detected using the SuperSignal West Pico Chemiluminescent Substrate (Thermo Scientific, Rockford, Ill).

RESULTS

A Novel Intragenic Duplication in the *PRSS1* Gene Is Associated With Hereditary Pancreatitis

The index patient is a 2-year-old boy from Denmark who presented with ascites and a history of recurrent attacks of abdominal pain, diarrhea, and vomiting for 4 months. A preoperative magnetic resonance cholangiopancreatography revealed a pancreatic fistula as the cause for the ascites and also showed pancreas divisum, duct irregularities, and multiple cysts in the pancreatic head and tail. The cauda of the pancreas was resected, and pancreaticojejunostomy was performed. After resection, the ascites production ceased, and the patient recovered. The father of the index patient was diagnosed with chronic pancreatitis at the age of 21 years, which was initially attributed to a bicycle accident, which had happened at age 13 years. The father underwent resection of the cauda of the pancreas at the age of 27 years because of repeated attacks of upper abdominal pain. The index patient's younger brother also developed abdominal pain, diarrhea, and elevated blood amylase at the age of 2 years,

but pancreatic edema was not detected by ultrasonography. The 3 affected members within this family satisfy the formal criteria of autosomal dominant hereditary pancreatitis (Fig. 1A). Curiously, however, no other case of pancreatitis could be confirmed in the rest of the extended family, suggesting that the causative mutation may have occurred de novo in the father. This assumption was later confirmed by the genetic studies detailed below. Nonpaternity was excluded by DNA microsatellite analysis (Identifiler kit; Applied Biosystems).

DNA sequence analysis of the *PRSS1* gene in the index patient found no known mutations but showed a yet unreported duplication in exon-2. As demonstrated by the electropherograms (see Supplementary Figure 1, Supplemental Digital Content 1, http://links.lww.com/MPA/A38), the forward sequencing of exon-2 showed mixed signals starting at nucleotide position c.72 because of a heterozygous 9-nucleotide insertion. The inserted sequence is TGACAAGAT, which corresponds to *PRSS1* sequence between c.63 and c.71. Thus, the insertion represents a short intragenic duplication (c.63_71dup), which has never been described in trypsinogen genes so far. Sequencing of exon-2 with a reverse primer confirmed the duplication (see Supplementary Figure 1, Supplemental Digital Content 1, http://links.lww.com/MPA/A38). No other mutations were identified in the *PRSS1* gene. The previously reported large-scale trypsinogen duplication and triplication were excluded.[14–17] The c.63_71dup mutation also was present in the father and the brother but not in the grandparents or in the father's sister and half brother, indicating that the mutation was de novo created in the father (Fig. 1A). All affected family members were negative for *SPINK1* mutations and a select panel of *CFTR* mutations (see "Materials and Methods" section). We did not find the c.63_71dup duplication in 200 healthy controls (400 chromosomes) from the same geographical region.

At the amino acid level, the c.63_71dup mutation creates an insertion of the Ile-Asp-Lys (IDK) sequence between amino acids Lys23 and Ile24 (p.K23_I24insIDK) (Fig. 1B). This region of trypsinogen is the so-called activation peptide, an 8 amino acid long N-terminal extension that is cleaved off during activation at the Lys23-Ile24 peptide bond by the physiological activator enteropeptidase or by the pathological activators trypsin and cathepsin B.

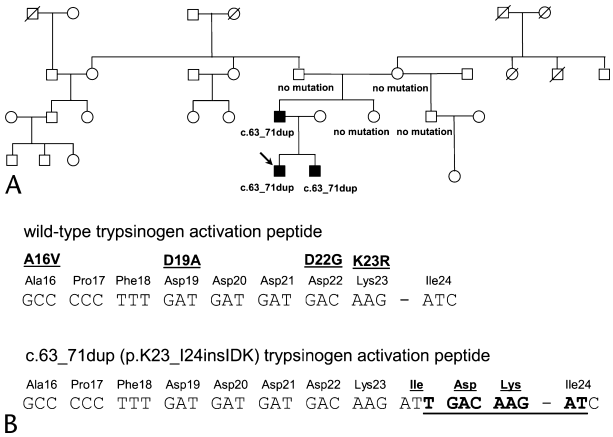

FIGURE 1. Association of the c.63_71dup intragenic duplication in the cationic trypsinogen (*PRSS1*) gene with hereditary pancreatitis in a family from Denmark. A, Pedigree of the study family. Heterozygous carriers of the c.63_71dup (p.K23_I24insIDK) mutation are indicated. Subjects affected with chronic pancreatitis are shown by solid black symbols. Crossed symbols designate deceased subjects. The arrow points to the index patient. B, Nucleotide and amino acid sequence of the wild-type and c.63_71dup (p.K23_I24insIDK) mutant cationic trypsinogen activation peptides. The location of the previously described pancreatitis-associated *PRSS1* mutations within the activation peptide also is indicated.

The tetra-Asp motif (Asp19-Asp22) preceding Lys23 is an important suppressor of trypsin-mediated activation (autoactivation).[23] In the p.K23_I24insIDK mutant, the tetra-Asp motif before the activating peptide bond is replaced with an Asp-Lys-Ile-Asp sequence. Previously described mutations that alter the tetra-Asp motif (p.D19A, p.D22G) were shown to increase autoactivation of cationic trypsinogen, suggesting a similar phenotype for the p.K23_I24insIDK mutant as well.[9,10,23,25]

Activation Characteristics of p.K23_I24insIDK Mutant Cationic Trypsinogen

To study the effect of the p.K23_I24insIDK mutation on the activation of cationic trypsinogen, we have generated recombinant versions of wild-type and mutant trypsinogens and purified them to homogeneity. The mutant trypsinogen preparations were highly unstable, and spontaneous conversion to trypsin occurred rapidly, suggesting that the p.K23_I24insIDK mutant exhibits markedly increased autoactivation. Indeed, when autoactivation of wild-type and mutant trypsinogens were compared in a quantitative manner (pH 8.0, 37°C), the mutant autoactivated at rates that were greater than 10-fold higher relative to wild-type trypsinogen (Fig. 2A). To better characterize the autoactivation kinetics, we generated catalytically inactive versions of wild-type and mutant trypsinogens by mutation of Ser200 to Ala (p.S200A). The use of the p.S200A-trypsinogens allowed us to measure exact rates of trypsin-mediated trypsinogen activation by controlling the trypsin concentration in the reactions. Because activation of p.S200A-trypsinogen does not result in enzymatic activity, the activation reactions were followed by the mobility shift on sodium dodecyl sulfate–polyacrylamide gel electrophoresis (SDS-PAGE). For comparison, in these experiments, we included the p.D22G mutant as a previously well-characterized example of the activation peptide mutants.[9,10,25] As shown in Figure 2B, 100 nM human cationic trypsin converted the 2 μM p.S200A (wild-type) trypsinogen to trypsin at a very slow rate, and appreciable trypsin levels were seen only after 60-minute incubation (pH 8.0, 37°C). In contrast, p.K23_I24insIDK/p.S200A trypsinogen was completely activated to trypsin within 30 minutes, whereas complete conversion of the p.D22G/p.S200A mutant took approximately 60 minutes. Thus, as judged from the half-lives of p.S200A trypsinogens, the rate of trypsin-mediated trypsinogen activation is greater than 10-fold higher for both the p.K23_I24insIDK and p.D22G mutants, relative to wild-type trypsinogen. These data are in agreement with the activity-based assay using catalytically competent trypsinogens, as shown in Figure 2A for the p.K23_I24insIDK mutant and published previously for the p.D22G mutant.[9]

Owing to the robust autoactivation of the p.K23_I24insIDK mutant, we were unable to measure enteropeptidase-mediated trypsinogen activation using the catalytically active proteins. Therefore, we monitored enteropeptidase-mediated activation of the p.S200A-trypsinogens on SDS-PAGE. Supplementary Figure 2 (Supplemental Digital Content 2, http://links.lww.com/MPA/A40) demonstrates that activation of the p.K23_I24insIDK and p.D22G mutants was comparable to that of wild type (pH 8.0, 37°C). The results are in accord with our previous studies showing that the trypsinogen activation peptide plays no significant role in the recognition of human cationic trypsinogen by human enteropeptidase.[23] This finding is somewhat surprising, as the

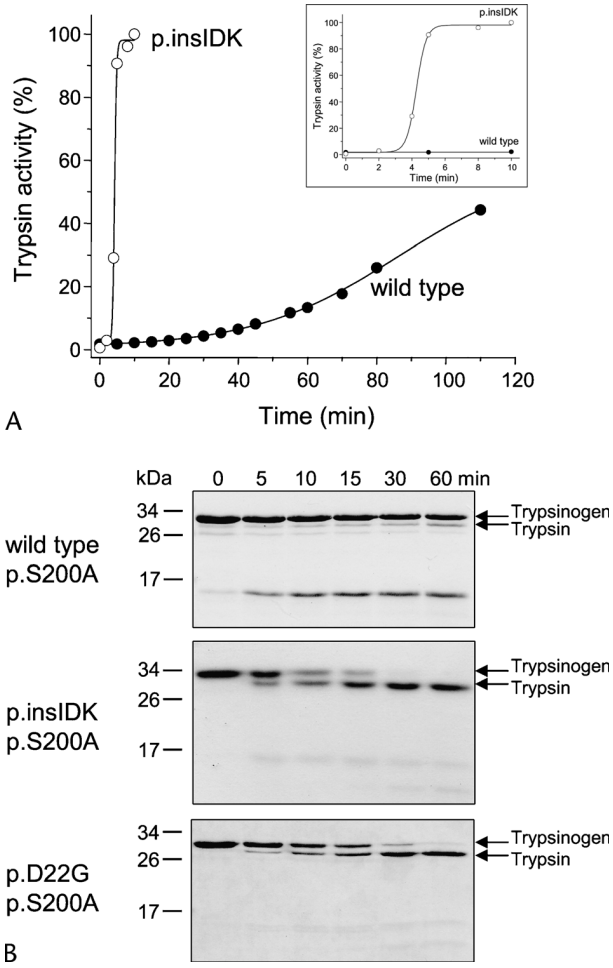

FIGURE 2. Effect of the p.K23_I24insIDK mutation on the activation of human cationic trypsinogen by trypsin (autoactivation). A, Trypsinogens at 2 μM concentration were incubated with 40 nM human cationic trypsin (initial concentration) at 37°C in 0.1 M Tris-HCl (pH 8.0), 1 mM $CaCl_2$, and 40 mM NaCl (final concentrations) in 100-μL final volume. Aliquots (2 μL) were withdrawn at indicated times, and trypsin activity was determined. Trypsin activity was expressed as percentage of the maximal activity. The inset shows the first 10 minutes of the time course. B, Trypsinogens carrying the p.S200A mutation were incubated with 100 nM human cationic trypsin at 37°C in 0.1 M Tris-HCl (pH 8.0) and 1 mM $CaCl_2$ in 100-μL final volume. At the indicated times, reactions were precipitated with 10% trichloroacetic acid (final concentration) and analyzed using 15% SDS-PAGE and Coomassie Blue staining. The lower molecular weight bands represent double-chain forms of trypsinogen and trypsin cleaved at the Arg122-Val123 peptide bond. p.insIDK = p.K23_I24insIDK.

tetra-Asp motif in the trypsinogen activation peptide has been known as a specific recognition motif for enteropeptidase, at least in the context of the bovine enzymes.[26]

The lysosomal cysteine protease cathepsin B has been recognized as a pathological activator of trypsinogen in acute models of experimental pancreatitis.[27–30] We tested the effect of the p.K23_I24insIDK mutation on cathepsin B–mediated trypsinogen activation at pH 4.0, where autoactivation is minimal. Remarkably, the mutant was activated by cathepsin B at a markedly elevated rate, which seemed approximately

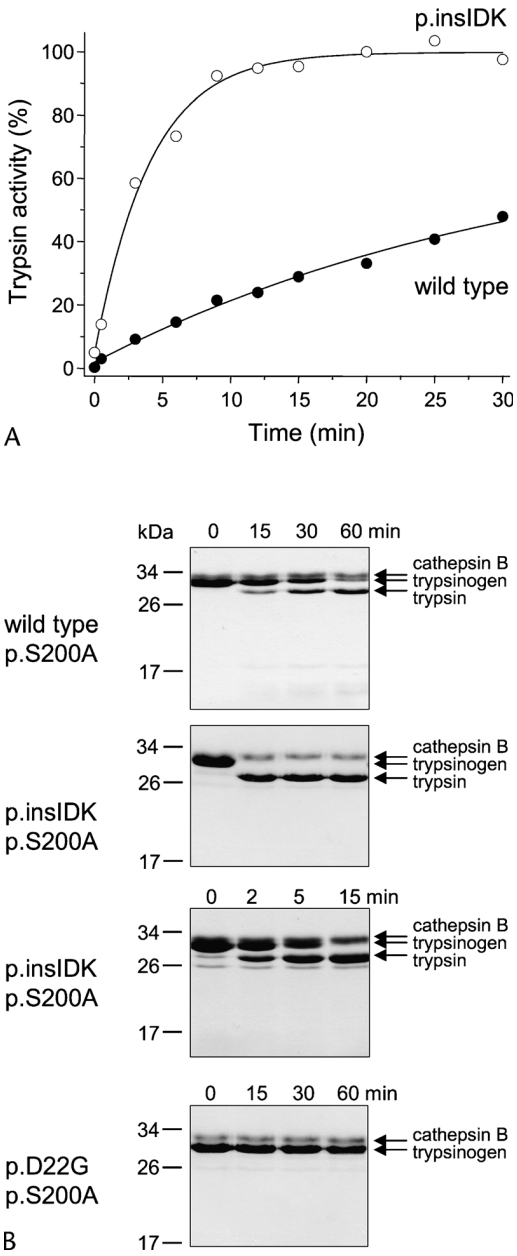

FIGURE 3. Effect of the p.K23_I24insIDK mutation on the activation of human cationic trypsinogen with cathepsin B. A, Trypsinogens at 2-μM concentration were activated with human cathepsin B (37 μg/mL, ~1.3 μM) at 37°C in 0.1 M Na-acetate buffer (pH 4.0), 1 mM EDTA, and 1 mM dithiothreitol (final concentrations) in 50-μL final volume. Aliquots (2 μL) were withdrawn at indicated times, and trypsin activity was determined. Trypsin activity was expressed as percentage of the maximal activity. B, Trypsinogens carrying the p.S200A mutation were activated with human cathepsin B (37 μg/mL, ~1.3 μM; 74 μg/mL, ~2.6 μM for p.D22G) at 37°C in 0.1 M Na-acetate buffer (pH 4.0) 1 mM K-EDTA, and 1 mM dithiothreitol in 100-μL final volume. At the indicated times, reactions were precipitated with 10% trichloroacetic acid (final concentration) and analyzed using 15% SDS-PAGE and Coomassie Blue staining. p.insIDK = p.K23_I24insIDK.

5- to 10-fold higher than that of wild type (Fig. 3A). Using p.S200A-trypsinogens, we measured the rates of conversion in a more precise manner and found that the p.K23_I24insIDK mutant was activated by cathepsin B 10-fold faster than wild-type cationic trypsinogen (Fig. 3B). As described previously, mutant p.D22G was resistant to cathepsin B–mediated activation.[10,31] More recently, cathepsin L was shown to degrade trypsinogen, and active trypsin accumulation during pancreatitis was attributed not only to cathepsin B–mediated activation but also to a defect in cathepsin L–mediated degradation.[32,33] We found no change in the degradation of the p.K23_I24insIDK mutant by cathepsin L (pH 4.0, 37°C) as compared with wild-type cationic trypsinogen (data not shown).

Cleavage of the Activation Peptide in the p.K23_I24insIDK Mutant Cationic Trypsinogen

The mutant activation peptide sequence contains 2 Lys-Ile peptides bonds (Fig. 1B). Although activation of trypsinogen to trypsin requires proteolysis of the second site, cleavage after the first Lys may modify the efficiency of the second cleavage. Therefore, we sought to clarify whether both sites were cleaved. For these experiments, we used the p.S200A-trypsinogens that we activated with trypsin (pH 8.0), enteropeptidase (pH 8.0), and cathepsin B (pH 4.0). The activation reactions were separated on SDS-PAGE, transferred to polyvinylidine fluoride membranes, and trypsin bands were subjected to N-terminal sequence analysis by Edman degradation. To capture cleavage intermediates, we sequenced trypsin bands early in the reaction when less than half of the trypsinogen was converted to a trypsin band. We found that trypsin and cathepsin B cleaved only the second (activating) Lys-Ile peptide bond, whereas enteropeptidase cleaved both Lys-Ile peptide bonds with equal efficacy. Cleavage after the first Lys-Ile peptide bond resulted in an N-terminally truncated trypsinogen, which was eventually completely cleaved at the second Lys-Ile peptide bond by enteropeptidase (see Supplementary Figure 3, Supplemental Digital Content 3, http://links.lww.com/MPA/A41).

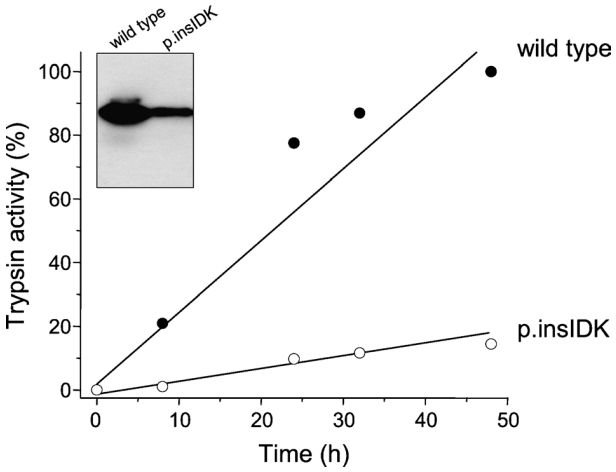

FIGURE 4. Secretion of the p.K23_I24insIDK cationic trypsinogen mutant from transiently transfected HEK 293T cells. At 8, 24, 32, and 48 hours after transfection, conditioned media were collected, and 20-μL medium was supplemented with 0.1 M Tris-HCl (pH 8.0) and 1 mM $CaCl_2$ in 50-μL volume, and trypsinogen was activated with 28 ng/mL human enteropeptidase for 1 hour at 37°C. Trypsin activity was then measured by adding 150 μL of the chromogenic substrate, *N*-benzyloxycarbonyl-Gly-Pro-Arg-*p*-nitroanilide, to 0.14-mM final concentration. Trypsin activities were expressed as percentage of the 48-hour wild-type activity. The average of 2 independent transfection experiments is shown. For clarity, the error bars have been omitted; the SEM was within 15%. Inset: 8 hours after transfection, 20-μL aliquots of conditioned media were electrophoresed on 15% SDS-PAGE and analyzed using Western blotting as described in the ''Materials and Methods'' section.

Secretion of the p.K23_I24insIDK Mutant From Transfected Cells

Recently, we demonstrated that activation peptide mutants that undergo robust autoactivation in the test tube also were autoactivating inside living cells.[10] Intracellular autoactivation resulted in diminished trypsinogen secretion. To test whether secretion of the strongly autoactivating p.K23_I24insIDK mutant would be reduced, we transfected HEK 293T cells with wild-type and p.K23_I24insIDK mutant cationic trypsinogen and measured secretion of trypsinogens from the conditioned medium by activity assays and immunoblot. The transfected cells exhibited healthy morphology during the time course studied with no signs of cell death. As shown in Figure 4, mutant p.K23_I24insIDK was secreted to significantly lower levels than wild-type cationic trypsinogen, suggesting that the p.K23_I24insIDK mutant suffered intracellular autoactivation.

DISCUSSION

There are a number of important observations in this study which set it apart from a typical mutation report. This is the first account of an intragenic duplication within the *PRSS1* gene in association with hereditary pancreatitis. The human trypsinogen genes are located on chromosome 7q35, intercalated between the beta T-cell receptor genes, at a locus highly active in recombination. This organization seems beneficial for the evolution of trypsinogens that tend to undergo extensive gene-duplication and gene-loss events during speciation, resulting in distinctive trypsinogen gene families.[9,34] On the other hand, unwanted genetic rearrangements, such as gene conversions, duplications, or triplications, can result in novel pathogenic alleles in hereditary pancreatitis.[13–17,34] In contrast to the previously reported large-scale gene duplications, in our family, the duplication was confined only to a 9-nucleotide segment within exon-2 without any evidence of more extensive genetic changes.

Interestingly, the duplication was identified only in the father and his 2 sons (Fig. 1A), whereas it was absent in the grandparents or the father's siblings, indicating that it was de novo generated in the father. Ours is the second report on capturing a mutational event leading to hereditary pancreatitis. Simon et al.[35] found a de novo p.R122H mutation in their cohort, and their subsequent studies indicated that *PRSS1* mutations are characteristically not inherited from a common founder, even when local clustering of families is observed.[36]

Intragenic duplications are likely to result in a frame shift and truncated, nonfunctional protein. In this case, however, the reading frame was kept, and at the amino acid level, the duplication generated an insertion within the trypsinogen activation peptide (Fig. 1B). As expected from this alteration, the activation properties of cationic trypsinogen have been affected in profound ways. Trypsin-mediated trypsinogen activation (autoactivation) and cathepsin B–mediated trypsinogen activation were both increased by an order of magnitude, an effect size never before seen with the known *PRSS1* mutants. With respect to autoactivation, the p.K23_I24insIDK mutant's phenotype is consistent with the reported properties of other *PRSS1* mutations

affecting the activation peptide (p.D19A, p.D22G, and p.K23R), which all result in markedly increased autoactivation.[9,10,23,25] Mechanistically, the increased autoactivation of p.K23_I24insIDK is explained by the disruption of inhibitory interactions between the negatively charged tetra-Asp motif in the activation peptide and trypsin.[23] In the p.K23_I24insIDK mutant, Asp21 is replaced with a hydrophobic Ile residue, and Asp20 is replaced with a positively charged Lys (Fig. 1B). A recent study found that, at the cellular level, increased autoactivation results in diminished trypsinogen secretion and eventual apoptotic death of acinar cells.[10] We confirmed using HEK 293T cells that the p.K23_I24insIDK mutant was secreted at markedly reduced rates, indicating that it also undergoes autoactivation inside living cells.

Cathepsin B has long been known as a pathological activator of trypsinogen in experimental models of acute pancreatitis, cerulein-induced pancreatitis in particular.[27–30] The effect of hereditary pancreatitis-associated mutations on cathepsin B–mediated trypsinogen activation has been studied in detail previously. Mutants p.D19A, p.N29I, p.N29T, p.E79K, and p.R122H exhibited unchanged activation characteristics, whereas mutant p.K23R was activated slowly, and mutant p.D22G was resistant to activation by cathepsin B.[10,29,31,37] Mutant p.K23_I24insIDK is the first cationic trypsinogen variant that exhibits increased sensitivity to cathepsin B–mediated activation and thus stands in contrast with all other PRSS1 mutants studied to date. We believe that this property is related to the longer activation peptide that allows extended contacts with the activating enzyme.

In summary, we identified a unique intragenic duplication within exon-2 of the *PRSS1* gene (c.63_71dup) in a hereditary pancreatitis family from Denmark. The duplication results in the p.K23_I24insIDK insertional mutation within the activation peptide of cationic trypsinogen. Activation of the p.K23_I24insIDK mutant by trypsin (autoactivation) or by cathepsin B is markedly increased, confirming the significance of the trypsin-dependent pathological pathway in hereditary pancreatitis.

ACKNOWLEDGMENTS

The authors thank all the family members who participated. The authors also thank Steen Gregersen for technical assistance; Rasmus Gaardskær Nielsen, Marianne S. Jakobsen (Department of Pediatrics, Odense University Hospital, Denmark), and Claus Hovendal (Department of Upper Surgery, Odense University Hospital, Denmark) for referring the index patient for genetic testing; and David McCourt (Midwest Analytical, Inc, St Louis, Mo) for performing the protein sequencing.

REFERENCES

1. Whitcomb DC, Gorry MC, Preston RA, et al. Hereditary pancreatitis is caused by a mutation in the cationic trypsinogen gene. *Nat Genet*. 1996;14:141–145.
2. Teich N, Rosendahl J, Tóth M, et al. Mutations of human cationic trypsinogen (PRSS1) and chronic pancreatitis. *Hum Mutat*. 2006;27:721–730.
3. Howes N, Lerch MM, Greenhalf W, et al. Clinical and genetic characteristics of hereditary pancreatitis in Europe. *Clin Gastroenterol Hepatol*. 2004;2:252–261.
4. Rebours V, Boutron-Ruault MC, Schnee M, et al. The natural history of hereditary pancreatitis: a national series. *Gut*. 2009;58:97–103.
5. Otsuki M, Nishimori I, Hayakawa T, et al. Hereditary pancreatitis: clinical characteristics and diagnostic criteria in Japan. *Pancreas*. 2004;28:200–206.
6. Keiles S, Kammesheidt A. Identification of CFTR, PRSS1, and SPINK1 mutations in 381 patients with pancreatitis. *Pancreas*. 2006; 33:221–227.
7. Szmola R, Sahin-Tóth M. Uncertainties in the classification of human cationic trypsinogen (*PRSS1*) variants as hereditary pancreatitis-associated mutations. *J Med Genet*. 2010;47:348–350.
8. Sahin-Tóth M. Biochemical models of hereditary pancreatitis. *Endocrinol Metab Clin North Am*. 2006;35:303–312.
9. Chen JM, Kukor Z, Le Maréchal C, et al. Evolution of trypsinogen activation peptides. *Mol Biol Evol*. 2003;20:1767–1777.
10. Kereszturi E, Sahin-Tóth M. Intracellular autoactivation of human cationic trypsinogen mutants causes reduced trypsinogen secretion and acinar cell death. *J Biol Chem*. 2009;284:33392–33399.
11. Chen JM, Raguenes O, Férec C, et al. A CGC>CAT gene conversion-like event resulting in the R122H mutation in the cationic trypsinogen gene and its implication in the genotyping of pancreatitis. *J Med Genet*. 2000;37:E36.
12. Howes N, Greenhalf W, Rutherford S, et al. A new polymorphism for the R122H mutation in hereditary pancreatitis. *Gut*. 2001;48:247–250.
13. Teich N, Nemoda Z, Kohler H, et al. Gene conversion between functional trypsinogen genes PRSS1 and PRSS2 associated with chronic pancreatitis in a six-year-old girl. *Hum Mutat*. 2005;25: 343–347.
14. Masson E, Le Maréchal C, Delcenserie R, et al. Hereditary pancreatitis caused by a double gain-of-function trypsinogen mutation. *Hum Genet*. 2008;123:521–529.
15. Le Maréchal C, Masson E, Chen JM, et al. Hereditary pancreatitis caused by triplication of the trypsinogen locus. *Nat Genet*. 2006; 38:1372–1374.
16. Masson E, Le Maréchal C, Chandak GR, et al. Trypsinogen copy number mutations in patients with idiopathic chronic pancreatitis. *Clin Gastroenterol Hepatol*. 2008;6:82–88.
17. Chauvin A, Chen JM, Quemener S, et al. Elucidation of the complex structure and origin of the human trypsinogen locus triplication. *Hum Mol Genet*. 2009;18:3605–3614.
18. Pál G, Sprengel G, Patthy A, et al. Alteration of the specificity of ecotin, an E. coli serine proteinase inhibitor, by site directed mutagenesis. *FEBS Lett*. 1994;342:57–60.
19. Pál G, Szilágyi L, Gráf L. Stable monomeric form of an originally dimeric serine proteinase inhibitor, ecotin, was constructed via site directed mutagenesis. *FEBS Lett*. 1996;385:165–170.
20. Lengyel Z, Pál G, Sahin-Tóth M. Affinity purification of recombinant trypsinogen using immobilized ecotin. *Protein Expr Purif*. 1998; 12:291–294.
21. Sahin-Tóth M. Human cationic trypsinogen. Role of Asn-21 in zymogen activation and implications in hereditary pancreatitis. *J Biol Chem*. 2000;275:22750–22755.
22. Sahin-Tóth M, Tóth M. Gain-of-function mutations associated with hereditary pancreatitis enhance autoactivation of human cationic trypsinogen. *Biochem Biophys Res Commun*. 2000;278:286–289.
23. Nemoda Z, Sahin-Tóth M. The tetra-aspartate motif in the activation peptide of human cationic trypsinogen is essential for autoactivation control but not for enteropeptidase recognition. *J Biol Chem*. 2005; 280:29645–29652.
24. Nemoda Z, Sahin-Tóth M. Chymotrypsin C (caldecrin) stimulates autoactivation of human cationic trypsinogen. *J Biol Chem*. 2006;281:11879–11886.
25. Teich N, Ockenga J, Hoffmeister A, et al. Chronic pancreatitis associated with an activation peptide mutation that facilitates trypsin activation. *Gastroenterology*. 2000;119:461–465.
26. Lu D, Fütterer K, Korolev S, et al. Crystal structure of enteropeptidase light chain complexed with an analog of the trypsinogen activation peptide. *J Mol Biol*. 1999;292:361–373.
27. Figarella C, Miszczuk-Jamska B, Barrett AJ. Possible lysosomal activation of pancreatic zymogens. Activation of both human trypsinogens by cathepsin B and spontaneous acid. Activation of human trypsinogen 1. *Biol Chem Hoppe Seyler*. 1988;369(suppl): 293–298.

28. Halangk W, Lerch MM, Brandt-Nedelev B, et al. Role of cathepsin B in intracellular trypsinogen activation and the onset of acute pancreatitis. *J Clin Invest*. 2000;106:773–781.
29. Kukor Z, Mayerle J, Krüger B, et al. Presence of cathepsin B in the human pancreatic secretory pathway and its role in trypsinogen activation during hereditary pancreatitis. *J Biol Chem*. 2002;277:21389–21396.
30. Saluja AK, Lerch MM, Phillips PA, et al. Why does pancreatic overstimulation cause pancreatitis? *Annu Rev Physiol*. 2007; 69:249–269.
31. Teich N, Bödeker H, Keim V. Cathepsin B cleavage of the trypsinogen activation peptide. *BMC Gastroenterol*. 2002;2:16.
32. Mareninova OA, Hermann K, French SW, et al. Impaired autophagic flux mediates acinar cell vacuole formation and trypsinogen activation in rodent models of acute pancreatitis. *J Clin Invest*. 2009;119: 3340–3355.
33. Wartmann T, Mayerle J, Kähne T, et al. Cathepsin L inactivates human trypsinogen, whereas cathepsin L-deletion reduces the severity of pancreatitis in mice. *Gastroenterology*. 2010;138:726–737.
34. Chen JM, Férec C. Gene conversion-like missense mutations in the human cationic trypsinogen gene and insights into the molecular evolution of the human trypsinogen family. *Mol Genet Metab*. 2000;71:463–469.
35. Simon P, Weiss FU, Zimmer KP, et al. Spontaneous and sporadic trypsinogen mutations in idiopathic pancreatitis. *JAMA*. 2002;288:2122.
36. Weiss FU, Zenker M, Ekici AB, et al. Local clustering of PRSS1 R122H mutations in hereditary pancreatitis patients from Northern Germany. *Am J Gastroenterol*. 2008;103:2585–2588.
37. Teich N, Le Marechal C, Kukor Z, et al. Interaction between trypsinogen isoforms in genetically determined pancreatitis: mutation E79K in cationic trypsin (PRSS1) causes increased transactivation of anionic trypsinogen (PRSS2). *Hum Mutat*. 2004;23:22–31.

Articles related to the subject of the thesis and cited in the thesis

III.

GASTROENTEROLOGY 2011;141:2228–2239

Trypsin Reduces Pancreatic Ductal Bicarbonate Secretion by Inhibiting CFTR Cl^- Channels and Luminal Anion Exchangers

PETRA PALLAGI,* VIKTÓRIA VENGLOVECZ,‡ ZOLTÁN RAKONCZAY Jr,* KATALIN BORKA,§ ANNA KOROMPAY,§ BÉLA ÓZSVÁRI,* LINDA JUDÁK,* MIKLÓS SAHIN–TÓTH,‖ ANDREA GEISZ,*,‖ ANDREA SCHNÚR,*,‖ JÓZSEF MALÉTH,* TAMÁS TAKÁCS,* MIKE A. GRAY,¶ BARRY E. ARGENT,¶ JULIA MAYERLE,# MARKUS M. LERCH,# TIBOR WITTMANN,* and PÉTER HEGYI*

**First Department of Medicine and ‡Department of Pharmacology, University of Szeged, Szeged, Hungary; §2nd Department of Pathology, Semmelweis University, Budapest, Hungary; ‖Department of Molecular and Cell Biology, Henry M. Goldman School of Dental Medicine, Boston University, Boston, Massachusetts; ¶Institute for Cell & Molecular Biosciences, Newcastle University, Newcastle upon Tyne, England; and #Department of Medicine A, Greifswald University Hospital, Greifswald, Germany*

BACKGROUND & AIMS: The effects of trypsin on pancreatic ductal epithelial cells (PDECs) vary among species and depend on the localization of proteinase-activated receptor 2 (PAR-2). We compared PAR-2 localization in human and guinea-pig PDECs, and used isolated guinea pig ducts to study the effects of trypsin and a PAR-2 agonist on bicarbonate secretion. **METHODS:** PAR-2 localization was analyzed by immunohistochemistry in guinea pig and human pancreatic tissue samples (from 15 patients with chronic pancreatitis and 15 without pancreatic disease). Functionally, guinea pig PDECs were studied by microperfusion of isolated ducts, measurements of intracellular pH and intracellular Ca^{2+} concentration, and patch clamp analysis. The effect of pH on trypsinogen autoactivation was assessed using recombinant human cationic trypsinogen. **RESULTS:** PAR-2 localized to the apical membrane of human and guinea pig PDECs. Trypsin increased intracellular Ca^{2+} concentration and intracellular pH and inhibited secretion of bicarbonate by the luminal anion exchanger and the cystic fibrosis transmembrane conductance regulator (CFTR) Cl^- channel. Autoactivation of human cationic trypsinogen accelerated when the pH was reduced from 8.5 to 6.0. PAR-2 expression was strongly down-regulated, at transcriptional and protein levels, in the ducts of patients with chronic pancreatitis, consistent with increased activity of intraductal trypsin. Importantly, in PAR-2 knockout mice, the effects of trypsin were markedly reduced. **CONCLUSIONS: Trypsin reduces pancreatic ductal bicarbonate secretion via PAR-2–dependent inhibition of the apical anion exchanger and the CFTR Cl^- channel. This could contribute to the development of chronic pancreatitis by decreasing luminal pH and promoting premature activation of trypsinogen in the pancreatic ducts.**

Keywords: Acinar Cells; Ductal Epithelium; Animal Model; Pancreatic Enzymes.

BASIC AND TRANSLATIONAL PANCREAS

Trypsinogen is the most abundant digestive protease in the pancreas. Under physiologic conditions, trypsinogen is synthesized and secreted by acinar cells, transferred to the duodenum via the pancreatic ducts, and then activated by enteropeptidase in the small intestine.[1] There is substantial evidence that early intra-acinar[2,3] or luminal[4,5] activation of trypsinogen to trypsin is a key and common event in the development of acute and chronic pancreatitis. Importantly, almost all forms of acute pancreatitis are due to autodigestion of the gland by pancreatic enzymes.[6]

Several studies have shown that trypsin stimulates enzyme secretion from acinar cells via proteinase-activated receptor 2 (PAR-2),[7,8] whereas the effect of trypsin on pancreatic ductal epithelial cells (PDECs) is somewhat controversial. Trypsin activates ion channels in dog PDECs[9] and stimulates bicarbonate secretion in the CAPAN-1 human pancreatic adenocarcinoma cell line,[10] whereas it dose-dependently inhibits bicarbonate efflux from bovine PDECs.[11] The effect of trypsin differs not only among species, but also with respect to the localization of PAR-2. When PAR-2 is localized to the basolateral membrane and activated by trypsin, the result is stimulation of bicarbonate secretion.[9,10] In contrast, when the receptor is localized to the luminal membrane, the effect is inhibition.[11] Interestingly, there are no data available concerning the effects of trypsin on guinea pig PDECs which, in terms of bicarbonate secretion, are an excellent model of human PDECs.[12]

The human pancreatic ductal epithelium secretes an alkaline fluid that may contain up to 140 mmol/L $NaHCO_3$.[12,13] The first step in HCO_3^- secretion is the accumulation of HCO_3^- inside the cell, which is driven by basolateral Na^+/HCO_3^- cotransporters, Na^+/H^+ exchangers, and H^+-adenosine triphosphatases.[12,13] Only 2 transporters have been identified on the apical membrane of

Abbreviations used in this paper: BAPTA-AM, 1,2-bis(o-aminophenoxy)ethane-*N,N,N′,N′*-tetraacetic acid; CFTR, cystic fibrosis transmembrane conductance regulator Cl^- channel; CFTRinh-172, CFTR inhibitor-172; $[Ca^{2+}]_i$, intracellular Ca^{2+} concentration; H_2DIDS, dihydro-4,4′-diisothiocyanostilbene-2,2′-disulfonic acid; PAR-2, proteinase-activated receptor-2; PAR-2-AP, PAR-2 activating peptide; PAR-2-ANT, PAR-2 antagonist; PDEC, pancreatic ductal epithelial cell; pH_i, intracellular pH; pH_L, luminal pH; SBTI, soybean trypsin inhibitor; SLC26, solute carrier family 26.

0016-5085/$36.00
doi:10.1053/j.gastro.2011.08.039

cells in the proximal ducts that are the major sites of HCO_3^- secretion: cystic fibrosis transmembrane conductance regulator (CFTR) and the solute carrier family 26 (SLC26) anion exchangers.[12,13] How these transporters act in concert to produce a high HCO_3^- secretion is controversial.[14] Most likely, HCO_3^- is secreted through the anion exchanger until the luminal concentration reaches about 70 mmol/L, after which the additional HCO_3^- required to raise the luminal concentration to 140 mmol/L is transported via CFTR.[15,16]

The role of PAR-2 in experimental acute pancreatitis is also controversial and highly dependent on the model of pancreatitis studied. PAR-2 was found to be protective in secretagogue-induced pancreatitis in mice[7,17–19] and rats.[20] However, PAR-2 is clearly harmful when pancreatitis is evoked by the clinically more relevant luminal administration of bile salts in mice.[17]

In this study, we show for the first time that (1) PAR-2 is localized to the apical membrane of the human proximal PDECs, (2) the localization of PAR-2 in the guinea pig pancreas is identical to that in the human gland, (3) trypsin markedly reduces bicarbonate efflux through a dihydro-4,4′-diisothiocyanostilbene-2,2′-disulfonic acid (H_2DIDS)-sensitive apical SLC26 anion exchanger and strongly inhibits CFTR, (4) a decrease in pH within the ductal lumen will strongly accelerate the autoactivation of trypsinogen, and (5) trypsin down-regulates PAR-2 expression at both transcriptional and protein levels in PDECs of patients with chronic pancreatitis.

Materials and Methods

A brief outline of the materials and methods is given in the following text. For further details, please see Supplementary Materials and Methods.

Solutions

The compositions of the solutions used for microfluorimetry are shown in Table 1.

Isolation of Pancreatic Ducts and Individual Ductal Cells

Small intralobular proximal ducts and individual ductal cells were isolated from guinea pigs or PAR-2 wild-type (PAR-$2^{+/+}$) and knockout (PAR-$2^{-/-}$) mice with a C57BL6 background by microdissection as described previously.[21]

Table 1. Composition of Solutions for Microfluorimetry Studies

	Standard HEPES	Standard HCO_3^-	Cl^--free HCO_3^-	Ca^{2+}-free HEPES
NaCl	130	115		132
KCl	5	5		5
$MgCl_2$	1	1		1
$CaCl_2$	1	1		
Sodium HEPES	10			10
Glucose	10	10	10	10
$NaHCO_3$		25	25	
Sodium gluconate			115	
Magnesium gluconate			1	
Calcium gluconate			6	
Potassium sulfate			2.5	

NOTE. Values are concentrations in mmol/L.

Measurement of Intracellular pH and Ca^{2+} Concentration

Intracellular pH (pH_i) and calcium concentration ($[Ca^{2+}]_i$) were estimated by microfluorimetry using the pH- and Ca^{2+}-sensitive fluorescent dyes 2,7-bis-(2-carboxyethyl)-5-(and-6-)carboxyfluorescein, acetoxymethyl ester (BCECF-AM) and 2-(6-(bis(carboxymethyl)amino)-5-(2-(2-(bis(carboxymethyl)amino)-5-methylphenoxy)-ethoxy)-2-benzofuranyl)-5-oxazolecarboxylic acetoxymethyl ester (FURA 2-AM), respectively.

Microperfusion of Intact Pancreatic Ducts

The luminal perfusion of the cultured ducts was performed as described previously.[22]

Electrophysiology

CFTR Cl^- channel activity was investigated by whole cell patch clamp recordings on guinea pig single pancreatic ductal cells.

Measuring Autoactivation of Trypsinogen

Autoactivation of human cationic trypsinogen was determined in vitro at pH values ranging from 6.0 to 8.5. Experimental details are described in Supplementary Materials and Methods.

Immunohistochemistry

Five guinea pig, 2 PAR-$2^{+/+}$, 2 PAR-$2^{-/-}$, and 30 human pancreata were studied to analyze the expression pattern of PAR-2 protein. Relative optical densitometry was used to quantify the protein changes in the histologic sections. Patients' data and the full methods are described in Supplementary Supplementary Materials and Methods.

Real-Time Reverse-Transcription Polymerase Chain Reaction

RNA was isolated from 30 human pancreata. Following reverse transcription, messenger RNA (mRNA) expression of PAR-2 and β-actin was determined by real-time polymerase chain reaction analysis.

Results

Expression of PAR-2 in Guinea Pig and Human Pancreata

PAR-2 was highly expressed in the luminal membrane of small intralobular and interlobular ducts (Figure 1*A* [i]; cuboidal epithelial cells forming the proximal pancreatic ducts) but was almost undetectable in the larger interlobular ducts (Figure 1*A* [ii]; columnar epithelial cells forming the distal pancreatic ducts). The localization of PAR-2 in the human pancreas was identical to that in the guinea pig gland (Figure 1*A* [iv–vi]). Measurements of relative optical density confirmed the significant differences between the expression of PAR-2 in small intralobular and interlobular ducts and the larger interlobular ducts in both species (Figure 1*C*).

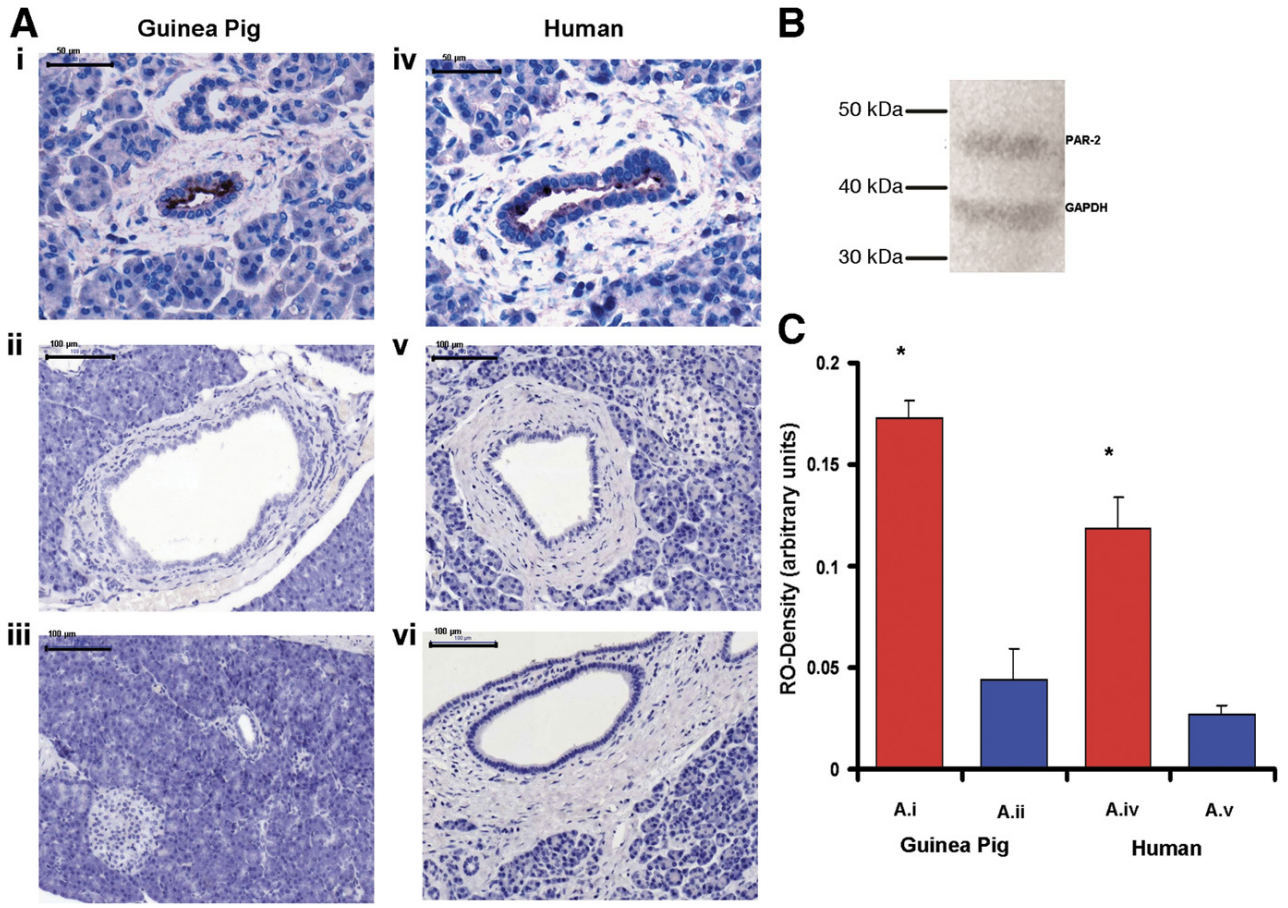

Figure 1. Localization of PAR-2 on human and guinea pig pancreatic ducts. Light micrographs of (*A* [i–iii]) guinea pig and (*A* [iv–vi]) human pancreas are shown. (i) PAR-2 is localized to the luminal membrane of PDECs in small intralobular and interlobular ducts (original magnification 400×). (ii) Large interlobular ducts do not express PAR-2 (original magnification 200×). (iii) No primary antiserum (original magnification 200×). (iv and v) Sections from human pancreas exhibit a similar localization of PAR-2 compared with the guinea pig gland (original magnification 400× and 200×). (vi) No primary antiserum (original magnification 200×). (*B*) Western blot analysis was used to determine the specificity of the PAR-2 antibody. Polyclonal anti–PAR-2 showed a single 44-kilodalton band. (*C*) Quantitative measurement of relative optical densities (RO-Density) of small intralobular and interlobular ducts (A.i,iv), and large interlobular ducts (A.ii,v) is shown. n = 12. $^{*}P < .05$ vs A.ii or A.v, respectively. *Scale bar* = 50 μm for *A* (i, iv) and 100 μm for *A* (ii and iii) and *A* (v and vi).

Luminal Administration of PAR-2-AP and Trypsin Induces Dose-Dependent $[Ca^{2+}]_i$ Signals

Because PAR-2 expression was detected only on the luminal membrane of intralobular duct cells, we used the microperfusion technique to see whether these receptors can be activated by PAR-2 agonists. First, the experiments were performed at pH 7.4 to understand the effects of trypsin and PAR-2 under quasi-physiologic conditions (Figure 2). The fluorescent images in Figure 2*A* clearly show that luminal administration of PAR-2 activating peptide (PAR-2-AP) increased $[Ca^{2+}]_i$ in perfused pancreatic ducts. The $[Ca^{2+}]_i$ response was dose dependent and consisted of a peak in $[Ca^{2+}]_i$ that decayed in the continued presence of the agonist, possibly reflecting PAR-2 inactivation or depletion of intracellular Ca^{2+} stores (Figure 2*B*). Pretreatment of PDECs with 10 μmol/L PAR-2 antagonist (PAR-2-ANT) for 10 minutes completely blocked the effects of 10 μmol/L PAR-2-AP on $[Ca^{2+}]_i$ (Figure 2*A* and *C*). Removal of extracellular Ca^{2+} had no effect on the increase in $[Ca^{2+}]_i$ evoked by luminal administration of 10 μmol/L PAR-2-AP; however, preloading ducts with the calcium chelator 1,2-bis(o-aminophenoxy)ethane-*N,N,N′,N′*-tetraacetic acid (BAPTA-AM) at 40 μmol/L totally blocked the response (Figure 2*A* and *C*).

Trypsin also induced a dose-dependent elevation in $[Ca^{2+}]_i$ similar to that evoked by PAR-2-AP (Figure 2*E* and *F*). Addition of 5 μmol/L soybean trypsin inhibitor (SBTI), 10 μmol/L PAR-2-ANT, and 40 μmol/L BAPTA-AM totally blocked the increase in $[Ca^{2+}]_i$ (Figure 2*D* and *F*). These data show that trypsin activates PAR-2 on the luminal membrane of the duct cell, which leads to release of Ca^{2+} from intracellular stores and an elevation of $[Ca^{2+}]_i$.

Because the pH of pancreatic juice can vary between approximately 6.8 and 8.0,[23,24] we also evaluated the effects of trypsin and PAR-2-AP on $[Ca^{2+}]_i$ at these pH values (Supplementary Figures 1 and 2, respectively). The

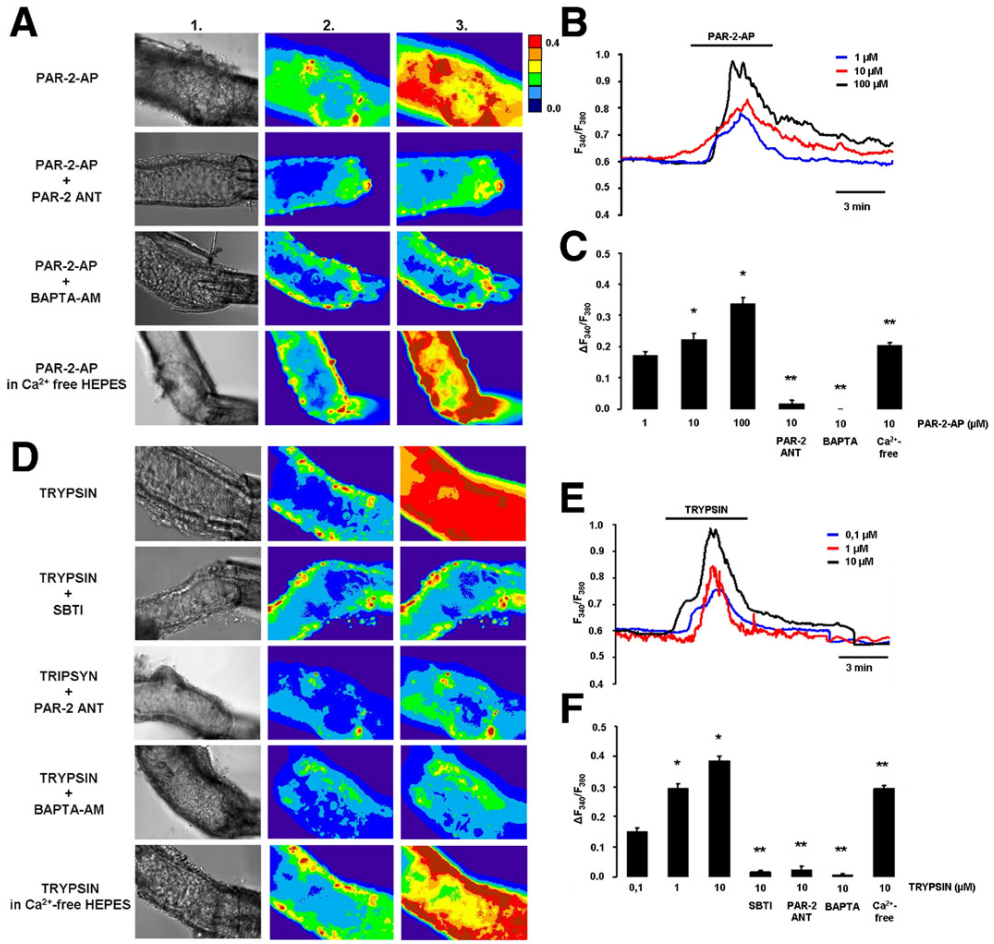

Figure 2. Effects of PAR-2-AP and trypsin on $[Ca^{2+}]_i$ in microperfused guinea pig pancreatic ducts at pH 7.4. (*A*) Light (1) and fluorescent ratio images (2 and 3) of microperfused pancreatic ducts showing the effects of luminal administration of 10 µmol/L PAR-2-AP, 10 µmol/L PAR-2-ANT, or 40 µmol/L BAPTA-AM on $[Ca^{2+}]_i$. Images were taken before (1 and 2) and after (3) exposure of the ducts to PAR-2-AP or trypsin. (*B* and *C*) Representative experimental traces and summary data of the changes in $[Ca^{2+}]_i$. (*D*) The same protocol was used to evaluate the effects of trypsin. Addition of 5 µmol/L SBTI was used to inhibit trypsin activity. (*E* and *F*) Representative experimental traces and summary data of the changes in $[Ca^{2+}]_i$. n = 5 for all groups. $^{*}P < .05$ vs 1 µmol/L PAR-2-AP or 0.1 µmol/L trypsin, respectively. $^{**}P < .001$ vs 10 µmol/L PAR-2-AP or 10 µmol/L trypsin, respectively.

elevations of $[Ca^{2+}]_i$ at pH 6.8 and 8.0 were generally very similar to the changes observed at pH 7.4. However, the increases in $[Ca^{2+}]_i$ evoked by 1 µmol/L PAR-2-AP and 0.1 µmol/L trypsin were significantly lower at pH 6.8 compared with either pH 7.4 or 8.0 (Supplementary Figure 3).

Luminal Exposure to PAR-2-AP and Trypsin Evokes Intracellular Alkalosis in PDECs

Figure 3 shows pH_i recordings from microperfused pancreatic ducts. Luminal application of the CFTR inhibitor (CFTRinh) 172 (10 µmol/L) and the anion exchanger inhibitor H_2DIDS (500 µmol/L) induced intracellular alkalization in PDECs (Figure 3*A* [i]). These data indicate that when bicarbonate efflux across the luminal membrane of PDECs (ie, bicarbonate secretion) is blocked, elevation of duct cell pH_i occurs, presumably because the basolateral transporters continue to move bicarbonate ions into the duct cell. Note also that the increase in pH_i evoked by the inhibitors is not sustained and begins to reverse before the inhibitors are withdrawn (Figure 3*A* [i]), which might be explained by the regulation of pH_i by basolateral acid/base transporters.

Both luminal PAR-2-AP and trypsin induced a dose-dependent elevation of pH_i (Figure 3*A* [ii and iii]), suggesting that activation of PAR-2 inhibits bicarbonate efflux across the apical membrane of the duct cell. Preincubation of PDECs with either 10 µmol/L PAR-2-ANT or 5 µmol/L SBTI or 40 µmol/L BAPTA-AM for 30 minutes totally blocked the effect of trypsin on pH_i (Figure 3*A* [iv]). The inhibitory effect of the calcium chelator BAPTA-AM suggests that the actions of trypsin and PAR-2-AP on pH_i are mediated by the increase in $[Ca^{2+}]_i$ that they evoke (Figure 2). Therefore, in this case, the transient nature of the pH_i response may reflect the transient effect that PAR-2 activators have on $[Ca^{2+}]_i$ (Figure 2*B* and *E*), as well as pH_i regulation by basolateral acid/base transporters.

Next we tested the effects of trypsin on pH_i in Cl^--free conditions and during pharmacologic inhibition of the

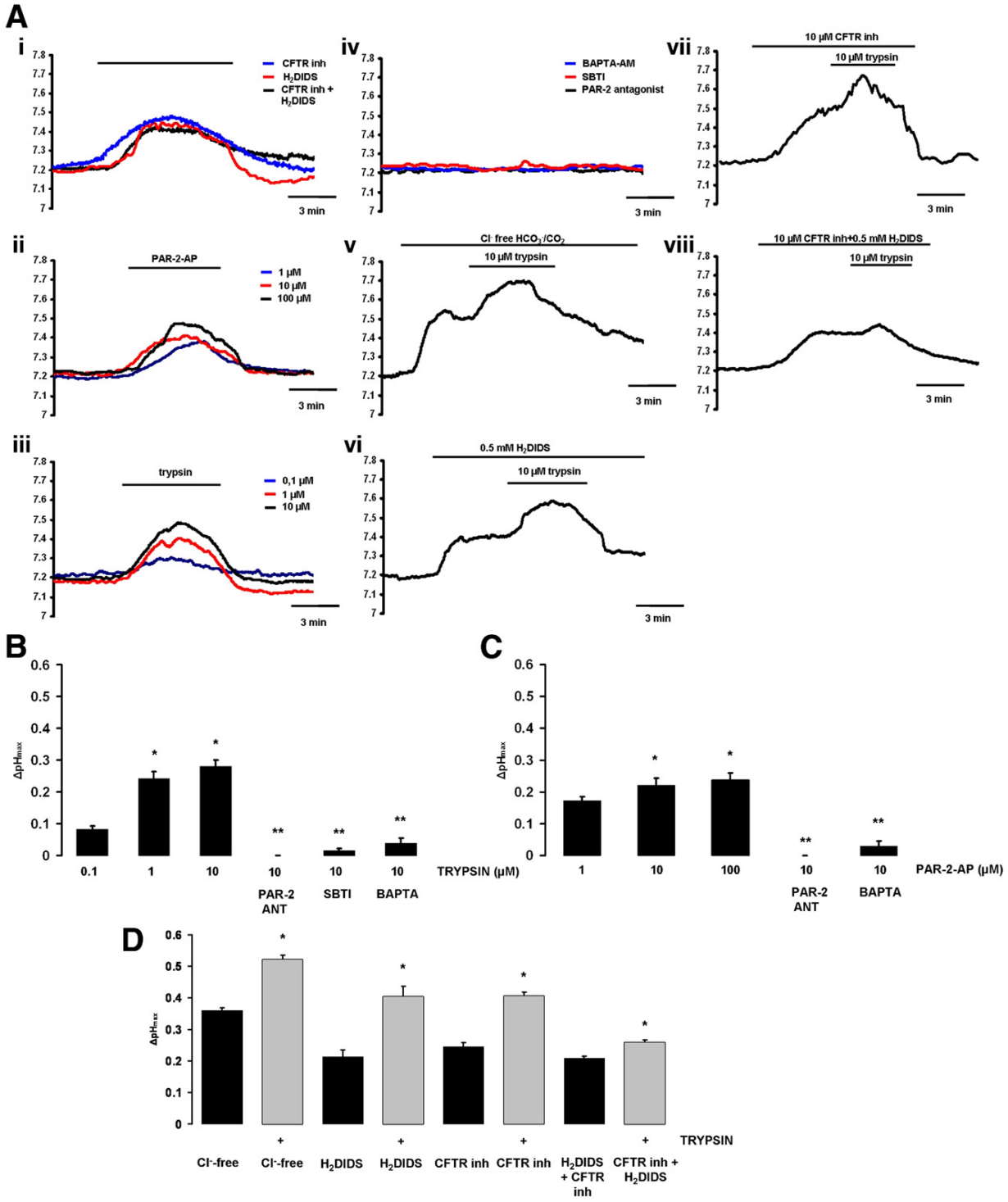

Figure 3. Effects of PAR-2-AP and trypsin on pH_i in microperfused guinea pig pancreatic ducts. (*A*) Representative pH_i traces showing the effects of luminal administration of different agents in microperfused pancreatic ducts. (i) A total of 10 μmol/L CFTRinh-172 and/or 500 μmol/L H_2DIDS caused alkalization of pH_i. (ii) PAR-2-AP and (iii) trypsin induced a dose-dependent pH_i elevation. (iv) Preincubation of ductal cells with 10 μmol/L PAR-2-ANT or 5 μmol/L SBTI or 40 μmol/L BAPTA-AM totally blocked the alkalization caused by 10 μmol/L trypsin. (v) Removal of luminal Cl^- or (vi) administration of H_2DIDS (500 μmol/L) decreased, but did not totally abolish, the effects of 10 μmol/L trypsin on pH_i. (vii) Pretreatment with 10 μmol/L CFTRinh-172 also decreased the effects of trypsin (10 μmol/L) on pH_i. (viii) Simultaneous administration of H_2DIDS and CFTRinh-172 strongly inhibited the effect of 10 μmol/L trypsin. (*B* and *C*) Summary of the effects of PAR-2-AP and trypsin on changes in pH_i. ΔpH_{max} was calculated from the experiments shown in *A*. (*D*) Effects of Cl^--free conditions. Cl^--free conditions, H_2DIDS, CFTRinh-172, and a combination of the inhibitors all induced an intracellular alkalosis. Trypsin further increased the alkalinization of pH_i, although the effect was markedly reduced when both H_2DIDS and CFTRinh-172 were present. n = 4–5 for all groups. (*B*) $^*P < .05$ vs 0.1 μmol/L trypsin; $^{**}P < .001$ vs 10 μmol/L trypsin. (*C*) $^*P < .05$ vs 0.1 μmol/L PAR-2-AP; $^{**}P < .001$ vs 10 μmol/L PAR-2-AP. (*D*) $^*P < .05$ vs the respective filled column.

luminal anion exchangers and/or CFTR (Figure 3*A* [v–viii]). Luminal Cl^--free conditions increased the pH_i of PDECs, presumably by driving HCO_3^- influx on the apical anion exchangers (Figure 3*A* [v]). Note that luminal administration of trypsin further elevated pH_i in Cl^--free conditions (Figure 3*A* [v]) and also in the presence of H_2DIDS (Figure 3*A* [vi]) and CFTRinh-172 (Figure 3*A* [vii]). However, pretreatment of ducts with a combination of H_2DIDS and CFTRinh-172 markedly reduced the effect of trypsin on pH_i (Figure 3*A* [viii]).

Figure 3*B–D* is a summary of the pH_i experiments. Trypsin (Figure 3*B*) and PAR-2-AP (Figure 3*C*) both induced statistically significant, dose-dependent increases in pH_i and these effects were blocked by PAR-2-ANT, SBTI, and BAPTA-AM. Exposure of the ducts to luminal Cl^--free conditions, H_2DIDS, CFTRinh-172, or a combination of the inhibitors also induced an intracellular alkalosis (Figure 3*D*). Also shown in Figure 3*D* is the additional, statistically significant increase in pH_i caused by trypsin in ducts exposed to Cl^--free conditions and the individual inhibitors. However, when ducts were exposed to both CFTRinh-172 and H_2DIDS simultaneously, the effect of trypsin on pH_i was markedly reduced, although it remained statistically significant (Figure 3*D*). We interpret these results as indicating that trypsin inhibits both Cl^--dependent (ie, anion exchanger mediated; revealed when CFTR is blocked by CFTRinh-172) and Cl^--independent (ie, CFTR mediated; revealed in Cl^--free conditions and when the luminal exchangers are blocked by H_2DIDS) bicarbonate secretory mechanisms in PDECs. Reduced bicarbonate secretion will lead to a decrease in intraductal pH.

Trypsin and PAR-2-AP Inhibit CFTR

Exposure of guinea pig PDECs to 5 μmol/L forskolin, which elevates intracellular adenosine 3′5′-cyclic monophosphate levels, increased basal whole cell currents (Figure 4*A–D* [i]) from 8.9 ± 2.3 to 91.2 ± 13.5 pA/pF (Figure 4*A–D* [ii]) at +60 mV in 78% of cells (38/49). The forskolin-activated currents were time- and voltage-independent, with a near linear I/V relationship and a reversal potential of −5.15 ± 1.12 mV (Figure 4*A–D* [iv]). These biophysical characteristics indicate that the currents are carried by CFTR.

Exposure of PDECs to 10 μmol/L trypsin did not affect the basal currents; however, administration of either 10 μmol/L PAR-2-AP (Figure 4*A* [iii]) or 10 μmol/L trypsin (Figure 4*B* [iii]) inhibited forskolin-stimulated CFTR currents by 51.7% ± 10.5% and 57.4% ± 4.0%, respectively. In both cases, the inhibition was voltage independent and irreversible. Pretreatment with either SBTI (10 μmol/L; Figure 4*C* [iii]) or PAR-2-ANT (10 μmol/L; Figure 4*D* [iii]) completely prevented the inhibitory effect of trypsin on the forskolin-stimulated CFTR currents. Figure 4*E* is a summary of these data, which suggest that trypsin inhibits CFTR Cl^- currents by activation of PAR-2.

Autoactivation of Trypsinogen Is pH Dependent

Trypsinogen can undergo autocatalytic activation during which trace amounts of trypsin are generated, which, in turn, can further activate trypsinogen in a self-amplifying reaction. Human trypsinogens are particularly prone to autoactivation, and mutations that facilitate autoactivation are associated with hereditary pancreatitis. To assess the effect of a decrease in intraductal pH (caused by reduced bicarbonate secretion) on trypsinogen activation, we measured autoactivation of human cationic trypsinogen in vitro at pH values ranging from 6.0 to 8.5 using a mixture of various buffers. As shown in Figure 5*A*, the rate at which cationic trypsinogen autoactivates was markedly increased as the pH was reduced from 8.5 to 7.0 when the buffer solution contained 1 mmol/L $CaCl_2$ and no NaCl. However, a further reduction in pH, from 7.0 to 6.0, had little effect (Figure 5*A* [i]).

To rule out that the differences observed in autoactivation were due to the different ionic strengths of the buffers used, we repeated the experiments in the presence of a higher concentration of sodium (100 mmol/L NaCl, Figure 5*A* [ii]) or lower concentration of calcium (0.1 mmol/L $CaCl_2$, Figure 5*A* [iii]). Although the overall autoactivation rates were much slower in the presence of NaCl, the pH profile of autoactivation was essentially identical to that observed in the absence of added salt (Figure 5*A* [ii]). Also, pH-dependent changes in the autoactivation of trypsinogen were still detectable when the experiments were performed using a low calcium buffer (Figure 5*A* [iii]).

PAR-2 Is Down-regulated in Patients With Chronic Pancreatitis

It has been documented that there is activated trypsin in the pancreatic ductal lumen in chronic pancreatitis in humans.[25–28] If trypsin activity is elevated in the duct lumen, PAR-2 down-regulation should occur, which could be due to either (1) changes in PAR-2 mRNA transcription and/or (2) receptor internalization and translocation to the cytoplasm. Our data show a marked reduction in membranous PAR-2 protein level but no significant changes in cytoplasmic PAR-2 protein in chronic pancreatitis (Figure 5*B* [i–iv] and *C*). Furthermore, PAR-2 mRNA expression was markedly reduced in chronic pancreatitis (Figure 5*D*), suggesting that reduced PAR-2 mRNA transcription may cause PAR-2 down-regulation in chronic pancreatitis.

Luminal Exposure to R122H Mutant Cationic Trypsin Induces Elevation of $[Ca^{2+}]_i$ and Evokes Alkalosis in PDECs

It has been shown that mutations in cationic trypsinogen increase the risk of chronic pancreatitis, most likely because of the enhanced autoactivation exhibited by the mutant trypsinogens.[29] Here we tested whether the commonest mutation in cationic trypsin, R122H, affected the ability of the protease to interact with PAR-2.

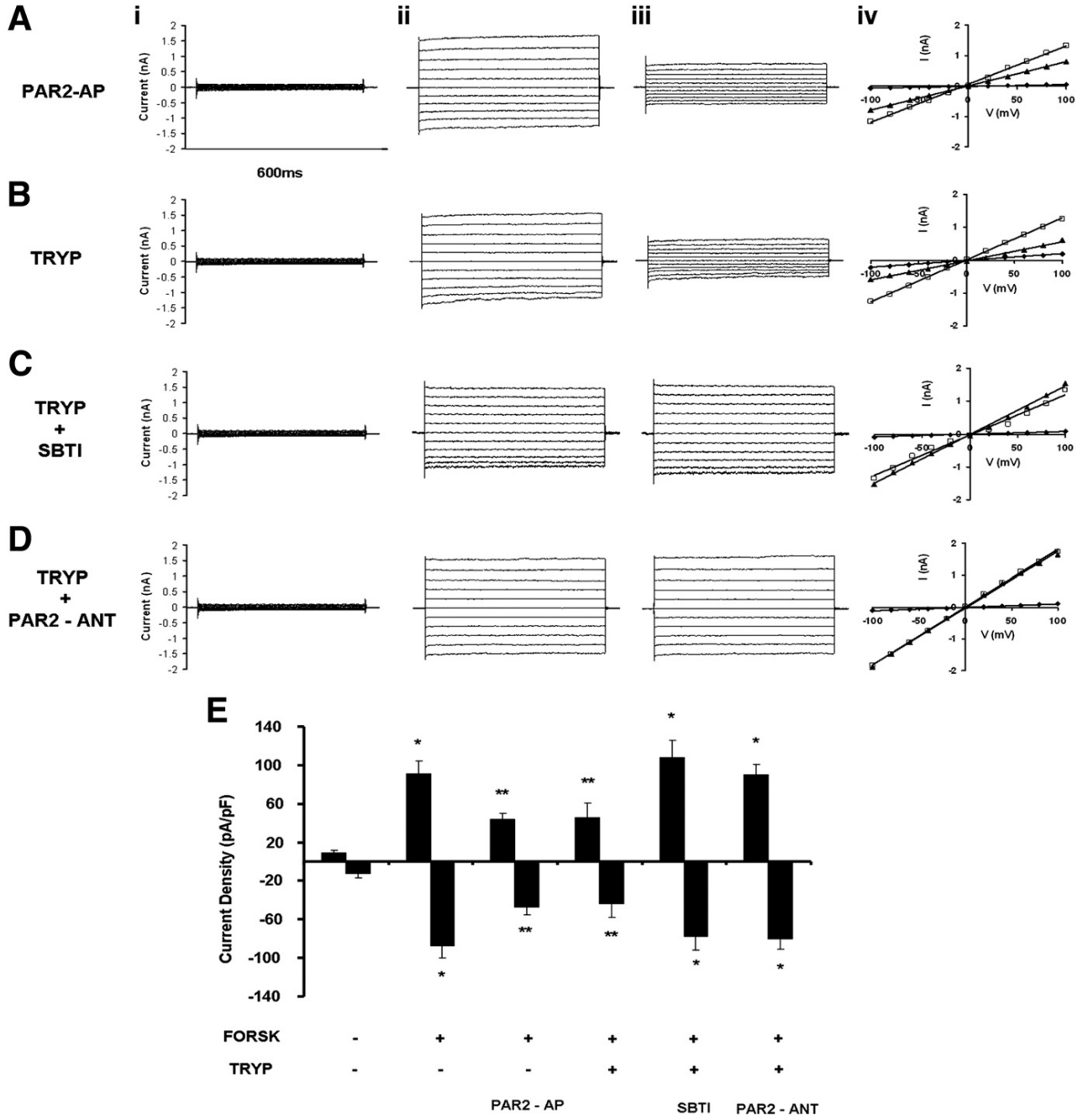

Figure 4. Effects of trypsin and PAR-2-AP on CFTR Cl^- currents of guinea pig pancreatic duct cells. Representative fast whole cell current recordings from PDECs. (*A–D*) (i) Unstimulated currents, (ii) currents after stimulation with 5 μmol/L forskolin, and (iii) currents following 3-minute exposure to (*A*) 10 μmol/L PAR-2-AP, (*B*) 10 μmol/L trypsin, (*C*) 10 μmol/L trypsin/5 μmol/L SBTI, and (*D*) 10 μmol/L trypsin/10 μmol/L PAR-2-ANT. (iv) I/V relationships. *Diamonds* represent unstimulated currents, *squares* represent forskolin-stimulated currents, and *triangles* represent forskolin-stimulated currents in the presence of the tested agents (see previous text). (*E*) Summary of the current density (pA/pF) data obtained from *A–D* measured at $E_{rev} \pm 60$ mV. Exposing PDECs to either PAR-2-AP or trypsin blocked the forskolin-stimulated CFTR Cl^- currents, while administration of SBTI or PAR-2-ANT prevented the inhibitory effect of trypsin. n = 6 for all groups. $^*P < .05$ vs the unstimulated cells, $^{**}P < .05$ vs forskolin. FORSK, forskolin; TRYP, trypsin.

Figure 6*A* and *B* shows that 1 μm of R122H human cationic trypsin causes comparable changes in pH_i and $[Ca^{2+}]_i$ to 0.4 μmol/L wild-type bovine trypsin, suggesting that a trypsin-mediated inhibition of bicarbonate secretion could play a role in the pathogenesis of hereditary as well as chronic pancreatitis.

Activation of PAR-2 Is Diminished in PAR-2$^{-/-}$ Mice

Finally, we investigated the effects of both PAR-2-AP and trypsin on PDECs isolated from PAR-$2^{+/+}$ and PAR-$2^{-/-}$ mice (Figure 6*C–E*). First we confirmed using

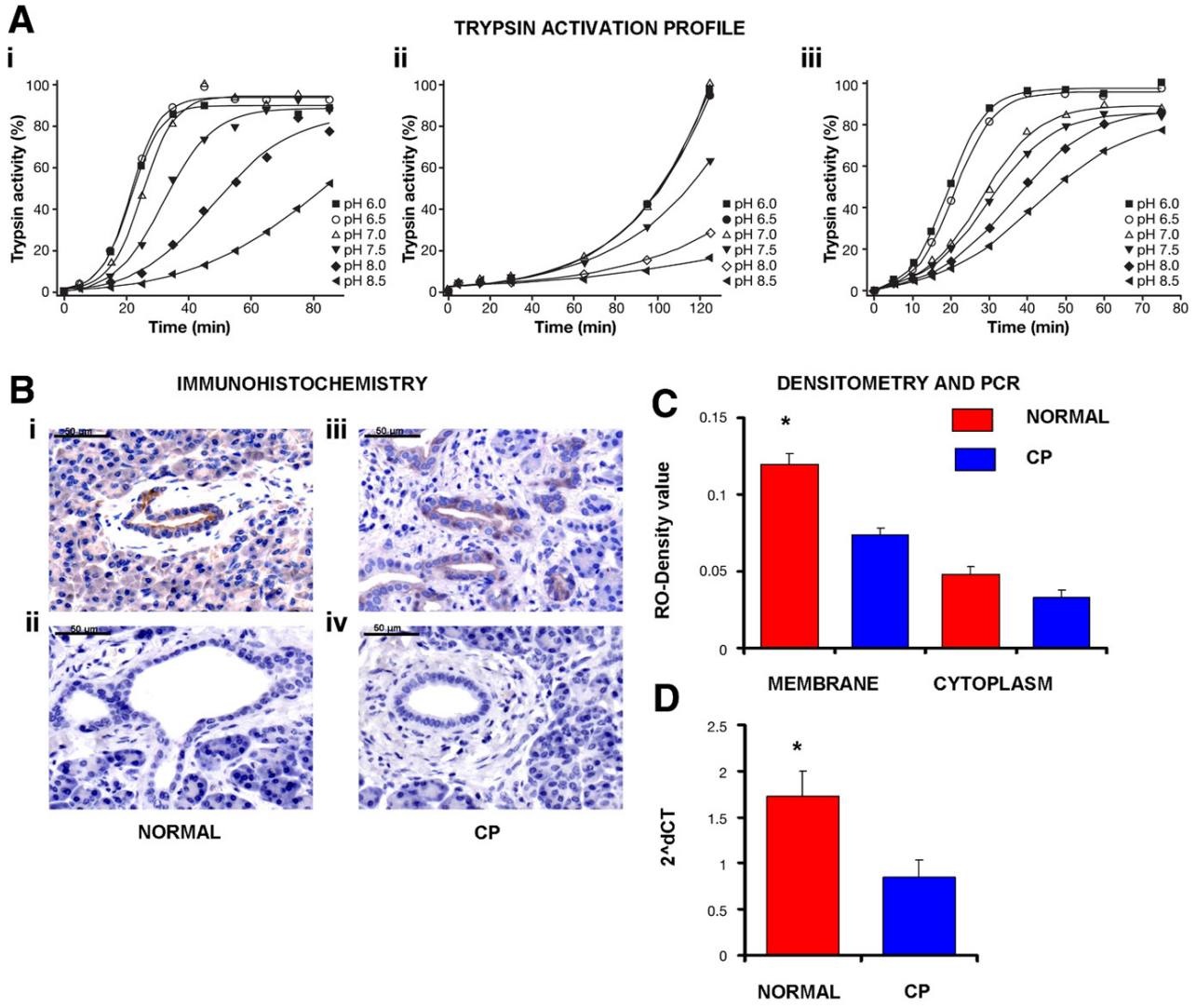

Figure 5. The effects of pH on trypsinogen activation and analyses of PAR-2 expression in human pancreatic samples. The autoactivation of human cationic trypsinogen was determined in vitro at pH values ranging from 6.0 to 8.5. (*A*) (i) Trypsinogen at 2 μmol/L concentration was incubated with 40 nmol/L trypsin at 37°C in 0.1 mol/L Tris + HEPES + 2-(*N*-morpholino)ethanesulfonic acid2-(*N*-morpholino)ethanesulfonic acid buffer mixture containing 1 mmol/L $CaCl_2$. (ii) The same protocol was used in high (100 mmol/L) NaCl buffer solution. Autoactivation of cationic trypsinogen significantly increased as the pH was reduced from 8.5 to 6.0. (iii) The same protocol was used in low (0.1 mmol/L) Ca^{2+}-buffered solution buffer solution. (*B*) (i–iv) PAR-2 expression. (i) Representative section of normal human pancreas. (ii) No primary antiserum. (iii) Representative section of human pancreas from a patient with chronic pancreatitis (CP). (iv) No primary antiserum. (*C*) Relative optical density. n = 15. $^*P < .05$ vs CP membrane. (*D*) Real-time reverse-transcription polymerase chain reaction analysis of PAR-2 mRNA expression of human pancreas. Data are given in 2^dCT. n = 15. $^*P < .05$ vs CP.

immunohistochemistry that PAR-$2^{+/+}$ mice do, whereas PAR-$2^{-/-}$ mice do not, express PAR-2 in their PDECs (Figure 6*C* [i and iii]). Accordingly, our functional data clearly show that the pH_i and $[Ca^{2+}]_i$ responses to luminal administration of either trypsin or PAR-2-AP were markedly diminished in PAR-$2^{-/-}$ PDECs (Figure 6*D* and *E*).

Discussion

The human pancreatic ductal epithelium secretes 1 to 2 L of alkaline fluid every 24 hours that may contain up to 140 mmol/L $NaHCO_3$.[12,13] The physiologic function of this alkaline secretion is to wash digestive enzymes down the ductal tree and into the duodenum and to neutralize acidic chyme entering the duodenum from the stomach. There are important lines of evidence supporting the idea that pancreatic ducts play a role in the pathogenesis of pancreatitis: (1) ductal fluid and bicarbonate secretion are compromised in acute and chronic pancreatitis,[30,31] (2) one of the main end points of chronic pancreatitis is the destruction of the ductal system,[32,33] (3) mutations in CFTR may increase the risk of pancreatitis,[30,31,34–36] and (4) etiologic factors for pancreatitis, such as bile acids or ethanol in high concentration, inhibit pancreatic ductal bicarbonate secretion.[37–39] Despite the previously men-

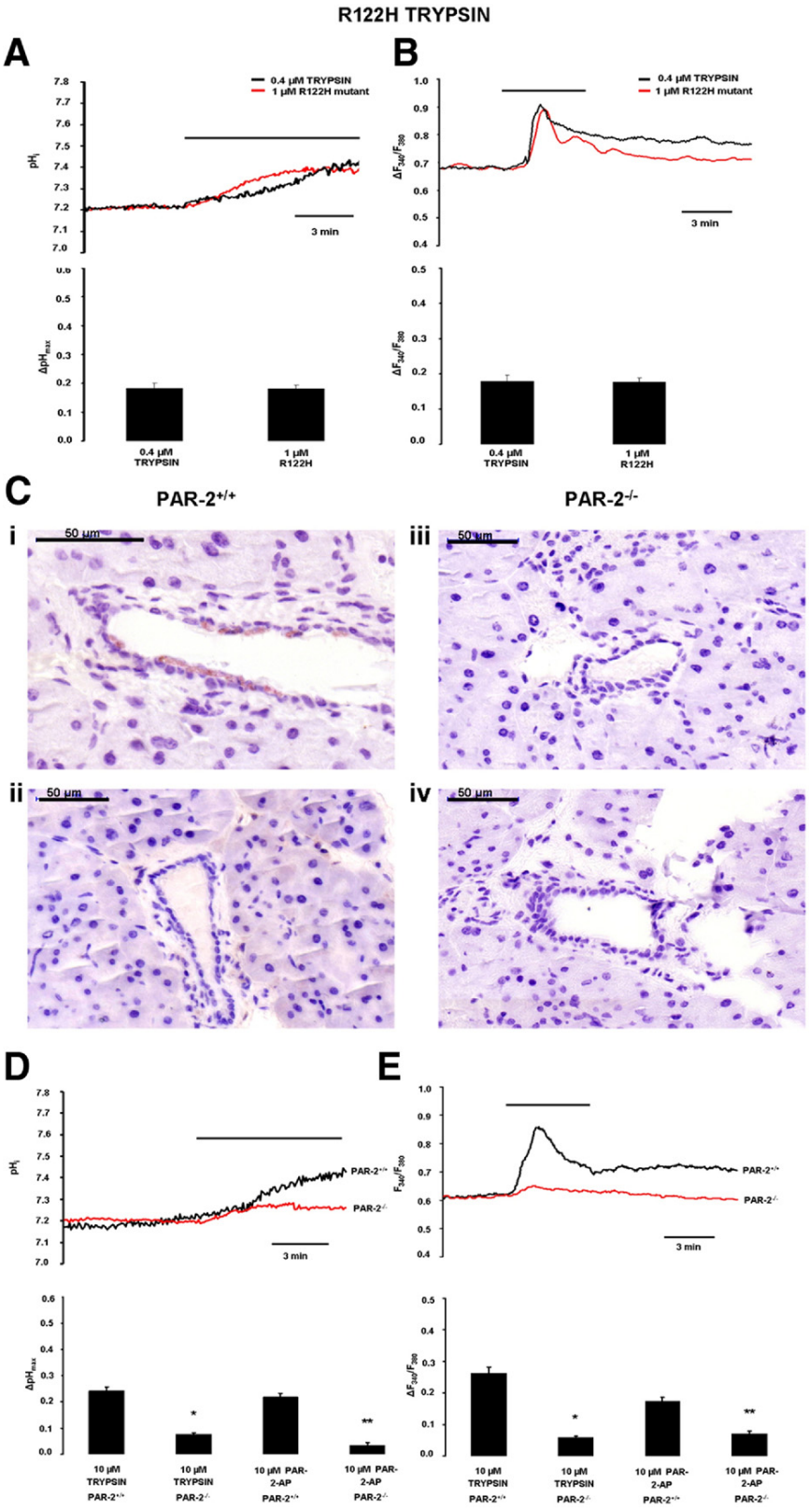

Figure 6. Experiments using R122H human mutant cationic trypsin and PAR-$2^{-/-}$ mice. Representative (*A*) pH_i and (*B*) $[Ca^{2+}]_i$ measurements using luminal administration of normal and R122H mutant cationic trypsin in microperfused guinea pig pancreatic ducts. n = 5 for all experiments. (*C*) (i–iv) PAR-2–expressing cells were visualized by immunohistochemistry as described in Figure 1. (i) Representative section of the pancreas removed from PAR-$2^{+/+}$ mice. (ii) Section without primary antiserum. (iii) Pancreas removed from PAR-$2^{-/-}$ mice. (iv) Section without primary antiserum. (*D*) pH_i and (*E*) $[Ca^{2+}]_i$ measurements using luminal administration of trypsin in microperfused pancreatic ducts isolated from PAR-2 knockout (*red curve*) and PAR-2 wild-type mice (*black curve*). n = 5 for all experiments. $^{*}P < .05$ vs 10 μmol/L trypsin PAR-$2^{+/+}$, $^{**}P < .05$ vs 10 μmol/L PAR-2-AP PAR-$2^{+/+}$.

tioned data, the role of PDECs in the development of pancreatitis has received relatively little attention.[40]

There are important species differences regarding the localization of PAR-2 in pancreatic ducts and in the effect of its activation on bicarbonate secretion. For example, CAPAN-1 cells[10] and dog PDECs[9] express PAR-2 only on the basolateral membrane, whereas bovine PDECs express PAR-2 on the luminal membrane.[11] Therefore, one of our

first aims was to determine which animal model best mimics human PAR-2 expression and thus would be the best for studying the effects of trypsin on PDEC function. Our results showed that in the human pancreas PAR-2 is localized to the luminal membrane of small proximal pancreatic ducts, which are probably the major site of bicarbonate and fluid secretion. Because CAPAN-1 cells and dog PDECs express PAR-2 only on the basolateral membrane, they do not mimic the human situation. Rats or mice are also not good models for the human gland because they secrete only 70 to 80 mmol/L bicarbonate.[41,42] However, the guinea pig pancreas secretes ~140 mmol/L bicarbonate, as does the human gland, and the regulation of bicarbonate secretion is similar in both species.[41,42] Because PAR-2 expression in the guinea pig pancreas was localized to the luminal membrane of duct cells, we performed our experiments on isolated guinea pig ducts.

First we characterized the effects of PAR-2 activation by trypsin and PAR-2-AP on PDECs. Previously, it has been shown that activation of the G protein–coupled PAR-2 by proteinases requires proteolytic cleavage of the receptor, which is followed by an elevation of $[Ca^{2+}]_i$.[43–45] As expected, luminal trypsin and PAR2-AP caused a dose-dependent elevation of $[Ca^{2+}]_i$ in guinea pig ducts. Importantly, the trypsin inhibitor SBTI, PAR-2-ANT, and the intracellular calcium chelator BAPTA-AM all completely blocked the elevation of $[Ca^{2+}]_i$, whereas removal of extracellular Ca^{2+} had no effect. Acidosis (pH 6.8) also slightly reduced the changes in $[Ca^{2+}]_i$ evoked by trypsin, most probably due to reduced cleavage activity of trypsin at an acidic pH. Next we characterized the effects of PAR-2 activation on pH_i. Luminal application of trypsin and PAR-2-AP both caused a dose-dependent intracellular alkalosis in PDECs. This alkalosis is most likely explained either by a reduction in the rate of bicarbonate efflux (ie, secretion) across the apical membrane of PDECs or by an increase in the rate of bicarbonate influx at the basolateral side of the cell. We favor the former explanation because luminal application of the anion exchange inhibitor H_2DIDS or the CFTR inhibitor CFTRinh-172 produced a similar intracellular alkalization.[22,46] Thus, PAR-2 activation inhibits bicarbonate secretion in PDECs by inhibiting SLC26 anion exchangers and CFTR Cl^- channels expressed on the apical membrane of the duct cell. In similarity with the $[Ca^{2+}]_i$ signals, the effect of PAR-2 activation on pH_i was blocked by SBTI, PAR-2-ANT, and BAPTA-AM, with the action of BAPTA-AM suggesting that the inhibition of bicarbonate secretion follows from the increase in $[Ca^{2+}]_i$. Interestingly, an elevation of $[Ca^{2+}]_i$ is crucial for both stimulatory (eg, acetylcholine,[13] low concentrations of bile acids,[39] and ethanol[38]) and inhibitory pathways (eg, basolateral adenosine triphosphate, arginine vasopressin, and high concentrations of ethanol) that control bicarbonate secretion by PDECs. Such marked differences in the outcome of $[Ca^{2+}]_i$ signals in PDECs probably reflect differences in the source of Ca^{2+} and/or in the intracellular compartmentalization of $[Ca^{2+}]_i$ signals generated by different secretory agonists and antagonists.

Remarkably, trypsin was still able to evoke an elevation of pH_i when Cl^- was removed from the duct lumen and when PDECs were pretreated with H_2DIDS, conditions that should inhibit bicarbonate efflux on the exchanger. These results suggested the involvement of CFTR, the only other known bicarbonate efflux pathway on the apical membrane, in the inhibitory effect of trypsin. This hypothesis was confirmed by patch clamp experiments in which trypsin decreased CFTR whole cell currents in isolated guinea pig PDECs by 50% to 60%. Finally, the fact that the trypsin-induced alkalinization was completely blocked by a combination of CFTRinh-172 and H_2DIDS confirms the involvement of both CFTR and SLC26 anion exchangers. Our conclusion from these pH_i and patch clamp data is that PAR-2 activation inhibits both the SLC26 anion exchanger (probably SLC26A6 [PAT-1][47] because SLC26A3 [DRA] is only weakly inhibited by disulfonic stilbenes[47,48]) and CFTR Cl^- channels expressed on the apical membrane of the duct cell.

The pH of pancreatic juice (and therefore the luminal pH [pH_L] in the duct) can vary between approximately 6.8 and 8.0. It has recently been shown that protons coreleased during exocytosis cause significant acidosis (up to 1 pH unit) in the lumen of the acini.[23] However, Ishiguro et al[49] have clearly shown that the pH_L in pancreatic ducts is dependent on the level of bicarbonate secretion. pH_L can be elevated from 7.2 to 8.5 by stimulation with secretin or forskolin, and this effect was strictly dependent on the presence of bicarbonate.[24,49,50] Also, inhibition of ductal bicarbonate secretion with H_2DIDS can decrease the pH_L to less than 8.0.[49] In view of these results, we tested whether trypsinogen autoactivation was affected by pH over the range of 6.0 to 8.5. Autoactivation of trypsinogen was relatively slow at pH 8.5, but decreasing the pH from 8.5 to 7 progressively stimulated autoactivation. These results suggest that under physiologic conditions bicarbonate secretion by PDECs is not only important for elevating the pH in the duodenum, but also for keeping pancreatic enzymes in an inactive state in the ductal system of the gland.

Receptor down-regulation is a phenomenon that occurs in the continued presence of an agonist and leads to a reduction in the sensitivity of the cell to the agonist. Potentially, there are 2 mechanisms that could underlie receptor down-regulation of PAR-2: (1) after proteolytic activation, the PAR-2 is internalized by a clathrin-mediated mechanism and then targeted to lysosomes[45] and (2) if trypsin is present for a longer time in the lumen, PAR-2 may be down-regulated at the transcriptional level. In this study, we provide evidence that the second mechanism, transcriptional down-regulation, explains the reduced expression of PAR-2 seen in chronic pancreatitis.

Conflicting data can be found in the literature concerning the role of PAR-2 in acute pancreatitis. Singh et al[7] showed that in secretagogue-induced experimental pancreatitis, PAR-2 deletion is associated with a more severe

pancreatitis. Although Laukkarinen et al[17] confirmed these results in cerulein-induced pancreatitis, they also clearly showed that in taurocholate-induced pancreatitis, PAR-2 deletion markedly reduced the severity of the disease. There is no evidence to suggest that clinical pancreatitis is evoked by supramaximal secretagogue stimulation; however, the taurocholate-induced pancreatitis model may mimic the clinical situation. Therefore, Laukkarinen et al[17] speculated that PAR-2 activation promotes the worsening of clinical pancreatitis and our data are consistent with that hypothesis.

Besides the clear pathophysiologic role of the trypsin/PAR-2 interaction in chronic pancreatitis, there is still a debate as to why PAR-2 are localized to the luminal membrane of PDEC in small ducts close to the acinar cells. What could the physiologic role of this PAR-2 be? A number of agents have been shown to have dual effects on PDECs at different concentrations. For example, bile acids in low concentrations stimulate but in high concentrations inhibit bicarbonate secretion.[39] The same applies to ethanol.[38] Under physiologic conditions, trypsin inhibitors are coreleased from acinar cells with trypsinogen and should block the activity of any trypsin that is generated spontaneously. Therefore, only very small amounts of active trypsin, if any, will be present in the duct lumen under normal conditions. However, there remains a possibility that very small amounts of active trypsin (ie, concentrations less than 0.1 μmol/L that would not cause an elevation of $[Ca^{2+}]_i$ or change in pH) could bind to PAR-2 on the luminal membrane of the ducts and augment other stimulatory mechanisms so as to enhance flushing of digestive enzymes down the ductal tree.

In conclusion, we suggest for the first time that one of the physiologic roles of bicarbonate secretion by PDECs is to curtail trypsinogen autoactivation within the pancreatic ductal system. However, if trypsin is present in the duct lumen (as may occur during the early stages of pancreatitis due to leakage from acinar cells), PAR-2 on the duct cell will be activated, leading to Ca^{2+} release from intracellular stores and an increase in cytosolic Ca^{2+} concentration. This causes inhibition of the luminal anion exchangers and CFTR Cl^- channels, reducing bicarbonate secretion by the duct cell. The decrease in bicarbonate secretion will increase the transit time of zymogens down the duct tree and decrease pH_L, both of which will promote the autoactivation of trypsinogen. The trypsin so formed will further inhibit bicarbonate transport, leading to a vicious cycle generating further decreases in pH_L and enhanced trypsinogen activation, which will favor development of the pancreatitis (Supplementary Figure 4). Finally, the R122H mutant cationic trypsin also elevated $[Ca^{2+}]_i$ and pH_i in duct cells, suggesting that this mechanism may be particularly important in hereditary pancreatitis in which the mutant trypsinogens more readily autoactivate.[29]

Supplementary Material

Note: To access the supplementary material accompanying this article, visit the online version of *Gastroenterology* at www.gastrojournal.org, and at doi: 10.1053/j.gastro.2011.08.039.

References

1. Petersen OH. Physiology of acinar cell secretion. In: Hans Beger, Andrew Warshaw, Markus Büchler, et al, eds. The pancreas. 2nd ed. Malden, MA: Blackwell Publishing, 2008:71–77.
2. Lerch MM, Gorelick FS. Early trypsinogen activation in acute pancreatitis. Med Clin North Am 2000;84:549–563.
3. Thrower EC, Gorelick FS, Husain SZ. Molecular and cellular mechanisms of pancreatic injury. Curr Opin Gastroenterol 2010;84:549–563.
4. Geokas MC, Rinderknecht H. Free proteolytic enzymes in pancreatic juice of patients with acute pancreatitis. Am J Dig Dis 1974;19:591–598.
5. Renner IG, Rinderknecht H, Douglas AP. Profiles of pure pancreatic secretions in patients with acute pancreatitis: the possible role of proteolytic enzymes in pathogenesis. Gastroenterology 1978;75:1090–1098.
6. Withcomb D, Beger H. Definitions of pancreatic diseases and their complications. In: Hans Beger, Andrew Warshaw, Markus Büchler, et al, eds. The pancreas. 2nd ed. Malden, MA: Blackwell Publishing, 2008:1–6.
7. Singh VP, Bhagat L, Navina S, et al. Protease-activated receptor-2 protects against pancreatitis by stimulating exocrine secretion. Gut 2007;56:958–964.
8. Kawabata A, Kuroda R, Nishida M, et al. Protease-activated receptor-2 (PAR-2) in the pancreas and parotid gland:Immunolocalization and involvement of nitric oxide in the evoked amylase secretion. Life Sci 2002;71:2435–2446.
9. Nguyen TD, Moody MW, Steinhoff M, et al. Trypsin activates pancreatic duct epithelial cell ion channels through proteinase activated receptor-2. J Clin Invest 1999;103:261–269.
10. Namkung W, Lee JA, Ahn W, et al. Ca^{2+} activates cystic fibrosis transmembrane conductance regulator- and Cl^--dependent HCO_3^- transport in pancreatic duct cells. J Biol Chem 2003;278:200–207.
11. Alvarez C, Regan JP, Merianos D, et al. Protease-activated receptor-2 regulates bicarbonate secretion by pancreatic duct cells in vitro. Surgery 2004;136:669–676.
12. Lee M, Muallem S. Physiology of duct cell secretion. In: Hans Beger, Andrew Warshaw, Markus Büchler, et al, eds. The pancreas. 2nd ed. Malden, MA: Blackwell Publishing, 2008:78–90.
13. Argent BE. Cell physiology of pancreatic ducts. In: Johnson LR, ed. Physiology of the gastrointestinal tract. Volume 2. 4th ed. San Diego, CA: Elsevier, 2006:1376–1396.
14. Hegyi P, Rakonczay Z Jr, Farkas K, et al. Controversies in the role of SLC26 anion exchangers in pancreatic ductal bicarbonate secretion. Pancreas 2008;37:232–234.
15. Ishiguro H, Steward MC, Sohma Y, et al. Membrane potential and bicarbonate secretion in isolated interlobular ducts from guinea-pig pancreas. J Gen Physiol 2002;120:617–628.
16. Sohma Y, Gray MA, Imai Y, et al. HCO_3^- transport in a mathematical model of the pancreatic ductal epithelium. J Membr Biol 2000;176:77–100.
17. Laukkarinen JM, Weiss ER, van Acker GJ, et al. Protease-activated receptor-2 exerts contrasting model-specific effects on acute experimental pancreatitis. J Biol Chem 2008;283:20703–20712.
18. Kawabata A, Matsunami M, Tsutsumi M, et al. Suppression of pancreatitis-related allodynia/hyperalgesia by proteinase-activated receptor-2 in mice. Br J Pharmacol 2006;148:54–60.
19. Sharma A, Tao X, Gopal A, et al. Protection against acute pancreatitis by activation of protease-activated receptor-2. Am J Physiol Gastrointest Liver Physiol 2005;288:G388–G395.

20. Namkung W, Han W, Luo X, et al. Protease-activated receptor 2 exerts local protection and mediates some systemic complications in acute pancreatitis. Gastroenterology 2004;126:1844–1859.
21. Argent BE, Arkle S, Cullen MJ, et al. Morphological, biochemical and secretory studies on rat pancreatic ducts maintained in tissue culture. Q J Exp Physiol 1986;71:633–648.
22. Hegyi P, Rakonczay Z Jr, Tiszlavicz L, et al. Protein kinase C mediates the inhibitory effect of substance P on HCO_3^- secretion from guinea pig pancreatic ducts. Am J Physiol Cell Physiol 2005; 288:C1030–C1041.
23. Behrendorff N, Floetenmeyer M, Schwiening C, et al. Protons released during pancreatic acinar cell secretion acidify the lumen and contribute to pancreatitis in mice. Gastroenterology 2010; 139:1711–1720.
24. Ishiguro H, Steward MC, Wilson RW, et al. Bicarbonate secretion in interlobular ducts from guinea-pig pancreas. J Physiol 1996;495:179–191.
25. Kukor Z, Mayerle J, Kruger B, et al. Presence of cathepsin B in the human pancreatic secretory pathway and its role in trypsinogen activation during hereditary pancreatitis. J Biol Chem 2002;277:21389–21396.
26. Tympner F, Rosch W. Viscosity and trypsin activity of pure pancreatic juice in chronic pancreatitis. Acta Hepatogastroenterol (Stuttg) 1978;25:73–76.
27. Fedail SS, Harvey RF, Salmon PR, et al. Trypsin and lactoferrin levels in pure pancreatic juice in patients with pancreatic disease. Gut 1979;20:983–986.
28. Tympner F. Selectively aspirated pure pancreatic secretion. Viscosity, trypsin activity, protein concentration and lactoferrin content of pancreatic juice in chronic pancreatitis. Hepatogastroenterology 1981;28:169–172.
29. Sahin-Tóth M, Tóth M. Gain-of-function mutations associated with hereditary pancreatitis enhance autoactivation of human cationic trypsinogen. Biochem Biophys Res Commun 2000;278:286–289.
30. Cavestro GM, Zuppardo RA, Bertolini S, et al. Connections between genetics and clinical data:Role of MCP-1, CFTR, and SPINK-1 in the setting of acute, acute recurrent, and chronic pancreatitis. Am J Gastroenterol 2010;105:199–206.
31. Hegyi P, Rakonczay Z. Insufficiency of electrolyte and fluid secretion by pancreatic ductal cells lead to increase patients risk to pancreatitis. Am J Gastroenterol 2010;105:2119–2120.
32. Kloppel G, Luttges J, Sipos B, et al. Autoimmune pancreatitis: pathological findings. Jop 2005;6:97–101.
33. Ectors N, Maillet B, Aerts R, et al. Non-alcoholic duct destructive chronic pancreatitis. Gut 1997;41:263–268.
34. Hegyi P, Pandol S, Venglovecz V, et al. The acinar-ductal tango in the pathogenesis of acute pancreatitis. Gut 2011;60:544–552.
35. Nousia-Arvanitakis S. Cystic fibrosis and the pancreas: recent scientific advances. J Clin Gastroenterol 1999;29:138–142.
36. Weiss FU, Simon P, Bogdanova N, et al. Functional characterisation of the CFTR mutations M348V and A1087P from patients with pancreatitis suggests functional interaction between CFTR monomers. Gut 2009;58:733–734.
37. Maleth J, Venglovecz V, Rázga Z, et al. The non-conjugated chenodeoxycholate induces severe mitochondrial damage and inhibits bicarbonate transport in pancreatic duct cells. Gut 2011;60:136–138.
38. Yamamoto A, Ishiguro H, Ko SB, et al. Ethanol induces fluid hypersecretion from guinea-pig pancreatic duct cells. J Physiol 2003;551:917–926.
39. Venglovecz V, Rakonczay Z Jr, Ozsvari B, et al. Effects of bile acids on pancreatic ductal bicarbonate secretion in guinea pig. Gut 2008;57:1102–1112.
40. Lee MG, Muallem S. Pancreatitis: the neglected duct. Gut 2008; 57:1037–1039.
41. Padfield PJ, Garner A, Case RM. Patterns of pancreatic secretion in the anaesthetised guinea pig following stimulation with secretin, cholecystokinin octapeptide, or bombesin. Pancreas 1989;4:204–209.
42. Steward MC, Ishiguro H, Case RM. Mechanisms of bicarbonate secretion in the pancreatic duct. Annu Rev Physiol 2005;67:377–409.
43. Vergnolle N. Review article: proteinase-activated receptors-novel signals for gastrointestinal pathophysiology. Aliment Pharmacol Ther 2000;14:257–266.
44. Bohm SK, Khitin LM, Grady EF, et al. Mechanisms of desensitization and resensitization of proteinase-activated receptor-2. J Biol Chem 1996;271:22003–22016.
45. Hoxie JA, Ahuja M, Belmonte E, et al. Internalization and recycling of activated thrombin receptors. J Biol Chem 1993;268:13756–13763.
46. Stewart AK, Yamamoto A, Nakakuki M, et al. Functional coupling of apical Cl^-/HCO_3^- exchange with CFTR in stimulated HCO_3^- secretion by guinea pig interlobular pancreatic duct. Am J Physiol Gastrointest Liver Physiol 2009;296:G1307–G1317.
47. Ko SB, Shcheynikov N, Choi JY, et al. A molecular mechanism for aberrant CFTR-dependent HCO_3^- transport in cystic fibrosis. EMBO J 2002;21:5662–5672.
48. Chernova MN, Jiang L, Shmukler BE, et al. Acute regulation of the SLC26A3 congenital chloride diarrhoea anion exchanger (DRA) expressed in Xenopus oocytes. J Physiol 2003;549:3–19.
49. Ishiguro H, Naruse S, Steward MC, et al. Fluid secretion in interlobular ducts isolated from guinea-pig pancreas. J Physiol 1998; 511:407–422.
50. Ishiguro H, Naruse S, Kitagawa M, et al. Luminal ATP stimulates fluid and HCO_3^- secretion in guinea-pig pancreatic duct. J Physiol 1999;519:551–558.

Received October 26, 2010. Accepted August 5, 2011.

Reprint requests

Address requests for reprints to: Péter Hegyi, MD, PhD, DSc, First Department of Medicine, University of Szeged, Faculty of Medicine, Korányi fasor 8-10, H-6720, Szeged, Hungary. e-mail: hegyi.peter@med.u-szeged.hu; fax: (36) 62 545-185.

Conflicts of interest

The authors disclose no conflicts.

Funding

Supported by grants from the Hungarian Scientific Research Fund to V.V., Z.R., and P.H. (PD78087, K78311, and NNF 78851), Bolyai postdoctoral fellowships to P.H. and Z.R. (00334/08/5, 00174/10/5) awarded by the Hungarian Academy of Sciences, a European Pancreatic Club travel grant, National Office for Research and Technology grants (TÁMOP-4.2.2-08/1/2008-0002 and 0013, TÁMOP 4.2.1.B-09/1/KONV), National Institutes of Health grant DK058088 (to M.S.-T.), and scholarships from the Rosztoczy Foundation (to A.G. and A.S.).

Supplementary Materials and Methods

Ethics

All experiments were conducted in compliance with the Guide for the Care and Use of Laboratory Animals (USA NIH publication No 85-23, revised 1985). Animal experiments were approved by the Regional Ethical Board at the University of Szeged, Hungary.

Solutions and Chemicals

HEPES-buffered solutions were gassed with 100% O_2, and their pH was set to 7.4 with HCl at 37°C. HCO_3^--buffered solutions were gassed with 95% O_2/5% CO_2 to set pH to 7.4 at 37°C. For patch clamp studies, the standard extracellular solution contained (in mmol/L): 145 NaCl, 4.5 KCl, 2 $CaCl_2$, 1 $MgCl_2$, 10 HEPES, and 5 glucose (pH 7.4 adjusted with NaOH). The osmolarity of the extracellular solution was 300 mOsm/L. The standard pipette solution for the patch clamp experiments contained (in mmol/L): 120 CsCl, 2 $MgCl_2$, 0.2 ethylene glycol-bis(β-aminoethyl ether)-*N,N,N′,N′*-tetraacetic acid (EGTA), 10 HEPES, and 1 Na_2ATP (pH 7.2 adjusted with NaOH). Chromatographically pure collagenase was purchased from Worthington (Lakewood, NJ). 2,7-Bis-(2-carboxyethyl)-5-(and-6-)carboxyfluorescein, acetoxymethyl ester (BCECF-AM), 2-(6-(bis(carboxymethyl)amino)-5-(2-(2-(bis(carboxymethyl)amino)-5-methylphenoxy)ethoxy)-2-benzofuranyl)-5-oxazolecarboxylic acetoxymethyl ester (FURA 2-AM), dihydro-4,4′-diisothiocyanostilbene-2,2′-disulfonic acid (H_2DIDS), and 1,2-bis(o-aminophenoxy)ethane- *N,N,N′,N′*-tetraacetic acid (BAPTA-AM) were from Invitrogen (Carlsbad, CA). PAR-2-ANT (H-Phe-Ser-Leu-Leu-Arg-Tyr-NH_2) and PAR-2-AP (H-Ser-Leu-Ile-Gly-Arg-Leu-amid trifluoroacetate salt) were from Peptides International (Louisville, KY). Forskolin were from Tocris (Ellisville, MO). Rabbit PAR-2 polyclonal antibody was purchased from Santa Cruz Biotechnology (Heidelberg, Germany). All other chemicals were obtained from Sigma-Aldrich (Budapest, Hungary).

Isolation of Pancreatic Ducts and Individual Ductal Cells

Male guinea pigs weighing between 150 and 250 g or mice (PAR-$2^{+/+}$ and PAR-$2^{-/-}$) weighing between 18 and 21 g were humanely killed by cervical dislocation, the pancreas was removed, and small intralobular proximal ducts were isolated by microdissection as described previously.[1] PAR-$2^{-/-}$ mice (B6.Cg-F2rl1$^{tm1Mslb/J}$) were previously generated by Schmidlin et al[1] and a kind gift from Ashok Saluja.[2] Isolated ducts were then cultured overnight in a 37°C incubator gassed with 5% CO_2/95% air.[3]

To obtain single pancreatic ductal cells, cultured ducts were incubated for 50 minutes at 37°C in 50 U/mL elastase dissolved in storage solution (Dulbecco's modified Eagle medium containing 3% [wt/vol] bovine serum albumin [pH 7.4 with NaOH]). Then the ducts were transferred to a Ca^{2+}/Mg^{2+}-free HEPES-buffered solution and incubated for a further 10 minutes at 37°C. After the incubation, the ducts were transferred to a coverslip and teased apart using stainless steel needles. The individual ductal cells were used for experiments within 3 to 4 hours after isolation.

Measurement of pH_i and Ca^{2+} Concentration

Ducts were bathed in standard HEPES solution and loaded with BCECF-AM (2 μmol/L) or FURA 2-AM (5 μmol/L) for 30 to 60 minutes at room temperature.

Ducts were then transferred to a perfusion chamber mounted on an IX71 inverted microscope (Olympus, Budapest, Hungary) and perfused continuously with solutions at 37°C both from the luminal and basolateral side at a rate of 10 to 30 μL/min and 4 to 5 mL/min, respectively. Four to 5 small areas (region of interests) of 5 to 10 cells in each intact duct were excited with light at a given wavelength. Excitation of BCECF was at 495 and 440 nm, with emitted light monitored at 535 nm. Excitation of FURA-2 was at 380 and 340 nm, with emitted light monitored at 510 nm. The fluorescence emissions were captured by a charge-coupled device camera and digitized by a Cell imaging system (Olympus, Budapest, Hungary). Ratio images were collected at 1-second intervals. In situ calibration of pH_i measured with BCECF was performed using the high K^+-nigericin technique.[4,5]

Electrophysiology

Guinea pig PDECs were isolated by an enzymatic microdissection procedure as described previously. Using a glass pipette, a few drops of cell suspension were placed within a perfusion chamber mounted on the stage of an inverted microscope (TMS; Nikon, Tokyo, Japan). The ductal cells were allowed to settle and attach to the bottom of the chamber for at least 30 minutes before the perfusion was started.

Patch clamp micropipettes were fabricated from borosilicate glass capillaries (Clark, Reading, England) by using a P-97 Flaming/Brown micropipette puller (Sutter Co, Novato, CA). These pipettes had resistances between 1.5 and 2.5 MΩ. Membrane currents were recorded with an Axopatch 1D amplifier (Axon Instruments, Union City, CA) using the whole cell configuration of the patch clamp technique at 37°C. After establishing a high-resistance seal (1–10 GΩ) by gentle suction, the cell membrane beneath the tip of the pipette was disrupted by suction or by application of short electrical pulses. The series resistance was typically 4 to 8 MΩ before compensation (50%–80%, depending on the voltage protocol). Current-voltage (I/V) relationships were obtained by holding V_m at 0 mV and clamping to ±100 mV in 20-mV increments. Membrane currents were digitized by using a 333-kHz analog-to-digital converter (Digidata 1200; Axon Instruments) under software control (pClamp 6;

Axon Instruments). Analyses were performed by using pClamp 6 software after low-pass filtering at 1 kHz.

Expression and Purification of Human Trypsinogens

Wild-type and R122H mutant human cationic trypsinogen was expressed in *Escherichia coli* and purified by ecotin-affinity chromatography as reported previously.[6]

Measuring Autoactivation of Trypsinogen

Autoactivation of trypsinogen was measured at 2 μmol/L concentration at 37°C in a polybuffer system (American Bioanalytical Inc, Natick, MA) containing 100 mmol/L 2-(*N*-morpholino)ethanesulfonic acid, 100 mmol/L HEPES, and 100 mmol/L Tris in 100 μL final volume. The pH of the Polybuffer was adjusted to given values with HCl (pH 6.0 and 6.5) or NaOH (pH 7.0, 7.5, 8.0, and 8.5). Reactions also contained 1 mmol/L or 0.1 mmol/L $CaCl_2$ and 100 mmol/L NaCl, as indicated. At given times, 2-μL aliquots were removed and trypsin activity was determined using the N-CBZ-Gly-Pro-Arg-p-nitroanilide substrate at 150 μmol/L final concentration.

Immunohistochemistry

Pancreatic tissue from 5 guinea pigs, 15 patient samples without pancreatic disease near neuroendocrine tumors (average age, 59.5; female/male, 7:8), and 15 patients (average age, 56.6; female/male, 4:11) who had chronic pancreatitis (13 alcohol, 2 gallstone) were investigated. The human samples were obtained with the permission of the Regional Ethical Committee of Semmelweis University (#172/2003).

The pancreatic tissues were fixed in 10% neutral buffered formalin for 24 hours, followed by paraffin embedding, and were then cut and stained with H&E to establish the diagnosis. Paraffin-embedded, 3- to 4-μm-thick sections were used for immunohistochemistry to detect PAR-2 expression. The slides were treated for 30 minutes with target retrieval solution (Dako, Glostrup, Denmark) in a microwave oven, followed by incubation with the primary rabbit polyclonal antibody (Santa Cruz Biotechnology Inc, Heidelberg, Germany) in 1:100 dilution overnight at 4°C. Signal detection was achieved by using ImPRESS reagent with secondary anti-rabbit immunoglobulin G antibody (20 minutes) (Vector Laboratories, Burlingame, CA). Diaminobenzidine was used to visualize immune complexes, and nuclear counterstaining was performed with hematoxylin. For negative controls, the appropriate antibody was omitted and either the antibody diluent alone or isotype-matched immunoglobulin G serum was used. The negative controls exhibited no signal. Normal skin epithelial cells were used as positive controls to confirm correct immunohistochemical staining for PAR-2 (results not shown).

The immunohistochemical reactions were digitalized with a Mirax MIDI slide scanner (3DHistech Ltd, Budapest, Hungary). Relative optical (RO) density was calculated using ImageJ program (National Institutes of Health, Bethesda, MD). Pixel values (PV) were normalized to erythrocyte density ($PV_{Norm} = PV_{Measured} - PV_{Erythrocyte}$) in all sections. RO-Density value was calculated from the $RO\text{-}Density = \log_{10}(255/PV_{Norm})$ equation, assuming that the brightest value in the image equals 255.

Western blot analysis was used to determine the specificity of the PAR-2 antibody. Proteins were extracted from fresh-frozen guinea pig (n = 3) and human (n = 3) pancreatic tissue stored at −80°C. Isolation was performed by using lysis buffer (20 mmol/L Tris, pH 7.5, 150 mmol/L NaCl, 2 mmol/L EDTA, 1% Triton X-100 containing protease inhibitor complex [Sigma Aldrich Co, Budapest, Hungary]). Samples (50 mg) were homogenized, followed by centrifugation at 13,200 rpm at 4°C for 5 minutes. Measurements of protein concentration were performed using Bradford analysis.[7] A total of 30 μg of protein samples were loaded in each lane, run on 10% sodium dodecyl sulfate/polyacrylamide electrophoresis at 200 V for 35 minutes, and then transferred to nitrocellulose membranes at 100 V, 4°C, for 75 minutes. For aspecific protein blocking, nonfat dry milk (5%, phosphate-buffered saline) was used for 30 minutes. Blots were incubated with polyclonal PAR-2 rabbit antibody (1:300; Santa Cruz Biotechnology Inc, Heidelberg, Germany) and anti-GAPDH antibody (1:5000; AbDSerotec, Kidlington, England) at 4°C overnight. After washing in 0.1% Tris, the secondary antibodies as anti-mouse GAPDH (1:2000; AbDSerotec, Düsseldorf, Germany) and horseradish peroxidase–conjugated anti-rabbit antibody (1:2000, Dako Cytomation, Ghostrup, Denmark) were applied at room temperature for 90 minutes. Following 3 series of washings in Tris-buffered saline with Tween 20, signals were visualized by enhanced chemiluminescent detection.

Real-Time Reverse-Transcription Polymerase Chain Reaction

RNA extraction. Fifteen formalin-fixed, paraffin-embedded normal pancreatic tissue samples and 15 samples of chronic pancreatitis tissue were selected for real-time reverse-transcription polymerase chain reaction analysis. Total RNA was isolated from five 5- to 10-μm macrodissected sections (connective tissue excluded) using RNeasy FFPE Kit (Qiagen, Hilden, Germany) in accordance with the manufacturer's instructions. RNA concentrations were obtained using a NanoDrop Spectrophotometer ND-1000 (Thermo Fisher Scientific Inc, Waltham, MA).

Reverse transcription of RNA. Complementary DNA samples were prepared from 1 μg total RNA using a High Capacity RNA-to-cDNA Kit (Applied Biosystems, Carlsbad, CA) as specified by the manufacturer.

Primer design. Gene-specific primers were designed by AlleleID 6.01 primer design software (Premier Biosoft International, Palo Alto, CA) for real-time reverse-

transcription polymerase chain reaction. Isoform specificity and primer sizes were checked by BioEdit biological sequence alignment editor software (Tom Hall Ibis Therapeutics, Carlsbad, CA). Primer specificity was checked by BiSearch software (Hungarian Academy of Sciences, Institute of Enzymology, Budapest, Hungary). Primer specific amplification degree (58°C) was optimized by gradient polymerase chain reaction. The used primer sequences are shown in Supplementary Table 1.

Reverse-transcription polymerase chain reaction. Real-time reverse-transcription polymerase chain reaction analysis was performed using SYBR Green technology on an ABI Prism 7000 Sequence Detection System (Applied Biosystems, Foster City, CA), according to the manufacturer's instructions. β-actin was used as the internal control gene. Primer-specific amplification was controlled by 2% agarose gel electrophoresis, as well as by melting temperature analysis. The final 20 μL reaction mixture contained Power SYBR Green PCR Master Mix (Applied Biosystems), 10 pmol/L of forward and reverse primers, and 100 ng complementary DNA as template. Amplification conditions were as follows: incubation at 95°C for 10 minutes, followed by 45 cycles at 95°C for 15 seconds, 60°C for 60 seconds, and 72°C for 15 seconds, with subsequent melting analysis, heating to 95°C for 20 seconds, cooling to 45°C for 10 seconds, and then reheating to 95°C.

Statistical Analysis

Data are expressed as means ± SEM. Significant difference between groups was determined by analysis of variance. Statistical analysis of the immunohistochemical data was performed using the Mann–Whitney *U* test. Probability values of $P < .05$ were accepted as being significant.

Supplementary References

1. Schmidlin F, Amadesi S, Dabbagh K, et al. Protease-activated receptor 2 mediates eosinophil infiltration and hyperreactivity in allergic inflammation of the airway. J Immunol 2002;169:5315–5321.
2. Singh VP, Bhagat L, Navina S, et al. Protease-activated receptor-2 protects against pancreatitis by stimulating exocrine secretion. Gut 2007;56:958–964.
3. Argent BE, Arkle S, Cullen MJ, et al. Morphological, biochemical and secretory studies on rat pancreatic ducts maintained in tissue culture. Q J Exp Physiol 1986;71:633–648.
4. Hegyi P, Rakonczay Z Jr, Gray MA, et al. Measurement of intracellular pH in pancreatic duct cells: a new method for calibrating the fluorescence data. Pancreas 2004;28:427–434.
5. Thomas JA, Buchsbaum RN, Zimniak A, et al. Intracellular pH measurements in Ehrlich ascites tumor cells utilizing spectroscopic probes generated in situ. Biochemistry 1979;18:2210–2218.
6. Sahin-Tóth M, Tóth M. Gain-of-function mutations associated with hereditary pancreatitis enhance autoactivation of human cationic trypsinogen. Biochem Biophys Res Commun 2000;278:286–289.
7. Bradford MM. A rapid and sensitive method for the quantitation of microgram quantities of protein utilizing the principle of protein-dye binding. Anal Biochem 1976;72:248–254.

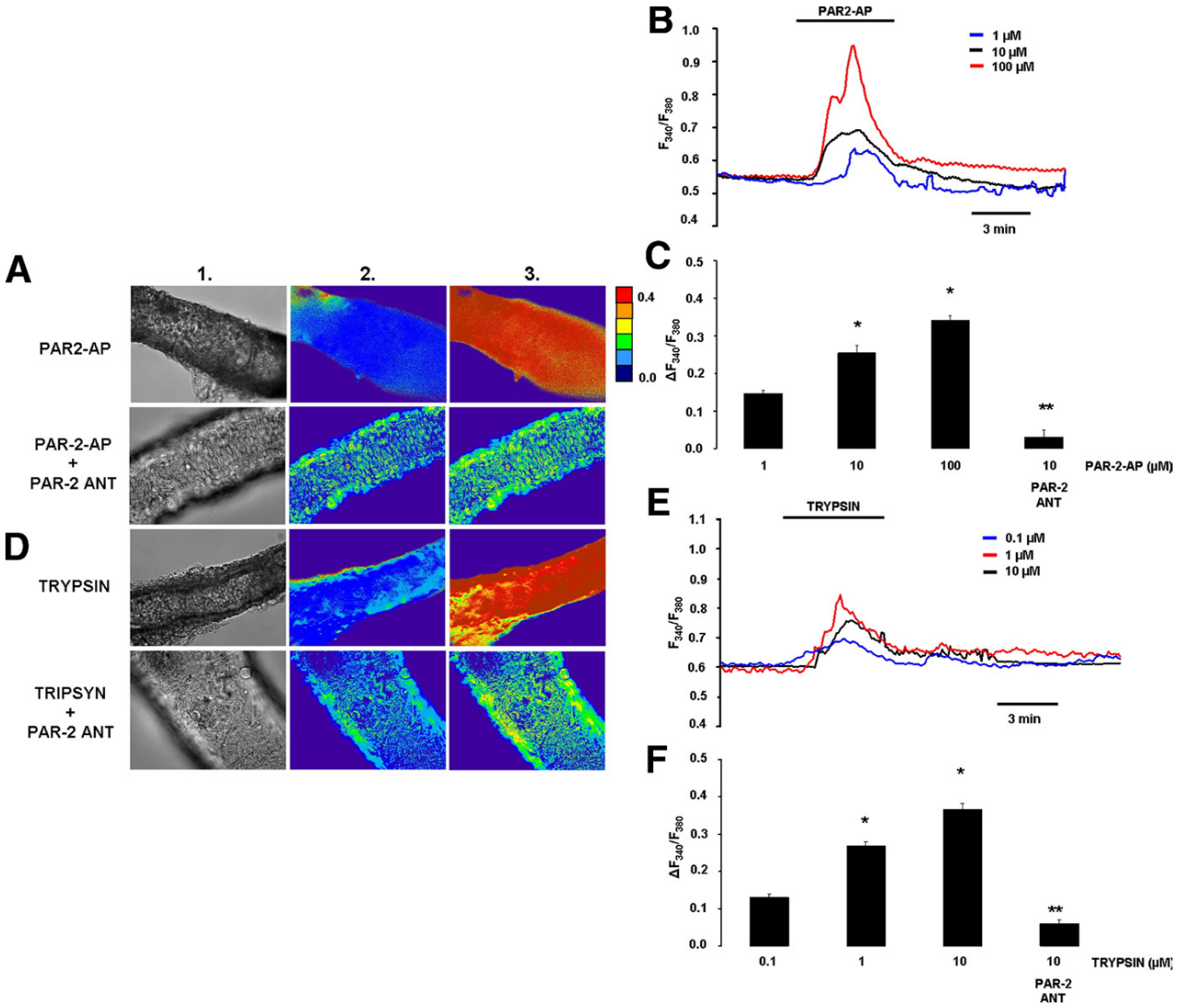

Supplementary Figure 1. Effects of PAR-2-AP and trypsin on $[Ca^{2+}]_i$ in microperfused guinea pig pancreatic ducts at pH 8.0. (*A*) Light (1) and fluorescent ratio images (2 and 3) of microperfused pancreatic ducts showing the effects of luminal administration of 10 μmol/L PAR-2-AP and 10 μmol/L PAR-2-ANT on $[Ca^{2+}]_i$ at pH 8.0. Images were taken before (1 and 2) and after (3) exposure of the ducts to PAR-2-AP or trypsin. An increase in $[Ca^{2+}]_i$ is denoted by a change from a "cold" color (*blue*) to a "warmer" color (*yellow to red*); see scale on the right. (*B* and *C*) Representative experimental traces and summary data of the changes in $[Ca^{2+}]_i$ at pH 8.0. (*D*) The same protocol was used to evaluate the effects of trypsin. (*E* and *F*) Representative experimental traces and summary data of the changes in $[Ca^{2+}]_i$. n = 3–4. $^{*}P < .05$ vs 1 μmol/L PAR-2-AP or 0.1 μmol/L trypsin, respectively. $^{**}P < .001$ vs 10 μmol/L PAR-2-AP or 10 μmol/L trypsin, respectively.

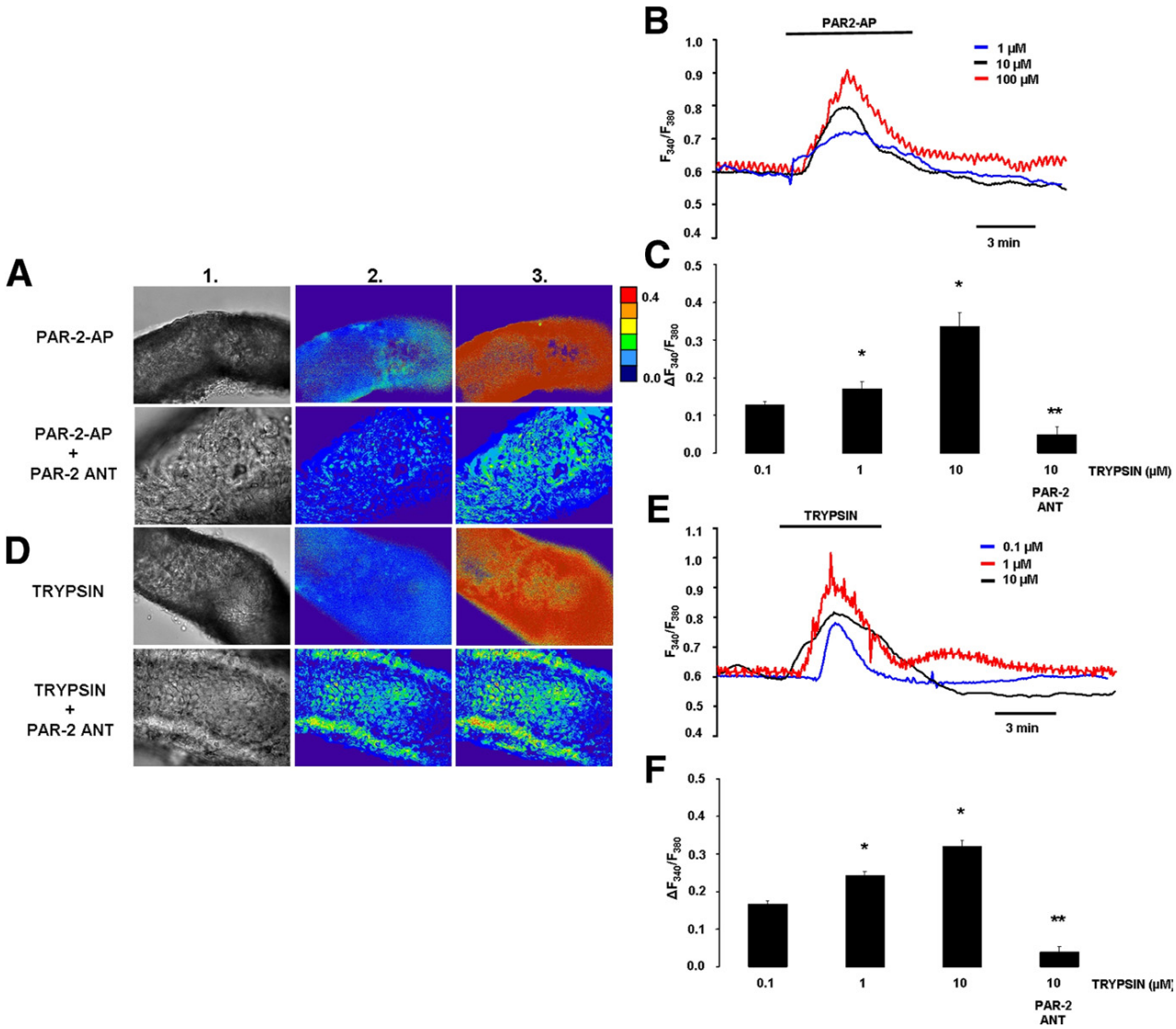

Supplementary Figure 2. Effects of PAR-2-AP and trypsin on $[Ca^{2+}]_i$ in microperfused guinea pig pancreatic ducts at pH 6.8. (*A*) Light (1) and fluorescent ratio images (2 and 3) of microperfused pancreatic ducts showing the effects of luminal administration of 10 μmol/L PAR-2-AP and 10 μmol/L PAR-2-ANT on $[Ca^{2+}]_i$ at pH 6.8. Images were taken before (1 and 2) and after (3) exposure of the ducts to either PAR-2-AP or trypsin. The colors are described in Supplementary Figure 1; see scale on the *right*. (*B* and *C*) Representative experimental traces and summary data of the changes in $[Ca^{2+}]_i$ at pH 6.8. (*D*) The same protocol was used to evaluate the effects of trypsin. (*E* and *F*) Representative experimental traces and summary data of the changes in $[Ca^{2+}]_i$ at pH 6.8. n = 3–4. $^{*}P < .05$ vs 1 μmol/L PAR-2-AP or 0.1 μmol/L trypsin, respectively. $^{**}P < .001$ vs 10 μmol/L PAR-2-AP or 10 μmol/L trypsin, respectively.

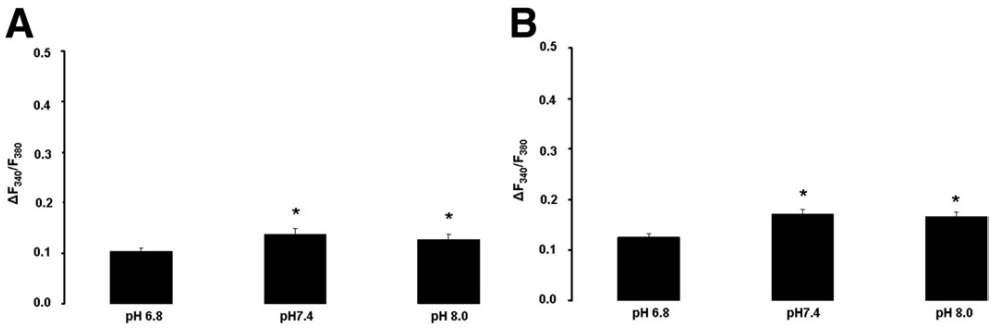

Supplementary Figure 3. Summary of the effects of PAR-2-AP and trypsin on $[Ca^{2+}]_i$ in microperfused guinea pig pancreatic ducts at different extracellular pH values. (*A*) The elevation in $[Ca^{2+}]_i$ evoked by 1 μmol/L PAR-2-AP and (*B*) 0.1 μmol/L trypsin at different extracellular pH values (6.8; 7.4; 8.0). n = 3–4. $^*P < .05$ vs at pH 6.8.

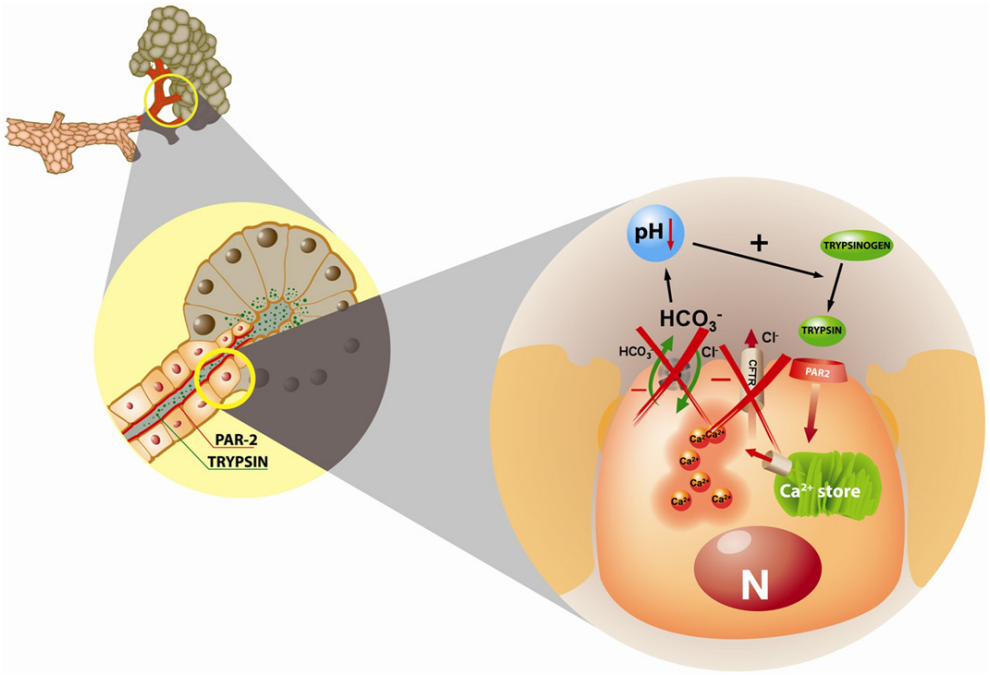

Supplementary Figure 4. The vicious trypsin cycle. If trypsin is present in the duct lumen, PAR-2 receptors on the duct cell are activated, leading to Ca^{2+} release from intracellular stores and an increase in cytosolic Ca^{2+} concentration. This causes inhibition of the luminal anion exchangers and CFTR Cl^- channels reducing bicarbonate secretion by the duct cell. The decrease in bicarbonate secretion will decrease luminal pH in the duct, which strongly accelerates the autoactivation of trypsinogen to trypsin. The activated trypsin will further inhibit bicarbonate transport by the duct cells, leading to a vicious cycle generating further decreases in luminal pH and enhanced trypsinogen activation with the potential for damaging the gland. The cycle may eventually be broken by the down-regulation of duct cell PAR-2 expression once pancreatitis is established. N, nucleus.

Supplementary Table 1. Nucleotid Sequences of the Primers Used in the Study.

Gene name	Primer sequence (5′ to 3′)	Product length (*base pairs*)	Annealing temperature (°*C*)
β-actin	GTACGCCAACACAGTGCTG (sense) CTTCATTGTGCTGGGTGCC (antisense)	100	55
PAR-2	GGCACCATCCAAGGAACCAATAG(sense) GCAGAAAACTCATCCACAGAAAAGAC (antisense)	128	58

IV.

Pflugers Arch - Eur J Physiol (2012) 463:459–475
DOI 10.1007/s00424-011-1059-6

SIGNALING AND CELL PHYSIOLOGY

NHE1 activity contributes to migration and is necessary for proliferation of human gastric myofibroblasts

Mátyás Czepán · Zoltán Rakonczay Jr. · Andrea Varró · Islay Steele · Rod Dimaline · Nantaporn Lertkowit · János Lonovics · Andrea Schnúr · György Biczó · Andrea Geisz · György Lázár · Zsolt Simonka · Viktória Venglovecz · Tibor Wittmann · Péter Hegyi

Received: 31 March 2011 / Revised: 31 October 2011 / Accepted: 2 November 2011 / Published online: 6 December 2011

Abstract Myofibroblasts play central roles in wound healing, deposition of the extracellular matrix and epithelial function. Their functions depend on migration and proliferation within the subepithelial matrix, which results in accelerated cellular metabolism. Upregulated metabolic pathways generate protons which need to be excreted to maintain intracellular pH (pH_i). We isolated human gastric myofibroblasts (HGMs) from surgical specimens of five patients. Then we characterized, for the first time, the expression and functional activities of the Na^+/H^+ exchanger (NHE) isoforms 1, 2 and 3, and the functional activities of the Na^+/HCO_3^- cotransporter (NBC) and the anion exchanger (AE) in cultured HGMs using microfluorimetry, immunocytochemistry, reverse transcription polymerase chain reaction and immunoblot analysis. We showed that NHE1–3, NBC and AE activities are present in HGMs and that NHE1 is the most active of the NHEs. In scratch wound assays we also demonstrated (using the selective NHE inhibitor HOE-642) that carbachol and insulin like growth factor II (IGF-II) partly stimulate migration of HGMs in a NHE1-dependent manner. EdU incorporation assays revealed that IGF-II induces proliferation of HGMs which is inhibited by HOE-642. The results indicate that NHE1 is necessary for IGF-II-induced proliferation response of HGMs. Overall, we have characterized the pH_i regulatory mechanisms of HGMs. In addition, we demonstrated that NHE1 activity contributes to both IGF-II- and carbachol-stimulated migration and that it is obligatory for IGF-II-induced proliferation of HGMs.

Keywords Fibroblast · Na^+/H^+ exchange · Gastrointestinal tract · Human

Abbreviations

AE	Anion exchanger
AMV	Avian myeloblastosis virus
AMV-RT	Avian myeloblastosis virus reverse transcriptase
BCECF-AM	2,7-Biscarboxyethyl-5(6)-carboxyfluorescein-acetoxymethylester
DAG	Diacyl-glicerol
DAPI	4,6-Diamidino-2-phenylindole
DMEM	Dulbecco's Modified Eagle's Medium

Specific author contributions György Lázár, Zsolt Simonka, Tibor Wittmann and János Lonovics were involved in patient selection and sample collection; Zoltán Rakonczay Jr., Viktória Venglovecz and Péter Hegyi were involved in tissue culturing and microfluorometric experiments; Andrea Varró, Rod Dimaline, Islay Steele, Nantaporn Lertkowit, Andrea Schnúr, György Biczó and Andrea Geisz performed molecular biology experiments and biological assay experiments. Mátyás Czepán was involved in all of the above mentioned experiments and drafted the manuscript. Péter Hegyi designed and supervised the project, the experiments and the manuscript. Mátyás Czepán spent 3 months in Liverpool as part of the project funded by the NIH and NIHR.

M. Czepán · Z. Rakonczay Jr. · J. Lonovics · A. Schnúr · G. Biczó · A. Geisz · T. Wittmann · P. Hegyi (✉)
First Department of Medicine, University of Szeged,
6720 Korányi fasor 8-10,
Szeged, Hungary
e-mail: hegyi.peter@med.u-szeged.hu

G. Lázár · Z. Simonka
Department of Surgery, University of Szeged,
Szeged, Hungary

V. Venglovecz
Department of Pharmacology and Pharmacotherapy,
University of Szeged,
Szeged, Hungary

A. Varró · I. Steele · R. Dimaline · N. Lertkowit
Department of Physiology, University of Liverpool,
Liverpool, UK

DMSO	Dimethyl sulfoxide
dNTP	Deoxyribonucleotide-triphosphate
EDTA	Ethylenediamine tetra-acetic acid
EdU	5-Ethynyl-2-deoxyuridine
ER	Endoplasmic reticulum
FITC	Fluorescein isothiocyanate
GAPDH	Glyceraldehyde 3-phosphate dehydrogenase
H_2DIDS	4,4′-Diisothiocyanatodihydrostilbene-2, 2′-disulfonic acid
HaCaT cells	Human adult low calcium temperature keratinocytes
HEPES	(4-(2-Hydroxyethyl)-1-piperazine-ethanesulfonic acid
HGM	Human gastric myofibroblast
HOE-642	4-Isopropyl-3-methylsulphonylbenzoyl-guanidin methanesulphonate also known as cariporide
IGF-II	Insulin like growth factor II
IP_3	Inositol 1,4,5-trisphosphate
$J(B^-)$	Base flux
NBC	Na^+/HCO_3^- cotransporter
NF-κB	Nuclear factor kappa B
NHE	Na^+/H^+ exchanger
NMDG	N-metil D-glucamine
PBS	Phosphate buffered saline
pH_i	Intracellular pH
PIP_2	Phosphatidylinositol 4,5-bisphosphate
PKC	Protein kinase C
PLC	Phospholipase C
PP	Proton pump
RPMI	Roswell Park Memorial Institute
RT	Room temperature
RT-PCR	Reverse transcription polymerase chain reaction
SEM	Standard error of mean
SMA	Smooth muscle actin
SR	Sarcoplasmic reticulum

Introduction

Myofibroblasts, also known as activated fibroblasts, are dynamic, spindle-like cells sharing the functional characteristics of both fibrocytes and smooth muscle cells [24]. They are crucial for the production of extracellular matrix and for morphogenesis [42]; moreover, they take part in inflammatory processes related to tissue repair and in the chronic inflammation–adenoma–carcinoma sequence by secreting a broad spectrum of cytokines thereby altering the microenvironment around epithelial cells [23, 41]. To accomplish their functions, myofibroblasts migrate and proliferate in the subepithelial compartment, generating acidic metabolites and consequently protons in the cytosol [21]. Protons are removed from cells mainly by acid/base transporters located on the plasma membrane [7], thus maintaining isoionic intracellular conditions.

Although many authors have investigated the regulation of acid/base transporters and their role in migration and proliferation of epithelial cells [16, 31, 39, 45] or fibroblasts [10, 11, 48, 57], no information is available concerning the effects of acid/base transporter activities on migration and proliferation of gastric myofibroblasts.

One of the main proton extrusion mechanisms is sodium/hydrogen exchange through the Na^+/H^+ exchangers (NHEs), which are members of a transporter family comprising of ten isoforms [32, 44]. It has been demonstrated that NHE1 functions not only as a cation exchanger, but also as a modulator of intracellular signalling thereby regulating motility in different animal species including mouse [53], rat [14], dog [30], guinea pig [57] and human cells including leukocytes [49], melanoma cells [55] and hepatoma cells [67]. NHE1 activity was found to be necessary for proliferation of brain-derived pericytes [25], fibroblasts [26], lymphocytes [60] and vascular smooth muscle cells [65]. Furthermore, inhibition of NHE1 activity significantly reduces proliferation rates in vascular smooth muscle cells [65].

It has been demonstrated that gastric epithelial cells secrete matrix metalloproteinase-7 which cleaves myofibroblast-produced insulin-like growth factor binding protein-5 thereby releasing insulin-like growth factor-II (IGF-II). IGF-II acts as a potent stimulant of both epithelial and myofibroblast proliferation [36]. The muscarinic acetylcholine receptor type 3 (M3) agonist carbachol has been shown to increase NHE activity in rabbit parietal cells [3] and in guinea pig pancreatic ductal epithelial cells [59]. Many inhibitors of NHE activity have been described as a consequence of intensive research on amiloride derivatives to develop isoform-specific NHE inhibitors for use in cardiovascular care. 4-Isopropyl-3-methylsulphonylbenzoyl-guanidin methanesulphonate (HOE-642), also known as cariporide, is one of the most effective compounds, which can dose-dependently inhibit specific NHE isoforms [47].

The aim of this study was to characterize the acid/base transporters of human gastric myofibroblasts (HGMs), focusing on the possible roles of NHE1 in cell migration and proliferation.

Materials and methods

Chemicals and solutions

Chemicals and solutions used for cell culture were purchased from Sigma-Aldrich (Budapest, Hungary). All reagents for

immunocytochemistry, unless indicated otherwise, were purchased from Jackson ImmunoResearch Laboratories (West Grove, PA, USA). Chemicals and reagents for polymerase chain reaction (PCR), unless indicated otherwise, were obtained from Promega (Southampton, UK). All primers were purchased from Eurogentec (Southampton, UK).

HOE-642 (cariporide) was kindly donated by Sanofi-Aventis (Frankfurt, Germany). 2,7-Biscarboxyethyl-5(6)-carboxyfluorescein-acetoxymethylester (BCECF-AM) and HOE-642 were dissolved in dimethyl sulfoxide. The composition of solutions used for the measurements of intracellular pH (pH_i) is given in Table 1. 4-(2-Hydroxyethyl)-1-piperazine-ethanesulfonic acid (HEPES) solutions were titrated to pH 7.4 at 37°C using either NaOH or HCl. HCO_3^--buffered solutions were gassed with 95% O_2 and 5% CO_2 at 37°C.

Ethics

The study was approved by the Ethics Committee of the University of Szeged, Hungary. All surgical patients gave informed consent.

Patients, isolation and culture of HGMs

Tissue specimens from patients undergoing gastric tumour resection in the Department of Surgery, University of Szeged, Hungary were obtained intraoperatively at least 3–4 cm away from the tumour and were transported immediately to the laboratory in ice-cold media for culturing (n=3). Two other specimens from multiple organ cadaver donors were obtained similarly. Patient details can be found in Table 2. Histopathology confirmed that all specimens were normal gastric tissue samples. The isolation of HGMs was performed using a previously described method [27]. Briefly, the specimens were washed and chopped into very small pieces and were then bathed in a shaking water bath at 37°C for 15 min with 1 mM dithiothreitol. After washing, the specimens were incubated for 30 min at 37°C with 1 mM ethylenediamine tetra-acetic acid (EDTA) four times. Specimens were cultured for 1–2 weeks in Roswell Park Memorial Institute (RPMI) medium supplemented with 10% fetal bovine serum, 1% penicillin–streptomycin and 2% antibiotic–antimycotic solution. After the cells became confluent, they were trypsinized with 0.25% trypsin-EDTA and were transferred into Dulbecco's Modified Eagle's Medium (DMEM) with 4 mM L-glutamine containing 10% fetal bovine serum, 1% amino acid solution, 1% penicillin–streptomycin and 2% antibiotic–antimycotic solution. The medium was replaced every 48 h and the cells were passaged after reaching confluency up to

Table 2 Patients' details

Patient no.	Gender	Age	Diagnosis
1	Female	71	Gastric cancer
2	Male	76	Gastric cancer
3	Male	66	Gastric cancer
4	Female	42	Subarachnoidal haemorrhage
5	Male	49	Traumatic head injury

Table 1 Composition of solutions. Values are in millimolar concentrations

	HEPES	HCO_3^-	NH_4Cl HEPES	NH_4Cl HCO_3^-	Cl^--free HEPES	Cl^--free HCO_3^-	Cl^--free NH_4Cl/ HEPES	Cl^--free NH_4Cl/ HCO_3^-	Na^+-free HEPES	Na^+-free HCO_3^-	Na^+-free NH_4Cl/ HEPES	Na^+-free NH_4Cl/ HCO_3^-	High K^+-HEPES
NaCl	130	115	110	95									5
KCl	5	5	5	5					5	5	5	5	130
Na-HEPES	10	25	10										10
$CaCl_2$	1	1	1	1					1	1	1	1	1
$MgCl_2$	1	1	1	1					1	1	1	1	1
Glucose	10	10	10	10	10	10	10	10	10	10	10	10	10
NH_4Cl			20	20							20	20	
$NaHCO_3$						25		25					
HEPES					10		10		10		10		
Na-gluconate					140	115	120	95					
K_2-sulfate					2.5	2.5	2.5	2.5					
Ca-gluconate					6	6	6	6					
Mg-gluconate					1	1	1	1					
NH_4-sulfate						20		20					
NMDG									140	115	120	95	
Atropine										0.01	0.01	0.01	
Choline-HCO_3										25	25	25	

passage 10. Cell cultures were continually incubated at 37°C in a mixture of 5% CO_2 and 95% air.

Immunocytochemistry

Twelve thousand HGMs were seeded onto chamber slides and were allowed to adhere overnight. Cells were fixed using 4% paraformaldehyde for 30 min and were washed twice with phosphate buffered saline (PBS, Invitrogen, Paisley, UK). Permeabilization was performed by incubation with a filtered, PBS-based solution containing 0.2% Triton X-100 and 0.3% protease-free bovine serum albumin for 30 min. Cells were then incubated with 10% donkey serum in PBS for 30 min. After washing twice with PBS, primary antibodies were added to the chambers and the slides were incubated in moist atmosphere at 4°C, overnight. The following primary antibodies were used: anti-α-smooth muscle actin (α-SMA) antibody raised in guinea pig (1:400), anti-vimentin antibody raised in mouse (1:400), anti-cytokeratin antibody raised in mouse (1:400), anti-desmin antibody raised in mouse (1:400, all four antibodies from Dako, Denmark) and anti-NHE1, -NHE2 and -NHE3 antibodies raised in goat (1:50, purchased from Santa Cruz Biotechnology, Santa Cruz, CA, USA). Primary antibodies were removed by a sequence of washes for 10 min each with 0.14, 0.5 and 0.14 M NaCl dissolved in PBS, respectively. Slides were then incubated with secondary antibodies for 60 min in dark and moist conditions. The following secondary antibodies were used: fluorescein isothiocyanate (FITC)-conjugated anti-guinea pig secondary antibody [1:400, diluted in 10 mM HEPES, pH 7.5], Texas Red- and FITC-conjugated anti-mouse antibody (1:400) and FITC-conjugated anti-goat secondary antibody (1:400). After hybridization, slides were washed three times with PBS and were covered with 4,6-diamidino-2-phenylindole (DAPI) containing Vectashield mounting medium (Vector Laboratories, Peterborough, UK), then cover slipped.

Intracellular pH measurement

One hundred thousand HGMs were seeded onto 24-mm-diameter round glass coverslips in full media. They were allowed to recover for 24 h before experiments. Coverslips were then transferred into a perfusion chamber and mounted on an inverted microscope (Olympus, Budapest, Hungary). Cells were bathed in HEPES solution at 37°C and were loaded with 2 μM pH-sensitive fluorescent dye BCECF-AM (Invitrogen, Paisley, UK) for 20 to 30 min. Thereafter, myofibroblasts were continuously perfused with solutions at a rate of 5 to 6 ml/min and pH_i was measured by using an imaging system (CellR; Olympus, Budapest, Hungary). Cells were excited at wavelengths of 490 nm and 440 nm, and the 490/440 fluorescence emission ratio was measured at 535 nm. One pH_i measurement was recorded per second.

In situ calibration of the fluorescence signal was performed using the high K^+-nigericin technique as previously described [22, 58]. The pH of high K^+–HEPES solution supplemented with 10 μM nigericin was set to 6.8 or 7.4 at 37°C, then cells loaded with BCECF were superfused by these solutions and the 490/440 fluorescence ratio was recorded. Multiple-point calibrations, i.e. sequential BCECF pH measurements (with high K^+–HEPES–nigericin solutions ranging pH from 6.2 by 0.4 step to 8.2) were performed to confirm data accuracy. Linear projections were made from the steady-state fluorescence pH data during high K^+-nigericin superfusion with known pH. Adaptation of projections to the resting fluorescence data of unknown pH_i in standard HEPES solution results in accurate resting pH_i.

In order to characterize the acid/base transporters, we used ion-withdrawal technique, and ammonium pulse technique in HEPES- and HCO_3^-/CO_2-buffered solutions. Initial rates (first 30–60 s) of recovery from acidosis were calculated by linear regression.

Determination of buffering capacity and calculation of base fluxes

The intrinsic buffering capacity (β_i) of HGMs was estimated by the NH_4^+ pre-pulse technique [62]. β_i refers to the ability of intrinsic cellular components (excluding the bicarbonate buffer system) to buffer changes of pH_i. Briefly, HGMs were exposed to various concentrations of NH_4Cl while Na^+ and HCO_3^- were omitted from the solution to block the Na^+-dependent pH regulatory mechanisms. β_i was estimated by the Henderson–Hasselbalch equation. The total buffering capacity (β_{total}) was calculated as $\beta_{total}=\beta_i+\beta_{HCO3^-}=\beta_i+2.3\times[HCO_3^-]_i$, where β_{HCO3^-} is the buffering capacity of the HCO_3^-/CO_2 system and $[HCO_3]_i$ is the intracellular concentration of HCO_3^-. Transmembrane base flux [$J(B^-)$] was calculated by using the equation $J(B^-)=dpH/dt\times\beta_{total}$. The β_{total} value used in the calculation of $J(B^-)$ was obtained from Fig. 2b by using the pH_i value at the start of the 30-s period over which dpH/dt was measured.

Reverse transcription polymerase chain reaction

RNA was isolated from myofibroblast cultures using a Qiagen RNEasy Mini Kit (Qiagen House, Crawly, UK) according to the manufacturer's instructions; human kidney RNA was isolated from whole tissue from surgical specimens utilizing TRIzol reagent. RNA was reverse transcribed to cDNA and RNA/primer annealing was performed with 0.5 μg oligo-dT primer at 65°C for 5 min. After cooling, samples were reverse transcribed in a final reaction volume of 30 μl containing the annealed RNA/primer set, 5× AMV (avian

myeloblastosis virus) buffer, 1.25 mM dNTP (deoxyribonucleotide-triphosphates) mix, 20 unit RNAse inhibitor and 15 unit AMV-RT (AMV-reverse transcriptase). Reactions were incubated at 42°C for 1 h; enzymes were inactivated at 85°C for 5 min. cDNA (1 μl) was used as template for each PCR in a final volume of 25 μl, containing 10× master mix Taq-buffer, 10 nM dNTPs, 2.5 unit Taq-polymerase and 1 μM NHE primer sets. The sequence of NHE primers is given in Table 3. PCR settings were as follows: denaturation at 95°C for 15 s, annealing at 60°C for 15 s, extension at 72°C for 45 s, 30 cycles. PCR products and DNA HyperLadderPlus (BioLine, Taunton, USA) were run on a 0.8% agarose gel containing 0.005% ethidium bromide in Tris-buffered EDTA solution at 80 V, then the gel was illuminated in a BioRad UV (ultraviolet) chamber and photographs were taken.

Immunoblot analysis

Confluent cells (3,000,000 cells at least) were washed with PBS after removing the media and were then incubated with 100 mM EDTA for 15 min. After centrifugation (500×*g*, 8 min), the supernatant was gently removed and was lysed with RIPA (radio-immuno precipitation assay) buffer supplemented with 1% protease inhibitor cocktail (Calbiochem-Merck Chemicals, Darmstadt, Germany). Samples were vortexed and frozen in liquid nitrogen for a few seconds then centrifuged at 11,000×*g* for 10 min at 4°C. The protein concentrations of supernatants containing whole cell protein lysates were determined by using Bradford's reagent. Samples were heat treated at 30°C for 30 min and 100 μg protein was electrophoresed on 8% sodium dodecylsulfate-polyacrylamide gels according to the method of Laemmli using a Hoefer Mighty Small II instrument (Harvard Bioscience Inc., Massachusetts, USA). After separation, proteins were blotted to matching-sized nitrocellulose membrane for 60 min at 100 V. Membranes were blocked in 5% nonfat dry milk for 1 h and were incubated with primary antibodies (1:100 for NHE) overnight at 4°C on a rocker. The same NHE primary antibodies were used as for immunocytochemistry. Primary antibodies were removed by washing with TBST for 3× 10 min. HRP-conjugated secondary antibodies (Dako, Denmark) were applied for 60 min at RT on a rocker. After 3×10 min TBST wash, the immunoreactive protein was visualized by enhanced chemiluminescence. Remaining antibodies were removed by washing with TBST, then anti-glyceraldehyde 3-phosphate dehydrogenase antibody (Dako, Denmark) was added to the membrane for 60 min at RT. Secondary antibody (1:10,000) was also applied for 60 min at RT then signals were recorded as described earlier.

Table 3 NHE primer sequences

Primer name	Sequence (5' - 3')
NHE1 forward	CCT-CTC-TGG-GTG-GAG-AAG-CT
NHE1 reverse	CCC-AGG-AAC-GAC-ACA-GAA-AG
NHE2 forward	CCA-TGG-AAC-CAC-TGG-GCA-AC
NHE2 reverse	TGC-AGG-GGG-AGA-CTT-CTC-AT
NHE3 forward	TCC-AAG-TCG-ACC-AAG-CTG-GG
NHE3 reverse	AAG-GCC-TCG-TCC-GGA-GAA-AA

Migration assays

HGMs (125,000 cells) were seeded onto six-well plates and allowed to adhere overnight in full media. On the following day, the confluent monolayer was gently scratched using a P2 tip. Only the wells containing even-sided and sharp-edged wounds were used for experiments. After gentle washing for three times with serum-free media, wounds were measured and photographed under inverted light microscope. Reagents were then added to the wells in serum-free media in all of the experiments and plates were incubated in CO_2 incubator at 37°C for 24 h. Migration was evaluated by counting the cells in the same area of the wound after 12 and 24 h as reported earlier [43].

Proliferation assays

Myofibroblasts (50,000 cells) were seeded onto cover glasses. After overnight incubation, HGMs were synchronized by incubation for 30 h in serum-free media. Thereafter, 10 μM 5-ethynyl-2-deoxyuridine (EdU; Alexa Fluor 488 Imaging Kit, Invitrogen, Oregon, USA; for further details, see reference [50]) was added to the cells for overnight incubation with or without treatment. After incubation, the manufacturer's protocol was applied to fix and permeabilize the cells and to detect EdU incorporation. We used DAPI to detect nuclear staining. The proliferation rate was calculated by normalizing the number of EdU positive cells to the DAPI-stained cells in 10 fields at 20x magnification.

Statistical analysis

Values are expressed as means±standard error of mean (SEM). Statistical analyses were performed using non-parametric Kruskal–Wallis tests with post-hoc Wilcoxon tests for pairwise comparisons and Bonferroni correction to test post-hoc significance. $p<0.05$ was accepted as significant. n numbers are given as follows: n = number of patients/number of independent experiments per patient.

Results

Identification of myofibroblasts

Cells showed positive staining for α-SMA and vimentin but not for cytokeratin and desmin, which are characteristics of myofibroblasts (Fig. 1). The purity of the HGM cell cultures was ~100%. As positive controls for cytokeratin and desmin antibodies, we used CAPAN-1 (human pancreatic adenocarcinoma cell line) cells and cultured human high grade pancreatic neuroendocrine carcinoma cells, respectively. In both cases, appropriate localisation was demonstrated (Fig. 1).

Determination of the resting pH_i of HGMs

The multiple-point calibration technique utilizing high K^+–HEPES/nigericin solution was used to determine the resting pH_i of HGMs. Our experiments showed that the resting pH_i of HGMs in HEPES solution was 7.09±0.02 (Fig. 2).

Characterization of the acid/base transporters of HGMs

Next we tried to identify the functionally active acid/base transporters expressed on the plasma membrane of HGMs. Na^+ withdrawal from the standard HEPES solution

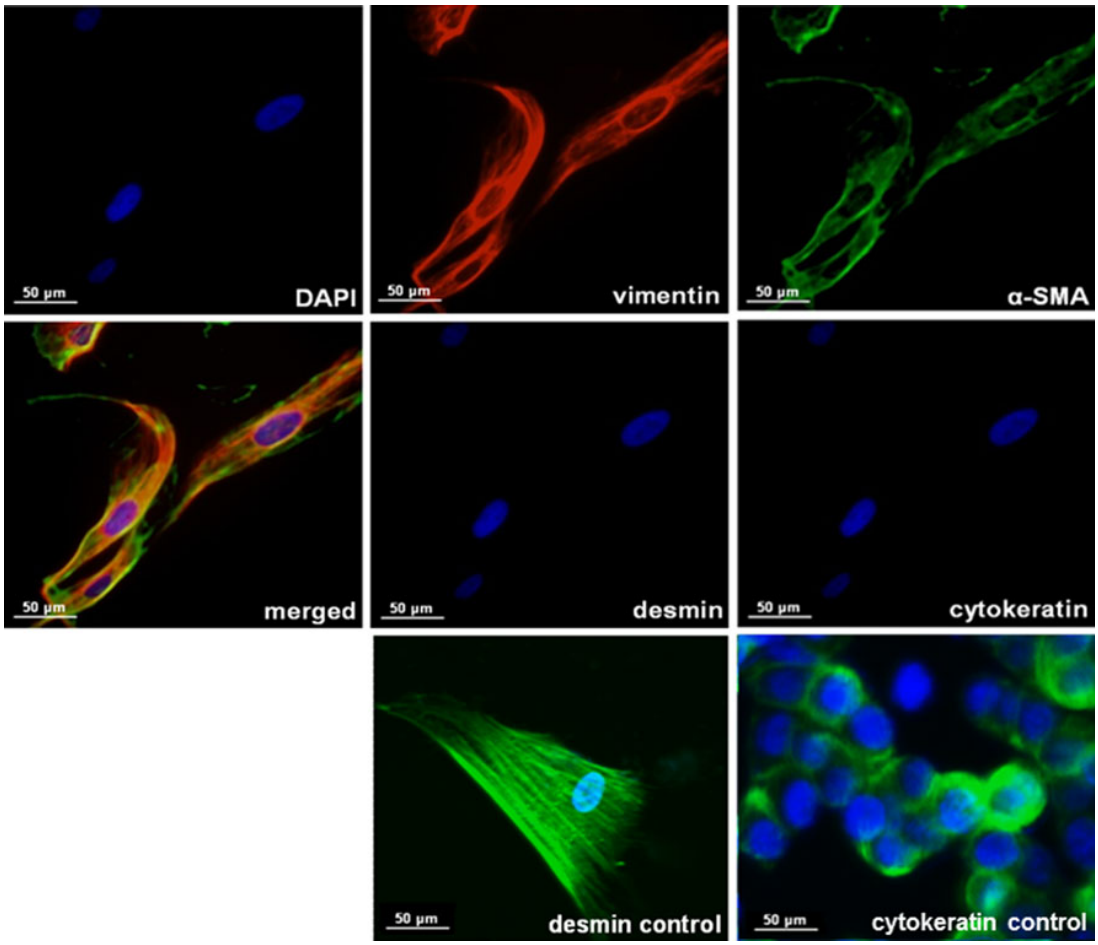

Fig. 1 Immunocytochemical identification of cell cultures. Cells isolated from human gastric samples were grown on chamber slides and were subjected to immunocytochemical analysis of vimentin and α-smooth muscle actin (α-SMA) expression as specific markers of myofibroblasts. Cytokeratin and desmin antibodies were used for detecting epithelial and muscle cells, respectively. Nuclei were counterstained with DAPI (*blue*). Vimentin (*red*) and α-SMA (*green*) verified the presence of myofibroblasts, whereas no epithelial or smooth muscle cells were detected (n=5/1–2). Control stainings were performed to test the desmin and cytokeratin antibodies. Cultured cancer cells (from human high grade pancreatic neuroendocrine carcinoma) were used as positive controls for desmin (*green staining*, n=1). To test the cytokeratin antibody, control staining was performed on CAPAN-1 (human pancreatic adenocarcinoma cell line) cells. *Green staining* shows cytokeratin; *blue staining* shows DAPI (n=1)

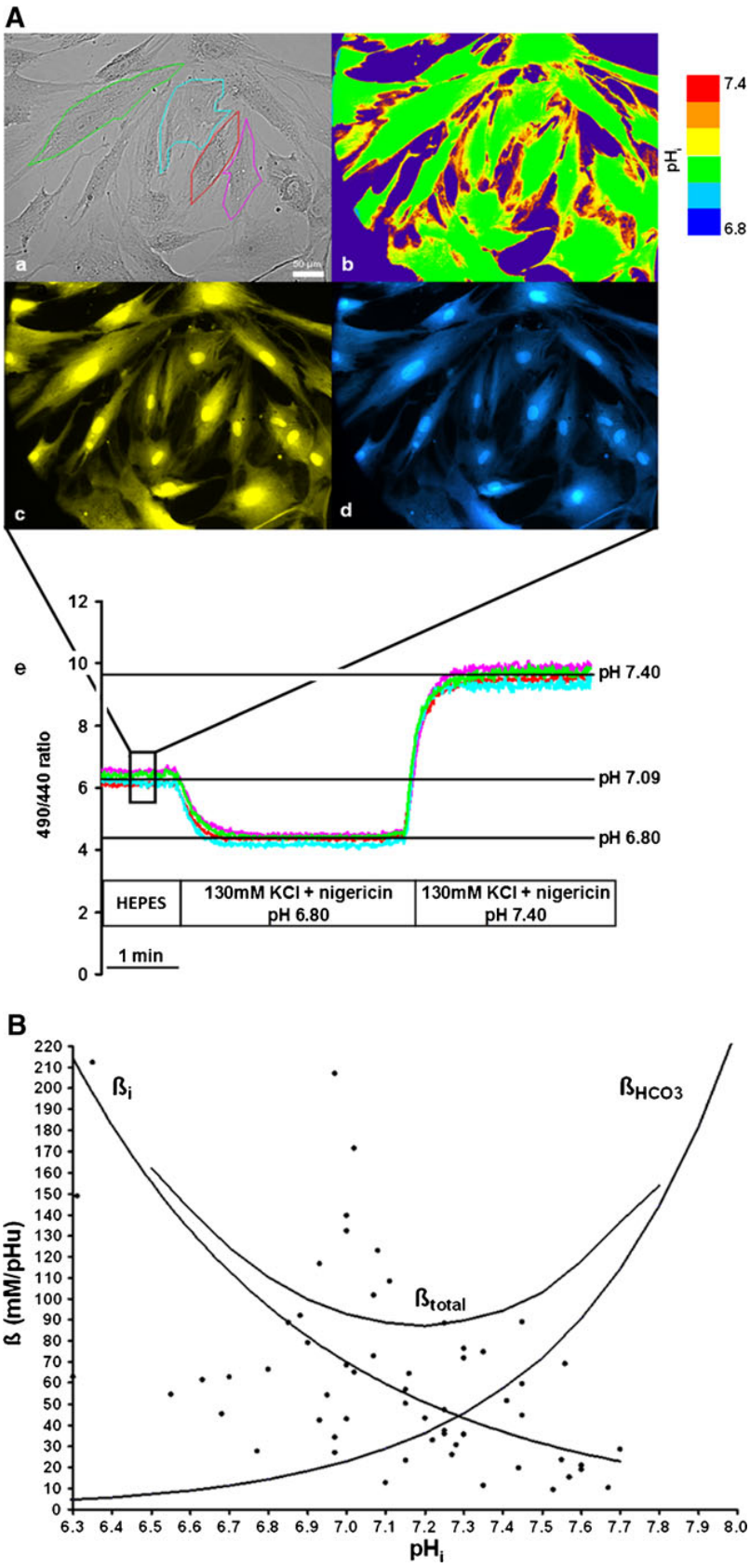

Fig. 2 The resting pH_i of gastric myofibroblasts and measurement of buffering capacity. **A** Human gastric myofibroblasts (HGMs, 100,000) were seeded onto cover glass to form monolayers. Cells were allowed to recover for 24 h. **a** Phase contrast image of myofibroblasts is shown. Four to seven cells as regions of interests (ROIs) were marked. **b** Thermal-adjusted image is shown to demonstrate homogenous BCECF dye distribution. Color coding shows the pH_i; **c** 490 and **d** 440 nm fluorescent images are also shown. **e** Cells were excited at wavelengths of 490 and 440 nm after loading the cells with the pH-sensitive fluorescent dye 2 μM BCECF-AM, and the 490:440 fluorescence emission ratio was measured at 535 nm. Cells were exposed to continuous perfusion with nigericin/high K^+–HEPES solutions of pH 6.80 and 7.40. The resting pH_i was calculated by multiple-point calibration (n=5/5–6). The figure shows a representative calibration curve; the mean resting pH_i in standard HEPES solution was 7.09±0.02. **B** The buffering capacity of HGMs was determined by exposing the cells to various concentrations of NH_4Cl while Na^+ and HCO_3^- were omitted from the solution to block Na^+-dependent pH regulatory mechanisms. The intrinsic buffering capacity (β_i) at different pH_i (*black circle*, n=85) was estimated by the Henderson–Hasselbalch equation. Regression analysis was performed using the curve-fitting protocol in Excel. The total buffering capacity (β_{total}) was calculated as $\beta_{total} = \beta_i + \beta HCO_3^- = \beta_i + 2.3 \times [HCO_3^-]_i$, where βHCO_3^- is the buffering capacity of the HCO_3^-/CO_2 system and $[HCO_3]_i$ is the intracellular concentration of HCO_3^-

caused strong reversible acidification suggesting the presence of an active Na^+-dependent H^+ efflux mechanism (Fig. 3a).

Switching the standard HEPES solution to standard HCO_3^-/CO_2 solution caused rapid intracellular acidification, most probably due to CO_2 diffusion into the cells. Thereafter, a small pH_i recovery was observed suggesting a HCO_3^- influx and/or H^+ efflux mechanism (Fig. 3b). In order to determine the Na^+ dependency of this HCO_3^- influx/H^+ efflux mechanism, the same experiment was performed in Na^+-free conditions (Fig. 3c). Since no recovery was found in the presence of HCO_3^-/CO_2 in Na^+-free solution, we can assume that the HCO_3^- influx/H^+ efflux mechanism in HGMs is Na^+-dependent. These results indicate that HGMs express functionally active NHE and/or NBC.

Next we tested whether HGMs contain functionally active anion exchangers (AE). Cl^- removal from the standard HCO_3^-/CO_2 solution caused reversible alkalization suggesting the presence of a Cl^--dependent HCO_3^- efflux mechanism (Fig. 3d). Importantly, omitting HCO_3^- from the extracellular solution in combination with Cl^- removal resulted in no significant change in pH_i (Fig. 3e). This indicates that HGMs express functionally active AE.

To confirm these findings, the activities of acid/base transporters were also investigated by the ammonium pulse technique. Exposure of HGMs to 20 mM NH_4Cl induced an immediate rise in pH_i due to the rapid entry of the lipophilic base, NH_3, into the cells, which binds intracellular protons generating NH_4^+ and causing alkalization. The recovery from this alkali load is promoted by AEs in the

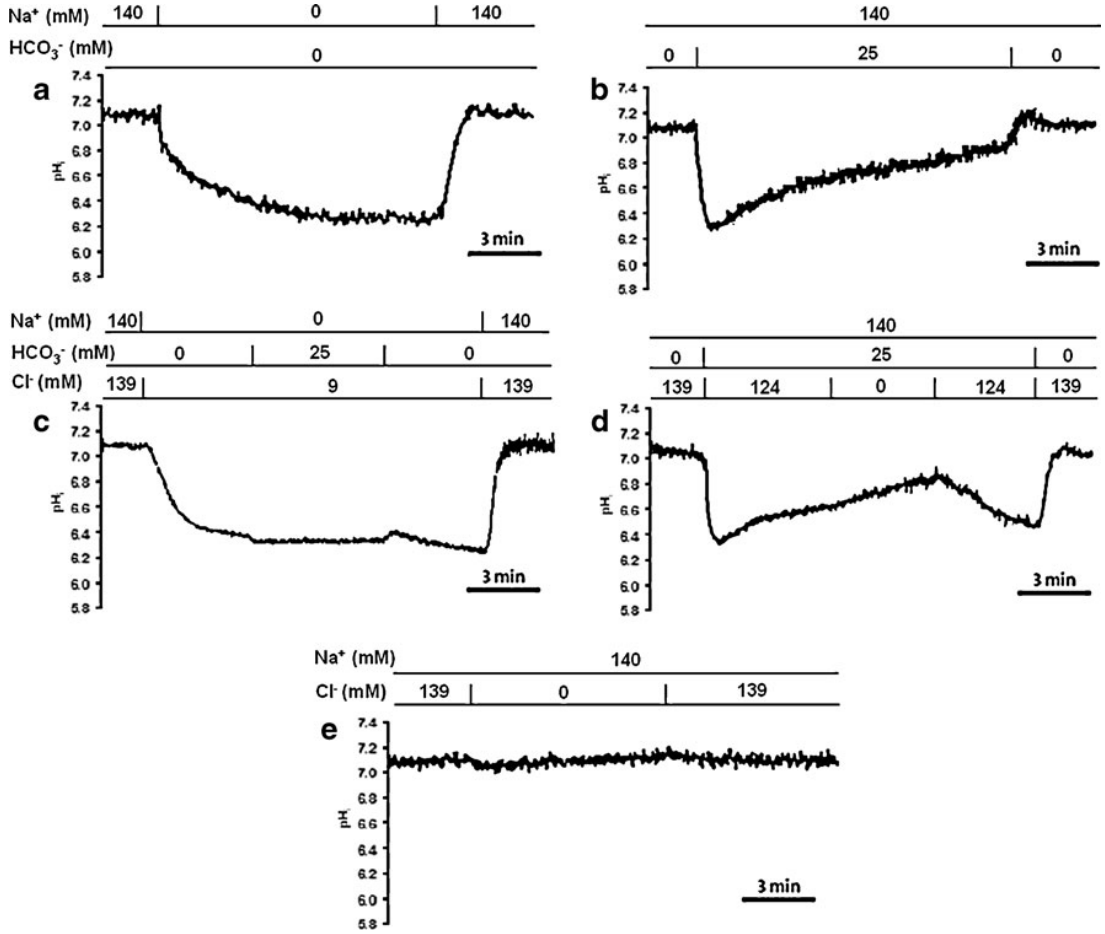

Fig. 3 Na^+-dependent HCO_3^- influx and Cl^--dependent HCO_3^- efflux mechanisms are present in HGMs. Representative pH_i curves of HGMs are shown. **a** The sudden removal of extracellular Na^+ from the standard HEPES solution caused rapid acidification, which was reversed by the re-addition of the ion. **b** Administration of HCO_3^-/CO_2-buffered solution after standard HEPES solution caused acidification of pH_i followed by alkalization (HCO_3^- influx). **c** Switching from Na^+-free HEPES solution to Na^+-free HCO_3^-/CO_2-buffered solution caused acidification, but no pH_i recovery was seen. **d** In HCO_3^-/CO_2-buffered solution, Cl^- removal resulted in alkalization of pH_i followed by a complete recovery after re-addition of Cl^-. **e** Cl^- removal from the standard HEPES solution did not alter significantly the pH_i, and it reached again the resting value before re-addition of Cl^- (n=5/5–6)

presence of HCO_3^- and Cl^- in the extracellular solution. In support of this, the recovery from alkali load was much steeper in the presence of HCO_3^-/CO_2 (Fig. 4c, d) compared with the absence (Fig. 4a, b) of HCO_3^-/CO_2. It is worth mentioning that the slow uptake of NH_4^+ is also a prerequisite for the acid loading. After the removal of NH_4Cl, NH_3 diffuses out of the cell, therefore facilitating the dissociation of intracellular NH_4^+ to H^+ and NH_3, which rapidly decreases pH_i. Thereafter, the pH_i starts to recover after this acidification owing to activation of pH_i regulatory mechanisms namely the NHE, NBC and proton pumps (PP; Fig. 4c). In the absence of extracellular HCO_3^- and in the presence of Na^+, the recovery from acidosis reflects the activity of NHE and PP (Fig. 4a). However, the lack of recovery in the absence of Na^+ excludes functionally active PP in HGMs (Fig. 4b). The addition of HCO_3^- to the extracellular solution strongly increases the pH_i recovery from acidosis (Fig. 4c). Since there is no pH_i recovery from acidosis in Na^+- and HCO_3^--free solution (Fig. 4d), it is assumed that the HCO_3^- influx mechanism is most probably accomplished by the Na^+-dependent NBC. Therefore, we tested the effects of the NBC inhibitor H_2DIDS in 0.5 mM concentration and the NHE1 and NHE2 inhibitor HOE-642 at 50 μM on the recovery rates during and following an acid load in HCO_3^-/CO_2-buffered solution (Fig. 4). We calculated $J(B^-)$ from these and from the above experiments (Fig. 4) and found that NBC inhibition greatly reduced pH_i recovery after acid load

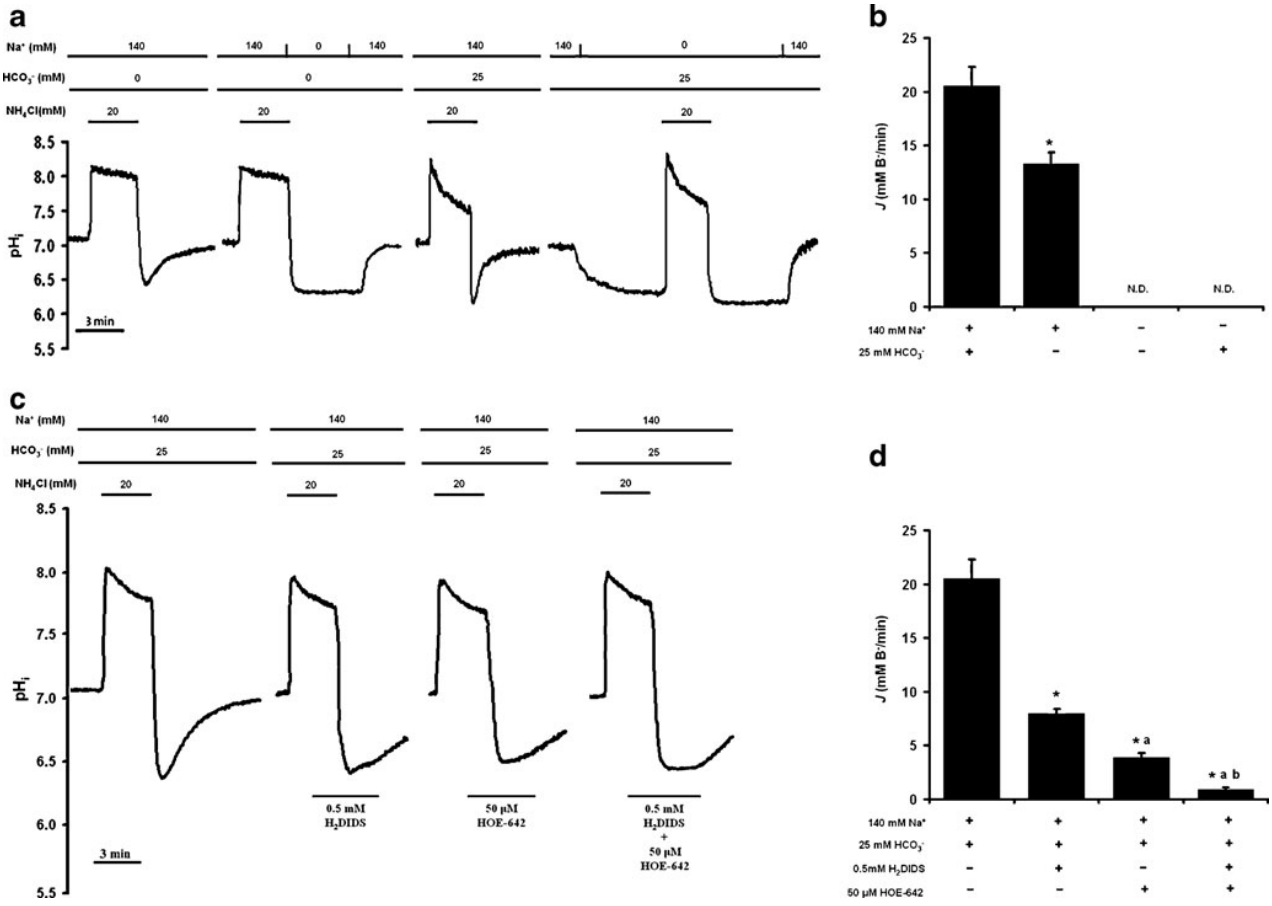

Fig. 4 Na^+-dependent H^+ efflux and Na^+-dependent HCO_3^- influx were detected in HGMs **a** Representative pH_i curves of HGMs are shown. Cells were exposed to 20 mM NH_4Cl pulse in HEPES-buffered solution for 3 min. After the acid load, recovery of pH_i could be observed. However, the administration of Na^+-free HEPES solution after the ammonium pulse inhibited pH_i recovery after the acid load. The same technique was applied in HCO_3^-/CO_2-buffered solution. Note that the initial phase of the pH_i recovery during the ammonium pulse is quicker than in HEPES solution and the recovery phase after the acid load is much steeper. Also in Na^+-free HCO_3^-/CO_2-buffered solution, no recovery could be seen after the ammonium pulse. **b** The *bar chart* shows the summary data of base fluxes after recoveries from acid load. Values are shown as means±SEM (n=5/10–12). *p<0.05 vs. 25 mM HCO_3^-. **c** Inhibition of Na^+/HCO_3^- co-transporter (NBC) with 0.5 mM H_2DIDS and/or inhibition of NHE1–2 with 50 μM HOE-642 during acid load in HCO_3^-/CO_2-buffered solution is shown. **d** The rates of recovery from acid load were determined and base fluxes were calculated from the experiments shown above. Absolute values are displayed for comparison (n=5/1–2); values are shown as means±SEM. *p<0.05 vs. 140 mM Na^+, 25 mM HCO_3^-; **a** p<0.05 vs. 25 mM HCO_3^-+0.5 mM H_2DIDS; **b** p<0.05 vs. 25 mM HCO_3^-+50 μM HOE-642

(20.54±1.76 vs. 7.99±0.39 mM B^-/min) revealing high transporter activity. 50 μM HOE-642 further decreased the recovery rate from acidosis (7.99±0.39 vs. 3.91±0.41 mM B^-/min) indicating high NHE1 and NHE2 activities. Simultaneous administration of the two inhibitors resulted in very slow recovery (0.98±0.09 mM B^-/min). Without HCO_3^-/CO_2 buffering in standard HEPES solution, cells showed much slower recovery than with bicarbonate buffering (13.36±0.41 vs. 20.54±1.76 mM B^-/min). As seen on Fig. 4b, d, eliminating Na^+ from the extracellular solution inhibited the cells to recover from an acid load in both HCO_3^-/CO_2-buffered solution and in standard HEPES solution.

Next, we focused our attention on characterizing the NHE isoforms expressed on the plasma membrane of HGMs. The HGMs were acid-loaded by exposure to a 3-min pulse of 20 mM NH_4Cl in HEPES solution followed by a 5-min exposure to Na^+-free HEPES solution (Fig. 5a). Since neither Na^+ nor HCO_3^- was present in the extracellular solution, acid/base transporters were inhibited and the pH_i was adjusted to a stable acidic level. NHE activity was induced by the re-addition of extracellular Na^+ and the activity of NHEs was determined by measuring the initial rates of pH_i recovery over the first 60 s (60 data points). The activities of the different NHE isoforms were determined by using the isoform selective NHE inhibitor HOE-642 (cariporide). At 1 μM HOE642 inhibits NHE1 whereas at 50 μM it inhibits both NHE1 and NHE2, but not NHE3 [69].

Our data indicate that NHE1 is responsible for about 85% of the Na^+/H^+ exchange activity, whereas NHE2 activity is around 10% and the remaining NHE activity is approximately 5% (Fig. 5b). Of course, we cannot exclude the possibility of the involvement of other NHEs. However, even if they were expressed, they would only have marginal influence on H^+ efflux.

mRNA and protein expression of NHE1-3 in HGMs

Based on results of the functional measurements, we investigated the presence of NHE transporters at the mRNA and protein levels. Reverse transcription polymerase chain reaction confirmed the expression of NHE1, NHE2 and NHE3 (Fig. 5c). We also analysed the expression of NHE isoforms in HGMs by Western blot. We found that NHE1 is present in HGMs, but we were unable to show NHE2 and NHE3 expression. Positive controls (human kidney) confirmed that the antibodies used for these studies were fit for purpose (Fig. 5d). We speculate that NHE2 and NHE3 protein abundance is low in our lysates so below the limit of detection. Using immunocytochemistry, we demonstrated NHE1-3 localisation to the plasma membrane of HGMs (Fig. 5e).

IGF-II and carbachol increases NHE activity

We then investigated the effects of IGF-II and carbachol on the activities of NHEs. Importantly, both IGF-II and carbachol dose-dependently stimulated NHE activity. Carbachol concentrations were tested in range of 1–1,000 μM. Carbachol (10 μM) had the greatest effect on NHE activity. 100 ng/ml IGF-II was more effective than 10 ng/ml in increasing NHE activity (Fig. 6).

Migration of HGMs is stimulated by carbachol and IGF-II

Next, we investigated the effects of carbachol and IGF-II on cell migration and the role of NHE1 in migration of HGMs using scratch wound assay. We found that both 100 ng/ml IGF-II and 10 μM carbachol stimulate the migration of HGMs (Fig. 7). Inhibition of NHE1 by HOE-642 had no effect on unstimulated cell migration, but it significantly inhibited both carbachol- and IGF-II-stimulated migration (by 29±7% and 33±8%, respectively).

IGF-II increases proliferation in an NHE1-dependent manner

Finally, we tested the effects of HOE-642, IGF-II and carbachol on HGM proliferation. EdU incorporation assays showed that 100 ng/ml IGF-II increased cell proliferation over two-fold. Carbachol and/or HOE-642 did not affect proliferation. However, NHE1 inhibition by 1 μM HOE-642 completely blocked the stimulatory effect of IGF-II on cell proliferation (Fig. 8).

Discussion

In this study, we have characterized the pH_i regulatory mechanisms of HGMs for the first time. The data demonstrate that NHE1 activity contributes to IGF-II- and carbachol-stimulated migration and that it is obligatory for IGF-II-induced proliferation of HGMs.

The resting pH_i of HGMs, 7.09±0.02, is similar to that in fibroblasts [12, 28, 46] and smooth muscle cells [64]. Myofibroblasts displayed three main acid/base transporters, namely NBC, AE and NHE. These are also the main mechanisms regulating pH_i in fibroblasts [2, 12, 29] and in smooth muscle cells [15]. Thus, AE decreases, whereas, NBC and NHE increase pH_i. $J(B^-)$ calculations revealed high NBC and high NHE activities which are the main transporters aiding recovery from an acid load in HGMs. In the present study we chose to focus on the roles of NHEs.

Carbachol (10 μM) strongly stimulated NHE activity of HGMs. It has been shown that carbachol also increases NHE (and AE) activity in lacrimal gland epithelia [59] and in rabbit

parietal cells [3]. In the latter study, carbachol strongly increased NHE activity and its effect was completely blocked by 1 μM HOE-642 suggesting the involvement of NHE1. Atropine or intracellular Ca^{2+} chelation inhibited the activation of NHE indicating a typical muscarinic receptor effect with a Ca^{2+}-dependent signalling pathway [4, 59]. In the

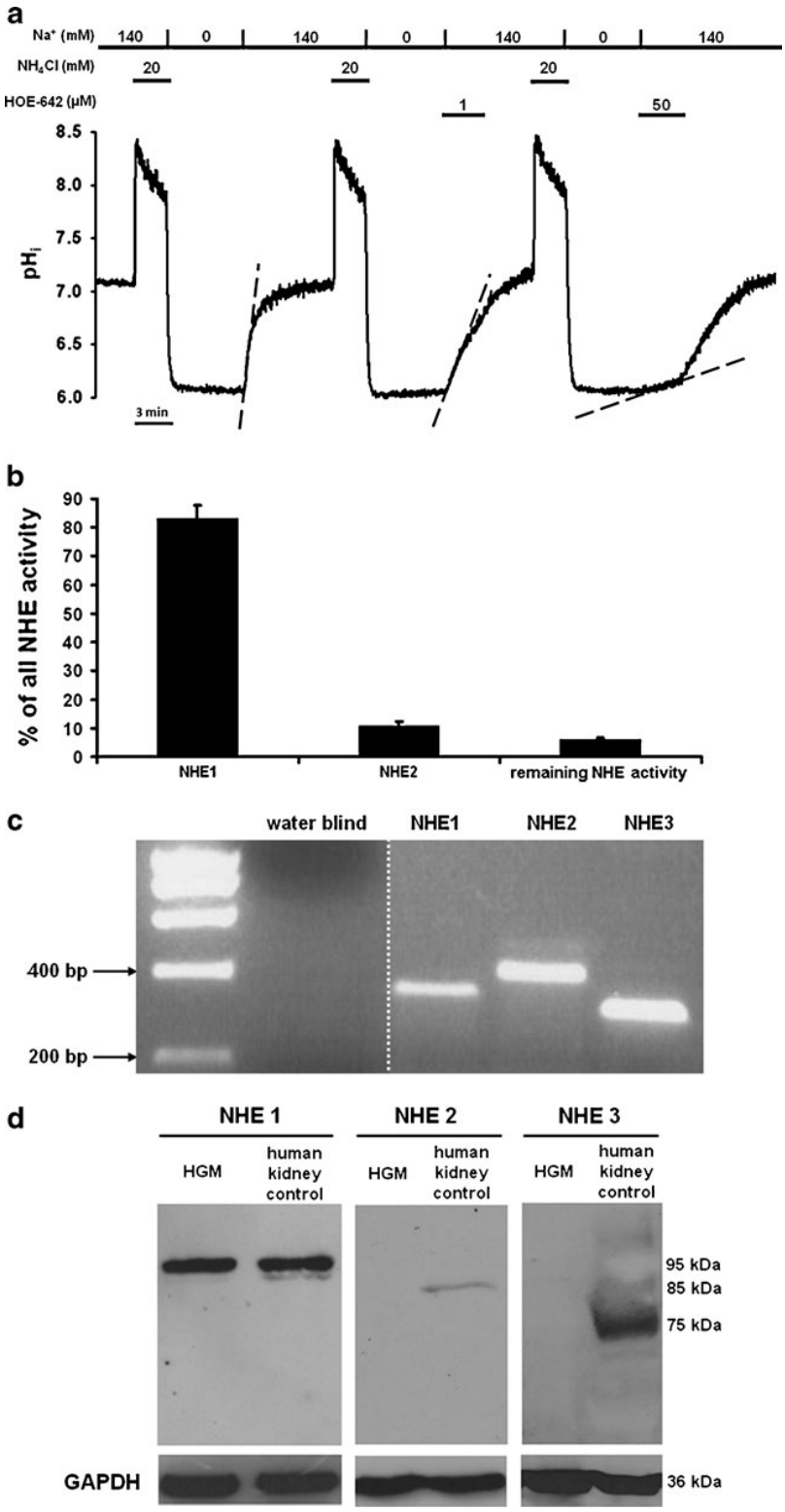

Fig. 5 Identification of NHE isoforms. **a** Representative pH_i curves of HGMs are shown. Cells were loaded with acid by using the ammonium pulse technique. After Na^+ withdrawal, the isoform-selective NHE inhibitor HOE-642 was administered in 1 μM (inhibits NHE1) or 50 μM (inhibits NHE1 and NHE2) concentration, together with re-addition of Na^+. The initial rates of the pH_i recovery during HOE-642 administration were calculated by linear regression analysis to determine the activity of NHE isoforms. **b** The *bar chart* demonstrates that NHE1 is responsible for 83 ±5%, NHE2 for 11±1% and other isoforms for 4.5±0.8% of all Na^+/H^+ exchange activity. Data are shown as means±SEM (n=5/5–6). **c** Reverse transcription PCR confirmed the expression of NHE1–3 isoforms (n=3/6–7). Expected PCR product sizes are as follows: NHE1, 341 bp; NHE2, 407 bp; NHE3, 299 bp. In water blind, we used water as template. **d** Immunoblot analysis showing different NHE isoforms in HGMs and human kidney controls. Protein sizes are as follows: NHE1, 95 kDa; NHE2, 85 kDa; NHE3, 75 kDa; GAPDH, 36 kDa (n=4–5/3–10). **e** NHE1, NHE2 and NHE3 were identified by immunocytochemistry in the plasma membrane of HGMs. Nuclei were counterstained with DAPI (*blue staining*). No specific staining was detected when the primary antibody was omitted (n=3/1–2)

Fig. 5 (continued)

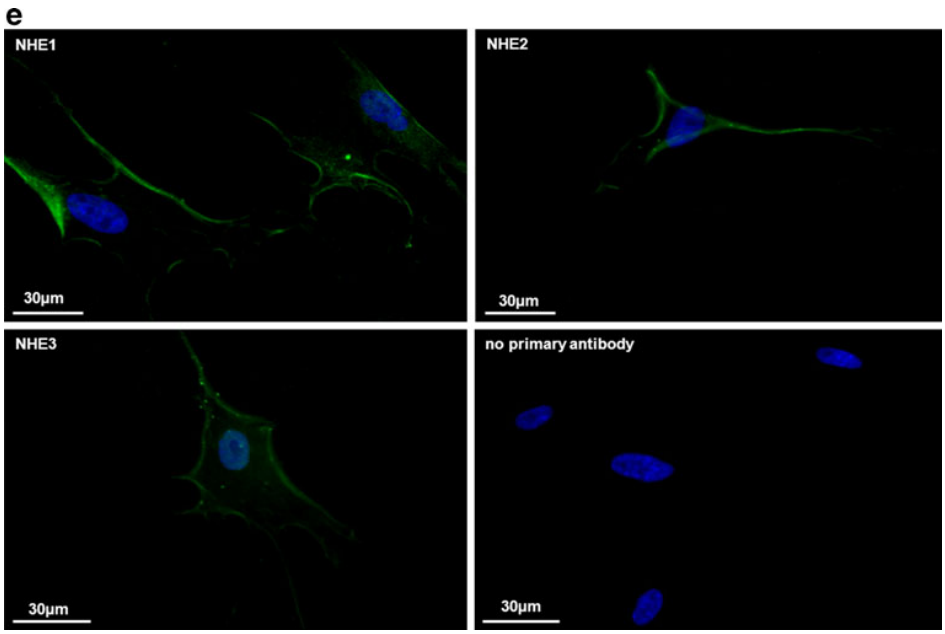

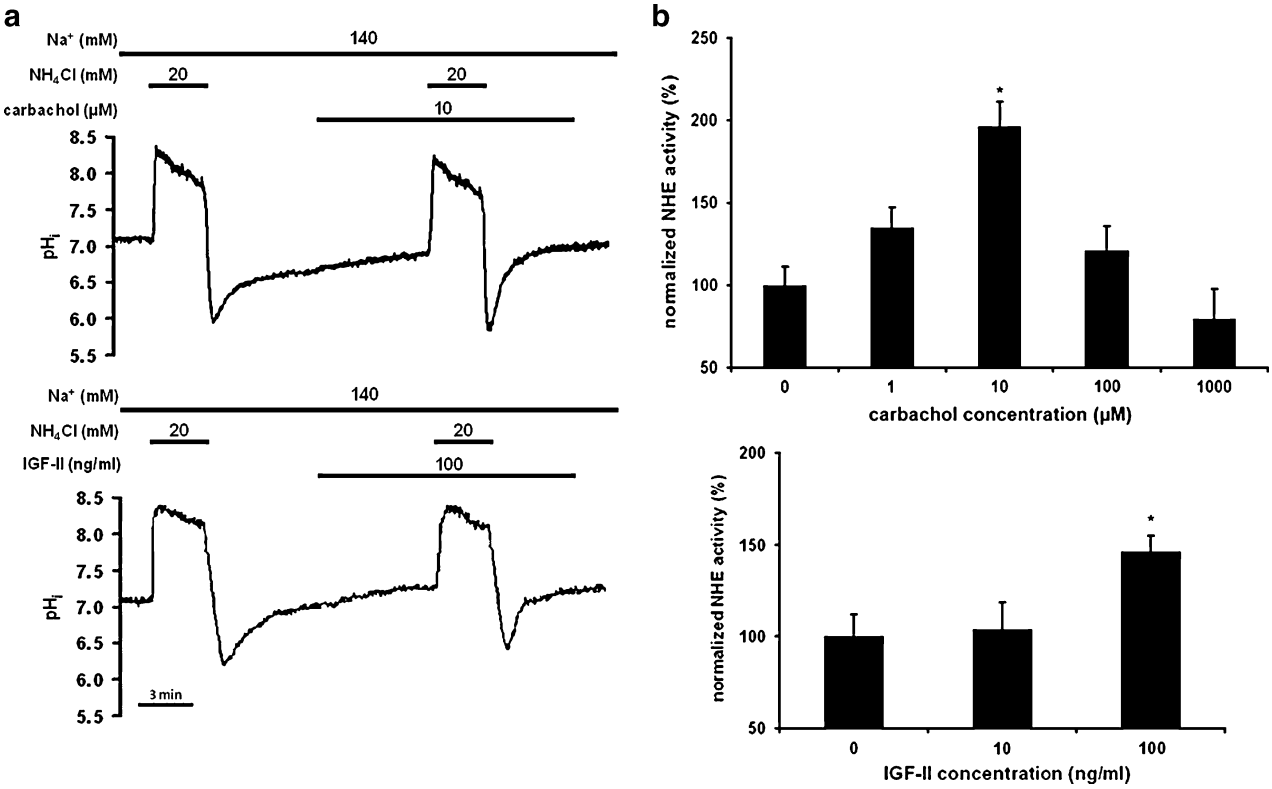

Fig. 6 The effects of carbachol and IGF-II on NHE activity. **a** Representative pH_i curves of HGMs are shown. We tested different carbachol and IGF-II concentrations on NHE activity using the ammonium pulse technique. The figure shows the effects of 10 μM carbachol and 100 ng/ml IGF-II treatment. Note that the changes in the rates of pH_i recovery from acidosis during treatment are much higher compared with the recovery rates without IGF-II or carbachol treatment. **b** The *bar diagram* shows the summary data obtained from the above mentioned experiments. Administration of 10 μM carbachol and 100 ng/ml IGF-II significantly increased NHE activity. Values are normalized to the basal NHE activity. Data are shown as means±SEM (n=5/5–6). *p<0.05 vs. 0 μM or 0 ng/ml

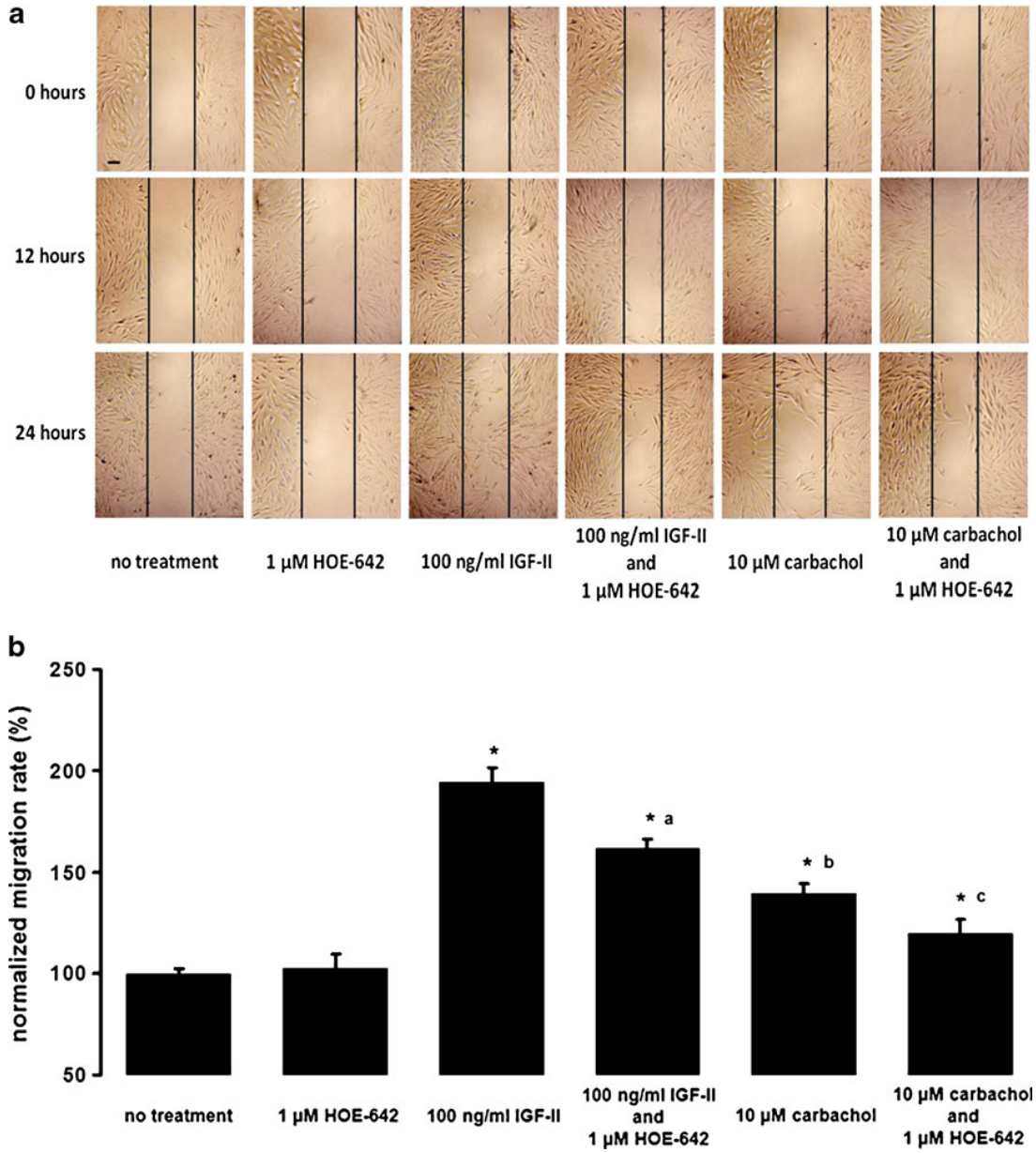

Fig. 7 Carbachol and IGF-II treatment increased migration rates of HGMs in a NHE1-dependent manner. **a** HGMs (100,000) were cultured in six-well plates. After reaching confluency, the monolayer was wounded by a P2 tip along an oriented line in the middle of the well and detached cells were removed by washing with serum-free media. Only wounds with sharp and even edges were used for experiments. Reagents were added to the wells in serum-free media and the plate was incubated for 24 h at 37°C, 5% CO_2. Images were taken at 0, 12 and 24 h from representative areas. Cells were treated with or without 10 µM carbachol or 100 ng/ml IGF-II, and/or 1 µM HOE-642 and cells which migrated into the wound were counted at 12 and 24 h. The *scale bar* on the first picture represents 100 µm. **b** The *bar chart* shows the migration rates normalized to the basal rate at 24 h. Values are shown as means±SEM, $n=5/1–3$; *$p<0.05$ vs. no treatment, *a* $p<0.05$ vs 100 ng/ml IGF-II, *b* $p<0.05$ vs 100 ng/ml IGF-II and 1 µM HOE-642, *c* $p<0.05$ vs 10 µM carbachol

latter publications, the authors suggested that Ca^{2+}-dependent stimulation causes a selective activation of NHE1, whereas cAMP-dependent stimulation with forskolin-activated NHE1, NHE2 and more strongly NHE4. In HCO_3^--containing solution, pH_i did not change indicating that activation of NHE and AE is primarily volume regulatory mechanisms, and they speculated that the physiological significance of secretagogue-induced NHE activity may be related to volume and not to pH_i regulation during acid secretion of rabbit parietal cells [3].

IGF-II, which has been shown to stimulate migration and proliferation of many cell types including myofibroblasts

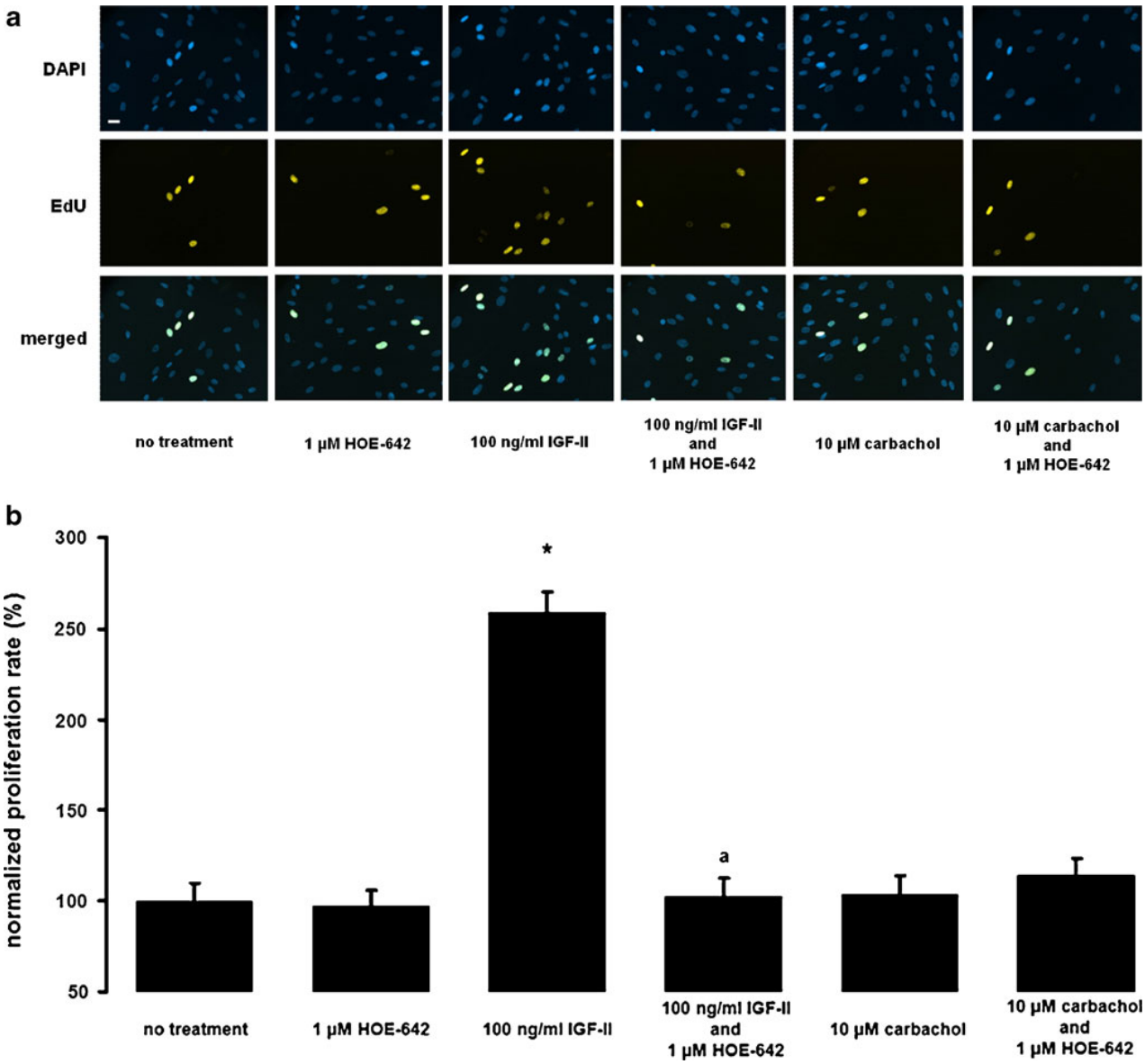

Fig. 8 IGF-II stimulates the proliferation of HGMs in a NHE1-dependent manner. **a** Representative images showing EdU localisation after treatment with 1 μM HOE-642, 100 ng/ml IGF-II and/or 10 μM carbachol compared to control. HOE-642 (1 μM) did not affect proliferation either on its own, or in a combination with 10 μM carbachol. IGF-II (100 ng/ml) increased the rate of proliferation. Furthermore, the inhibition of NHE1 suppressed the IGF-II stimulatory response. Nuclei were counterstained with DAPI (*blue staining*). The *scale bar* on the first picture represents 50 μm. **b** The *bar chart* shows the proliferation rates of *a* normalized to the basal proliferation rate; *$p<0.05$, *a* $p<0.05$ vs 100 ng/ml IGF-II ($n=5/1–2$)

[36, 52], also stimulated NHE activity. It is known that IGF-II exerts its effects through the tyrosine kinase receptor IGF-IR and it is also well known that NHE1 is mainly regulated by phosphorylation. Meima et al. reported that IGF-IR activates Ser/Thr kinases in the Akt signalling pathway and increases myofibroblast migration, growth and NHE activity by phosphorylating intracellular NHE regulatory domains thus enhancing transporter activity [37]. The distal region of the cytoplasmic tail of NHE corresponding to amino acids 700–815, is enriched in serine and threonin residues that are phosphorylated by different protein kinases in response to hormones and/or growth factors [51]. It has also been suggested that Ser/Thr kinases not only stimulate NHE1 activity, but also increase NHE1 promoter transcription [5]. ERK1/2 regulates gene expression via the MAPK cascade [40] after NHE1 phosphorylation/activation through $p90^{RSK}$ (a downstream substrate of ERK1/2) [56]. $p90^{RSK}$ directly phosphorylates NHE1 at position 703(Ser) in vascular

smooth muscle cells after growth hormone treatment and the exchanger activity was found to be increased [56]. Another important factor in the regulation of NHE is protein 14-3-3, which binds to position 703(Ser) after its phosphorylation and limits dephosphorylation by protein phosphatases [33]. Additional Ser/Thr phosphorylation sites have been recently identified in the ERK pathway, but their importance must be confirmed [35].

Our experiments demonstrate that reagents increasing NHE activity also increase HGM migration and proliferation, so the question arises whether in turn NHE inhibition may inhibit cell migration and proliferation. The effects of parasympathomimetics on cell migration are conflicting, though they are thought to stimulate NHE activity in general. In HaCaT cells, carbachol did not alter single random cell locomotion compared to non-treated cultures [38]. Epidermal keratinocytes showed enhanced migration after long-term muscarinic stimulation with acetylcholine in an agarose gel outgrowth system [18], whereas carbachol treatment arrested wound healing in epidermal keratinocytes [9]. Besides the differences between species and tissues, it seems that various muscarinic receptors can mediate different migration responses even in the same cell [63]. Our experiments clearly showed that 10 μM carbachol stimulated migration of HGMs, at least partly in a NHE1-dependent manner, but higher or lower doses had no further effect on migration (data not shown). It is known that protein kinase C (PKC) might mediate M3 receptor signals causing PLC to cleave membrane phospholipids. PIP2 is cleaved into diacyl glycerol and IP3 which is released into the cytosol and binds to IP3 receptors localised at the ER (or SR) causing consequent increase of the cytosolic calcium concentration and a cascade of activity including locomotion of contractile cells [1]. M3 receptors, through PLC, may also activate PI3K/Akt cascade. In the context of gastric cancer, it is worth mentioning that apoptosis can be suppressed through the PI3K/Akt/mTOR pathway allowing vigorous proliferation and better survival [68]. PKC modulates gene regulation via NF-κB and by joining Raf/MAPK cascade. It has been shown recently that PKC may phosphorylate the potent activation transcription factor-2, which controls c-Jun-mediated activation of transcription [66]. The observed increase in migration in our studies suggests, however, a permissive or supporting role of NHE1 in enabling migratory mechanisms to take effect in response to bioactive compounds. Others have found that not only NHE1 activity, but also intact NHE1 protein structure is required for locomotion, since mutations/modifications of protein structure or inhibition of the exchanger activity also inhibits migration [30]. Notably, NHE1 is a scaffolding-organizing protein functioning as a transmembrane signal transducer for various agents modulating cell volume, cell migration and growth through NHE1 activity [27]. Muscarinic agonists have also been shown to evoke differential effects on proliferation depending on the type of the muscarinic receptor [63]. We found that the M3 agonist carbachol does not induce proliferation of HGMs.

IGF-II stimulates the proliferation of many cell types, including myofibroblasts [19, 36]. NHE1 may act as an organizer of different cell growth inducing signals through modulation of transporter activity via receptor tyrosine kinases and joint pathways. Denker et al. reported that NHE1 protein contains an intracellular esrin/radixin/moesin (ERM) motif close to the plasma membrane, which anchors the protein to the subcortical actin filament network and serves as a host to actin polymerization [14]. In a wound healing assay, migration was impaired when mutations disrupted the ERM site. Not only ERM site mutations, but also mutations of the transporter sequence (resulting in diminished NHE1 activity), impair de-adhesion resulting in failure to retract lamellipodia. Besides this membrane anchoring, NHE1 is important in regulating cell volume and local pH at changing membrane sites of a moving cell; it is known that in fibroblasts NHE1 is most abundant at the rear and front pole of a spatially polarized migrating cell [14].

We showed that inhibition of NHE1 blocks migration and proliferation of HGMs. Since stromal cells play an important role in cancer initiation and progression [6, 13, 31], our results may have both physiological and therapeutic relevance. It is well documented that proliferation is reduced by NHE1 inhibition in human cancer cells [20, 49]. However, it is also possible that intracellular alkalization simply promotes or permits proliferative responses, because as the pH_i becomes more alkaline, cellular metabolism becomes more rapid mainly due to the more effective energy producing mechanisms [20]. For example, in tumour cells, acid/base conditions are of particular importance, because cancer cells share an aberrant intracellular alkalization facilitating their malignant behavior, whereas the microenvironment becomes more acidic [8]. Nevertheless, as mentioned before, NHE1 is highly regulated by phosphorylation and Akt kinases that phosphorylate NHE1 increasing its activity also stimulate proliferation at the same time [17, 34, 54].

In conclusion, we have demonstrated that HGMs express functionally active NHE, NBC and AE transporters which regulate pH_i. Furthermore, we have shown that NHE1 contributes to IGF-II- and carbachol-stimulated migration, and that it is obligatory for IGF-II-induced proliferation.

Acknowledgements We would like to thank Graham Dockray, professor at the Department of Physiology, University of Liverpool (Liverpool, UK) for his kind help and supervision of the molecular biology experiments. We would also like to thank Drs. László Tiszlavicz and István Balázs Németh, pathologists at the Department of Pathology, University of Szeged (Szeged, Hungary) for their continuous technical support and accurate histological evaluations of our gastric tissue specimens. Cariporide was a generous gift from Sanofi-Aventis,

(Frankfurt, Germany). Our funding sources were Hungarian Scientific Research Fund K76844, K73141, National Development Agency (TÁMOP) 4.2.1.B-09/1/KONV, 4.2.2-08/1/2008-0002 and 4.2.2-08/1/2008-0013, Hungarian Academy of Sciences BO/00334/08/5 and BO/00174/10/5, NIH PHS398/2590 and NIHR L115931.

Conflict of interest statement The authors hereby declare that there is no conflict of interest to disclose.

References

1. Alberts B, Alexander J, Julian L, Martin R, Keith R, Peter W (2002) Molecular Biology of the Cell, 4th edn. Garland Science, New York, US
2. Alexandratou E, Dido Y, Panagiotis H, Dimitris K, Spyros L (2002) Human fibroblast alterations induced by low power laser irradiation at the single cell level using confocal microscopy. Photochem Photobiol Sci 8:547–552
3. Bachmann O, Sonnentag T, Siegel WK, Lamprecht G, Weichert A, Gregor M, Seidler U (1998) Different acid secretagogues activate different Na+/H+ exchanger isoforms in rabbit parietal cells. Am J Physiol 275:G1085–G1093
4. Bachmann O, Reichelt D, Tuo B, Manns MP, Seidler U (2006) Carbachol increases Na+−HCO3- cotransport activity in murine colonic crypts in a M3-, Ca2+/calmodulin-, and PKC-dependent manner. Am J Physiol Gastrointest Liver Physiol 291:G650–G657
5. Besson P, Fernandez-Rachubinski F, Yang W, Fliegel L (1998) Regulation of Na+/H+ exchanger gene expression: mitogenic stimulation increases NHE1 promoter activity. Am J Physiol 274: C831–C839
6. Bhowmick NA, Neilson EG, Moses HL (2004) Stromal fibroblasts in cancer initiation and progression. Nature 432:332–337
7. Cala PM, Anderson SE, Cragoe EJ (1988) Na/H exchange-dependent cell volume and pH regulation and disturbances. Comp Biochem Physiol 90:551–555
8. Cardone RA, Casavola V, Reshkin SJ (2005) The role of disturbed pH dynamics and the Na+/H+ exchanger in metastasis. Nat Rev Cancer 5:786–795
9. Chernyavsky AI, Arredondo J, Wess J, Karlsson E, Grando SA (2004) Novel signaling pathways mediating reciprocal control of keratinocyte migration and wound epithelialization through M3 and M4 muscarinic receptors. J Cell Biol 166:261–272
10. Chung MK, Kim HC (2002) Volume-activated chloride currents from human fibroblasts: blockade by nimodipine. Gen Physiol Biophys 21:85–101
11. Damkier HH, Aalkjaer A, Praetorius J (2010) Na+-dependent HCO3- import by the slc4a10 gene product involves Cl- export. J Biol Chem 285:26998–27007
12. Davies JE, Ng LL, Kofoed-Enevoldsen A, Li LK, Earle KA, Trevisan R, Viberti G (1992) Intracellular pH and Na+/H+ antiport activity of cultured skin fibroblasts from diabetics. Kidney Int 42:1184–1190
13. De Wever O, Demetter P, Mareel M, Bracke M (2008) Stromal myofibroblasts are drivers of invasive cancer growth. Int J Cancer 123:2229–2238
14. Denker SP, Barber DL (2002) Cell migration requires both ion translocation and cytoskeletal anchoring by the Na-H exchanger NHE1. J Cell Biol 159:1087–1096
15. Duquette RA, Wray S (2001) pH regulation and buffering power in gastric smooth muscle. Eur J Physiol 442:459–466
16. Gleeson D (1992) Acid–base transport systems in gastrointestinal epithelia. Gut 33:1134–1145
17. Goss GG, Woodside M, Wakabayashi S, Pouyssegur J, Waddell T, Downey GP, Grinstein S (1994) ATP dependence of NHE-1, the ubiquitous isoform of the Na+/H+ antiporter. Analysis of phosphorylation and subcellular localization. J Biol Chem 269:8741–8748
18. Grando SA, Crosby AM, Zelickson BD, Dahl MW (1999) Agarose gel keratinocyte outgrowth system as a model of skin re-epithelization: requirement of endogenous acetylcholine for outgrowth initiation. J Invest Dermatol 101:804–810
19. Grotendorst GR, Rahmanie H, Duncan MR (2004) Combinatorial signaling pathways determine fibroblast proliferation and myofibroblast differentiation. FASEB 18:469–479
20. Harguindey S, Orive G, Pedraz JL, Paradiso A, Reshkin SJ (2005) The role of pH dynamics and the Na+/H+ antiporter in the etiopathogenesis and treatment of cancer. Two faces of the same coin—one single nature. Biochim Biophys Acta 1756:1–24
21. Hayashi H, Aharonovitz O, Alexander RT, Touret N, Furuya W, Orlowski J, Grinstein S (2008) Na+/H+ exchange and pH regulation in the control of neutrophil hemokinesis and chemotaxis. Am J Physiol Cell Physiol 294:C526–C534
22. Hegyi P, Rakonczay Z, Gray MA, Argent BE (2004) Measurement of intracellular pH in pancreatic duct cells: a new method for calibrating the fluorescence data. Pancreas 28:427–434
23. Hinz B (2010) The myofibroblast: paradigm for a mechanically active cell. J Biom 43:146–155
24. Hinz B, Phan SH, Thannickal VJ, Galli A, Bochaton-Piallat M-L, Gabbiani G (2007) The myofibroblast: one function, multiple origins. Am J Pathol 170:1807–1816
25. Iida M, Nakamura N, Kamouchi M, Kitazono K, Kuroda J, Matsuo R, Hagiwara N, Ishikawa E, Ooboshi H, Ibayashi S (2008) Role of NHE1 in calcium signaling and cell proliferation in human CNS pericytes. Am J Physiol Heart Circ Physiol 294: H1700–H1707
26. Kapus A, Grinstein S, Wasan S, Kandasamy R, Orlowski J (1994) Functional characterization of three isoforms of the Na+/H+ exchanger stably expressed in Chinese hamster ovary cells. ATP dependence, osmotic sensitivity, and role in cell proliferation. J Biol Chem 269:23544–23552
27. Koliakos G, Paletas K, Kaloyianni M (2008) NHE-1: a molecular target for signalling and cell matrix interactions. Connect Tissue Res 49:157–161
28. L'Allemain G, Paris S, Pouysségur J (1984) Growth factor action and intracellular pH regulation in fibroblasts. Evidence for a major role of the Na+/H+ antiport. J Biol Chem 259:5809–5815
29. L'Allemain G, Paris S, Pouysségur J (1985) Role of a Na+-dependent Cl-/HCO3- exchange in regulation of intracellular pH in fibroblasts. J Biol Chem 260:4877–4883
30. Lagana A, Vadnais J, Le PU, Nguyen TN, Laprade R, Nabi IR, Noël J (2000) Regulation of the formation of tumor cell pseudopodia by the Na(+)/H(+) exchanger NHE1. J Cell Sci 113:3649–3662
31. LaPointe MS, Batlle DC (1994) Na+/H+ exchange and vascular smooth muscle proliferation. Am J Med Sci 307:S9–S16
32. Lee SH, Kim T, Park E-S, Yang S, Jeong D, Choi Y, Rho J (2008) NHE10, an osteoclast-specific member of the Na+/H+ exchanger family, regulates osteoclast differentiation and survival. Biochem Biophys Res Commun 369:320–326
33. Lehoux S, Ji A, Florian JA, Berk BC (2001) 14-3-3 Binding to Na+/H+ exchanger isoform-1 is associated with serum-dependent activation of Na+/H+ exchange. J Biol Chem 276:15794–15800
34. Luo J, Sun D (2007) Physiology and pathophysiology of Na(+)/H(+) exchange isoform 1 in the central nervous system. Curr Neurovasc Res 4:205–215
35. Malo ME, Fliegel L (2006) Physiological role and regulation of the Na+/H+ exchanger. Can J Physiol Pharmacol 84:1081–1095
36. McCaig C, Duval C, Hemers E, Steele I, Pritchard DM, Przemeck S, Dimaline R, Ahmed S, Bodger K, Kerrigan DD, Wang TC, Dockray GJ, Varro A (2006) The role of matrix metalloproteinase-7

in redefining the gastric microenvironment in response to Helicobacter pylori. Gastroenterology 130:1754–1763
37. Meima ME, Webb BA, Witkowska HE, Barber DL (2009) The sodium-hydrogen exchanger NHE1 is an Akt substrate necessary for actin filament reorganization by growth factors. J Biol Chem 284:26666–26675
38. Metzger M, Just L, Boss A, Drews U (2005) Identification and functional characterization of the muscarinic receptor M3 in the human keratinocyte cell line HaCaT. Cells Tissues Organs 180:96–105
39. Moolenaar WH, Tsien RY, van der Saag PV, de Laat SW (1983) Na+/H+ exchange and cytoplasmic pH in the action of growth factors in human fibroblasts. Nature 304:645–648
40. Moor AN, Fliegel L (1999) Protein kinase-mediated regulation of the Na(+)/H(+) exchanger in the rat myocardium by mitogen-activated protein kinase-dependent pathways. J Biol Chem 274:22985–22992
41. Mutoh H, Sashikawa M, Hayakawa H, Sugano K (2010) Monocyte chemoattractant protein-1 is generated via TGF-beta by myofibroblasts in gastric intestinal metaplasia and carcinoma without H. pylori infection. Cancer Sci 101:1783–1789
42. Nakayama H, Enzan H, Miyazaki E, Toi M (2002) Alpha smooth muscle actin positive stromal cells in gastric carcinoma. J Clin Pathol 55:741–744
43. Noble A, Towne C, Chopin L, Leavesley D, Upton Z (2003) Insulin-like growth factor-II bound to vitronectin enhances MCF-7 breast cancer cell migration. Endocrinology 144:2417–2424
44. Orlowski J, Grinstein S (2004) Diversity of the mammalian sodium/proton exchanger SLC9 gene family. Eur J Physiol 447:549–565
45. Pedersen SF (2006) The Na+/H+ exchanger NHE1 in stress-induced signal transduction: implications for cell proliferation and cell death. Eur J Physiol 452:249–259
46. Perona R, Portillo F, Giraldez F, Serrano R (1990) Transformation and pH homeostasis of fibroblasts expressing yeast H(+)-ATPase containing site-directed mutations. Mol Cell Biol 10:4110–4115
47. Radhakrishnan J, Kolarova JD, Ayoub IM, Gazmuri RJ (2011) AVE4454B-a novel sodium-hydrogen exchanger isoform-1 inhibitor-compared less effective than cariporide for resuscitation from cardiac arrest. J Lab Clin Med 157:71–80
48. Rentsch ML, Ossum CG, Hoffmann EK, Pedersen SF (2007) Roles of Na+/H+ exchange in regulation of p38 mitogen-activated protein kinase activity and cell death after chemical anoxia in NIH3T3 fibroblasts. Eur J Physiol 454:649–662
49. Ritter M, Fuerst J, Wöll E, Chwatal S, Gschwentner M, Lang F, Deetjen P, Paulmichl M (2001) Na(+)/H(+)exchangers: linking osmotic dysequilibrium to modified cell function. Cell Physiol Biochem 11:1–18
50. Salic A, Mitchison TJ (2008) A chemical method for fast and sensitive detection of DNA synthesis in vivo. Proc Natl Acad Sci 105:2415–2420
51. Sardet C, Fafournoux P, Pouysségur J (1991) Alpha-thrombin, epidermal growth factor, and okadaic acid activate the Na+/H+ exchanger, NHE-1, by phosphorylating a set of common sites. J Biol Chem 266:19166–19171
52. Schmid C (1995) Insulin-like growth factors. Cell Biol Int 19:445–457
53. Schneider L, Stock C-M, Dieterich P, Jensen BH, Pedersen LB, Satir P, Schwab A, Christensen ST, Pedersen SF (2009) The Na+/H+ exchanger NHE1 is required for directional migration stimulated via PDGFR-alpha in the primary cilium. J Cell Biol 185:163–176
54. Slepkov ER, Rainey JK, Sykes BD, Fliegel L (2007) Structural and functional analysis of the Na+/H+ exchanger. Biochem J 401:623–633
55. Stock C, Gassner B, Hauck CR, Arnold H, Mally S, Eble JA, Dieterich P, Schwab A (2005) Migration of human melanoma cells depends on extracellular pH and Na+/H+ exchange. J Physiol 567:225–238
56. Takahashi E, Abe J, Gallis B, Aebersold R, Spring DJ, Krebs EG, Berk BC (1990) p90(RSK) is a serum-stimulated Na+/H+ exchanger isoform-1 kinase. Regulatory phosphorylation of serine 703 of Na+/H+ exchanger isoform-1. J Biol Chem 274:20206–20214
57. Taves J, Rastedt D, Canine J, Mork D, Wallert MA, Provost JJ (2008) Sodium hydrogen exchanger and phospholipase D are required for alpha1-adrenergic receptor stimulation of metalloproteinase-9 and cellular invasion in CCL39 fibroblasts. Arch Biochem Biophys 477:60–66
58. Thomas JA, Buchsbaum RN, Zimniak A, Racker E (1979) Intracellular pH measurements in Ehrlich ascites tumor cells utilizing spectroscopic probes generated in situ. Biochemistry 18:2210–2218
59. Tóth-Molnár E, Venglovecz V, Ózsvári B, Rakonczay Z, Varró A, Papp JG, Tóth A, Lonovics J, Takács T, Ignáth I, Iványi B, Hegyi P (2007) New experimental method to study acid/base transporters and their regulation in lacrimal gland ductal epithelia. Investig Ophthalmol Vis Sci 48:3746–3755
60. Vereninov AA, Vassilieva IO, Yurinskaya VE, Matveev VV, Glushankova LN, Lang F, Matskevitch JA (2001) Differential transcription of ion transporters, NHE1, ATP1B1, NKCC1 in human peripheral blood lymphocytes activated to proliferation. Int J Exp Cell Physiol Biochem Pharmacol 11:19–26
61. Watanabe M, Hirano T, Asano G (1995) Roles of myofibroblasts in the stroma of human gastric carcinoma. Nippon Geka Gakkai Zasshi 96:10–18
62. Weintraub WH, Machen TE (1989) pH regulation in hepatoma cells: roles for Na-H exchange, Cl-HCO3 exchange, and Na-HCO3 cotransport. Am J Physiol 257:G317–G327
63. Wessler I, Kirkpatrick CJ (2008) Acetylcholine beyond neurons: the non-neuronal cholinergic system in humans. Br J Pharmacol 154:1558–1571
64. Wray S (1988) Smooth muscle intracellular pH: measurement, regulation, and function. Am J Physiol Cell Physiol 254: C213–C225
65. Wu S, Song T, Zhou S, Liu Y, Chen G, Huang N, Liu L (2008) Involvement of Na+/H+ exchanger 1 in advanced glycation end products-induced proliferation of vascular smooth muscle cell. Biochem Biophys Res Commun 375:384–389
66. Yamasaki T, Takahashi A, Pan J, Yamaguchi N, Yokoyama KK (2009) Phosphorylation of activation transcription factor-2 at serine 121 by protein kinase C controls c-Jun-mediated activation of transcription. J Biol Chem 284:8567–8581
67. Yang X, Wang D, Dong W, Song Z, Dou K (2011) Suppression of Na(+)/H (+) exchanger 1 by RNA interference or amiloride inhibits human hepatoma cell line SMMC-7721 cell invasion. Med Oncol 28:385–390
68. Yap TA, Garrett MD, Walton MI, Raynaud F, de Bono JS, Workman P (2008) Targeting the PI3K-AKT-mTOR pathway: progress, pitfalls, and promises. Curr Opin Pharmacol 8:393–412
69. Yeruva S, Farkas K, Hubricht J, Rode K, Riederer B, Bachmann O, Cinar A, Rakonczay Z, Molnár T, Nagy F, Wedemayer J, Manns M, Raddatz D, Musch MW, Chang EB, Hegyi P, Seidler U (2010) Preserved Na(+)/H(+) exchanger isoform 3 expression and localization, but decreased NHE3 function indicate regulatory sodium transport defect in ulcerative colitis. Inflamm Bow Dis 16:1149–1161

TRIPSZINOGÉN AKTIVÁCIÓS PEPTID MUTÁCIÓK ÖRÖKLETES PANKREATITISZBEN

Tézis kivonat

BEVEZETÉS

A krónikus pankreatitisz a hasnyálmirigy visszatérő vagy folyamatos gyulladásos megbetegedése, amelyet visszafordíthatatlan morfológiai változások, fájdalom, valamint az exokrin és endokrin pankreatikus funkciók tartós károsodása jellemez. A krónikus pankreatitisz genetikai hátterének kutatása az örökletes pankreatitisz vizsgálatával kezdődött. A klasszikus értelemben vett örökletes forma egy ritka autoszómális domináns öröklésmenetet mutató betegség, melyet a humán kationos tripszinogént kódoló *PRSS1* gén mutációi okoznak. A tripszinogén mutációk okozta megbetegedések 90%-ért felelős az R122H és az N29I mutáció, míg az esetek 10%-ban olyan ritka variánsokat azonosítottak, melyek közé tartoznak a tripszinogén aktivációs peptidet érintő mutációk A16V, D19A, D22G és a K23R. A mutációk a tripszin pankreaszon belüli fokozott ektopiás aktiválódását, illetve a tripszin inaktiválásáért felelős védőmechanizmusok elégtelen működését okozhatják. A kórosan emelkedett intrapankreatikus tripszin aktivitás a hasnyálmirigy önemésztődéséhez, szöveti károsodáshoz, és következményes gyulladásos reakcióhoz vezet.

Munkacsoportunk megfigyelése, hogy egy másik hasnyálmirigy proteáz, nevezetesen a kimotripszin C (CTRC), nem csupán emésztő funkcióval rendelkezik, hanem szabályozza a tripszinogén aktiválódását is. A CTRC egyrészt stimulálja a tripszinogén autoaktivációját azáltal, hogy tripszinogén propeptidjét a Phe18-Asp19 peptidkötésnél hasítja, másrészt elősegíti a tripszinogén és tripszin lebomlását a kalcium kötő hurokban elhelyezkedő Leu81-Glu82 peptidkötés emésztése útján. A CTRC ezen szabályozó hatása felveti annak lehetőségét, hogy a tripszinogén mutációk befolyásolhatják a CTRC szabályozó működését és ezáltal idézhetnek elő emelkedett tipszin aktivitást a pankreaszon belül.

CÉLKITŰZÉSEK

Korábbi kutatások bizonyították, hogy a három humán tripszinogén izoenzim génje közül kizárólag a kationos tripszinogént kódoló *PRSS1* génben azonosított mutációk hozhatók összefüggésbe a krónikus pankreatitisz kialakulásával. A biokémiai vizsgálatok kimutatták, hogy ezen mutációk esetében az autoaktivációra való hajlam fokozott, mely fokozott kockázatot jelenthet krónikus pankreatitisz kialakulására. Azon hipotézis mely szerint a pankreatitisz-asszociált mutációk a CTRC-szabályozó útvonalon is kifejthetik hatásukat, olyan kísérletsorozatot indított el nemrégiben, mely elsősorban a mutáns tripszinogének CTRC jelenlétében bekövetkező autoaktivációjára fókuszált.

K23_I24insIDK tripszinogén aktivációs peptid mutáció biokémiai karakterizálása (I.)

Munkánk során azonosítottunk egy örökletes pankreatitisszel asszociált új intragenikus duplikációt (c.63_71dup) a humán kationos tripszinogént kódoló *PRSS1* génben, melynek a továbbiakban biokémiai jellemzését tűztük ki célul. Fő céljaink a következők voltak:

1. A K23_I24insIDK mutáció tripszinogén autoaktivációra kifejtett hatásának vizsgálata
2. A K23_I24insIDK mutáció hatásának vizsgálata az enteropeptidáz és a katepszin B mediálta tripszinogén aktivációra
3. A K23_I24insIDK mutáció tripszinogén szekrécióra kifejtett hatásának vizsgálata

Tripszinogén autoaktiváció vizsgálata CTRC jelenlétében (II.)

Annak eldöntésére, hogy a tripszinogén aktivációs peptid mutációk, a már korábban tapasztalt robusztus autoaktiváció növekvést önmagukban avagy a CTRC szabályozó útvonalon keresztül érik el, célul tűztük ki ezen variánsok autoaktivációra kifejtett hatásának vizsgálatát önmagukban és CTRC jelenlétében. Fő céljaink a következők voltak:

1. A tripszinogén aktivációs peptidet érintő mutációk autoaktivációra kifejtett hatásának vizsgálata
2. A CTRC tripszinogén aktivációs peptid mutánsok autoaktivációra kifejtett hatásának vizsgálata
3. Az aktivációs peptid mutáns tripszinogének CTRC általi lebontásának vizsgálata
4. A mutációk hatása a tripszinogén aktivációs peptid CTRC általi hasításának specificitása
5. A mutációk hatásának vizsgálata az aktivációs peptid Ca^{2+} kötő affinitására
6. Az aktivációs peptid mutációk tripszinogén szekrécióra kifejtett hatásának vizsgálata

ANYAGOK ÉS MÓDSZEREK

Expressziós plazmidok készítése

A génvariánsokat PCR-mutagenezissel állítottuk elő majd az emésztőenzimek kódoló DNS-ét pTrapT7 illetve pcDNA3.1(-) expressziós vektorokba klónoztuk.

Az emésztő proenzimek termelése

A tripszinogéneket aminopeptidáz P deficiens LG-3 *E. coli* törzsben, míg a proelasztáz 2 fehérjét *E. coli* BL21(DE3) törzsben termeltük. A tenyészet centrifugálása után a zárványtestekben képződő fehérjét ultrahang kezelés segítségével izoláltuk, melyet az enzimek in vitro renaturálása követett. A kimotripszinogének (CTRC, CTRB1, CTRB2, CTRL1), a proelasztáz 3A valamint proelasztáz 3B termelése humán embrionális vese sejtekben (HEK 293T) történt tranziens transzfekcióval.

Az emésztőenzimek tisztítása

A tripszinogéneket illetve a proelasztáz 2 fehérjét ekotin afffinitás kromatográfiával míg a kimotripszinogéneket nikkel affinitás kromatográfia segítségével tisztítottuk meg.

A proteázok aktivitásának meghatározása

Az enzimaktivitást szintetikus peptid szubsztrátokon mértük. A proteolitikus hasítás eredményeképpen sárga p-nitroanilin keletkezett, amelynek felszaporodását spektrofotométer segítségével követtük.

A fehérjék elektroforetikus elválasztása

A fehérjéket SDS-gélelektroforézissel tettük láthatóvá. Az elektroforetikus elválasztás Tris-glicin géleken történt. Az N-terminális aminosavak azonosítása céljából a mintákat szekvenáló membránokra transzferáltuk és N-terminális szekvenálásnak vetettük alá.

EREDMÉNYEK

I. Új mutációt írtunk le a humán kationos tripszinogént kódoló *PRSS1* génben, amely domináns módon öröklődő krónikus pankreatitisszel társul.

1. A DNS szekvencia analízis során egy eddig ismeretlen intragenikus duplikációt azonosítottunk a humán kationos tripszinogént kódoló *PRSS1* génben. A mutáció egy 3 aminosavnyi inszerciót eredményezett a tripszinogén aktivációs peptidjében, mely alapján feltételeztük, hogy a tripszinogén aktivációs tulajdonságai jelentősen megváltoznak.
2. Eredményeink azt mutatták, hogy az újonnan felfedezett mutáció jelentősen fokozta a tripszinogén autoaktivációját. A mutáns tripszinogént a lizoszomális proteáz katepszin B is gyorsabban aktiválta mint a vadtípusú triszinogént. Ez utóbbi jelenség ezidáig nem volt megfigyelhető a többi *PRSS1* génben talált mutációnál.
3. Az inszerciós mutáció tripszinogén szekrécióra kifejtett hatását vizsgálva a mutáns enzim csökkent szekrécióját detektáltuk.

II. Megvizsgáltuk továbbá az inszerciós mutáns tripszinogén K23_I24insIDK mellett a már korábban jellemzett aktivációs peptid mutáns D19A, D22G, és K23R tripszinogének autoaktivációját CTRC nélkül és annak jelenlétében.

1. Eredményeink azt mutatták, hogy a mutáns enzimek jelentősen gyorsabban autoaktiválódtak a vad típusú tripszinogénhez képest, illetve autoaktivációjuk csak kis mértékben fokozódott tovább CTRC jelenlétében.
2. A mutációk közül egy esetben, a D19A variánsnál volt megnövekedett a CTRC katalizálta N-terminális processzálás, de ennek hatására az autoaktiváció sebességében nem történt jelentős változás.
3. Az aktivációs peptid mutációk a CTRC általi tripszinogén lebontásában nem okoztak változást.
4. A mutációk a tripszinogén aktivációs peptid Ca^{2+} kötő affinitásában nem okoztak változást.
5. Végül az aktivációs peptid mutációk szekrécióját vizsgálva mind a négy vizsgált aktivációs peptid mutáns csökkent szekréciót mutatott HEK 293T sejtekből.

KÖVETKEZTETÉSEK

Munkánk során azonosítottuk az első örökletes pankreatitisszel asszociált intragenikus duplikációt a *PRSS1* génben. A duplikáció egy K23_I24insIDK inszerciós mutációt eredményezett a kationos tripszinogén aktivációs peptidjében melynek következtében erősen fokozódott a mutáns tripszinogén autoaktivációja. A K23_I24insIDK mutáns tripszinogénnek a lizoszomális enzim; katepszin B általi aktivációja is megnövekedett, mely korábban nem volt detektálható a többi pankreatitisszel asszociált *PRSS1* génben talált mutációnál.
Kimutattuk továbbá, hogy a vizsgált négy aktivációs peptid mutáció, D19A, D22G, K23R és K23_I24insIDK, jelentős mértékben stimulálta a tripszinogén autoaktivációt, azonban ezt a CTRC csak kis mértékben növelte tovább.

Végül kimutattuk, hogy az aktivációs peptid mutációk kivétel nélkül tripszinogén szekréció csökkenést okoztak, mely csökkenés fordítottan arányos volt a mutáns fehérjék megnövekedett autoaktivációjával. Feltételezhetően ez egy védekező mechanizmust takar, mely során a sejtek az intracellulárisan autoaktiválódott enzimeket lebontják. Ez a jelenség tompíthatja a mutáns enzimek markánsan fokozott autoaktivációjának a hatását és csökkentheti a hasnyálmirigyen belül a tripszin aktivitás fokozódásának mértékét a krónikus pankreatitisz patomechanizmusában.